DOCTOR OF PHILOSOPHY

Effects of in situ oceanic warming on marine benthic recruitment and community development in Antarctica

Villota Nieva, Leyre

Award date:
2019

Awarding institution:
Bangor University

Effects of *in situ* oceanic warming on marine benthic recruitment and community development in Antarctica

PRIFYSGOL
BANGOR
UNIVERSITY

by Leyre Villota Nieva

Thesis submitted for the degree of Doctor of Philosophy

BANGOR UNIVERSITY

School of Ocean Sciences

2018

Table of Contents

Author's declaration

I declare that the thesis has been composed by myself and I confirm that the work submitted is my own, except where work which has formed part of jointly-authored publications has been included. My contribution and those of the other authors to this work have been explicitly indicated below and in the relevant chapters. I confirm that appropriate credit has been given within this thesis where reference has been made to the work of others.

The work presented in Chapter 4 was a collaboration between the British Antarctic Survey and Edinburgh Genomics. I conducted the fieldwork, collected the samples, performed the RNA isolates and amplifications and also the biological annotation of the data. Edinburgh Genomics (Urmi Trivedi and Francis Turner) performed the bioinformatics analyses.

Except where stated above, I declare that the data presented in the rest of this thesis is an original report of my research, has been written by me and has not been submitted for any previous degree. The experimental work is my own work; the collaborative contributions have been indicated clearly and acknowledged. Due references have been provided on all supporting literatures and resources.

Leyre Villota Nieva

June, 2018

Acknowledgements

I am grateful to my supervisors Melody Clark, Lloyd Peck and Andrew Davies for their guidance and support during this project. Thank you Melody for the unconditional support and encouragement during the project and for always being there. Thank you Andy for making me feel so welcome in the Ocean Sciences department and for providing endless support with the Bangor panels. Thank you Lloyd for the support and guidance throughout the project and during the summer season in Rothera.

Thank you to Gail Ashton for your support and guidance, this project wouldn't have been possible without your work and monitoring of the panels in Rothera. Thank you to Urmi Trivedi and Frances McDonald at Edinburgh Genomics for the collaborative work we undertook together. A special thank you to Gwynne Parry Jones for the endless early mornings, late afternoons sampling the panels and the immense support throughout the deployment and monitoring. It wouldn't have been possible without you. Thank you to all the volunteers that got up at 6am to come out on the boat with me. Thank you to Elaine Fitzgerald, Michelle King and Guy Hillyard for the support in the lab. Thank you to the Rothera dive team for monitoring the panels.

Finally, thank you to all my colleagues at BAS and Bangor and in particular to my officemates at BAS for all the support, cups of tea, food and laughs. Thank you to my family, dogs and friends for always supporting me in pursuing my goals. Thank you to Fleetwood Mac, your music got me through the final stages of writing to the tune of "thunder only happens when it's raining."

List of Figures

List of Tables

Abstract

With coastal sea temperature predicted to increase 1.5-2°C by 2050, it is important to assess how the communities of coastal marine habitats will respond, in order to predict overall biodiversity and ecosystem level impacts. In this study I used the novel technology of heated settlement panels which heated the surface of each panel and a thin layer of overlying water to 1°C or 2°C above ambient temperatures, thus mimicking oceanic warming predictions for 2050 (IPCC, 2014). This technology was used to assess the effects of *in situ* elevated warming on benthic early community development.

In a first experiment, panels were deployed at the BAS Rothera Research station, Antarctica for a period of 18 months. To evaluate whether the encrusting species had acclimated to the warmer temperatures, I performed upper thermal limit and heat shock experiments on one of the main benthic colonisers, the spirorbid worm *Romanchella perrieri*. These data indicated a lack of both acclimation and a heat shock response in this species. This suggested that *R. perrieri* were resisting at the higher temperatures rather than successfully acclimating. An RNA-Seq approach was also was with another major spirorbid coloniser, *Protoleospira stalagmia*. The transcriptome data suggested the gradual shutting down of cellular pathways in the organisms in the 2°C treatment, supporting the observations of lack of acclimation in *R. perrieri*. Biofilm analyses were also carried out on the same panels. In contrast to the invertebrate results, there were very few differences observed in the microbial community across experimental treatments. Thus indicating that microbial communities may be more robust in the face of future climate change compared with metazoans.

In a second experiment, these panels were deployed in a temperate region, the Menai Strait, Wales. Development of the communities was monitored on a seasonal basis over a period of 13 months. Whilst communities varied seasonally, there was no significant difference in overall composition or species biodiversity between treatments. The exception to this was the overlapping evaluations in June 2015 and June 2016. Overall percentage cover was higher in June 2016 compared with June 2015, compromising three dominant species: the barnacle *Balanus crenatus*, the encrusting worm *Spirobranchus triqueter* and the bryozoan *Electra pilosa*.

Furthermore species composition was different in June 2016 and June 2015 was different in the control panels compared to the heated panels. Thus in warmer years even a +1°C or a +2°C

temperature rise can significantly affect temperate benthic ecosystems, producing a thermal tipping point for some species. These data validate the application of this heated settlement panel technology in temperate ecosystems.

Chapter 1

Introduction

Drastic human and economic consequences of biodiversity loss are widely recognised but poorly understood and quantified. Although a multitude of biologically significant environmental changes are projected to occur as a consequence of anthropogenic climate change, it is still difficult to predict how life and biodiversity on Earth will respond to the current and projected climate change (IPCC, 2014). Scientists and policy makers recognise that this is one of the most important questions in science at the moment, since predicting ecosystem level responses to change is a fundamental requirement for the future management of biodiversity, agriculture, fisheries and ecosystem services (Millennium Ecosystem Assessment (https://www.millenniumassessment.org/en/index.html), UN convention on Biological Diversity) (Dobson, 2005). The study of biodiversity has many different aspects. It has traditionally concentrated on documenting species and evaluating community compositions, but there is an increasing focus on functional aspects i.e. how species' respond to environmental challenges with an assessment of their abilities to cope in the new conditions.

The oceans cover over 70% of the Earth's surface and influence climate on a global scale (Reid & Beaugrand, 2012). The predicted increase in ocean temperatures is one of the most important impacts of climate change on biodiversity, as temperature influences fundamental physiological and ecological processes across biological scales, from genes to ecosystems. To date, predictions of responses to change in animals have been primarily at the species level and based around two approaches. The first uses current species range (climate envelopes) and predicts future ranges by assessing where similar conditions are likely to be from climate models (Araujo et al., 2012; Beale et al., 2008; Pearson et al., 2002). The second approach evaluates an organism's physiological capacity to cope with experimentally altered conditions in the laboratory (Huey et al., 2012; Peck, 2011; Pörtner, 2002; Somero, 2010).

Although widely used, both approaches have limitations. Studies of species ranges do not include measures of acclimation and adaptation rates (the rate at which genetic complements in populations can be altered either by gene-flow or mutation) or genetic and functional tolerance differences within and between populations. Similarly, the conclusions that can be drawn from

using physiological approaches are limited. They predominantly evaluate small numbers of species', often in isolation, over relatively short time periods using experimental rates of change that are faster than natural change. Experimental multi-generational experiments are rare and hence these types of experiments rarely evaluate genetic adaptation rates.

In addition, the majority of these studies are conducted in aquaria or mesocosms. Whilst these experiments provide valuable information, the highly controlled nature of the physio-chemical and biological environment reduces realism (Carpenter, 1996). Species, populations and individuals in nature experience a constantly changing environment. Moreover biological communities are connected across a range of spatial and temporal scales that extends beyond the confines of an aquarium (Borthagaray et al., 2009) e.g. biological communities are connected via the recruitment and settlement of marine larval, an essential process in establishing marine communities. Furthermore, few studies evaluate changes beyond metazoan communities i.e. changes to bacterial communities. This is particularly relevant as biofilms play a vital role in establishing benthic marine communities via the induction of settlement cues (Whalan et al., 2014), a process well documented in the polychaete literature (Kirchman et al., 1982; Hadfield et al., 1994).

There is therefore a pressing need for studies that link laboratory experiments with field observation that involve *in situ* experiments. Such field based manipulations conducted at environmentally relevant temperatures looking at impacts across different levels of biological organisation, from metazoans to bacteria, structures and interactions will provide a better holistic understanding of the effects of future warming on communities. In the terrestrial realm, some of the most valuable insights into the effects of predicted changes on communities come from field manipulation experiments in mesocosms (Grime et al., 2008), but to date such studies in marine systems are rare.

1.1 Marine *in situ* warming experiments

In situ experiments that provide realistic scenarios mimicking projected oceanic warming can provide predictions of future biodiversity responses and also provide a crucial experimental link to the numerous laboratory studies on thermal tolerances and acclimation. There is a noticeable lack of *in situ* studies in the marine environment, due to the inherent difficulties of manipulating temperature in marine systems (Wernberg et al., 2012a; Ashton et al. 2017). This represents a serious knowledge gap.

Marine data in this area generally come from mesocosm experiments (McElroy et al., 2015) where conditions are still somewhat artificial and from long term correlation studies based on historical collections (Barnes et al., 2011). Nevertheless there have been a number of opportunistic studies investigating warming in the field (Schiel et al., 2010; Wernberg et al., 2012b) and a few field thermal manipulation experiments (Kordas et al., 2014). The recent development of heated panels capable of recreating predicted oceanic warming conditions *in situ* is a key contribution in addressing this gap in the literature (Ashton et al., 2017; Smale et al., 2011; Smale et al., 2017). These panels warm a thin layer of water overlying their surface above the ambient temperature, thus simulating oceanic warming effects on encrusting communities. The design and operation of the panel predicates the level of heating achieved above ambient temperatures: the panels in Smale et al., (2017) heated the surface water layers by 3°C and 5°C, whilst those of Ashton et al., (2017) provided a much more ecologically relevant 1-2°C temperature increase and representative of near future warming predictions (IPCC, 2014). It is the panel design used in Ashton et al., (2017) which is employed in this thesis, which will primarily evaluate molecular data from encrusting communities in heated panels deployed at sites near the British Antarctic Survey Rothera research station on the Antarctic Peninsula, and in a pilot deployment in a temperate site in the Menai Straits, north Wales.

1.2 Antarctica

1.2.1 The Antarctic marine ecosystem and organisms

Antarctica is a unique environment. The Southern Ocean has a very stable and narrow temperature range (Barnes et al., 2006), with much of the fauna surviving around 0°C; temperature rises of +5°C have not occurred for at least 10 million years (Clarke & Crame, 2010). Although temperatures are stable, there is a strong seasonal variability in light and primary productivity (Clarke et al., 2008; Peck et al., 2006). Across the year, light varies from no direct sunlight in winter, to 24h of direct sunlight in summer, resulting in an intense seasonality of phytoplankton productivity in the summer, with chlorophyll standing stock levels in excess of 25 mg Chl-*a* m^{-3} (Clarke et al., 2008; Peck et al., 2017). Growth in Antarctic benthic organisms is therefore highly seasonal with feeding primarily restricted in many species to the summer period (Bowden et al., 2006; Clarke, 2008), although some have been shown to feed all year round (Barnes & Clarke 1994; 1995). These seasonal patterns are also reflected in the marine bacterial community composition, where the dramatic seasonal variation in Antarctic water causes shifts in

bacterial richness and composition to reflect this seasonality (Murray and Grzymski, 2007). Photoautotroph bacteria are highly abundant in the summer due to the plankton bloom, generating organic matter as a by product. This productivity drives the succession of the microbial community structure from summer to winter, where photoautotrophs become less abundant as light levels vary to no direct light and the phytoplankton bloom disappears (Luria et al., 2014).

In spite of the near freezing temperatures and intense seasonality, life in the Southern Ocean is highly abundant and rich, comparable to the benthic diversity in temperate areas (Clarke & Johnston, 2004, Peck, 2017). The most abundant benthic group in shallow rocky sites in the Antarctic both in terms of number of recruits and area coverage are the Cheliostome bryozoans together with Spirorbid polychaetes (Barnes et al., 2006). (Barnes et al., 2006). The spirorbid polychaetes *Romanchella perrieri* and *Protolaeospira stalagmia* are some of the most abundant benthic organisms found on shallow rocky sites in the Antarctic (Barnes et al., 2006). They were originally proposed as subgenera of *Spirorbis* from which they were separated by small differences in setae and reproduction: these tube-incubating organisms do not attach their embryos to the walls of their tubes (Knight-Jones et al., 1972). Their distribution is mainly polar, with *R. perrieri* extending as far north as Patagonia (Knight-Jones, 1984) and *P. stalagmia* extending as far north as the South Orkney islands (Knight-Jones et al., 1972). Not only is there a high metazoan diversity but also a high diversity at the prokaryotic level. Although Antarctic marine microbial communities still remain highly underrepresented in microbial diversity studies, recent advances in sequencing technology have allowed for an increase in the number of studies looking at marine bacteria (Wilkins et al., 2013). These studies suggest that Antarctic marine bacterial communities are also like benthic ones, highly diverse and rival to those found in other ocean systems (Tytgat et al., 2014).

1.2.2 A region under threat

As a consequence of having evolved in a stable temperature environment, organisms here are highly stenothermal (Bilyk & Devries, 2011; Pörtner et al., 2007; Peck, 2016). Most live within a 4°C temperature range in their natural environment and have poor acclimatory abilities (Morley et al., 2011; Peck et al., 2014; Peck et al., 2010; Barnes & Peck, 2008). Temperature manipulation experiments have shown that not only do Antarctic invertebrates start to lose essential biological functions, such as swimming in scallops and burrowing in clams with temperatures changes of only 1-2°C above current summer maxima, but long term survival is also compromised by similar temperature rises (Peck et al., 2004; Pörtner et al., 2007; Peck et al., 2009; Peck et al., 2014).

Hence Antarctic marine life is highly biodiverse (Arntz et al., 1997; Clarke & Johnston, 2003; De Broyer et al., 2014), but also very sensitive to even small increases in water temperature (Peck et al., 2009), such as those resulting from heated settlement panels. This region, where we have significant gaps in our knowledge on ecosystem functioning, is at high risk from climate change. The Western Antarctic Peninsula is one of the regions of the world currently experiencing the greatest rates of warming due to climate change. Although recent analysis suggest that the atmospheric warming seen along the Peninsula during the second half of the 20th century has ceased (Turner et al., 2016), it is still uncertain whether these trends are also reflected in the oceanographic data, where sea ice changes and glacier retreat are still occurring (Barnes & Souster, 2011; Cook et al., 2016). Since a principal factor determining benthic assemblage structure in near shore waters is the gradient of decreasing physical disturbance by ice with increasing depth (Brown et al., 2004), warming in the peninsula is particularly important.

Warming is likely to increase sea ice scour and change the composition of benthic assemblages, where deeper seabed benthic assemblages are likely to become richer and hard shallow surfaces are likely to be dominated by rapidly colonising pioneers and responsive scavengers (Barnes et al., 2014). Such changes have already been observed in the West Antarctic Peninsula, where increased iceberg scouring on the benthos has increased the mortality of the pioneer species *Fenestrulina rugula* (Barnes & Souster, 2011). Warming has already been shown to change benthic assemblage composition (Ashton et al., 2017) and alter competition between species (Poloczanka et al., 2008). Reduction in annual sea ice and glacier retreat (Venebles et al., 2014; Cook et al., 2016) in the Antarctic Peninsula is also likely to result in a loss of habitat for marine bacterial communities and affect sea ice-melting related oceanic processes like seeding plankton blooms. An increase in primary productivity in the austral summer as a consequence of oceanic warming has already been observed in Antarctica due to enhanced stratification and abundance of macronutrients, causing shifts in bacterial communities i.e. diatoms have been replaced by cryptophytes (Moline et al., 2004).

As such warming, ice loss and changes in iceberg scour will have implications for the whole ecosystem, such as the effects on productivity, food webs and carbon capture (Peck et al., 2010; Barnes, 2015; Barnes, 2017). Because of these changes the Western Antarctic Peninsula is still considered a vulnerable area (Ducklow et al., 2013), and there is an urgent need to characterise ecosystem functioning in this region.

1.3 Organism responses to change

Organisms can cope with environmental change by adjusting physiologically (Peck, 2011; Somero, 2010) if the extent of environmental variability is small. However, when a population of organisms experiences an environmental challenge outside the normal range of phenotypic variability, they may respond in one of three ways:

1) Migration: species move to a more favourable area
2) Adaptation: species evolve and shift their phenotype to better fit the new environment
3) Extinction: species fail to adapt or migrate and as a result, become extinct

The continental shelf fauna of Antarctica is isolated from the rest of the world by a strong frontal system associated with the Antarctic circumpolar current (ACC) and a wide expanse of deep ocean, thus restricting the migration of Antarctic species to more favourable areas (Clarke & Crame, 1997; Peck, 2017). It must be noted that oceanographic mechanisms for transporting larval benthic invertebrates in and out from Antarctica exist, but the thermal sensitivities of dispersing larvae to rapid temperature gradients during the transit from Antarctica to sub-polar sites poses a major limitation (Barnes & Peck, 2008). This makes migration to more favourable areas, unlikely. Antarctic species have long generation times and reduced number of eggs produced per female per reproductive event (Peck et al., 2005; Peck, 2017) which means that rapid genetic adaptation to the new conditions is also unlikely.

In this context, (Somero, 2010) argues that acclimation via physiological flexibility is the most important process that will dictate the survival or failure of long-lived species in a climate change scenario. However, this will be highly dependent on the rate of climate change and the time required for any given process or mechanism to become effective. For example, if the rate of change is too fast for evolutionary mechanisms to take place, then an intermediate stage whereby physiological flexibility occurs is necessary in order to provide enough time for the slower evolutionary processes to take place (Peck, 2011). Hence, there is a requirement to understand the mechanisms that underlie a species capacity for acclimation, but these are not well defined yet and are still subject of debate. Pörtner et al., (2001, 2002, 2007) argue that oxygen limitation through reduced aerobic capacity will be the limiting mechanism dictating whether a species can acclimate or not. Peck et al., (2009, 2010) on the other hand argues that it is the rate of temperature change together with a range of mechanisms that will limit survival: energy trade-

offs associated with metabolism at higher temperatures (Sørensen and Loeschcke, 2007), increase formation of reactive oxygen species (ROS) due to heat stress (Heise et al., 2002) and the already poor acclimation capabilities of Antarctic species (Peck et al., 2010).

1.4 Acclimation and life histories in Antarctic species

In acclimation work which subjected 6 species of Antarctic invertebrates to acclimation trials at 3 °C for 60 days: 5 out of 6 species failed to acclimate to temperatures only 1-2°C above current summer maxima (Peck et al., 2010). Additional work on Antarctic bivalve molluscs showed that the upper limit for acclimation in these species is low, around 3–4°C (Peck et al., 2014). Whilst further work examining the long-term (beyond 60 days) acclimation abilities of Antarctic marine species showed that they required at least 2-5 months to acclimate to even small temperature rises. Morley et al. (2011) reported the Antarctic limpet *Nacella concinna* taking 9 months to acclimate to 2.9°C. The poor acclimation capabilities is not only seen in invertebrates but also in Antarctic fish: they take longer to acclimate to altered temperatures than warmer water fishes (Bilyk & Devries, 2011). Nevertheless, they have a higher degree of thermal flexibility than the invertebrates mentioned above (Peck et al., 2009), as they seem to acclimate faster to altered temperatures (Bilyk & Devries, 2011). There is therefore a growing body of work, indicating the very slow acclimation capacities of Antarctic organisms, however all these data are based on evaluations of adults and age impacts significantly on Antarctic species' responses to change (Clark et al., 2013).

In contrast to Antarctic invertebrates, Antarctic marine bacteria have a higher thermal flexibility and wider temperature range. For example a *Pseudoalteromonas* species from the South Shetlands demonstrated a temperature range from -2°C to 18°C, whilst a *Cellulophaga* species from the same area survived up to 41°C (Jeong et al., 2014). Their much higher degree of thermal plasticity and potential for adaptation due to their shorter life histories means prokaryotic responses to climate change may be very different to those from metazoans. Current studies and climate prediction envelopes do not take into consideration these potentially differing responses that may cause significant changes to metazoan communities. This represents a gap in the literature.

One of the parameters that need to be considered when developing approaches to understand how communities or assemblages will respond to environmental change is the identification of the

most vulnerable stages of the population. The loss of such stages could have a great impact on the overall biodiversity. In this context, early life history stages have been identified as the most vulnerable stages to change (Pedersen et al., 2008): the largest mortality across life histories occurs in early development and recruitment. Their small body size, reasonably high (mass-specific) metabolic rates and lower energy reserves increases their vulnerability to climate change (Rijnsdorp et al., 2009). This is not true however for all species. Early life stages of 4 species of marine invertebrates: the clam *Laternula elliptica*, the sea cucumber *Cucumaria georgiana,* the sea urchin *Sterechinus neumayeri*, and the seastar *Odontaster validus* out-perform adults in warming experiments (Peck et al., 2013), suggesting that at least some early life stages are robust (See Clark et al., 2016 for another example). There are no studies looking at the thermal tolerance of adult and larval stages in Antarctic marine polychaetes but studies from temperate species suggest that early life stages and juveniles are more vulnerable than adults. Qiu & Qian (1997) studied tolerances to various experimental salinities among developmental stages of the worm *Hydroides elegans* and reported that early developmental stages were more sensitive to environmental stress than late juveniles and adults. This is particularly important as in polychaetes such as *Spirobranchus triqueter* (formerly known as *Pomatoceros triqueter*) there is already over 90% natural mortality observed in juveniles (Klockner, 1976).

Early life stages are therefore still considered vulnerable since small changes in balance in early life history and colonisation stages in marine species are likely to give very large changes in community structure and ecosystem balance. These factors, coupled with the very high ecologically-driven mortality in early life history stages, means that investigations of warming effects on recruitment and early community development in Antarctic marine benthic groups are an essential step towards understanding how ecosystems will respond to change. It is this stage that is under investigation in this thesis using heated settlement panels and the evaluation of the performance of encrusting communities.

1.5 Understanding molecular responses to acclimation: the environmental stress response

The data in Ashton et al. (2017) demonstrated significant differences in colonisation and massive increases in growth rates of encrusting species when heated 1°C and 2°C above ambient on settlement panels deployed near Rothera for 9 months. This time-scale is beyond the maximum of nine months, so far described for acclimation requirements of Antarctic species (Morley et al.,

2011), hence the question arises as to whether these rapidly growing encrusting species are truly acclimated and what are the underlying mechanisms behind their enhanced performance? What is their environmental stress response?

In face of predicted oceanic warming, understanding environmental stress responses in organisms is becoming increasingly important in order to predict when a species is threatened and the extent of such threats. This will allow us to identify what factors set species range boundaries and how they will be affected by anthropogenic stress. Identifying environmental stress responses can be carried out at different experimental levels from ecological observation (Walther et al., 2002), behavioural, physiological (Peck et al., 2004; Pörtner et al., 2006) and molecular (Clark et al., 2004; Clark et al., 2017). Whilst all contribute to understanding ecosystem function, the ability to predict the vulnerability of a species to stress is best achieved at the molecular level, as sub-lethal effects across a range of functions can be quantified (Truebano et al., 2010). The understanding of the cellular responses is key, in order to determine early on when a species is threatened. This has led to the proposal of a generic universal cellular stress response (CSR), which comprises a series of biochemical changes aimed at maintaining homeostasis (Kultz, 2005; Clark et al., 2016). These biochemical changes, or rather the expression levels of genes and proteins underlying them can potentially be used as molecular biomarkers to predict sensitivities and resiliencies to change in higher levels of biological organisation (Clark et al., 2013; 2017).

1.6 Heat shock proteins

In general, exposure to external stressors results in the activation of members of the CSR and the production of heat shock proteins (Hsps) (Kültz, 2003; Gross, 2004). The most studied Hsp family members are the 70kDA proteins (Hsp70) that act as chaperones to stabilise and re-fold denatured proteins and prevent the aggregation of damaged proteins (Bucciantini et al., 2002). The highly conserved nature of Hsps makes them proteins of interest for ecological physiologists studying the biological consequences of the physical environment. The production of Hsps is thought to have an adaptive value: synthesis of Hsps may reduce the cost of environmentally-induced irreversible protein damage, decreasing the proportion of the organism's energy budget that is dedicated to maintaining the protein pool (See Houlihanet et al., 1995). This is particularly the case of intertidal ectotherms that experience unpredictable and extreme variations in temperature (e.g. Helmuth & Hofmann, 2001).

1.7 Heat shock proteins in Antarctic species

The induction and expression of *hsp70* genes is highly plastic. Levels of induction are influenced by seasonal temperature variations and biogeography (Hofmann, 2005; Somero, 2002). Patterns of expression of Hsps in Antarctic marine organisms differ to those that are highly conserved across the vast majority of species. The only species where Hsps have not been induced in response to temperature are in the Antarctic (Clark et al., 2008b; Hofmann et al., 2000; Terza et al., 2004). The classical heat shock response is absent in the Antarctic notothenoid fishes (Hofmann et al., 2000) due to a mutation in the promoter region of the *hsp70* gene, which prevents Hsf1 binding and the transcription of the gene (Place et al., 2004). In contrast to their temperate species, Antarctic bivalve molluscs permanently express *hsp70* (Clark et al., 2008a) under no heat stress which is thought to be a response to the problems of protein folding at cold temperatures (Privalov, 1990).

Experimental thermal challenges in a range of Antarctic invertebrates showed no increase in expression of Hsps in the fish *Harpagifer antarcticus*, the amphipod *Paraceradocus gibber*, and the starfish *Odontaster validus* (Clark & Peck, 2009a). There was induction of *hsp70* in two molluscs, but only at abnormally high "environmental" temperatures: 15°C in the Antarctic limpet (*Nacella concinna*) and at 8°C in the Antarctic clam (*Laternula elliptica*). These abnormally high induction temperatures compared to those experienced in the natural environment were presumed to be the relic of a temperate ancestor. However, further studies in *N. concinna* showed that animals did express *hsp70* at much lower temperatures under natural conditions and in response to a variety of stresses including emersion in the intertidal zone (Clark & Peck, 2009b). Moreover, transcriptome led discovery approaches (using candidate gene approaches) have reported that species that were previously thought to lack a heat shock response are in fact capable of inducing one indeed (Clark et al., 2017). Some species such as *Euphausia superba* (krill) and *Laternula elliptica* have species-specific duplications of *hsp* genes, so the fact that the genes are still present, and in some cases multiplied, implies advantageous selective pressures, the reason behind which is still unknown.

Therefore, despite the limited number of examples and the vast distribution across taxa, there is no rule for the expression or loss of the classical heat shock response in Antarctic marine organisms and there is still a big question over whether more Antarctic species may lack a heat shock response. This response in Antarctic organisms might be important in dealing with multiple stressors' and therefore in this study Hsps were evaluated to determine if the encrusting worm

Romanchella perrieri exhibited such a response and these genes were also used as molecular markers of acclimation along with the classic physiological metrics of upper thermal limits.

1.8 Objectives and thesis structure

This PhD is a tied studentship on the NERC standard grant (NE/J007501/1): Effects of *in situ* oceanic warming on marine benthic recruitment and community development in Antarctica. The main aim of this project was to study the effects of *in situ* elevated temperature on marine benthic recruitment and community development in Antarctica at the molecular level. This was achieved by using a novel technology, "heated settlement panels". The panels were set to heat the panel surface and a thin layer of water overlying the surface to 1°C and 2°C above ambient temperature, thus mimicking end of century oceanic warming predictions (IPCC, 2014) in the natural environment. The heated panel technology allows the study of early community development under ecologically relevant temperatures that match the IPCC's oceanic warming predictions *in situ* alongside the additional natural environmental variables such seasonality of food supply, light etc. Panels were deployed on the benthos, at 15m and at three different sites near the British Antarctic Survey Rothera research station on the Antarctic Peninsula.

The post-doctoral researcher on the grant (Dr Gail Ashton) was responsible for setting up the heated panel experiment in Rothera, monitoring the panels and describing the community compositions, growth rates and competitive interactions. Part of this work on the ecology associated with the panels has recently been published (Ashton et al., 2017). The Antarctic chapters in this thesis complement the ecological research on the heated panels of the post-doctoral researcher, by carrying out genetic analyses on the encrusting communities. In addition Chapter 6 of this thesis describes the results of a pilot project deploying the heated panels in the Menai Strait, UK. This was an independent experiment set up, monitored and analysed during the course of this PhD, with the aim of determining if a 1°C and a 2°C increase in water temperature would affect UK encrusting communities. The thesis is divided into seven chapters including a general introduction and conclusions.

Chapter 2

Chapter two is a general material and methods chapter that describes the heated settlement panel technology and compares the methodologies used in the Antarctic and Menai Strait panels.

This chapter also discusses potential improvements that could be made to the heated settlement panels and additional capabilities to be explored.

Chapter 3

Chapter three describes the differences in the expression of heat shock proteins and the thermal tolerance in response to heat stress in one of the main Antarctic colonisers, the spirorbid worm *Romanchella perrieri.* The ecological evaluations of the panels showed a massive increase in growth rates with temperature across the encrusting communities. Hence key questions tested in this chapter are: Have the organisms acclimated to the experimental temperatures? Does *Romanchella perieri* have a heat shock response and if so, how does it differ between panel treatments?

Chapter 4

In Chapter four I explored further how the organisms were functionally performing in the heated treatments at the cellular level using an RNA-Seq approach. A *de novo* transcriptome for *Protoleospira stalagmia*, one of the other Antarctic spirorbid worms was performed and up and down regulation of genes involved in thermal stress, oxidative stress and ATP synthesis in the heated treatments were explored. This data complemented the thermal stress results reported in Chapter three for the other spirorbid worm, *R. perrieri* and yielded an understanding on how the organisms were performing at the molecular level and whether they would be able to survive predicted end of century oceanic warming (IPCC, 2014). I also interrogated RNA-Seq data Single Nucleotide Polymorphisms (SNPs) to investigate post-selection recruitment using a population genetics approach in *P. stalagmia*.

Chapter 5

Biofilms are integral parts of communities, play a significant role in the development of new communities, and can have significant effects on the settlement of new recruits. The differences in the microbial composition of biofilm of the heated and non-heated Antarctic settlement panels, using 16s amplicon sequencing is presented in Chapter five. The incorporation of biofilm data into the findings presented in Chapter three and four lays a foundation for understanding the effects of oceanic warming on marine communities across different levels of biological organisation.

Chapter 6

Chapter six describes the experimental outcome of using heated settlement panels in a temperate environment, the Menai Straits, Wales, UK. This chapter describes the differences in community composition and biodiversity on heated versus non-heated panels for trials run in different seasons. It further describes the effects of elevated temperature on the growth rates of the main coloniser, the calcifying worm *Spirobranchus triqueter.*

Chapter 7

Finally Chapter 7 synthesises the results of the earlier chapters to address the main paradigms in organismal responses to oceanic warming and to test hypothesis such as the universal stress response. It also discusses future directions for research and the potential applications of heated settlement across other ecosystems and industries.

Chapters three to six are presented in the format of a scientific paper, including an introduction, methods, results, discussion, conclusion and references per chapter.

1.9 References

Arntz, W. E., Gutt, J. and Klages, M. (1997). Antarctic marine biodiversity: an overview. Cambridge University Press (UK).

Abele, D., Heise, K., Pörtner, H. O. and Puntarulo, S. (2002). Temperature-dependence of mitochondrial function and production of reactive oxygen species in the intertidal mud clam *Mya arenaria*. *J. Exp. Biol.* **205***,* 1831–1841.

Araujo, M. B. and Peterson, A. T. (2012). Uses and misuses of bioclimatic envelope modeling. *Ecology.* **93**, 1527–1539.

Ashton, G. V., Morley, S. A., Barnes, D. K. A., Clark, M. S. and Peck, L. S. (2017). Warming by 1°C Drives Species and Assemblage Level Responses in Antarctica's Marine Shallows. *Curr. Biol*. **27**, 2698–2705.

Barnes, D. K. A. and Clarke, A. (1994). Seasonal variation in the feeding activity of four species of Antarctic bryozoan in relation to environmental factors. *J. Exp. Mar. Biol. Ecol.* **181**, 117-133.

Barnes, D. K. A. and Clarke, A. (1995). Seasonality of feeding activity in Antarctic suspension feeders. *Polar. Biol.* **15**, 335-340.

Barnes, D. K. A., Fuentes, V., Clarke, A., Schloss, I. R. and Wallace, M. I. (2006). Spatial and temporal variation in shallow seawater temperatures around Antarctica. *Deep. Sea. Res. Part II. Top. Stud. Oceanogr*. **53**, 853–865.

Barnes, D. K. A. and Peck, L. S. (2008). Vulnerability of Antarctic shelf biodiversity to predicted regional warming. *Clim. Res.* **37***,* 149–163.

Barnes, D. K. A. and Souster, T. (2011). Reduced survival of Antarctic benthos linked to climate-induced iceberg scouring. *Nat. Clim. Change.* **1**, 365–368.

Barnes, D. K. A., Fenton, M. and Cordingley, A. (2014). Climate-linked iceberg activity massively reduces spatial competition in Antarctic shallow waters. *Curr. Biol.* **24**, 553–554.

Barnes, D. K. A. (2015). Antarctic sea ice losses drive gains in benthic carbon drawdown. *Curr. Biol*. **25**, R789–R790.

Barnes, D. K. A. (2017). Polar zoobenthos blue carbon storage increases with sea ice losses , because across-shelf growth gains from longer algal blooms outweigh ice scour mortality in the shallows. *Glob. Change. Biol*. **00**, 1–9.

Beale, C. M., Lennon, J. J. and Gimona, A. (2008). Opening the climate envelope reveals no macroscale associations with climate in European birds. *PNAS.* **105**, 14908-14912.

Bilyk, K. T. and Devries, A. L. (2011). Heat tolerance and its plasticity in Antarctic fishes. *Comp. Biochem. Physiol. Part A Mol. Integr. Physiol.* **158**, 382–90.

Borthagaray, A. I., Brazeiro, A. and Giménez, L. (2009). Connectivity and patch area in a coastal marine landscape : Disentangling their influence on local species richness and composition. *Austral. Ecol*. **34**, 641–652.

Bowden, D., Clarke, A., Peck, L. and Barnes, D. (2006). Antarctic sessile marine benthos: colonisation and growth on artificial substrata over three years. *Mar. Eco. Prog. Ser.* **316**, 1–16.

Brown, K. M., Fraser, K. P. P., Barnes, D. K. A. and Peck, L. S. (2004). Links between the structure of an Antarctic shallow-water community and ice-scour frequency. *Oecologia.* **141**, 121–129.

Bucciantini, M., Giannoni, E., Chiti, F., Baroni, F. and Formigli, L. (2002). Inherent toxicity of aggregates implies a common mechanism for protein misfolding diseases. *Nature.* **416***,* 507–511.

Carpenter, S. R. and Pace, M. L. (1997). Dystrophy and eutrophy in lake ecosystems: implications of fluctuating inputs. *Oikos.* **78**, 3-14.

Clark, M. S., Clarke, A., Cockell, C. S., Convey, P., Lii, H. W. D., Fraser, K. P. P. et al. (2004). Antarctic genomics. *Comp. Funct. Genomics.* **5**, 230–238.

Clark, M. S., Fraser, K. P. P. & Peck, L. S. (2008a). Antarctic marine molluscs do have an HSP70 heat shock response. *Cell. Stress. Chaperones.* **33**, 39–49.

Clark, M. S., Fraser, K. P. P. and Peck, L. S. (2008b). Lack of an HSP70 heat shock response in two Antarctic marine invertebrates. *Polar Biol.* **31**, 1059–1065.

Clark, M. S. and Peck, L. S. (2009). Triggers of the HSP70 stress response : environmental responses and laboratory manipulation in an Antarctic marine invertebrate (*Nacella concinna*). *Cell. Stress. Chaperones*. **70**, 649–660.

Clark, M. S., Husmann, G., Thorne, M. A. S. and Burns, G. (2013). Hypoxia impacts large adults first : consequences in a warming world. *Glob. Change. Biol.* **19**, 2251–2263.

Clark, M. S., Thorne, M. A. S., Burns, G. and Peck, L. S. (2016). Age-related thermal response: the cellular resilience of juveniles. *Cell. Stress. Chaperones*. **21**, 75-85

Clark, M. S., Sommer, U. L. F., Sihra, J. K. and Thorne, M. A. S. (2017). Biodiversity in marine invertebrate responses to acute warming revealed by a comparative multi-omics approach. *Glob. Change. Biol.* **23**, 318–330.

Clarke, A. and Crame, J. A. (1997). Diversity, lattitude and time: patterns in the shallow sea. *Marine Diversity: Patters and Processes* (eds R.F.G. Ormond, J.D. Gage & M.V. Angel), 122-147. Cambridge University Press. Cambridge, U.K.

Clarke, A. and Johnston, N. M. (2003). Antarctic marine benthic diversity. *Oceanogr. Mar. Biol. Ann. Rev.* **41**, 47-114.

Clarke, A., Murphy, E. J., Meredith, M. P., King, J. C., Peck, L. S., Barnes, D. K. A. and Smith, R. C. (2007). Climate change and the marine ecosystem of the Western Antarctic Peninsula. *Philos. Trans. R. Soc. Lond. B. Biol. Sci.* **362**, 149–166.

Clarke, A. (2008). Journal of Experimental Marine Biology and Ecology Antarctic marine benthic diversity : patterns and processes. *J. Exp. Mar. Biol. Ecol.* **366,** 48–55.

Clarke, A., Meredith, M. P., Wallace, M. I., Brandon, M. A. and Thomas, D. N. (2008). Seasonal and interannual variability in temperature , chlorophyll and macronutrients in northern Marguerite Bay , Antarctica. *Deep. Sea. Res. Part 2. Top. Stud. Oceanogr.* **55**, 1988–2006.

Clarke, A. and Crame, J. A. (2010). Evolutionary dynamics at high latitudes : speciation and extinction in polar marine faunas. *Philos. Trans. R. Soc. Lond. B. Biol. Sci.* **365**, 3655–3666.

Cook, A. J., Holland, P. R., Meredith, M. P., Murray, T., Luckman, A. and Vaughan, D. G. (2016). Ocean forcing of glacier retreat in the western Antarctic Peninsula. *Science.* **353**, 283–287.

De Broyer, C., Koubbi, P., Griffiths, H., Raymond, B., D'Udeken, C. et al. (2014). Biogeographic Atlas of the Southern Ocean.

Dietmar, K. (2005). Molecular and evolutionary basis of the cellular stress response. *Annu. Rev. Physiol.* **67**, 225-257.

Dobson, A. (2005). Monitoring global rates of biodiversity change : challenges that arise in meeting the Convention on Biological Diversity (CBD) 2010 goals. *Philos. Trans. R. Soc. Lond. B. Biol. Sci.* **360**, 229–241.

Ducklow, H. W., Fraser, W. R., Meredith, M. P., Stammerjohn, S. E., Doney, S. C., Martinson, D. G., Schofield, O. M. et al. (2013). *Oceanography.* **26**, 190-203.

Grime, J. P., Fridley, J. D., Askew, A. P., Thompson, K., Hodgson, J. G. and Bennett, C. R. (2008). Long-term resistance to simulated climate change in an infertile grassland. *PNAS.* **105**, 10028-10032.

Gross, M. (2004). Emergency services: a bird's eye perspective on the many different functions of stress proteins. *Curr. Protein. Pept. Sci.* **5**, 213-223.

Hadfield, M. G., Unabia, C. C., Smith, C. M. and Michael, T. M. (1994). Settlement preferences of the ubiquitous fouler Hydroides elegans. In: Thompson, M. F., Nagabhushanam, R., Sarojini, R., Fingerman, M. (eds). Recent development in biofouling control. Oxford and IBH Pub. Co., New Delhi, pp 65-74.

Helmuth, B. S. T. and Hofmann, G. E. (2001). Microhabitats , Thermal Heterogeneity , and Patterns of Physiological Stress in the Rocky Intertidal Zone. *Biol. Bull.* **201**, 374–384.

Hofmann, G. E., Buckley, B. A., Airaksinen, S., Keen, J. E. and Somero, G. N. (2000). Heat-shock protein expression is absent in the antarctic fish *Trematomus bernacchii* (family Nototheniidae). *J. Exp. Biol.* **203***,* 2331–2339.

Hofmann, G. E. (2005). Patterns of Hsp gene expression in ectothermic marine organisms on small to large. *Integr. Comp. Biol.* **45**, 247–255.

Huey, R. B., Kearney, M. R., Krockenberger, A., Holtum, J. A. M., Jess, M. and Williams, S. E. (2012). Predicting organismal vulnerability to climate warming : roles of behaviour, physiology and adaptation. *Philos. Trans. R. Soc. Lond. B. Biol. Sci.* **367**, 1665–1679.

IPCC. (2014). Climate Change 2014 Synthesis Report Summary for Policymakers.

Jeong, H. H., Jeong, S. G., Park, A., Jang, S. C., Hong, S. G. and Lee, C. S. (2014). Effect of temperature on biofilm formation by Antarctic marine bacteria in a microfluidic device. *Anal. Biochem.* **446***,* 90–95.

Kirchman, D., Graham, S., Reish, D. and Mitchell, R. (1982). Bacteria induce settlement and metamorphosis of *Janua* (Dexiospira) *brasiliensis* Grube (Polychaeta: Spirorbidae). *J. Exp. Mar. Biol. Ecol.* **56**, 153-163.

Klockner, K. (1976). Zur Okologie von *Pomatoceros triqueter* (Serpulidae, Polychaeta) I. Reproduktionsablauf, Substratwahl, Wachstum and Mortalitat. *Helgoländer. Wissenschaftliche. Meeresuntersuchungen*. **28**, 352-400.

Knight-Jones, P. and Walker, A. J. M. (1972). Spirorbidae (Serpulidae: Polychaeta) on limpets from the South Orkney Islands. *BAS. Bulletin.* **31**, 33-40.

Knight-Jones, P. and Knight-Jones, E. W. (1984). Systematics, ecology and distribution of southern hemisphere spirorbids (Polychaeta; Spirorbidae). Proceedings of the first international polychaete conference, Sydney edited by P.A. Hutchings, published by Linnean Society of New South Wales, pp 196-210.

Kordas, R. and Dudgeon, S. (2014). Intertidal community responses to field-based experimental warming warming. *Oikos.* **124**, 888-898.

Kültz, D. (2003). Evolution of the cellular stress proteome : from monophyletic origin to ubiquitous function. *J. Exp. Biol.* **206**, 3119-3124.

La Terza, A., Miceli, C. and Luporini, P. (2004). The gene for the heat-shock protein 70 of *Euplotes focardii*, an Antarctic psychrophilic ciliate. *Antarct. Sci.* **16**, 23–28.

Luria, C. M., Ducklow, H. W. and Amaral-Zettler, L. A. A. (2014). Marine bacterial, archaeal and eukaryotic diversity and community structure on the continental shelf of the western Antarctic Peninsula*. Aquat. Microb. Ecol*. **73**, 107-121.

McElroy, D. J., Gorman, E. J. O. and Schneider, F. D. (2015). Size-balanced community reorganization in response to nutrients and warming. *Glob. Change. Biol.* **21**, 3971–3981.

Moline, M. A., Claustre, H., Frazer, T. K., Schofield, O. and Vernet, M. (2004). Alteration of the food web along the Antarctic Peninsula in response to a regional warming trend. *Glob. Change. Biol*. **10**, 1971-1980.

Morley, S. A., Lemmon, V., Obermüller, B. E., Spicer, J. I., Clark, M. S. and Peck, L. S. (2011). Duration tenacity : A method for assessing acclimatory capacity of the Antarctic limpet , *Nacella concinna*. *J. Exp. Mar. Biol. Ecol.* **399**, 39–42.

Murray, A. E. and Grzymski, J. J. (2008). Diversity and genomics of Antarctic marine micro-organisms. *Philos. Trans. R. Soc. Lond. B. Biol. Sci*. **362**, 2259-2271.

Peck, L. S., Webb, K. E. and Bailey, D. M. (2004). Extreme sensitivity of biological function to temperature. *Funct. Ecol.* **18**, 625–630.

Peck, L. S. (2005). Prospects for survival in the Southern Ocean : vulnerability of benthic species to temperature change. *Antarc. Sci.* **17**, 497–507.

Peck, L. S., Convey, P., Barnes, D. K. A., Peck, L. S., Convey, P. and Barnes, D. K. A. (2006). Environmental constraints on life histories in Antarctic ecosystems : tempos , timings and predictability. *Biol. Rev.* **81**, 75–109.

Peck, L. S., Clark, M. S., Morley, S. A., Massey, A. and Rossetti, H. (2009). Animal temperature limits and ecological relevance : effects of size , activity and rates of change. *Funct. Ecol.* **23**, 248–256.

Peck, L. S., Morley, S. A. and Clark, M. S. (2010). Poor acclimation capacities in Antarctic marine ectotherms. *Mar. Biol.* **157**, 2051–2059.

Peck, L. S. (2011). Marine Genomics Organisms and responses to environmental change. *Mar. Genomics*. **4**, 237–243.

Peck, L. S., Souster, T. and Clark, M. (2013). Juveniles are more resistant to warming than adulst in 4 species of Antarctic Marine Invertebrates. *PLoS ONE.* **8**, e66033.

Peck, L. S., Morley, S. A, Richard, J. and Clark, M. S. (2014). Acclimation and thermal tolerance in Antarctic marine ectotherms. *J. Exp. Biol*. **217**, 16–22.

Peck, L. S. (2016). Opinion A Cold Limit to Adaptation in the Sea. *Trends. Ecol. Evol.* **31**, 13–26.

Peck, L.S. (2017) – OMBAR in press

Place, S. P., Zippay, M. L., Hofmann, G. E., Sean, P., Zippay, M. L. and Hoffman, G. E. (2004). Constitutive roles for inducible genes : evidence for the alteration in expression of the inducible hsp70 gene in Antarctic notothenioid fishes. *Am. J. Physiol. Integr. Comp. Physiol.* **287**, 429–436.

Poloczanska, E. S., Hawkins, S. J., Southward, A. J. and Burrows, M. T. (2008). Modeling the response of populations of competing species to climate change. *Ecology.* **89**, 3138-3149.

Pörtner, H. O. (2001). Climate change and temperature-dependent biogeography: oxygen limitation of thermal tolerance in animals. *Naturwissenschaften*, **88**, 137-146.

Pörtner, H. O. (2002). Climate variations and the physiological basis of temperature dependent biogeography : systemic to molecular hierarchy of thermal tolerance in animals. *Comp. Biochem. Physiol. A. Mol. Integr. Physiol.* **132**, 739–761.

Pörtner, O. H., Peck, L. S. and Hirse, T. (2006). Hyperoxia alleviates thermal stress in Antarctic bivalve, *Laternulla elliptica*: evidence for oxygen limited thermal tolerance. *Polar. Biol.* **29**, 688-693.

Pörtner, O. H., Peck, L. and Somero, G. (2007). Thermal limits and adaptation in marine Antarctic ectotherms : an integrative view. *Philos. Trans. R. Soc. Lond. B. Biol. Sci.* **362**, 2233–2258.

Privalov, P. L. (1990). Cold Denaturation of Proteins. *Crit. Rev. Biochem. Mol. Biol.* **25**, 281-306.

Qiu, J. W. and Qian, P. Y. (1997). Combined effects of salinity, temperature and food on early development of the polychaete *Hydroides elegans*. *Mar. Ecol. Prog. Ser*. **152**, 79-88.

Reid, P. and Beaugrand, G. (2012). Global synchrony of an accelerating rise in sea surface temperature. *J. Mar. Biol. Assoc. U.K.* **92**, 1435-1450.

Rijnsdorp, A. D., Peck, M. A., Engelhard, G. H., Mo, C. and Pinnegar, J. K. (2009). Resolving the effect of climate change on fish populations. *ICES. J. Mari. Sci.* **66**, 1570–1583.

Schiel, D. R., Steinbeck, J. R. and Foster, M. S. (2004). Ten years of induced ocean warming causes comprehensive changes in marine benthic communities. *Ecology.* **85**, 1833–1839.

Smale, D. A, Wernberg, T., Peck, L. S. and Barnes, D. K. A. (2011). Turning on the heat: ecological response to simulated warming in the sea. *PLoS One*. **6**, e16050.

Smale, D. A., Taylor, J. D., Coombs, S. H., Moore, G. and Cunliffe, M. (2017). Community responses to seawater warming are conserved across diverse biological groupings and taxonomic resolutions. *Pro. R. Soc. Lond. B. Biol. Sci.* **284***,* 20170534.

Somero, G. N. (2002). Thermal Physiology and Vertical Zonation of Intertidal Animals : Optima , Limits , and Costs of Living. *Integr. Comp. Biol.* **789***,* 780–789.

Somero, G. N. (2010). The physiology of climate change : how potentials for acclimatization and genetic adaptation will determine " winners " and " losers ". *J. Exp. Biol.* **213***,* 912–920.

Sørensen, J. G. and Loeschcke, V. (2007). Studying the stress responses in the post-genomic era: it's ecological and evolutionary role. *J. Biosci*. **32**, 447-456.

Truebano, M., Burns, G., Thorne, M. A. S., Hillyard, G., Peck, L. S., Skibinski, D. O. F., & Clark, M. S. (2010). Transcriptional response to heat stress in the Antarctic bivalve *Laternula elliptica*. *J. Exp. Mar. Biol. Ecol*. **391**, 65–72.

Turner, J., Lu, H., White, I., King, J. C., Phillips, T., Hosking, J. S. et al. (2016). Absence of 21st century warming on Antarctic Peninsula consistent with natural variability. *Nature*. **535**, 411–415.

Tytgat, B., Verleyen, E., Obbels, D., Peeters, K., De Wever, A., D'hondt, S., De Meyer, T., Van Criekinge, W., Wyverman, W. and Willems, A. (2012). Bacterial diversity assessment in Antarctic terrestrial and aquatic microbial mats: a comparison between bidirectional pyrosequencing and cultivation. PLoS. ONE. **9**, e97564.

Sørensen, J. G. and Loeschcke, V. (2007). Studying the stress responses in the post-genomic era: it's ecological and evolutionary role. *J. Biosci*. **32**, 447-456.

Venebles, H. J. and Meredith, M. P. (2014). Feedbacks between ice cover, ocean stratification and heat content in Ryder Bay, western Antarctic Peninsula. *J. Geophys. Res. Oceans*. **119**, 5323-5336. Walther, G., Post, E., Convey, P., Menzel, A., Parmesan, C., Beebee, T. J. C. et al. (2002). Ecological responses to recent climate change. *Nature.* **416***,* 389–395.

Wernberg, T., Smale, D. A. and Thomsen, M. S. (2012a). A decade of climate change experiments on marine organisms : procedures , patterns and problems. *Glob. Change. Biol.* **18***,* 1491–1498.

Wernberg, T., Smale, D. A., Tuya, F., Thomsen, M. S., Langlois, T. J., Bettignies, T. De, Bennett, S. and Rousseaux, C. S. (2012b). An extreme climatic event alters marine ecosystem structure in a global biodiversity hotspot. *Nat. Clim. Change*. ***3***, 78–82.

Whalan, S. and Webster, N. S. (2014). Sponge larval settlement cues: the role of microbial biofilms in a warming ocean. *Sci. Rep.* **4**, 4072.

Chapter 2

General Materials and Methods

2.1 Abstract

The experimental basis of this thesis is the use of a novel technology heated settlement panels, designed by the engineering department at the British Antarctic Survey (High Cross, Madingley road, Cambridge, CB3 0ET). These panels are capable of recreating end of century oceanic warming predictions (IPCC, 2014) *in situ* and were originally deployed by Dr. Gail Ashton during the Austral summer of 2014 at Rothera Research Station. As discussed previously, Dr Gail Ashton was responsible for setting up the heated panel experiment in Rothera, monitoring the panels and describing the community compositions, growth rates and competitive interactions. Chapters 3, 4 and 5 in this thesis are based on this experimental set-up. Chapter 6 is based on an independent experimental set up using the same heated settlement panels on a temperate ecosystem, the Menai Strait (UK). Given the differences in the experimental set up between the sites, this general material and methods chapter aims to compare the methodologies for both systems and highlight differences in the deployment of the panels and the experimental protocols used. Furthermore, this chapter will discuss potential improvements that could be made to the heated settlement panels and additional capabilities that could be explored.

2.2 Panel design

Heated panels were designed by the engineering department at the British Antarctic Survey (High Cross, Madingley road, Cambridge, CB3 0ET). Cables were purchased from Scorpions Oceanic Ltd (Park Farm, Great Chesterford, Saffron Walden, Essex CB10 1RN, United Kingdom). A heating element was embedded in a PVC block allowing the temperature on the panel surface to be regulated using power supplied to the panel. By keeping the power supply constant to the panels, the resulting temperature increase at the surface of the panel is also constant. The thickness of the layer of water warmed to the same temperature as the panel surface varies with the flow rate of water across the panel. Trials in a flume system showed it is always more than 1.5 mm and can be as much as 3-5 mm in low flow conditions (Peck, pers. comm.).

The power necessary to uniformly warm the experimental panel surface was calibrated prior to deployment (14.2V and 20.1V for +1°C and +2°C of warming respectively). The degree of warming was accurate to within 0.2°C at a distance of 1mm from the panel surface at flow rates up to 2cm sec^{-1} (Figure 2.1.). This created a water layer of >2mm from the surface with uniform heating in the accuracy of ±0.03°C (S.E.) and no animal grew beyond the 2mm layer for the duration of this experiment. The extent and evenness of warming was rigorously verified both in a flow flume during the design phase and in aquaria after the deployment.

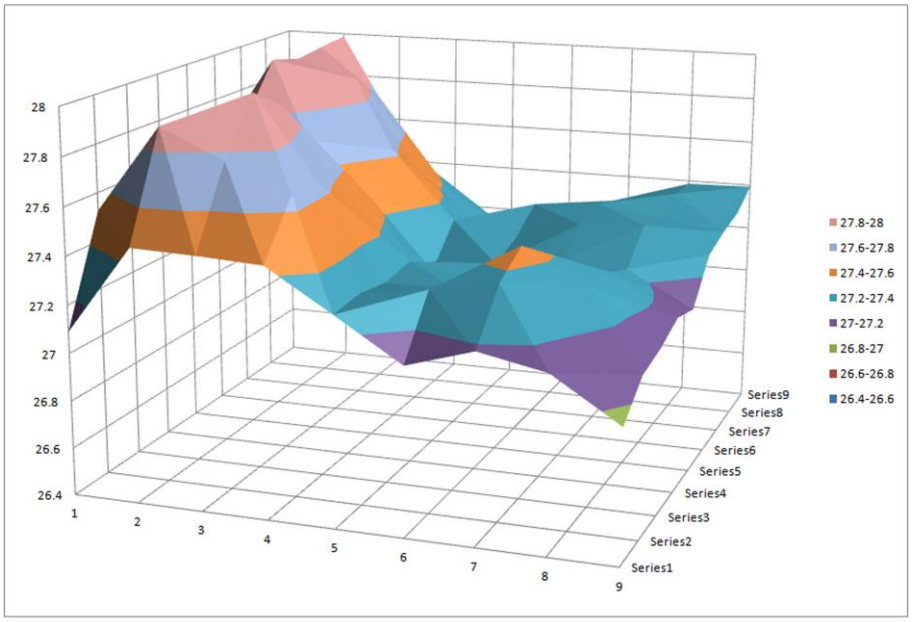

Figure 2.1. Surface temperature vs distance above the panel from calibration trials during panel development.

2.3 Panel deployment: Sites and methodology

2.3.1 Antarctic deployment sites

Panels at Rothera Research Station were deployed in 3 sites: South Cove (Biscoe Wharf), North Cove and Hangar Cove (See Figure 2.2). Hangar Cove panels were heavily grazed by urchins and as such, these panels were excluded from any further analysis. For the purpose of this thesis, only panels on the South Cove and North Cove sites were used. South Cove panels were used to investigate acclimation and the heat shock response in the encrusting worm *Romanchella perrieri* in Chapter 3. South Cove panels were also used in Chapter 4 in an RNA-seq approach and population genetic study in the other encrusting worm *Protolaeospira stalagmia*. North Cove panels were used to compare the upper thermal limit of *Romanchella perrieri* worms maintained in the natural environment (North Cove) vs aquaria (South Cove) in Chapter 3. These panels were also used in the biofilm analysis in Chapter 5.

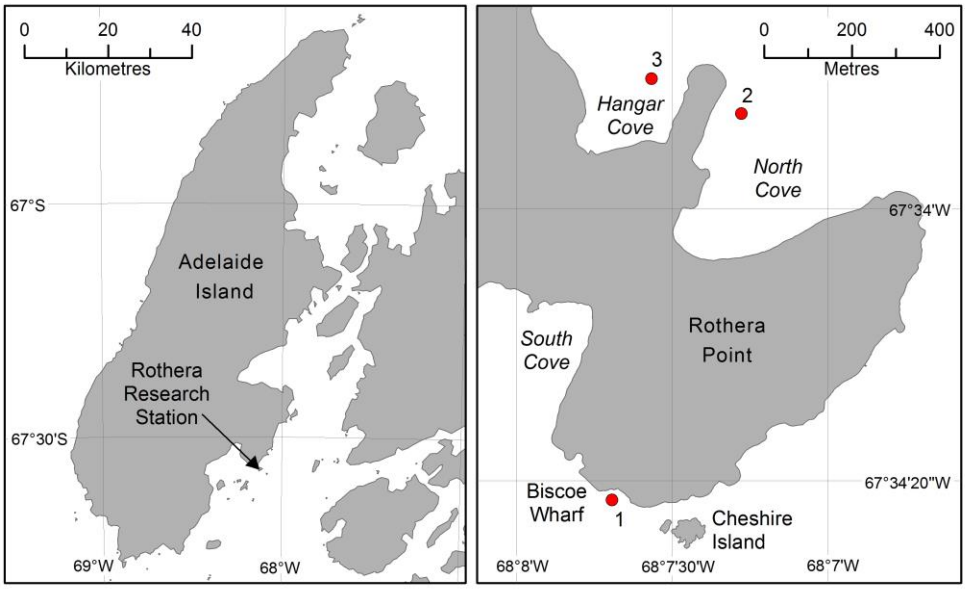

Figure 2.2. Deployment sites of Antarctic panels. 1 = Biscoe Wharf (South Cove panels), 2 = North Cove panels and 3 = Hangar Cove panels.

2.3.2 Menai Strait deployment sites

Panels in the Menai Strait were deployed at one site near Ynys Faelog Island in a fan shape design (Figure 2.3). The data from these panels was used in Chapter 6. Site selection was restricted by the requirement for close proximity to a power supply, in this case the SEACAMS building located on Ynys Faelog Island, Menai Bridge, UK (Marked with an X). Furthermore, the site needed to be easily accessible by boat and away from strong currents to enable monthly photographing of panels. This project was excluded from the need for a permit from the Marine License Team, Natural Resources Wales.

Figure 2.3. Deployment site of steel frames numbered 1-4 near Ynys Faelog Island, Menai Bridge, UK. Each frame contained three panels. The power supply used to heat the panels was located on the SEACAMS building, marked with an X.

2.3.3 Comparison of the panel deployment methodologies

Panels at Rothera Research Station were deployed using SCUBA at a depth of 15m. One replicate of each treatment (Control, +1C and +2C) was deployed on each of 4 concrete slabs in a random block design, secured in place using an elastic cord (n = 12 panels total) (Figure 2.4.)

Figure 2.4. Photograph of concrete slabs and panels deployed at 15m at Rothera Research Station.

Due to HSE diving regulations and the lack of qualified diving personnel, panels in the Menai strait were not deployed via SCUBA. In contrast, four panel arrays were mounted onto a cross-shaped tubular steel frame with anchor points and a central rope (Figure 2.5 B). Up to three panels (150x150x4mm) could be mounted onto an acrylic base plate (750x250x4mm) (Figure 2.5 A) and held in place by a plastic frame. This was known as an array. A 20mm gap was left between the upper surface of the base plate and the lower surface of the settlement panel making the surface of the plates less accessible to larger grazing and predatory macrofauna.

Panel treatment (control, +1°C, +2°C) was randomly distributed around the array. The tubular steel acted as an anchor and each steel frame was attached to a mooring rope that followed the cables back to land, where it was attached to a steel pole. Due to the strength of the flow through the Menai Strait and the risk of equipment loss due to the latter, only three panels (one each of 1°C, 2°C and control) were attached at random to each frame. This was to ensure that the loss of any single frame would not negatively impact data collection. The rest of the spaces were left empty. Panels were deployed at a depth of 10m below lowest tide and 50-100m from the bank to ensure minimal disturbance to the panels from waves and anthropogenic activities.

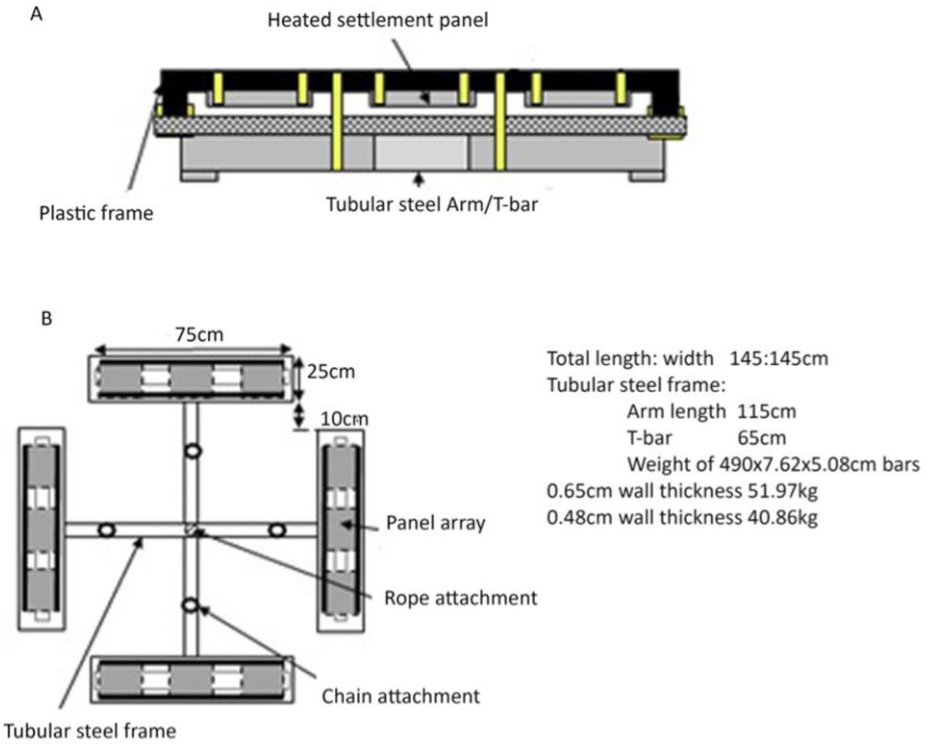

Figure 2.5. Designs of arrays and streel frames. A: Side view of an array which can hold up to three panels. B: Steel frame which compromises four arrays

On both the Antarctic and Menai strait panels, cables were protected by a 50mm diameter plastic conduit in the intertidal and shore line regions. On both sites panels were connected to a shore-based (mains supplied) control unit via a 100m cable. On the Antarctic panels, power supply to each cable (and thus panel) was controlled using resistors within the unit and verified using an inline voltmeter. Indicator lights within the control unit were monitored 1-2 times per week, up to once a month depending on weather conditions, to confirm continuance of the power supply. On the Menai strait panels, power was supplied using a shore-based mains supply located in the SEACAMS building (School of Ocean Sciences Bangor University, Menai Bridge, Anglesey, LL59 5AB, UK) with a transformer. Current and voltage were monitored 1-2 times per week to confirm correct continuance of the power supply and thus, *in situ* temperatures.

2.4 Panel Monitoring

Panels on both the Antarctic and Menai strait sites were photographed regularly for the duration of the experiment (Table 2.1). In the Antarctic, South Cove panels were not monitoring from July 2014 to October 2014 due to adverse weather conditions. Furthermore, South Cove panels were brought back to an aquarium holding on the 13/03/17 due to the panel site being destroyed by an iceberg impact. After this, the panels were maintained in through flow aquaria with seawater supplied at background ambient temperature for the duration of the experiment (9 months).

Table 2.1. Sites and dates the Antarctic panels were deployed, photographed and retrieved/sampled.

Site	Deployment date	Photographed	Retrieved and sampled
North Cove	29/01/14	31/03/14	20/02/16
		23/05/14	
		27/08/14	
		19/12/14	
		23/01/15	
		19/03/15	
		08/01/16	
		20/02/16	
South Cove	17/07/14	23/10/14	13/03/15
		25/11/14	
		05/01/15	
		09/02/15	
		13/03/15	
Put in aquarium			
		15/05/15	19/12/15
		08/08/15	
		09/24/15	
		10/11/15	
		19/12/15	

In the Menai Strait, panels could not be deployed continuously for 13 months and separate trials were run in Summer, Autumn, Winter and Spring. This was to preclude any organisms growing beyond the heated layer. Panels that were deployed during the Winter period (December-March) were only photographed at the start and end of the deployment, due to low recruitment and slow growth during the winter months (Table 2.2).

Table 2.2. Season and date the Menai Strait panels were deployed, photographed and sampled.

Deployment Season/year	Deployment date	Photographed	Retrieved and sampled
Summer 15	05/06/15	15/07/15 06/08/15 02/09/15	02/09/15
Autumn 15	10/09/15	26/10/15 24/11/15	24/11/15
Winter 15/16	26/11/15	05/04/16	05/04/16
Spring 16	07/04/15	05/05/16 03/06/16	03/06/16
Summer 16	06/06/16	20/07/16	20/07/16

Antarctic panels were monitored *in situ* by SCUBA divers via photography using a Nikon D7000 with a 60mm macro lens. The elastic cord securing the panel to the seabed was removed and the panel was turned over so that the experimental surface was facing up. A sliding frame was used to keep the camera lens at a constant distance from the panel to ensure images were captured on optimum settings and to assist with image analysis. Each image captured approximately 3.5x2.5cm of the panel; more than 25 overlapping images of each panel were taken on each sampling event so that the entire panel surface was captured at least once. The sampling took approximately 5min for each panel, after which time the panel was turned over and secured in place using the elastic cord.

In the Menai Strait panels, the lack of SCUBA diving capability and resources precluded the panels to be photographed *in situ*. Instead, steel frames (n=4) containing the panels were lifted from the seabed to the side of a boat and brought to the shore near the sampling sites, but held under water at all times. The plastic frame securing the panels to the array was removed and the panels were moved onto an *in situ* tank filled with filtered sea water. Panels were turned over so that the experimental surface was facing up and photographs of the associated fauna were taken. Following image capture of all panels the arrays were reattached to the frame and the frames returned to the relevant site. Throughout the whole process panels were kept underwater at all times.

Both Antarctic and Menai Strait panels were photographed using a Nikon D7000 with a Nauticam Nikon D7000 Underwater housing and a 60mm macro lens. The underwater housing was fitted on to a sliding frame that in turn was rested on the panel, thus keeping the camera lens at a constant distance from the panel. The camera was slid across the panel to a series of roughly predetermined positions, and a total of 24 photographs or more (lens focal ratio 1:2) were taken per panel, with a 50% overlap between image. Each photograph captured approximately an area of 3.5-2.5cm of the panel. Photographs were taken in both RAW and JPEG formats and were subsequently merged in to a single image using Photoshop CS5. Images were cropped to the central 9.8 x 9.8cm heated area of each panel. A flowchart summarising the deployment and monitoring methodologies for both Antarctic and Menai Stait panels can be visualised in Figure 2.6.

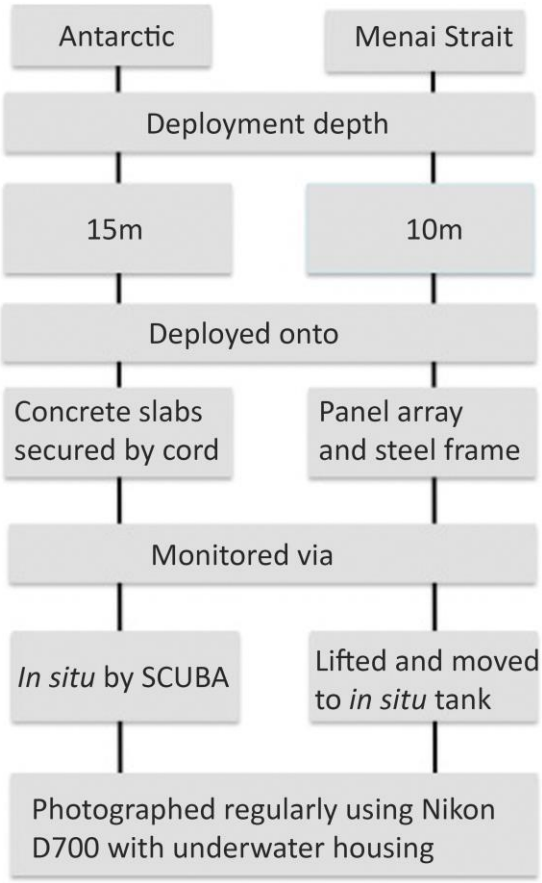

Figure 2.6. Panel deployment and panel monitoring methodology flowchart comparing the Antarctic and Menai Strait panels

2.5 Panel performance

As discussed previously, the power necessary to uniformly warm the experimental panel surface was calibrated prior to deployment (14.2V and 20.1V for +1°C and +2°C). Indicator lights using the control unit (in the Antarctic panels) and current and voltage (in the Menai Strait panels) were monitored 1-2 times a week to confirm correct continuance of the power supply and thus, *in situ* temperatures. To further ensure the panels were performing to the correct temperatures, surface panel temperature readings using a precision RTD handheld data logger thermometer (accuracy of ±0.5°C) of six panels from South Cove (2 of each Control, +1°C and +2°C) held in aquaria were taken in February 2016. The Control panels were at 0.8°C (±0.5°C), the +1°C panels were heating to 1.8 °C (±0.5°C) and the +2°C panels were heating to 2.8°C (±0.5°C) (Figure 2.7). Panels were therefore heating to the expected temperatures when compared to the control: +1°C and +2°C respectively. These data further support the weekly monitoring of the panel power supply indicating the panels were heating to the calibrated temperatures.

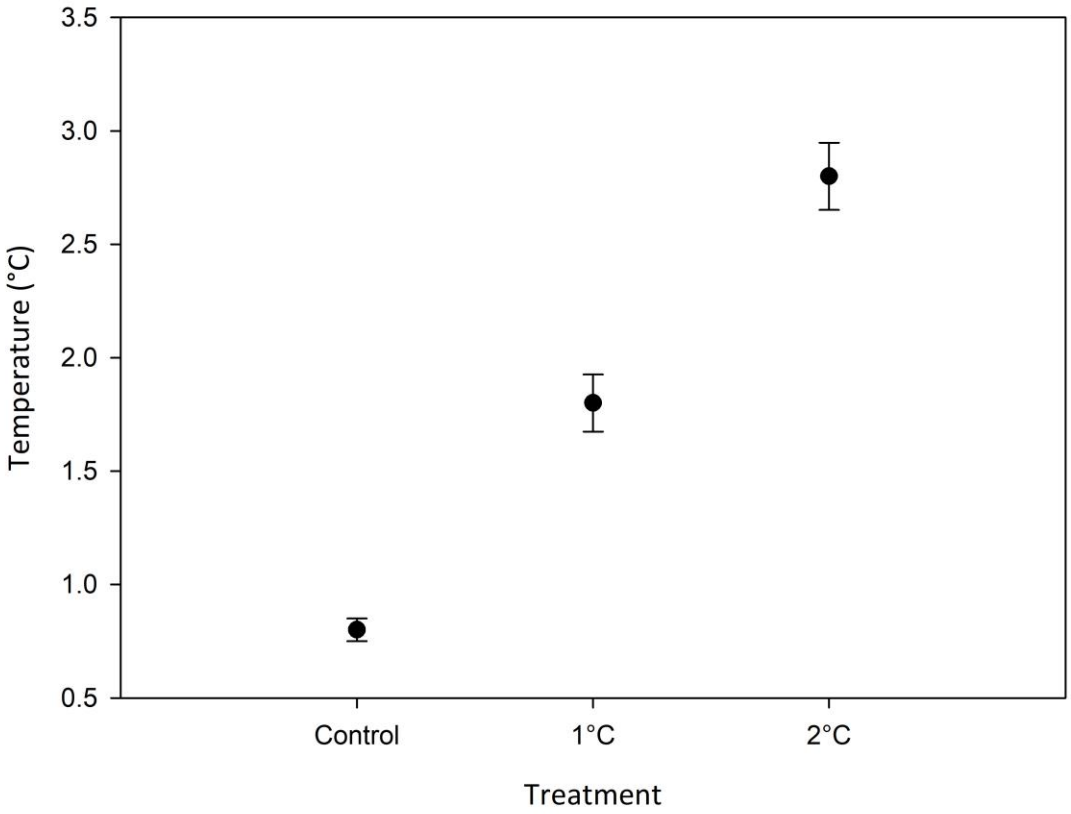

Figure 2.7. Mean ± SE surface panel temperatures (°C) for the different panel treatments (Control, +1°C, +2°C) recorded from South Cove panels

In the Menai strait, three iButton thermal loggers (accuracy of ±1°C) were placed on the heated surface of three panels (one of each +1°C, +2°C and control) and deployed at the experimental site on September 2016 (for 3 months) to further verify the extent of warming on the panel surfaces. The iButton sensor was within the heated layer and the iButtons were programmed to record the temperature every hour. One of the iButton sensors stopped recording data after 2 weeks and as such only the first 2 weeks of data have been plotted. The Control panel was at 16.4°C (±1°C), the +1°C panel was heating to 17.7 °C (±1°C) and the +2°C panel was heating to 18.8°C (±1°C) (Figure 2.8). Panels were therefore heating to 1.3°C and 2.4°C in comparison to the control. These differences compared to the temperatures observed in the Antarctic panels could be due to the accuracy of the iButton thermal loggers (accuracy of ±1°C). As discussed previously, the panels were calibrated to the correct voltage (14.2V and 20.1V for +1°C and +2°C) and were monitored weekly to ensure they were heating to the calibrated temperatures.

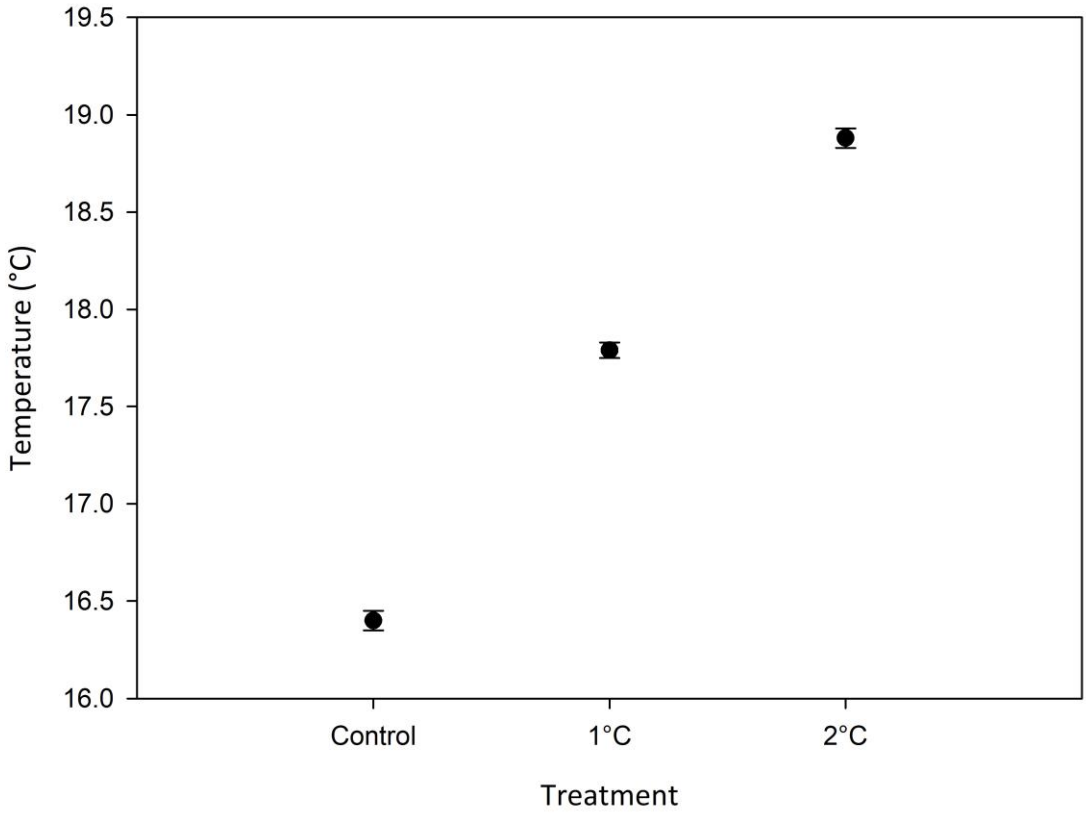

Figure 2.8. Mean ± SE surface panel temperatures (°C) for the different panel treatments (Control, +1°C, +2°C) recorded from panels in the Menai Strait

2.6 Improvements and additional capabilities of the panels

A major limitation of the heated settlement panels is the lack of an embedded thermal logger within the panels capable of monitoring experimental temperatures continuously. Although the panels have been calibrated to the correct voltage that ensures *in situ* temperatures (monitored weekly) and the temperature readings taken from the Antarctic and Menai Strait panels supported the weekly monitoring, future versions of the heated settlement panels should consider re-designing these to include an embedded temperature logger. The temperature readings provided by the embedded logger would then be monitored along with the voltage weekly. This would provide further assurance that the panels are in fact heating to the correct temperatures.

As discussed previously, the panels warm a 2mm layer of water, making deployments in temperate environments such as the Menai Strait challenging. Although panels cannot be deployed long term in temperate ecosystems as organisms will quickly grow beyond the 2mm layer, they can be deployed in short-term experimental periods successfully (please refer to Chapter 6 in this thesis for further detail). These short term deployments do however, preclude studying long-term growth and assemblage development of individual organisms across time. This can be studied by deploying panels in Antarctic ecosystems, where the slow growth rate of organisms (Clarke et al., 2003) allows for panels to be deployed for an extended period of time (See Ashton et al., 2017).

Heated settlement panels could be applied to other fast warming ecosystems such as the Arctic and tropical ecosystems (with limitations). Heated settlement panels could also be used to answer much broader questions beyond the ones explored in this thesis, some of which are explored further in Chapter 7 e.g. Heated settlement panels can be used to answer questions about how changes in temperature modulate toxicity of chemical contaminants, they can be used to test anti-fouling compounds etc. Nevertheless even with their limitations, heated settlement panels prove to be a useful technology capable of recreating end of century oceanic warming predictions *in situ* (IPCC, 2014) and can be successfully used in the field.

2.7 References

Ashton, G. V., Morley, S. A., Barnes, D. K. A., Clark, M. S. and Peck, L. S. (2017). Warming by 1°C drives species and assemblage level responses in Antarctica's marine shallows. *Curr. Biol*. **27**, 2698–2705.

Clarke, A. and Johnston, N. M. (2003). Antarctic marine benthic diversity. *Oceanogr. Mar. Biol. Ann. Rev.* **41**, 47-114.

IPCC. (2014). Climate Change 2014 Synthesis Report Summary for Policymakers.

Chapter 3

Acclimation capacity and the heat shock response in the Antarctic spirorbid worm *Romanchella perrieri*

3.1 Abstract

Antarctic marine organisms have evolved in one of the coldest and most temperature stable marine environments on Earth. As such, they have very poor acclamatory abilities, requiring at least 2-5 months to acclimate to small temperature rises. Acclimation and responses to environmental change can be measured at the physiological level via upper thermal limit experiments but the ability to predict the vulnerability of a species to environmental stress is best achieved at the molecular level, as sub-lethal effects can be quantified more readily. The heat shock response (HSR) has been suggested as a suitable biomarker of environmental stress and a key predictor of the vulnerability of a species to changing conditions. In this study acclimation success of an Antarctic spirorbid polychaete, *Romanchella perrieri* at +1°C and +2°C above ambient conditions over a period of 18 months was measured via upper thermal limit (UTL) and heat shock experiments. *R. perrieri* individuals were most resistant to acute thermal challenge in the control treatment, followed by those in the +1°C and +2°C. The expression of HSP70 family members was surveyed via quantitative PCR after an acute heat shock response (2h) at 15°C and a long term heat shock response (30 days) at 4°C. The long term heat shock at 4°C for 30 days showed a significant down-regulation of *hsp90* in the +1°C and +2°C heated panels ($P < 0.05$) and no significant up-regulation or down-regulation of *hsp60* and *hsp70* in either of the panel treatments (+1°C, +2°C and control). This study suggests that *R. perrieri* did not acclimate to the heated temperatures, even though the time-scale was much longer than any previously identified as necessary for the acclimation of Antarctic marine invertebrates. Previous laboratory experiments on other Antarctic marine invertebrates have shown the lack of the classical heat shock response in Antarctic organisms. However in this study, the lack of acclimation in the species might explain the lack of a heat shock response. The data here indicate that *Romanchella perrieri* has a very poor capacity to acclimate to warming of even 1°C and is unable to cope with predicted end of century oceanic warming (IPCC, 2014).

3.2 Introduction

Antarctica has experienced some of the fastest rates of warming on the planet, where shallow seawater temperatures along the Western Antarctic Peninsula (WAP) rose 1°C during the last half of the 20th century (Meredith and King, 2005; Turner et al., 2017). Antarctic marine organisms are suggested to be particularly vulnerable to these changes in temperature, due to their highly stenothermal nature (Peck et al., 2009a). For example, the brittle star *Ophionotus victoriae* is unable to survive long term at 2°C, just 2.5°C above mean annual temperatures (Peck et al., 2009b). Acclimation and physiological flexibility have been proposed as the most important mechanisms that will dictate the success or the failure of polar species in future climate change scenarios (Somero, 2010). This is based on the premise that genetic adaptation in such long-lived species will not be rapid enough to enable the animals to cope with the current rate of change. Acclimation is defined as the change from one stable physiological state to another stable physiological state in experiments when conditions are altered (Schmidt-Nielsen, 1990).

Antarctic marine organisms have very poor acclimatory capacities (Peck et al., 2014). In a study by Peck et al. (2010), 6 species of Antarctic invertebrates were subjected to acclimation trials at 3 °C for 60 days: 5 out of 6 species failed to acclimate to temperatures only 1-2°C above current summer maxima. Furthermore studies examining the long-term (beyond 60 days) acclimation abilities of Antarctic marine species report that they require at least 2-5 months to acclimate to even small temperature rises. For example, Morley et al., (2011) reported that the Antarctic limpet *Nacella concinna* took 9 months to acclimate to 2.9°C. To date all of these acclimation studies have been carried out in aquaria and whilst extremely useful for understanding physiological mechanisms, relative sensitivities and resilience of species, they do not exactly mimic natural environmental conditions, a gap that this study attempts to address.

Our current understanding of the mechanisms limiting species exposed to elevated experimental temperatures centres around limitations to physiological capacities (Pörtner et al., 2002; 2007). The oxygen limitation hypothesis (Pörtner, 2002) suggests that a drop in aerobic scope is the first mechanism to limit survival at low and high ends of the thermal envelope, involving a mismatch between oxygen demand and supply to the tissues. This limits the capacity of the circulatory and ventilator systems, leading to organism failure. Physiological studies have identified the thermal limits and changes in metabolism in response to temperature and oxygen availability (Pörtner et al., 2002; 2006; 2007) using ramping experiments such as upper thermal limits (UTL) (Peck et al.,

2009a). The UTL is defined as the temperature at which mortality of the experimental organisms reaches 50% and is used as a way of measuring whether acclimation has occurred (Bilyk & Devries, 2011). This is because, as Peck et al., (2010) suggests, if acclimation occurs, then responses to altered temperatures at the whole animal level should change the temperature tolerances of the organisms studied (Brett, 1956; Schmidt-Nielsen, 1990, Jumbam et al., 2008; Tomanek, 2008). Furthermore, an analysis of the relationship between upper temperature limits and the rate of temperature change allows for an estimation of the long-term survival potential of communities (Peck et al., 2009a; Richard et al., 2012). This has been recognised for over 70 years (Fry et al., 1942; Pörtner et al., 2007; Peck et al., 2010) and is a commonly used metric to evaluate whole-animal acclimation.

Although responses to environmental change can be measured at the physiological level as described above, the ability to predict the vulnerability of a species to environmental stress is best achieved at the molecular level, as sub-lethal effects can be quantified more readily (Truebano et al., 2010). In this context, the heat shock response (HSR) has been suggested as a suitable biomarker of environmental stress (Feder & Hofmann, 1999) and a key predictor of the vulnerability of a species to changing conditions. Exposure to external stressors results in the unfolding of proteins, the activation of the HSR and the production of heat shock proteins (Hsps). These highly conserved proteins act as chaperones to stabilise and refold denatured proteins, maintaining the functioning of the cell (Parsell and Lindquist, 1993). The most studied family members are the 70kDa proteins (Hsp70s), comprised of constitutive (Hsc70) and inducible forms (Hsp70) (Ritossa 1962).

The HSR in Antarctic marine organisms often differs to that of temperate species, in that the classical heat shock response involving a strong up-regulation of Hsp70 production in response to environmental challenge, such as heat is sometimes absent in Antarctic species. In the Antarctic notothenoid fish *Trematomus bernacchii* (Hofmann et al., 2000) this lack of up-regulation is due to a mutation in the promoter region of the gene (Buckley et al., 2004) and although these genes are present in the sea star *Odontaster validus* they also did not present a discernable heat shock response under experimental warming (Clark et al., 2008c). However, in the laboratory some Antarctic marine invertebrates expressed these genes, but only at temperatures far higher than those experienced by the species in their natural environment. Clark et al., (2008b) reported the expression of the inducible *hsp70* gene in the Antarctic clam, *Laternula elliptica* at temperatures between 8-10°C. Similar findings were reported in the limpet *Nacella concinna*, with the

expression of *hsp70* gene family members at 15°C (Clark et al., 2008b). However, studies in *N. concinna* showed that although animals in laboratory warming experiments did not increase HSR expression until 15°C, this did occur at much lower temperatures under natural conditions and in response to a variety of stresses including emersion in the intertidal zone (Clark & Peck, 2009a; Clark et al., 2008c). Such findings highlight the importance of evaluating the HSR under both laboratory and natural conditions.

In the first study to evaluate the acclimation to *in situ* warming, heated settlement panels were deployed for a period of 18 months in Ryder Bay near Rothera research station on the Antarctic Peninsula. This timescale is well above that required for acclimation in Antarctic marine invertebrates (Peck et al., 2014). The panels were set to heat a thin layer of water overlying the surface to 1°C or 2°C above ambient temperature, thus mimicking oceanic warming predictions in the natural environment and yet maintaining natural cycles of temperature variation, light regime, food supply etc. To match the local predictions for the area, a third treatment was introduced, a +1°C that was switched off during the winter period, as winter temperatures at this site will still fall to -1.8°C in the end of century scenarios (Barnes pers comm).

Ashton et al., (2017) describes one of the main benthic colonisers in the area, the spirorbid worm *Romanchella perrieri*, which performed better in terms of growth rates and settlement success under the experimental warmer regimes. Individuals growing on +1°C treatments were on average 70% larger than those in the control treatments. Although seemingly performing well, the main question arising given this data is whether the organisms were maintaining their growth rate at the expense of their physiology i.e. have they acclimated to the experimental temperatures or not. *Romanchella perrieri* is a marine encrusting worm belonging to the Spirorbinae subfamily, highly abundant on the sublittoral coasts of Antarctica. It's distribution spreads as far south as the shore in Patagonia but it is again exclusively sublittoral (on shells, crustaceans carapaces or bryozoans) in the few places where it has been found north of the antiboreal convergence (Knight-Jones et al., 1984). To date, there are no descriptions of the thermal limit or acclimatory capacities of the species.

This is the first study to evaluate the acclimation of an Antarctic marine invertebrate, the spirorbid polychaete *Romanchella perrieri* under *in situ* warming using heated settlement panels. I measured the UTL and conducted Q-PCR of Hsps to determine acclimation success at +1°C and +2°C above ambient conditions over a period of 18 months. Two main questions were asked: 1)

Have the organisms acclimated to the experimental temperatures or are they physiologically resisting the change? 2) Does *Romanchella perrieri* have a heat shock response and if so, how does it differ between treatments?

3.3 Methods

Two independent experiments were carried out to investigate the heat shock response in *R. perrieri.* An initial heat shock was carried out on wild *R. perrieri* to assemble a transcriptome and identify heat shock proteins (Hsps) in this species. A subsequent thermal limit experiment was carried out on heated/non-heated panels deployed at South Cove colonised by *R. perrieri* to assess acclimation of the animals to predicted future oceanic warming temperatures. The same thermal limit experiment was carried out on heated/non-heated panels from a second site in North Cove, Rothera point to assess whether acclimation of *R. perrieri* was affected by the South Cove panels being partially maintained in through flow aquaria with seawater supplied at background ambient temperature for 9 months. The aquarium holding period was required because the South Cove panel site was destroyed by an iceberg impact. The panels were rescued and maintained in an aquarium for 9 months over the Antarctic winter to enable comprehensive sampling of the panels in the following summer. Heat shock experiments were also performed on heated/non-heated panels deployed at North Cove colonised by *R. perrieri* to assess the heat shock response (HSR) in this species using Q-PCR on Hsps previously identified from the transcriptome data.

3.3.1 Identification of heat shock proteins in Romanchella perrieri

3.3.1.1 Stock population

Rocks colonised by *R. perrieri* were collected by SCUBA divers between 18 and 25m water depth in January 2014 at Rothera Research Station, Adelaide Island, Antarctic Peninsula (67° 4' 07" S, 68° 07' 30" W). Animals were immediately transferred, underwater at all times to the laboratory and maintained in a flow-through aquarium at ambient temperature, under a 12:12 simulated natural light: dark cycle. Animals were transferred to the British Antarctic Survey aquarium facilities in Cambridge, UK and were habituated to aquarium conditions for 6 months (closed water system at water temperature and salinity of 0 ± 0.5°C and 35 ± 3.8ppt respectively, 12:12 h light: dark) prior to experimentation.

3.3.1.2 *Heat shock*

To maximise the identification of heat shock proteins in *R. perrieri*, 2 different temperatures were used: acute (15°C for 2 hours) and chronic (+4°C for 30 days). To induce acute heat shock response, rocks (n=3) colonised by *R. perrieri* were exposed to a thermal shock by immediate

transfer to seawater: 15°C for 2 hours. Animals kept at 0°C were used as controls. Post experimental treatment, individuals (n=12) were dissected from their outer calcified skeleton under low power microscopy (10x), snap frozen in liquid nitrogen and stored at −80°C prior to RNA extraction. To induce a chronic heat shock response, a single rock colonised by 60 *R. perrieri* was transferred to a 60 L jacketed acrylic tank (Engineering Design and Plastics, Cambridge, Cambs.) attached to a LTD20G thermocirculator (Grant instruments Ltd, Shepreth, Cambs.) and exposed to +4°C sea water for 30 days. As a control, another rock colonised by 50 *R. perrieri* was kept in a 60 L jacketed tank with aerated sea water at the same temperature as the main stock aquarium and field (0°C) for 30 days. Water temperature was checked twice a day for the duration of the experiment. After this period, 12 individuals were selected at random from both treatments and the controls and dissected as described previously, snap frozen in liquid nitrogen and stored at −80°C prior to RNA extraction.

3.3.1.3 RNA extraction and sequencing

Total RNA was extracted from the whole organism using ReliaPrep TM RNA Miniprep Systems (Promega) according to manufacturer's instructions. RNA samples were assessed for concentration and quality using a NanoDrop ND-100 Spectrometer (NanoDrop Technologies) and an Agilent 2200 Tapestation (Agilent Technologies). RNA of equal quantities from 6 individuals were pooled for each experimental treatment to make a total of 4 libraries (0°C for 2 hours, 15°C for 2 hours, 0°C and 4°C for 30 days). Library preparation and sequencing was carried out by the Department of Biochemistry at the University of Cambridge. For each pool, RNA was converted to a sequencing library using the Illumina TruSeq stranded mRNA-seq library Prep kit (RNA input 1ug, fragmentation time 8 min, 10 PCR cycles), and barcoded libraries were pooled and sequenced on an Illumina MiSeq using 300 base paired-end reads, to generate 25 million raw reads per pool.

3.3.1.4 Bioinformatic analysis

All analyses were carried out using default parameters unless otherwise specified. Adapters were trimmed from the raw reads using Trimmomatic v.0.33 (Bolger et al., 2014). The reads were further trimmed based on quality and length using Fastq-mcf v.1.04.636 (Aronestry, 2011). The Phred quality score was set to 30 and minimum read length to 80 bp. The reads were normalised *in silico* with different coverage values and contigs were assembled using Trinity v.2.0.6 (Grabherr et al., 2013), with the SS_lib_type_parameter set to RF to match the stranded library construction.

Contigs were assembled using *de novo* mode. The read alignment bam file for input to the Trinity genome guided mode was generated using TopHat v.2.0.13 (Kim et al., 2013) and sorted using SAMtools v.1.1 (Li et al., 2009). All protein similarity searches were carried out using BLAST (blastx or blastp) v.2.2.30 (Altschul et al., 1990) with an E-value cutoff less than l e^{-10} against SwissProt (17 January 2017). The BLAST results were summarized based on the best sequence similarity match for each transcript.

3.3.2 Heat shock experiments on the panels

3.3.2.1 Upper lethal limits

1 panel per treatment (1 each of control, +1°C, +2°C, seasonal) from South Cove and North Cove sites (3 panels in total from South Cove and 3 panels in total from North Cove) colonised by *R. perrieri* were transferred to a 60 L jacketed tank with aerated sea water at the same temperature as the ambient sea water (0°C) and connected to a thermocirculator (Grant LTD 20g, Grant Instruments Ltd, Cambridge, UK). The temperature was raised at the rate of 1°C h^{-1} (Peck et al., 2014). When the animals no longer responded to tactile stimuli (n=25 per panel, per treatment), it was considered that the upper thermal limit had been reached and the temperature for each animal was noted. The Upper Thermal Limit (UTL) was considered as the temperature at which mortality of the experimental animals reached 50%. It must be noted that although the UTL of 25 *R. perrieri* per panel, per treatment was measured, only one panel per treatment was used i.e. the unit of replication for the panel was one. This was due to limitations in the number of panels available for further heat shock experiments and population genetic analysis in Chapter 5.

3.3.2.2 Thermal shocks

The same aquarium system was used to assess response to thermal shocks. Panels (1 each of control, +1°C, +2°C, seasonal) from South Cove colonised by *R. perrieri* were transferred to 15°C sea water for 2h. Specimens of *R. perrieri* (n=12) were then dissected and snap frozen in liquid nitrogen. A subset of panels (1 each of control, +1°C, +2°C, seasonal) were transferred directly to 4°C sea water for 30 days. At the same time, a set of control panels (1 each of control, +1°C, +2°C, seasonal) were kept in 60 L jacketed tank with aerated sea water at the same temperature as the main stock aquarium (0°C) for both 2h and 30 days. Post the experimental treatment period the *R.*

perrieri (n=12 per panel, per treatment) were dissected, snap frozen in liquid nitrogen and stored at −80°C prior to RNA extraction.

3.3.3 RNA extraction and reverse transcription

Total RNA was extracted from the whole organism using ReliaPrep TM RNA Miniprep Systems (Promega) according to manufacturer's instructions. RNA samples were assessed for concentration and quality using a NanoDrop ND-100 Spectrometer (NanoDrop Technologies) and an Agilent 2200 Tapestation (Agilent Technologies). 250ng of total RNA was DNAse treated using gDNA Wipeout Buffer and reverse transcribed using a first strand synthesis kit, Quantitect Reverse Transcription kit (Qiagen) according to manufacturer's instructions.

3.3.4 Primer design

Three contigs were identified in the backbone transcriptome by BLAST sequence similarity searching which shared sequence similarity with heat shock proteins. These 3 sequences had sufficient overlap to enable them to be identified as distinct family members and to allow comparative analyses with other species. The transcripts were putatively identified as *hsp70*, *hsp90* and *hsp60* based on BLAST sequence similarity and motif searches. One contig was identified in the backbone transcriptome as elongation factor transcript (*efa1*) (as defined by Blast sequence similarity searching). Gene-specific Hsp primers were designed based on the above sequences identified from the assembled transcriptome, using the Primer 3 software (http://frodo.wi.mit.edu) to produce single amplicons with a size of approximately 200–400bp, annealing temperature of 58-62°C and a GC content between 55–60%. The candidate Hsps (*hsp70, hsp90* and *hsp60*) were successfully amplified and the elongation factor transcript (*efa1*) was used as a positive control and reference housekeeping gene (Table 3.1). Testing of *efa1* amplification on control and heated samples demonstrated that it was a suitable control.

3.3.5 Q-PCR

Hsps previously designed from sequences contained in the assembled transcriptome were amplified using Brilliant SYBR Green Master Mix (Agilent) according to manufacturer's instructions on an Eco Real-Time PCR System (Ilumina). The *efa1* gene of *R. perrieri* was used as a reference to normalise the expression levels between samples. Samples were run in triplicate and data were

collected as Ct (PCR cycle number where fluorescence is detected above a threshold and decreases linearly with increasing input target quantity). Amplification efficiencies for each assay were calculated by the EcoStudy Software (Illumina) from a standard curve produced through serial dilutions of cDNA template pools (per panel, per experimental treatment). Each standard curve was made of 4 dilutions, starting from undiluted and with a dilution factor of 10. Polymerase chain reaction conditions were as follow: 95°C, 3 min, 50 cycles of 95°C, 5 s and 61°C, 20s followed by a melt curve analysis (95°C, 15s, 55°C, 15s and 95°C at a ramping rate of 0.25°C/s).

Table 3.1. PCR primers used for Q-PCR analysis of four genes. Primer sequence, RSq and PCR efficiency values are included for each gene, as calculated using the EcoStudy Software v 5.0 from the Eco Real-Time PCR System software (Illumina).

Gene	Primer sequence		RSq	PCR efficiency
hsp70	HSP70Rev HSP70F	CCTATGCCACACCAGAAACG TGGCTACGTACTGTGTGTGT	0.97	97
hsp60	HSP60Rev HSP60F	CAATAACATTCCCTCGCGCA GAGGAGCCGGGTGATGATAA	0.95	94
hsp90	HSP90Rev HSP90F	AGGTACTCTCACGTCCCTCT AGCTTCTTCAGAGCCCACAT	0.99	98
efa1	EFA1Rev EFA1F	GCAGGTGCCTCTACCTCAAG CAATGCTATGGCCACCTTTT	0.96	91

3.3.6 Statistical analysis

3.3.6.1 Upper thermal limit

Upper thermal limits were analysed using a Two-way ANOVA in the R environment for statistical computing. Post-hoc Tukey tests were performed using the *agricolae* package.

3.3.6.2 Q-PCR

Relative gene expression of the target genes (*hsp90*, *hsp70*, *hsp60* and *efa1)* was analysed using the Relative Expression Software Tool (REST). REST compares two or more treatments groups or

conditions (in REST-MCS), with up to 100 data points in a sample or control group (in REST-XL), for multiple reference genes and up to 15 target genes (in REST-384). The mathematical model used is based on the correction for exact PCR efficiencies and the mean crossing point deviation between sample group(s) and control group(s). Subsequently the expression ratio results of the investigated transcripts are tested for significance by a Pair Wise Fixed Reallocation Randomisation Test and plotted using standard error (SE) estimation via a complex Taylor algorithm (Pfaffl et al., 2002).

3.4 Results

3.4.1 Upper thermal limit experiment

R. perrieri individuals were most resistant to an acute thermal challenge in the control treatment (UTL = 20.4°C) followed by those in the +1°C (UTL = 19.4°C), +2°C (UTL = 18.9°C) and seasonal (UTL = 18.6°C)(Figure 3.1). An analysis of variance (ANOVA) on these scores yielded significant variation among treatments, F (3), = 5.72, $P < 0.01$. A post-hoc Tukey test revealed that the control treatment was significantly different from the +2°C and seasonal treatment ($P < 0.01$) but was not significantly different from the +1°C treatment ($P < 0.1$). Heated treatments (+1°C, +2°C and seasonal) were not significantly different from each other ($P > 0.05$).

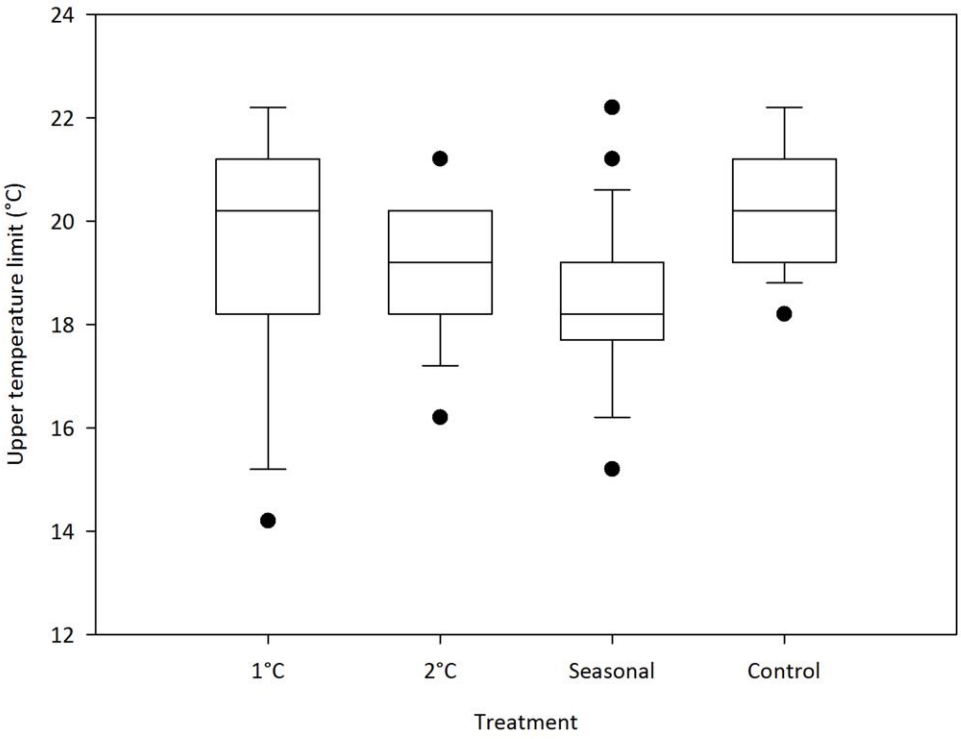

Figure 3.1. The range of maximum temperature reached by individuals of *Romanchella perrieri* (n=25) recruited on heated/non-heated panels in South Cove warmed at a rate of 1 degree h^{-1}. The black dots indicate points outside the interquartile range.

Further analysis comparing the upper thermal limits of *R. perrieri* individuals in panels maintained in the natural environment (North Cove) vs aquaria (South Cove) revealed similar upper thermal limit temperatures for the respective treatments: Control = 20°C as opposed to 20.4°C, +1°C = 19.2°C as opposed to 19.4°C, seasonal = 18.2°C as opposed to 18.6°C and +2°C = 18.3 as opposed to 18.9°C (Figure 3.2). An analysis of variance (ANOVA) on the North Cove panels also yielded significant variation among treatments, F (3), = 9.95, $P < 0.01$. A post-hoc Tukey test revealed that the control treatment was significantly different from the +2°C and seasonal treatment ($P < 0.01$) but not from the +1°C treatment ($P < 0.1$). Heated treatments (+1°C, +2°C and seasonal) were not significantly different from each other ($P > 0.05$). This had the same pattern as the one observed in the South Cove panels, which indicate there was no effect on South Cove panels after being held in the aquarium over winter.

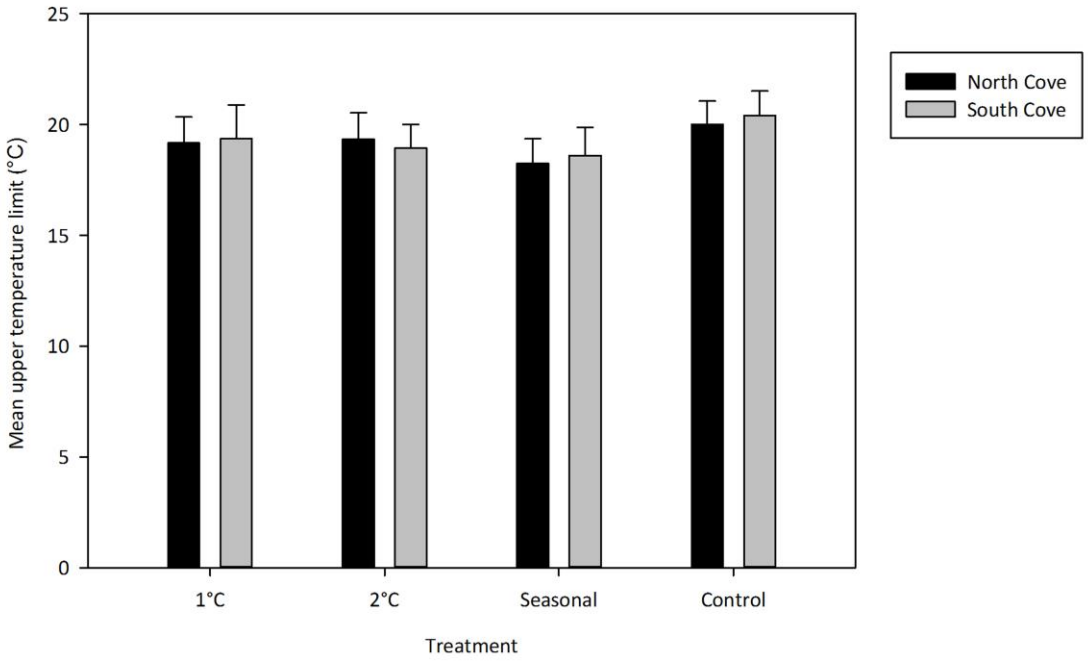

Figure 3.2. Mean ± SE upper temperature limit (UTL) (°C) in individuals of *Romanchella perrieri* (n=25) recruited in heated/non-heated panels in North Cove and South Cove sites warmed at a rate of 1 degree h^{-1}.

3.4.2 Q-PCR experiment

3.4.2.1 Identification of heat shock protein transcripts and transcriptome profiling

Three contigs were initially identified in the reference backbone transcriptome, which shared sequence similarity with heat shock proteins (as defined by BLAST sequence similarity searching) and also had sufficient overlap in sequence to enable them to be identified as distinct family members (Table 3.2). Of the 3 sequences analysed in more detail, one showed highest sequence similarity to Hsp90 (contig ID DN2076) with 58.86% identity (Table 3.2). The contig DN2076 contained four motifs characteristic of the Hsp90 family (NKEIFLRELISNSSDALDKIR; LGTIAKSGT; IGQFGVGFYSAYLVAD; IKLYVRRVFI and the C-terminus with the cellular localisation motif (Gupta, 1995). The contig DN36793 showed highest sequence similarity to Hsp60 with 57.33% identity. It contained a pre-sequence of 26 amino acids at the N terminus that is required for importation into the mitochondria (Yang et al., 2014) and had a conserved ATP-binding/Mg^{2+} binding site (Marchler-Bauer et al., 2007). The remaining contig (DN43886) was putatively identified as Hsp70, both on BLAST sequence similarity and motif searches. It shared a 63.42% identity with this gene. The contig DN43886 contained the motif R-A-[RK]-F-E-[ED]-[LM] characteristic of Hsp70 (Rensing & Maier, 1994) and the motifs [TS]-[VC]-P-A-[YN]-[FY]-N, D-[LF]-G(3)-T-F-D and [IVL]-D-[LF]-G-T-T-x-S which are also family signatures of the Hsp70 family (Rensing & Maier, 1994).

Table 3.2. Designation of *hsp* gene family member status based on BLAST match results from database sequence similarity searches.

Primer set	Gene designation	Closest database match	Score	% Identity	Probability
HSP70Rev HSP70F	*hsp*70	Q6L6T3_ANTYA: HSP70 *Antheraea yamamai* (Japanese oak silkmoth)	439	63.42	8.90E-071
HSP60Rev HSP60F	*hsp60*	CH60_DROME: HSP60 *Drosophila melanogaster* (Fruit fly)	372	57.33	9.45E-044
HSP90Rev HSP90F	*hsp90*	HSP90_BRUPA: HSP90 *Brugia pahangi* (nematode worm)	426	58.86	4.57E-122
EFA1Rev EFA1F	*efa1*	EF1A1_EUPCR:EFA1 *Euplotes crassus* (ciliate)	373	81.49	3.89E-089

These three different Hsp gene family members were successfully cloned from *R. perrieri: hsp90*, *hsp70* and *hsp60* (See Table 3.1) and *efa1* which was used as a reference gene. The acute heat shock at 15°C for 2 hours showed no significant up-regulation or down- regulation of *hsp90*, *hsp70* or *hsp60* in any of the panel treatments (+1°C, +2°C and control) (P = 0.1) (Figure 3.3).

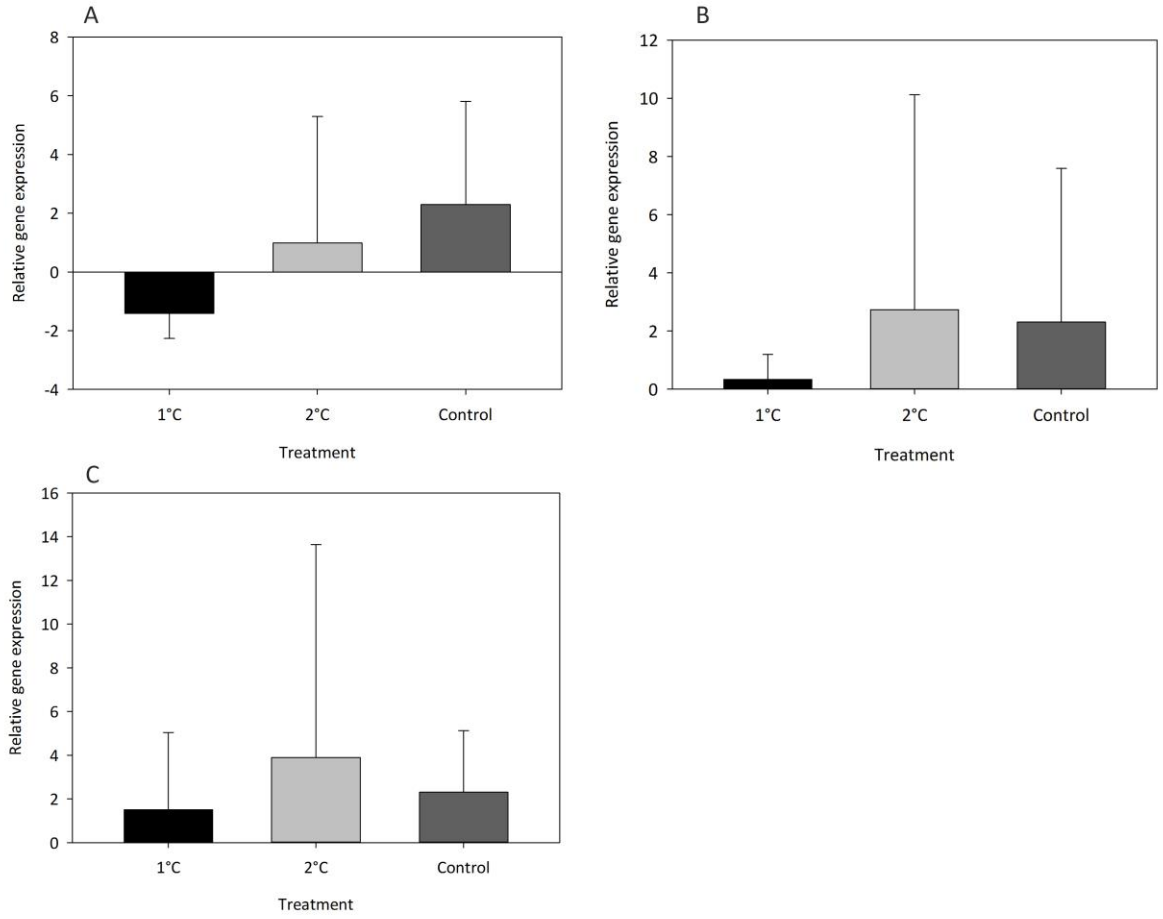

Figure 3.3. qPCR results for *Romanchella perrieri* after a short term heat shock at 15°C for 2 hours for the genes A) *hsp90* B) *hsp70* and c) *hsp60*. Fold changes (ddCT) in gene expression level calculated by REST using *efa1* as a gene reference.

The long term heat shock at 4°C for 30 days showed a significant down-regulation of *hsp90* in the +1°C and +2°C heated panels ($P < 0.05$). For *hsp70* and *hsp60* genes there was no significant up-regulation or down-regulation of the genes in either of the panel treatments (+1°C, +2°C and control) ($P > 0.9$) (Figure 3.4).

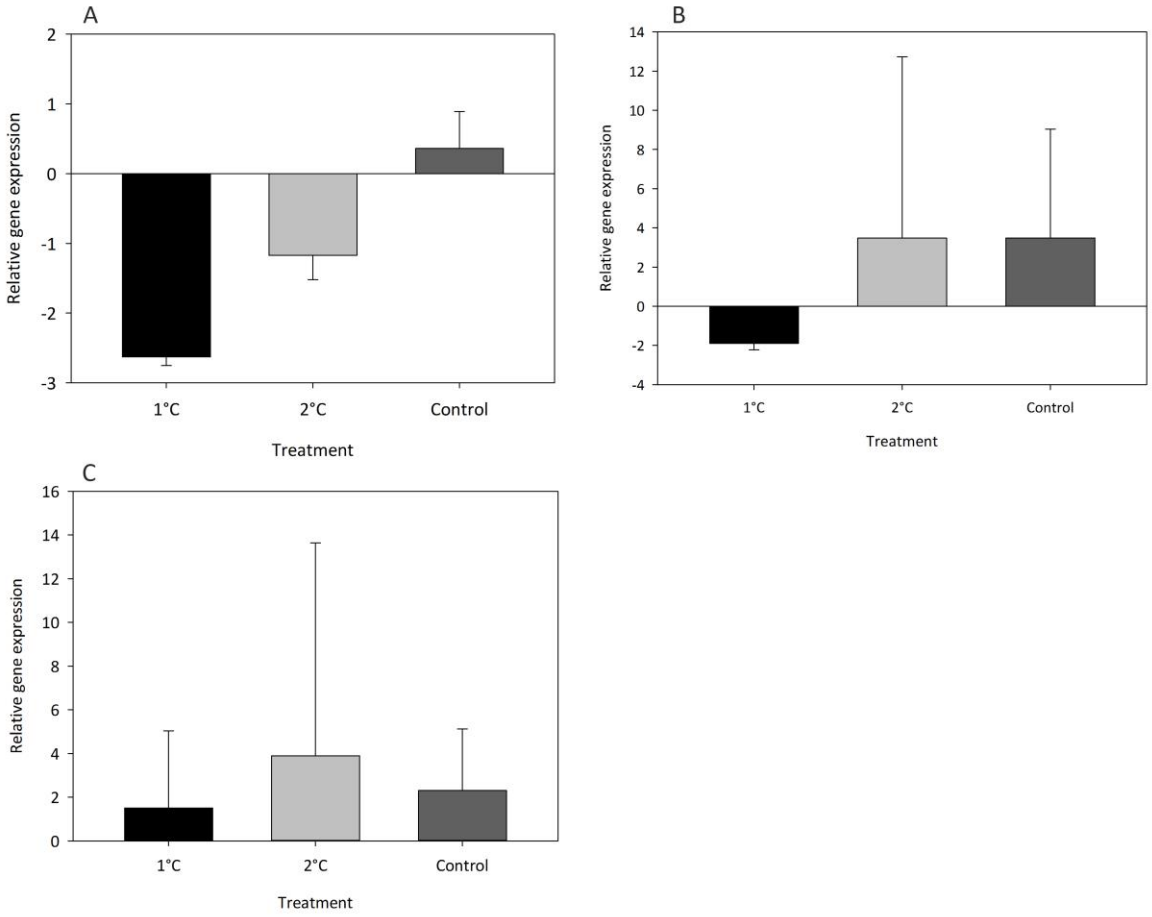

Figure 3.4. qPCR results for *Romanchella perrieri* after a long term heat shock at 4°C for 30 days for the genes A) *hsp90* B) *hsp70* and C) *hsp60*. Fold changes (ddCT) in gene expression level calculated by REST using *efa1* as a reference gene.

3.5 Discussion

R. perrieri recruited on heated panel treatments had a significantly lower UTL than those in the non-heated panels (Figure 3.1), suggesting that the organisms had not acclimated to the heated temperatures over the 18 month period. This was much longer than the time-scale, which was likely long enough for them to have done so and much longer than any previous period identified as necessary for the acclimation of Antarctic marine invertebrates (Morley et al., 2011; Morley et al., 2012; Peck et al., 2014; Suckling et al., 2015). Upper thermal limit experiments are widely used in ecological studies as a proxy for acclimation across terrestrial (Hoffmann et al., 2013; Kellermann et al., 2017) and marine systems (Peck et al., 2009; Bennett et al., 2018) as they identify thermal tolerances of species, a key factor contributing to species distributional limits (Chown et al., 2001). Ramping experiments such as the above can be adjusted to reflect the rate of thermal change experienced in the field (Please refer to Terblanche et al., 2007 for an example). This approach allows the average species survival for a community or ecosystem to be estimated and if applied to ecologically divergent groups, it also allows the potential for perturbation of communities to be assessed, for instance, if predators on average are more resistant than prey species. As such, the UTL data for *R. perrieri* in this study reflects the lack of acclimation in the species and could be extrapolated to estimate the survival for the rest of the community.

R. perrieri is a filter feeder and it may be that the animals were not able to ingest sufficient food to fuel the increased metabolism at the higher temperatures and were therefore resisting rather than acclimating. Overall, very few Antarctic marine species appear able to acclimate and perform biological functions over periods of months at temperatures above 4°C e.g. the brittle star *Ophionotus victoriae* is incapable of acclimating to 2°C and both the bivalve *L. elliptica* and the amphipod *P. miersi* cannot acclimate to 3°C (Peck et al., 2010). In the first paper demonstrating the use of heated settlement panels in Antarctica, significant increases in growth rates of colonising species were observed with +1°C and +2°C of warming (Ashton et al. 2017). After nine months of deployment the spirorbid worm *Romanchella perrieri* showed a near doubling of growth rates on the heated plates compared with controls. The data here, however suggest that although the organisms were seemingly performing well, they had not acclimated to the heated treatments and were living close to their thermal limit.

UTL data were further validated by the lack of a HSR, especially when *R. perrieri* were exposed to acute warming, even under control conditions (Figure 3.3). There was no significant up-regulation

of heat shock protein activity in the acute temperature experiment (15°C for 2 hours) above the level of individual variation/experimental noise for any of the family members (Figure 3.3) and for any of the treatments tested. To date, there are no other published experiments looking at the heat shock response in Antarctic polychaetes, probably due to the difficulty of extracting RNA in the organisms due to their small size. However, previous laboratory based experiments on other Antarctic marine invertebrates have shown the lack of the classical heat shock response at 10°C and 15°C in the Antarctic sea star *Odontaster validus* (Clark et al., 2008). The lack of the HSR has also been recorded in other Antarctic species, namely the microbial eukaryote, *Euplotes focardii* (LaTerza et al., 2011) and *R. perrieri* may be another example of an Antarctic species lacking an HSR. Whilst 10°C and 15°C are temperatures exceeding those Antarctic marine organisms would experience in the natural environment, laboratory based experiments on the clam *Laternula elliptica* and the limpet *Nacella concinna* have demonstrated the classical heat shock response at such temperatures and consequently such tests have been used as a test bed for evaluations in the natural environment (Clark and Peck 2009b). Hence there are Antarctic organisms that still possess the ability to up-regulate heat shock genes (*hsps*) (Clark and Peck, 2009a).

Since *R. perrieri* did not acclimate to the temperatures in this study, the added stress imposed by an acute heat shock might be energetically too costly for *R. perrieri* to induce the HSR. There is a demonstrable energetic cost associated with the production of heat shock proteins, in particular the inducible form of *hsp70* and its overproduction may be cytotoxic (reviewed in Sørensen & Loeschcke, 2007). It is also possible that this particular stress did not induce a HSR but that under a different stress or multiple stressors a HSR would be induced. As global climate change progresses, the Southern Ocean is predicted to undergo changes in oceanic temperature and also in pCO_2 (Hofmann et al., 2010) and as such it is important to consider changes in multiple environmental variables when assessing the HSR in a species (Byrne et al., 2013; Suckling et al., 2015). For example, previous acute thermal stress studies on the Antarctic fish *Trematomus bernacchii* suggested the lack of a heat shock response in the species was due to a mutation in the promoter region of the gene. However, the organism was shown to be capable of mounting a short-term response after a multi-stressor exposure to elevated temperature and pCO_2 stress (Huth & Place, 2016).

However, the results from the long term heat shock at 2°C for 30 days showed a significant down regulation of *hsp90* in *R. perrieri* that recruited on the heated panels (+1°C and +2°C) in comparison to those on control panels but no significant activity in other heat shock proteins

(Figure 3.4 A). This suggests that there might be a cellular trade-off at the higher temperatures, as described above. This response contrasts to that previously found in long term heat shocks in other Antarctic invertebrates, with *hsp90* being constitutively expressed in the sea urchin *Sterechinus neumayeri* (González et al., 2016) and *hsp70b* (an isoform of *hsp70*) also being constitutively expressed in the limpet *N. concinna* (Clark & Peck, 2009b). This pattern of expression is also observed in other polychaete worms that inhabit extreme environments such as hydrothermal vents. *hsp90* and *hsp70* are constitutively expressed in the polychaete worm *Paralvinella sulfincola* to cope with the rapid changes in temperature typically encountered by this species, which includes maintaining physiological function near the organism's UTL (Dilly et al., 2012).

In *N. concinna,* the constitutive expression of *hsp70b* may be due to a pre-emptive mechanism to protect cells against stressors triggered by life in the intertidal region (Dong et al., 2008; Clark et al., 2008). In both *S. neumayeri* and *N. concinna* there was also constitutive expression of *hsc70* under routine conditions with further up-regulation under long term thermal stress. *hsc70* is considered a major family member involved in both routine protein folding and chronic heat stress in marine organisms (Place et al., 2008). Chaperone proteins of the Hsp70 family are routinely constitutively expressed in Antarctic species, a situation not often found in temperate species. For example, in the clam *L. elliptica*, it was *grp*78 that was constitutively expressed and not *hsc70* as in *N. concinna* (Clark et al., 2008a). It is thought that this "extra" constitutive expression of Hsp70 protein family members is due to the problems of protein folding in the cold (Peck, 2016). Unfortunately it was not possible to survey *hsc70* in this experiment, as a contig of suitable length was not identified in the transcriptome.

Therefore, although the number of examples is limited with regard to the production of an HSR in response to thermal stress in Antarctic species, the distribution across taxa is vast: from a microbial eukaryote, *Euplotes focardii* (LaTerza et al., 2001) to an Antarctic fish (Hofmann et al. 2000; Clark et al., 2008). There is no strict rule for the expression or loss of the heat shock response in Antarctic organisms. As more species are studied, the more complex the picture becomes. More extensive analyses are required to investigate whether *R. perrieri*, which failed to exhibit a HSR response in this study, does in fact lack one in other environmental conditions. Transcriptomic analysis and construction of gene networks in *R. perrieri* might indeed reveal the induction of one. This has been demonstrated in *Paraceradocus miersi*, originally thought to lack a HSR after an acute heat shock at 10°C using a candidate gene approach (Clark et al., 2008a) but

was found to up-regulate *hsp70* after an NGS transcriptome-led approach (Clark et al., 2017). In fact, such NGS discovery-led approaches are essential to be able to prove whether Antarctic species have an HSR, as candidate gene approaches are limited and *hsp70* genes are often duplicated in Antarctic species, with complicated expression patterns (Temblay et al., 2014).

It is evident that *R. perrieri* in the heated panels have not acclimated to predicted future oceanic warming (IPCC, 2014) after 18 months and that this lack of acclimation could possibly explain the absence of a heat shock response on the treated panels. This may be due to the high energy costs and other trade-offs associated with expression of these genes. These data demonstrates that although Ashton et al., (2017) observed accelerated invertebrate growth and colonisation rate in *R. perrieri* on the heated panels in warmed treatments throughout the summer (the exception being a decline in growth rate in March on all treatments including the control), this situation was clearly not sustainable. Thus is it entirely possible that a longer deployment of the panels would have led to the mortality of the organisms over time. The data here demonstrate the importance of UTLs and molecular evaluations of acclimation and indicate that *Romanchella perrieri* has a very poor capacity to acclimate to warming of even 1°C and is unable to cope with predicted end of century oceanic warming (IPCC, 2014).

3.6 References

Altschul, S. F., Gish, W., Miller, W., Myers, E. W. and Lipman, D. J. (1990). Basic local alignment search tool. *J. Mol. Biol*. **21***5*, 403–410.

Ashton, G. V., Morley, S. A., Barnes, D. K. A., Clark, M. S. and Peck, L. S. (2017). Warming by 1°C Drives Species and Assemblage Level Responses in Antarctica's Marine Shallows. *Curr. Biol*, **27**, 2698–2705.

Bennett, J. M. *et al.* (2018). GlobTherm, a global database on thermal tolerance for aquatic and terrestrial organisms. *Sci Data*. 180022.

Bilyk, K. T. and Devries, A. L. (2011). Heat tolerance and its plasticity in Antarctic fishes. *Comp. Biochem. Physiol. A. Mol. Integr. Physiol.* **158**, 382–90.

Bolger, A. M., Lohse, M. and Usadel, B. (2014). Genome analysis Trimmomatic : a flexible trimmer for Illumina sequence data. *Bioinformatics*. **30**, 2114–2120.

Bosch, T. C. G., Krylow, S. M., Bode, H. R. and Steele, R. E. (1988). Thermotolerance and synthesis of heat-shock proteins – these responses are present in *Hydra attenuata* but absent in *Hydra oligactis*. *Proc. Natl. Acad. Scie. USA*. **85**, 7927-7931.

Brennecke, T., Gellner, K. and Bosch, T. C. G. (1998). The lack of a stress response in *Hydra oligactis* is due to reduced hsp70 mRNA stability. *Eur. J. Biochem.* **255**, 703–709.

Brett, J. R. (1956). Some principles in the thermal requirements of fishes. *Q. Rev. Biol*. **31**, 75-87.

Byrne, M. and Przeslawski, R. (2013). Multistressor Impacts of Warming and Acidification of the Ocean on Marine invertebrates' life histories. *Integr. Comp. Biol.* **53**, 582-596.

Chown, S. L. (2001). Physiological variation in insects: hierarchical levels and implications. J*. Insect. Physiol*. **47**, 649-660.

Clark, M. S., Fraser, K. P. P. and Peck, L. S. (2008a). Antarctic marine molluscs do have an HSP70 heat shock response. *Cell. Stress. Chaperones.* **13**, 39–49.

Clark, M. S., Fraser, K. P. P. and Peck, L. S. (2008b). Lack of an HSP70 heat shock response in two Antarctic marine invertebrates. *Polar. Biol.* **31**, 1059–1065.

Clark, M. S., Geissler, P., Waller, C., Fraser, K. P. P., Barnes, D. K. A. and Peck, L. S. (2008c). Low heat shock thresholds in wild Antarctic inter-tidal limpets (*Nacella concinna*). *Cell. Stress. Chaperones.* **31**, 51–58.

Clark, M. S. and Peck, L. S. (2009a). Marine Genomics HSP70 heat shock proteins and environmental stress in Antarctic marine organisms : A mini-review. *Mar. Genomics*. **2**, 11–18.

Clark, M. S. and Peck, L. S. (2009b). Triggers of the HSP70 stress response : environmental responses and laboratory manipulation in an Antarctic marine invertebrate (*Nacella concinna*). *Cell. Stress. Chaperones.* **14**, 649–660.

Clark, M. S., Sommer, U. L. F., Sihra, J. K. and Thorne, M. A. S. (2017). Biodiversity in marine invertebrate responses to acute warming revealed by a comparative multi-omics approach. *Glob. Change. Biol.* **23**, 318–330.

Dilly, G. F., Young, C. R., Lanse, W. S., Pangilinan, J. and Girguis, P.R. (2012). Exploring the limit of metazoan thermal tolerance via comparative proteomics: thermally induced changes in protein abundance by two hydrothermal vent polychaetes. *Proc R Soc Lond*. *Biol*. **279.**

Dong, Y. W. and Williams, G. A. (2011). Variations in cardiac performance and heat shock protein expression to thermal stress in two differently zoned limpets on a tropical rocky shore. *Mar. Biol.* **158**, 1223-1231.

Feder, M. and Hofmann, G. (1999). Heat-shock proteins, molecular chaperones, and the stress response: Evolutionary and Ecological Physiology. *Annu. Rev. Physiol*. **61**, 243–282.

González, K., Gaitán-Espitia, J., Font, A., Cárdenas, C. A. and González-Aravena, M. (2016). Expression pattern of heat shock proteins during acute thermal stress in the Antarctic sea urchin, *Sterechinus neumayeri. Rev. Chil. Hist. Nat.* 1–9.

Grabherr, M. G., Haas, B. J., Yassour, M., Levin, J. Z., Thompson, D. A. et al. (2011). Full-length transcriptome assembly from RNA-Seq data without a reference genome. *Nat. Biotechnol***. 15**, 644-52.

Hoffmann, A. A., Chown, S. L. and Crusella-Trullas S. (2013). Upper thermal limits in terrestrial ectotherms: how constrained are they? *Funct. Ecol*. **27**, 934-49.

Hofmann, G. E., Buckley, B. A., Airaksinen, S., Keen, J. E. and Somero, G. N. (2000). Heat-shock protein expression is absent in the antarctic fish *Trematomus bernacchii* (family Nototheniidae). *J Exp Biol,* **203**, 2331–2339.

Hofmann, G. E., Barry, J. P., Edmunds, P. J., Gates, R. D., Hutchins, D. A., Klinger, T. and Sewell, M. A. (2010). The Effect of Ocean Acidification on Calcifying Organisms in Marine Ecosystems : An Organism- to-Ecosystem Perspective. *Annu. Rev. Ecol. Evol. Syst.* **41**, 127-147.

Huth, T. J. and Place, S. P. (2016). Transcriptome wide analyses reveal a sustained cellular stress response in the gill tissue of *Trematomus bernacchii* after acclimation to multiple stressors. *BMC Genom*. **17**, 1–18.

IPCC. (2014). Climate Change 2014 Synthesis Report Summary for Policymakers.

Jumbam, K. R., Jackson, S., Terblanche, J. S., McGeoch, M. A. and Chown, S. L. (2008). Acclimation effects on critical and lethal thermal limits of workers of the Argentine ant, *Linepithema humile. J. Insect. Physiol.* **54**, 1008-1014.

Kellermann, V., Van Heerwaarden, B. and Sgro, C.M. (2017). How important is thermal history? Evidence for lasting effects of developmental temperature on upper thermal limits in *Drosophila melanogaster*. *Proc. R. Soc. B*. **284**, 20170447.

Kim, D., Pertea, G., Trapnell, C., Pimentel, H., Kelley, R. and Salzberg, S. L. (2013). TopHat2 : accurate alignment of transcriptomes in the presence of insertions, deletions and gene fusions. *Genome. Biol.* **14**, 1–13.

Knight-Jones, P. and Knight-Jones, E. W. (1984). Systematics, ecology and distribution of southern hemisphere spirorbids (Polychaeta; Spirorbidae). Proceedings of the first international polychaete conference, Sydney edited by P.A. Hutchings, published by Linnean Society of New South Wales, pp 196-210.

Li, H., Handsaker, B., Wysoker, A., Fennell, T., Ruan, J., Homer, N. et al. (2009). The Sequence Alignment / Map format and SAMtools. *Bioinformatics.* **25**, 2078–2079.

LaTerza, A., Papa, G., Miceli, C. and Luporini, P. (2001). Divergence between two Antarctic species of the ciliate Euplotes , *E . focardii* and *E . nobilii*, in the expression of heat-shock protein 70 genes. *Mol Ecol.* **10**, 1061–1067.

Machler-Bauer, A., Anderson, J. B., Derbyshire, M. K., DeWeese-Scott, C. et al. (2007). CDD: a conserved fomain database for interactive domain family analysis. *Nucleic. Acids. Res* **35**, D237-D240.

Morley, S. A., Peck, L. S., Tan, K. S., Martin, S. M. and Pörtner, H. O. (2007). Slowest of the slow : latitudinal insensitivity of burrowing capacity in the bivalve *Laternula*. *Marine Biol.* **151**, 1823–1830.

Morley, S. A., Lemmon, V., Obermüller, B. E., Spicer, J. I., Clark, M. S. and Peck, L. S. (2011). Duration tenacity : A method for assessing acclimatory capacity of the Antarctic limpet, *Nacella concinna*. *J. Exp. Mar. Bio. Ecol*, **399**, 39–42.

Morley, S. A., Hirse, T., Thorne, M. A. S., Pörtner, H. O. and Peck, L. S. (2012). Physiological plasticity, long term resistance or acclimation to temperature, in the Antarctic bivalve, *Laternula elliptica*. *Comp. Biochem. Physiol. A.* **162**, 16-21.

Parsell, D. A. and Lindquist, S. (1993). The function of heat-shock protein in stress tolerance-degradation and reactivation of damaged proteins. *Ann. Rev. Genet.* **27**, 437-496.

Peck, L. S., Pörtner, H. O. and Hardewig, I. (1999). Metabolic Demand, Oxygen Supply, and Critical Temperatures in the Antarctic Bivalve *Laternula elliptica*. *Physiol. Biochem. Zool.* **75**, 123-33.

Peck, L. S., Clark, M. S., Morley, S. A., Massey, A. and Rossetti, H. (2009a). Animal temperature limits and ecological relevance : effects of size, activity and rates of change. *Funct. Ecol.* **23**, 248–256.

Peck, L. S., Massey, A., Thorne, M. A. S. and Clark, M. S. (2009b). Lack of acclimation in *Ophionotus victoriae* : brittle stars are not fish. *Polar Biol.* **32**, 399–402.

Peck, L. S., Morley, S. A. and Clark, M. S. (2010). Poor acclimation capacities in Antarctic marine ectotherms. *Polar Biol.* **157**, 2051–2059.

Peck, L. S., Morley, S. A, Richard, J., & Clark, M. S. (2014). Acclimation and thermal tolerance in Antarctic marine ectotherms. *J Exp Mar Bio Ecol*, *217*, 16–22.

Place, S. P., Zippay, M.L. and Hofmann, G. E. (2004). Constitutive roles for inducible genes: evidence for the alteration in expression of the inducible hsp70 gene in Antarctic notothenioid fishes. *Am. J. Physiol. Reg. Integr. Comp. Physiol.* **287**, 429-436.

Pfaffl, M.W., Horgan, G.W. and Dempfle, L. (2002). Relative expression software tool (REST) for group-wise comparison and statistical analysis of relative expression results in real-time PCR. Nucleic. Acids. Res. **30**, 9.

Pörtner, H. O. (2002). Climate variations and the physiological basis of temperature dependent biogeography : systemic to molecular hierarchy of thermal tolerance in animals. *Comp. Biochem. Physiol. A. Mol. Integr. Physiol.* **132**, 739–761.

Pörtner, H. O., Peck, L. S. and Hirse, T. (2006). Hyperoxia alleviates thermal stress in the Antarctic bivalve, *Laternula elliptica* : evidence for oxygen limited thermal tolerance. *Polar Biol.* **29**, 688–693.

Pörtner, H. O., Peck, L. S. and Somero, G. (2007). Thermal limits and adaptation in marine Antarctic ectotherms : an integrative view. *Philos. Trans. R. Soc. Lond. B. Biol. Sci*. **362**, 2233–2258.

Rensing, S. A. and Maier, U. G. (1994). Phylogenetic analysis of the stress-70 protein family. *J. Mol. Evol.* **38***,* 80-86.

Richard, J., Morley, S.A., Thorne, M.A.S. and Peck, L.S. (2012). Estimating long-term survival temperatures at the assemblage level in the marine environment: towards macrophysiology. *PLoS. One*. **7**, e34655.

Ritossa, F. (1962). A new puffing pattern induced by temperature shock and DNP in *Drosophila. Experimentia*. **18**, 571-573.

Schmidt-Nielsen, K. (1990). Animal Physiology: Adaptation and Environment, 4th edn, 602. Cambridge University Press.

Somero, G. N. (2010). The physiology of climate change: how potentials for acclimatization and genetic adaptation will determine “winners” and “losers”. *J. Exp. Biol*. **213**, 912–20.

Sørensen, J. G. and Loeschcke, V. (2002). Decreased heat-shock resistance and down-regulation of Hsp70 expression with increasing age in adult *Drosophila melanogaster*. *Func. Ecol.* **16**, 379-384.

Sørensen, J. G., Nielsen, M. M. and Loeschcke, V. (2007). Gene expression profile analysis of *Drosophila melanogaster* selected for resistance to environmental stressors. *J. Evol. Biol.* **20**, 1624–1636.

Suckling, C., Clark, M. S., Richard, J., Morley, S. A., Thorne, M. A. S., Harper, E. M. and Peck, L. S. (2015). Adult acclimation to combined temperature and pH stressors significantly enhances reproductive outcomes compared to short-term exposures. *J. Anim. Ecol.* **84**, 773-784.

Temblay, N., Cascella, K., Touellec, J-Y., Held, C., Fielding, S., Tarling, G. A. and Abele, D. (2014). Gene expression of the Antarctic krill *Euphasia superba* under different hypoxia intensities. *Pangea*.

Terblanche, J.S., Deere, J.A., Clusella-Trullas, S., Janion, C. and Chown, S.L. (2007). Critical thermal limits depend on methodological context. *Proc Biol Sci*, **274**, 2935-2943.

Tomanek, L. (2008). The importance of physiological limits in determining biogeographical range shifts due to global climate change: the heat-shock response. *Physiol. Biochem. Zool.* **81**, 709-717.

Truebano, M., Burns, G., Thorne, M. A. S., Hillyard, G., Peck, L. S., Skibinski, D. O. F. and Clark, M. S. (2010). Transcriptional response to heat stress in the Antarctic bivalve *Laternula elliptica*. *J. Exp. Mar. Bio. Ecol.* **391**, 65–72.

Turner, J., Orr, A., Gudmundsson, G. H., Jenkins, A., Bingham, R. G., Hillenbrand, C-D. and Bracegirdle, T. J. (2017). Atmosphere-ocean-ice interactions in the Amundsen Sea embayment, West Antarctica. *AGU.* **55**, 235-276.

Vaughan, D. G., Marshall, G. J., Conrolley, W. M., Parkinson, C., Mulvaney, R., Hodgson, D. A., King, J. C., Pudsey, C. J. and Turner, J. (2003). Recent rapid regional climate warming on the Antarctic Peninsula. *Clim. Change*. **60**, 243-274.

Yang, J., Yawen, Mu., Siming, D., Jian, Q. and Yang, J. (2014). Changes in the expression of four heat shock proteins during the aging process in *Brachionus calyciflorus* (rotifera). *Cell. Stress. Chaperones.* **19**, 33-52.

Chapter 4

Differential gene expression in response to *in situ* elevated temperature in the Antarctic spirorbid worm *Protolaeospira stalagmia*

4.1 Abstract

Antarctic marine invertebrates have very poor capacities to acclimate. Phenotypic plasticity is therefore a key mechanism for the future survival of Antarctic marine organisms as it allows genotypes to produce different phenotypes in response to environmental variation. We currently have no measure of how much standing genetic variation is available within Antarctic species and whether this provides a sufficient buffer for a population to respond to changing conditions. In this study, an RNA-Seq approach was used to examine how the Antarctic Spirorbid worm, *Protolaeospira stalagmia* were functionally responding at the cellular level to the heated treatments at +1°C and +2°C above ambient conditions over a period of 18 months. RNA-Seq data was also interrogated for Single Nucleotide Polymorphisms (SNPs) to investigate post-selection recruitment using a population genetics approach. There was massive up-regulation of the cellular stress response in the warmed worms with almost one third of the transcripts comprising ribosomal genes. There was a high up-regulation of transcripts involved in translation in the warmer worms, indicating a substantial requirement for the enhanced generation of proteins, protein turnover and cell renewal in the warmer conditions. This transcriptional profile indicated that the animals were exhibiting cellular stress and starting to shut down cellular pathways. Population genetic analyses showed little evidence of post-recruitment selection and genetic adaptation. Overall this data suggests that the organisms had not acclimated to the heated temperatures and were resisting. This combined with the little evidence of genetic adaption means it is unlikely that these Antarctic benthic organisms are going to be able to cope with predicted end of century oceanic warming.

4.2 Introduction

Antarctic marine organisms are particularly vulnerable to environmental change due to their highly stenothermal nature and poor capacity to resist elevated temperatures (Somero and DeVries, 1967; Peck, 2002). Such characteristics are therefore concerning given climate change effects and recent rates of warming seen in the polar-regions (Meredith & King, 2005; Turner et al., 2017). Somero (2010) argues that phenotypic plasticity via physiological flexibility and genetic adaptation are the most important process determining the success of a species under future environmental conditions. Furthermore, he argued that acclimation via physiological flexibility will critically dictate the survival or failure of long-lived species under changing conditions, as given the current rates of change, these species will have very few generations in which they can genetically adapt. Knowledge of the extent of phenotypic plasticity within populations and the capacity of genotypes to produce different phenotypes in response to environmental variation is therefore crucial in order to predict biodiversity change in face of end of century predicted oceanic warming (Peck, 2011; IPCC, 2014; Somero, 2015; Peck, 2018,).

The traditional view of all populations in the marine environment being genetically homogeneous is beginning to change as our abilities to perform whole genome scans, especially using RNA-Seq and single nucleotide polymorphism (SNP) discovery, is becoming routine for non-model species (Buckley, 2007; Chown et al., 2015). This is particularly true of marine polychaetes where the lack of genetic information for non-model species limited research. However the recent use of RNAseq in polychaete toxicological studies (Neave et al., 2012; Rhee et al., 2011) has aided our understanding of gene pathways (Gao et al., 2015) and developmental phenotypes (Lesoway et al., 2016) in these organisms. For example, Lv et al., (2017) recently sequenced the transcriptome of somatic muscles in the polychaete worm *Perinereis aibuhitensis*, characterising heat shock proteins in the species, as well as identifying SNPs. Studies such as these are showing that the environmental variation in the marine environment may exert strong selection on populations to adapt to an environmental change or may allow small-scale adaptation of populations to particular local conditions (Hereford, 2009). Genetic adaptation in marine invertebrates occurs along a variety of selective gradients (both abiotic and biotic), generating spatially complex mosaics of local adaptation and across a range of life histories (Sanford and Kelly, 2011).

Recent RNA-Seq studies of marine species at the whole-genome level increasingly demonstrate cases of particularly strong differentiation of some loci in the face of environmental change (Nielsen et al., 2009, Pespeni & Palumbi, 2010). For example, Pespeni et al., (2013) observed that

there was enough standing genetic variation in natural populations of the purple sea urchin *Strongylocentrotus purpuratus*, such that experimental exposure to high acidity conditions led to marked gene frequency evolution over very short timescales. Such whole-genome approaches are well suited to understanding the relationship of environmental stress to potential adaptation for climate change effects. Further work on the purple sea urchin demonstrated that urchin populations most frequently exposed to low pH seawater responded to experimental acidification via the enhanced expression of genes with major ATP-producing pathways. These same metabolic pathways were significantly over-represented among genes both expressed in a population-specific manner and putatively under selection to enhance low pH tolerance (Evans et al., 2017). These studies thus suggest that natural selection is acting on metabolic gene networks to redirect ATP and enhance the tolerance of seawater acidification. Similarly, De Wit et al., (2013) confirmed low levels of genetic differentiation of the red abalone *Haliotis rufescens* between different geographic locations along the Californian coast. However, they also showed that a substantial number of loci involved in biomineralization, resistance to hypoxia and response to heat and energy metabolism were under different selective pressures in different geographical regions.

Among intertidal organisms, there are several examples in which larval/juvenile survival or post-settlement selection leads to different genotypes becoming established in different physical or biotic conditions. For example, individuals of the barnacle *Semibalanus balanoides* have different allelic variants of the enzyme mannose 6-phosphate isomerise that correlate to different vertical positions in the intertidal zone, which in turn are also influenced by the presence of a species of alga that provides cover for the animals (Schmidt and Rand, 2001). This genotypic patterning is thought to have resulted from genotype specific mortality following larval settlement and may reflect a combination of physical stress and access to mannose-containing compounds in the barnacle's diet.

Similarly, a cline in the allele frequencies of the *Lap* allozyme in a population of *Mytilus edulis* mussels was shown to correspond with a salinity gradient that separated mussels with genotypes specific to oceanic habitats from those genotypes specific to brackish waters (Hilbish, 1985). Furthermore these allozymes were found to be functionally different and resulted in lower fitness for mussels with oceanic genotypes in brackish waters. In the marine worm *Arenicola marina*, Hummel et al., (1997) reported that the expression of the *Idh2* isoform, involved in cell metabolism and energy production was predominantly influenced by temperature, creating a geographic cline in genotypes between different populations. These studies support the evidence

that local adaptation and polymorphism-based selection in marine animals have the potential for replenishing populations of conspecifics that face local extinction in warming environments (Panova et al., 2004). Species with adequate genetic variation to generate phenotypes with different thermal tolerances and optima may prove to be the most successful in the predicted end of century oceanic warming (Peck, 2011; IPCC, 2014).

Studies have shown that in general Antarctic marine invertebrates have very poor capacities to acclimate with low values for CT_{max}. In the species where acclimation has been demonstrated, they require long times, from 2-9 months to do so (Morley et al., 2011; Peck et al., 2014; Suckling et al., 2015). Given these poor acclimation capacities, phenotypic plasticity is therefore a key mechanism for the future survival of Antarctic marine organisms (Peck, 2011; Somero, 2010, 2012). What we currently have no measure of, is how much standing genetic variation is available within Antarctic species and whether this provides a sufficient buffer for a population to respond to changing conditions.

Given the above studies and the important role that genetic adaption plays in the survival of marine organisms facing future climate change (IPCC, 2014), in this chapter I built upon the previous work using the heated settlement panels and examined phenotypic plasticity processes across heated and non heated treatments in one of the main benthic colonisers, the Antarctic spirorbid worm *Protolaeospira stalagmia.* Heated settlement panels were deployed for a period of 18 months in Ryder Bay near Rothera research Station on the Antarctic Peninsula. The panels were set to heat the panel surfaces and a thin layer of water up to 5 mm thick (See Chapter 2), overlying the surface to 1°C or 2°C above ambient temperature. This system simulates end of century oceanic warming predictions (IPCC, 2014) in the natural environment while maintaining natural cycles of temperature variation, light regime, food supply etc. Previous work in chapter 3 examined the thermal tolerance and heat shock response of one of the other main colonisers, the spirorbid worm *Romanchella perrieri*. Work on this organism indicated that the worms that had settled and grown in warmed conditions had not acclimated to the heated treatments and that they had a very limited if any, discernable heat shock response. This indicated the very poor capacity of *R. perrieri* to cope with predicted end of century warming, at least via physiological flexibility.

In this study, I used populations of *Protolaeospira stalagmia*, the other main spirorbid coloniser (it was not possible to perform the same experiments on *R. perrieri* due to limited numbers present on the panels) to examine how the animals were functionally responding to the heat treatments

at the cellular level (phenotypic plasticity). *P. stalagmia* is a marine encrusting worm belonging to the Spirorbinae subfamily. Like *R. perrieri*, individuals have a stalk for the attachment of embryos and an asymmetrical distribution of setae and uncini (Knight-Jones and Walker, 1972). *P. stalagmia* is highly abundant in Antarctica and has been found as far north as the South Orkney Islands (Knigh-Jones and Walker, 1972). As with *R. perrieri*, there are no descriptions of the thermal limit or acclamatory capacities of the species.

To test how animals were functionally responding to the heat treatments, I used an RNA-Seq approach and sequenced the transcriptome of 9 pools of *P. stalagmia* (3 replicates per treatment) from three different panel treatments (control, +1°C and +2°C) to compare gene expression differences in animals on the +1°C and +2°C panels with those on control plates. I also interrogated the RNA-Seq data for Single Nucleotide Polymorphisms (SNPs) to investigate post-recruitment selection using a population genetics approach.

4.3 Methods

This chapter represents a collaboration between the British Antarctic Survey and Edinburgh Genomics. L V-N helped conduct the fieldwork and collected the samples for this experiment, performed the RNA isolations and amplifications and also the biological annotation of the data. Edinburgh Genomics (Urmi Trivedi and Francis Turner) performed the bioinformatics analyses.

4.3.1 Sample collection

Heated and non heated panels (3 each of control, +1°C, +2°C) colonised by *Protolaeospira stalagmia* worms were transferred to a 60 L jacketed tank with aerated sea water at the same temperature as the ambient sea water (0°C) to ensure all organisms were kept at the same temperature whilst they were dissected. *P. stalagmia* (n=6 per panel, per treatment) were dissected from their calcified structure, snap frozen in liquid nitrogen and stored at -80°C prior to RNA extraction. In total 54 individuals were preserved at -80°C for this experiment.

4.3.2 RNA extraction

Total RNA was extracted from the whole organism using ReliaPrep TM RNA Miniprep Systems (Promega) according to manufacturer's instructions. RNA samples were assessed for concentration and quality using a NanoDrop ND-100 Spectrometer (NanoDrop Technologies) and an Agilent 2200 Tapestation (Agilent Technologies). RNA samples (n=6 per panel, per treatment) were pooled to obtain a total of 3 replicates per treatment (control, +1°C, +2°C) producing a final total of 9 samples and of 150ng RNA for each sample.

4.3.3 cDNA amplification

For each RNA pool cDNA was amplified using the ovation RNA-seq system v2 kit (NuGEN) according to manufacturer's instructions. In this method total RNA (150ng) was reverse-transcribed to synthesize the first-strand cDNA with a combination of random hexamers and a poly-T chimeric primer. The RNA template was then partially degraded by heating and the second-strand cDNA was synthesized using DNA polymerase. The double-stranded DNA was amplified using single primer isothermal amplification (SPIA). SPIA is a linear cDNA amplification process in which RNase H degrades RNA in DNA/RNA heteroduplex at the 5'-end of the double-stranded DNA, after which the SPIA primer binds to the cDNA and the polymerase starts replication at the

3-end of the primer by displacement of the existing forward strand. Random hexamers were then used to amplify the second-strand cDNA.

4.3.4 Library preparation and sequencing

Library preparation and sequencing was carried out by Edinburgh Genomics (Edinburgh, UK). For each sample, cDNA was converted to a sequencing library using the TruSeq standed mRNA-seq library for NeoPrep (Ilumina) and barcoded libraries were pooled and sequenced on an Illumina HiSeq 4000 using 125 base paired-end reads, to generate 50 million raw reads per sample.

4.3.5 Bioinformatic analysis of Differential gene expression

Reads were trimmed using Cutadapt version cutadapt-1.9 dev2 (Martin, 2011) for quality at the 3' end using a quality threshold of 30 and for adapter sequences of the TruSeq Nano DNA kit (AGATCGGAAGAGC) and a minimum length of 35bp. rRNA reads were removed using sortMeRNA (version 2.1) (Kopylova et al., 2012). The filtered reads were assembled using Trinity (version 2.5) (Grabherr et al., 2011) and over 5 million sequences were produced from the Trinity program. Transcripts were quantified using the RSEM method (Li et al., 2011) and any sequences with TPM < 1 and isopct < 1 were discarded. This reduced the number of sequences to 32,000. In order to further reduce any redundancy, transcripts with 95% similarity were clustered using CD-HIT-EST (version 4.7) (Fu et al., 2012; Li et al., 2006). Reads were annotated using Trinotate (version 3.1.1) (Grabherr et al., 2011) to identify putative protein coding sequences from the assembled transcriptome. Peptide sequences were predicted using transdecoder, which were further searched against the SwissProt non-redundant database using BLASTP (Camacho et al., 2009). BLASTX (Camacho et al., 2009) search was also performed with Trans-D as the query and the SwissProt non-redudant database as the target.

The Pfam databases (Eddy, 2011; Bateman et al., 2004) were used to predict protein domains using HMMER (Mistry et al., 2013). SignalP (version 4.1) (Nielsen et al., 2017) was used to predict the presence of signal peptides, and the TMHMM (Sonnhammer et al., 1998) was used to predict transmembrane helices within the predicted peptide sequences. The trimmed reads free from rRNA were aligned against the reference transcriptome using bwa mem (vesion 0.7.13-r1126) (Li et al., 2010) with parameter '-M' which marks split alignments as secondary and which can later be excluded by downstream tools. Duplicates were marked using Picard tools (version 2.8.1) (http://broadinstitute.github.io/picard).

4.3.5.1 Alignment-tree quantification

Read counts by transcript were generated using Salmon (version 0.9.1)(Patro et al., 2017). The assembly produced in 3.2.5.1 was used to produce a quasi-mapping index. The quantification step was carried out with parameter '-1 U' to specify a unstranded library and bias correction parameters –seqBias, --gcBias and –posBias (Patro et al., 2017).

4.3.5.2 Count pre-processing

Reads were filtered on counts per million (CPM) to remove transcripts consisting of near-zero counts and to avoid artefacts due to library depth. Transcripts were required to have a CPM >0.3 in at least 3 samples, corresponding to the smallest sample group as defined by Group, once any samples were removed. Reads were normalised using the weighted trimmed mean of M-values method (Robinson et al., 2010). 'TMM' was passed as the method to the calcNormFactors method of edgeR.

4.3.5.3 Differential expression analysis

EdgeR (version 3.16.5)(Robinson et al., 2010) was used to perform differential expression analysis with contrasts shown in Table 3.1. Fold changes were estimated as per the default behaviour of edgeR. Statistical assessment of differential expression was carried out with the quasi-likehood (QL) F-test using the following contrasts: Control vs 1°C, Controls vs 2°C and 1°C vs 2°C .To adjust for confounding covariates such as batch effects, a blocking factor was incorporated as part of the additive model. The following Gene Ontology (GO) gene sets were used: GO molecular function, GO Cellular component and GO Biological Process (Ashbirner et al., 2000; Subramanian et al., 2005).

For GO enrichment analyses, the GO annotations were extracted from the Trans-D_trinotate_annotation_report.txt. ROAST was executed using 9,999 rotations. GO terms that were not associated with at least five genes were excluded from the analysis. All transcripts in the contrasts of interest with either a BLASTX and/or a BLASTP annotation were re-searched against the human SwissProt database (Bairoch and Apweiler, 2005). A list of unique human protein identifiers was then entered into both the STRING (Szklarczyk et al., 2015) and PANTHER (Mi et al., 2017) databases to evaluate enrichment of functional groups.

4.3.6 Bioinformatic analysis of Population genetics

4.3.6.1 Generation, alignment and mapping of supertranscripts

Supertranscripts were generated from the assembled transcriptome using the script 'Trinity_gene_splice_modeler.py' provided with Trinity (version 2.5.0) (Haas et al., 2011). Trimmed and filtered reads were aligned to the supercontigs using STAR (version 2.5.2b) (Dobin et al., 2013). Potential PCR duplicates were marked using Picard tools MarkDuplicates. In accordance with GATK (DePristo et al., 2011) best practices, reads with split mappings were split into separate reads in the BAM files using GATK (version 3.7) tool SplitNCigarReads with parameters: -rf ReassignOneMappingQuality -RMQF 255 -RMQT 60 -U ALLOW_N_CIGAR_READS. Local realignment around indels was performed using GATK tools RealignerTargetCreator and IndelRealigner. A single pileup file was generated from the nine BAM files using samtools (Li et al., 2009) mpileup (version 1.3) with the parameters '-B -q 20-Q30'. These parameters result in bases with a base quality phred score of less than 30, and an alignment quality of less than 20, being discarded. A single '.sync' file was generated from the pileup file using 'mpileup2sync.jar' from PoPoolation2 (Kofler et al., 2011) (version 1.201).

4.3.6.2 Comparison of allele frequencies between groups

Bayenv2 (Günther & Coop, 2013) was used to measure the extent to which the allele frequencies of each SNP correlate with temperature. Bayenv2 is designed to take into account the extra level of sampling error arising from pooled data from a small number of individuals. In accordance with recommendations for running Bayenv2, a set of SNPs were selected to generate a matrix of covariance between samples. Only SNPs covered by at least five reads in at least six samples, and with a minor allele supported by at least five reads in total across all samples, were selected, and only one SNP per transcript was included. The covariance matrix was generated using Bayenv2 with the following parameters: -p 9 -k 200000, and specifying specifies four diploid individuals per sample with the '-s' flag. Z-scores for each SNP were calculated using Bayenv2 with the parameters: -p 9 k 200000 -r 8372 -n 1 -e standard_env.txt -x -m pool_matrix.txt –t. Where file 'pool_matrix.txt' contains the covariance matrix produced in the previous step, and 'standard_env.txt' contains standardised measures of temperature (in degrees centigrade).

4.3.6.3 Filtering of SNPs and estimation of FDRs for individual SNPs

Due to the various sources of noise in this dataset, we wanted to filter out SNPs that are most likely affected by sampling error. Before attempting to calculate FDRs or perform GSEA, the SNPs were filtered to remove low coverage SNPs. Specifically, we removed SNPs that were not covered by at least five reads in each sample, or which had a minor allele supported by less than 15 reads in total across the nine samples. Because Bayenv2 does not produce p-values, we estimated the statistical significance of our results by reference to a null distribution of Z-scores. This was created by randomly permuting the labels in file 'standard_env.txt' 100 times and recalculating the Z-scores for each SNP. The null distribution of Z-scores allowed us to calculate the probability of a high Z-score arising by chance. The false discovery rate (FDR) for each SNP was then calculated as follows: FDR=ip/n. Where i=number of SNPs in the dataset that achieved an equal or greater Z-score, n=total number of SNPs in all null permutations that achieved an equal or greater than Z-score, and p=number of permutations.

4.3.6.4 Estimation of FDRs for supertranscripts

A score for each supertranscript was calculated by taking the mean Z-score of all SNPs from that supertranscript. FDRs for each supertranscript with more than five SNPs that passed the filter were calculated from the null distribution as follows: FDR=ip/n. Where i=number of supertranscripts in dataset that achieved an equal or greater mean Z-score, n=total number of supertranscripts with at least five SNPs passing the filter in all null permutations that achieved an equal or greater mean Z-score, and p=number of permutations.

4.3.6.5 Calculation of minor allele frequencies

For each SNP, the minor allele frequency (MAF) was calculated for each of the three groups (see table 1) of samples. The MAF was calculated for each individual sample as MAF=m/t where m=number of reads supporting minor allele and t=total number of reads covering site. The effective allele number was also calculated for each sample at each SNP, using the formula e=((nc)-1)/(n+c) (Wiberg et al., 2017). MAF was calculated for each of the three groups by taking the average MAF for each sample weighted by the effective allele number for that sample. This allows varying the sampling error arising from the varying depths of coverage between samples to be accounted for.

4.4 Results

Samples were pooled due to the small amounts of RNA available in the individual *P. stalagmia* samples and in order to obtain sufficient RNA for sequencing. The TruSeq Total stranded RNA-Seq protocol requires 1200ng of input RNA (Edinburgh Genomics https://genomics.ed.ac.uk/resources/sample-requirement), which was not achievable using individual *P. stalagmia* samples in this study as total amounts of RNA were around 500ng per replicate. *P. stalagmia* are very small, the tubes of the worm are up to 6mm in length but the actual size of the worm is less than 6mm (Knight-Jones et al., 1972). Post pooling, there were a total of 3 replicates per treatment (Control, +1°C and +2°C) producing a final total of 9 samples.

4.4.1 Transcriptome assembly of P. stalagmia

After initial assembly with Trinity, there were 5,755,612 sequences. Contigs with a TPM < 1 and isoprct < 1 were filtered further, reducing the above number to a total of 75,132. Similar contigs were then clustered together, producing a final total of 61, 421 contigs. 23.86% of these transcripts contained protein sequences, out of which 63.45% showed matches to known proteins from the SwissProt database and 33.92% possessed functional information based on GO terms. Whilst comprehensive searches were conducted using different sequence databases (e.g. Pfam, SignalP, TmHMM, eggnog, KEGG and GO), the most comprehensive annotations were provided by the SWISS-PROT database (BLASTX and BLASTP).

3.5.1 Differential expression in the heated P. stalagmia samples compared with controls

Differential expression analysis was then performed on the contrasts specified in Table 4.1.

Table 4.1. Table of statistics showing the numbers of differentially expressed transcritps in each contrast according to the threshold on minimum fold-change (2) and maximum false discovery rate (0.05).

Contrast name	Up	Down	Level of annotation (%)
2°C vs Control	1,013	7	29.8
1°C vs Control	13,034	1,597	12.2
1°C vs 2°C	4,835	228	47.9

The principal component analysis (PCA) revealed a clear separation between each set of contrasts (control, 1°C and 2°C) (Figure 4.1.). In the 1°C vs Control contrast, a total of 14,631 transcripts were differentially expressed. The majority of these transcripts (13,034) were up-regulated in the 1°C samples compared with the controls, while 1,597 were down-regulated. Fewer transcripts were differentially expressed in the 2°C vs Control (1,020 in total) of which 1,013 were up-regulated in the 2°C samples and only 7 were down-regulated. In the PCA plot, two of the 2°C samples clustered closely together with good discrimination from the other samples, however the third sample (2B13) clustered more closely with the control samples. This may have resulted in fewer genes differentially expressed in the 2°C vs Controls and the 1°C vs Controls (1,020 and 5,063 respectively). However, the striking feature of the 2°C comparisons was the almost complete lack of down-regulation in the 2°C vs Control comprising only 7 transcripts.

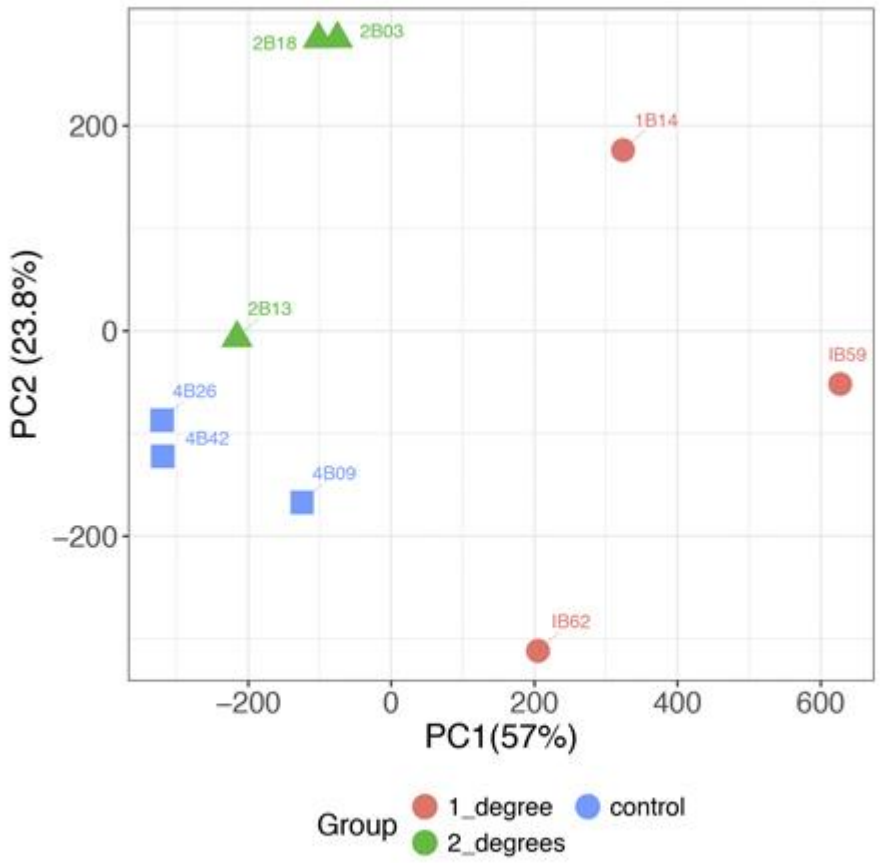

Figure 4.1. Principal component analysis (PCA) plot showing clustering of treatment groups and samples. Principal component 1 (PC1, x-axis) represents 57% and PC2 (y-axis) represents (23.8%) of total variation in the data.

The latter was reflected further by the GO analyses. GO enrichment analyses on these datasets showed significant enrichment below the threshold of the false discovery rate (FDR) of 0.05 only for the control versus 2°C comparison. There was a significant lack of representation of GO categories involved in transcription (Molecular Function: rRNA binding and DNA directed 5'-3' RNA polymerase activity) in the control samples compared with the 2°C samples (Table 4.2.) i.e. these processes were up-regulated and enriched in the 2°C samples.

Table 4.2. Enriched GO processes in the control versus 2°C transcriptome comparisons. Direction of "down" means that the processes were less represented in controls compared with 2°C and thus effectively enriched in 2°C compared to control samples.

	No of Genes	Proportion Down	Proportion Up	Direction	P-Value	FDR
GO Biological Process						
GO:0015031 PROTEIN_TRANSPORT	10	0.60	0.00	Down	0.001	0.011
GO:0006351 TRANSCRIPTION_DNA-TEMPLATED	29	0.59	0.14	Down	0.001	0.011
GO Molecular Function						
GO:0019843 RRNA_BINDING	24	0.75	0.00	Down	0.001	0.016
GO:0003899 DNA-DIRECTED_5'-3'_RNA_POLYMERASE_ACTIVITY	22	0.73	0.09	Down	0.001	0.016

Further analysis looking at logCPM values of the transcripts revealed the up-regulation of ribosomal genes in the 1°C vs Control contrast such as translation initiation factors (translation inhibition factor IF-3), elongation factors (elongation factor 1-alpha) and protein degradation transcripts such as E3 ubiquitin (Detailed in Appendix 1). Of the transcripts involved in respiration, ATP synthase and cytochrome transcripts (e.g. EXM, cytochrome P450 and cytochrome c oxidase) were also up-regulated. Cytoskeleton transcripts such as collagen, myosin and titin were also up-regulated in the 1°C vs Control contrast. These genes are required for thermal tolerance as they are involved in shaping cells and in many cell signaling pathways (Fletcher et al., 2010). Transcripts involved in antioxidant defenses: catalase, glutathione peroxidase, NFkappaβ, NOS and peptidyl-prolyl cis-trans isomerase were also up-regulated in the 1°C vs Control contrast (Detailed in Appendix 1). Glutathione peroxidase is one of the main antioxidant enzymes that catalyzes the dismutation of reactive oxygen species (ROS), which are severely harmful for cell survival (Sharma

et al., 2012). Of particular interest was the up-regulation of heat shock protein transcripts such as *hsp83*, *hsp70* and *hsp90* as some of these were previously explored in heat shock experiments using qPCR data in Chapter 3. Finally the up-regulation of caspase and death associated proteins indicating apoptosis were also observed.

There was a high number of ribosomal transcripts up-regulated in the 2°C vs Control samples. Transcripts involved in the cell cycle were up-regulated in the higher temperature treatment along with actin cytoskeleton transcripts and transcripts involved in ATP production (ATP synthase) (Detailed in Appendix 2). These results corroborate the GO enrichment analyses described above (Table 4.2.). Heat shock protein transcripts (*hsp70*, *hsc70* and *hsp90*) were also up-regulated in the 2°C vs Control contrast.

To identify critical biochemical pathways, the STRING program was used to visualise protein-protein interactions. This uncovered statistically significant enrichment of certain functional groups of proteins ($P < 1.0e^{-16}$), with a major cluster of transcription and translation proteins and satellite clusters of proteins involved in post-translational modification, the cell cycle, cytoskeleton, energy production and proliferation (data not shown). The PANTHER enrichment results were dominated by GO terms associated with RNA metabolism and cell division (Table 4.3.). Overall these data indicated the induction of the classical stress response to the warmer conditions and a lack of acclimation. This latter was previously observed in Chapter 3 on the qPCR and UTL data in the congeneric species *Romanchella perrieri*.

Table 4.3. PANTHER v13.1 GO-slim overrepresentation tests for biological processes and molecular functions assigned to 2°C differentially regulated transcripts under study.

Process	GO identifier	FDR
Biological processes for 2°C up-regulated transcripts		
Translation	0006412	2.02 e^{-13}
rRNA metabolic process	0016072	4.05 e^{-06}
Protein folding	0006457	8.62 e^{-03}
Generation of precursor metabolites and energy	0006091	4.05 e^{-03}
Cellular component biogenesis	0044085	7.04 e^{-10}
Cell cycle	0007049	2.90 e^{-04}
Organelle organisation	0006996	8.26 e^{-07}
Biosynthetic process	0009058	8.95 e^{-06}
Molecular function for 2°C up-regulated transcripts		
Structural component of ribosome	0003735	2.57 e^{-42}
Translation elongation factor activity	0003746	7.32 e^{-03}
Translation initiation factor activity	0003743	4.55 e^{-02}
Translation regulator activity	0045182	5.76 e^{-04}
Hydrogen ion transmembrane transporter activity	0015078	3.46 e^{-03}
Structural component of cytoskeleton	0005200	2.23 e^{-08}
Nucleotide binding	0000166	6.70 e^{-05}
mRNA binding	0003729	2.44 e^{-04}

4.4.2 Population genetic analysis

In order to test for allele frequency differences among the treatments, a total of 13,843 SNPs were called from the RNA-seq data according to strict criteria as described in the methods. Analysing each SNP individually resulted in no significant allele frequency differences among the groups after FDR correction (Table 4.4.). However, when the SNPs were analysed collectively as supertranscripts, 91 out of 521 genes (17.5%) showed a significant association with temperature after FDR correction (Table 4.4.). Go annotations could only be recovered for 14 of these genes (Detailed in Appendix 3) while Blast matches were obtained against ribosomal sequences, cytoskeletal proteins and serine/threonine kinases (Detailed in Appendix 3). The former are

involved in translation a result, which correlates with the transcriptome GO enrichment results. Cytoskeletal proteins such as tubulin and actin are structural proteins are often involved in the cellular stress response, whilst serine/threonine kinases are proteins that play critical roles in signal transduction affecting cellular processes such as cell division, proliferation and apoptosis (Manning et al., 2002).

Table 4.4. SNPs, genes and GO terms found to correlate with temperature

Analysis results	**Number**
Number of SNPs	13,843
Number of SNPs with Z-score >0.4999	839
Number of SNPs with FDR <=0.05	0
Number of genes with >=5 SNPs	521
Number of genes with FDR <=0.05	91
Number of GO terms with FDR <=0.05	0

4.5 Discussion

Protolaeospira stalagmia recruited on the heated panel treatments were not performing optimally in terms of their cellular response. Expression profiling of the 1°C animals revealed a highly active response to the warmer conditions with thousands of genes up-regulated compared to control organisms. Relatively little differential expression would be expected between these two treatments, if acclimation had occurred, with the physiology of the 1°C organisms being re-set to that of the controls. Clearly, the 1°C organisms were still trying to acclimatise their physiologies to the warmer conditions. At the more extreme temperature increase, analysis of the annotations associated with the up-regulated transcripts in the 2°C organisms revealed indications of cell stress. Almost one third of the transcripts comprised ribosomal genes. Similarly, there was up-regulation of transcripts putatively involved in translation (e.g. translation elongation factors), protein degradation (e.g. ubiquitin and proteomsome transcripts), cellular respiration (e.g. ATP synthase) and cell division (e.g. G2/mitotic-specific cyclin), indicating a substantial requirement for the enhanced generation of proteins, protein turnover and cell renewal in the warmer conditions. This probably therefore indicates a long-term thermal limit for this species on Adelaide Island.

As previously stated in the results, there was a clear separation between the 1°C and control samples resulting in a large number of transcripts being expressed differently between these two groups. There were fewer differentially expressed transcripts between the 2°C and control group due to the clustering of sample 2B13 with the control. Further analysis of this sample looking at photographs taken from the panels by Ashton et al., (2017) showed that the panel from which these samples were taken was not an outlier i.e. there were no distinct differences in community structure in this panel in comparison to the other 2°C panels. Thus it was likely that the clustering of this sample with the control group was due to biological variation. Given the small number of biological replicates in each treatment group, it was therefore not possible to remove this sample from the analyses.

Further analysis of the up-regulated transcripts in the 1°C vs Control contrast revealed the up-regulation of heat shock proteins (*hsp70*, *hsp90* and *hsp83*), one of the main molecular responses that is activated in a cell under thermal stress (Parsell & Lindquist, 1993; Gross, 2004). These proteins are of great interest as they have been suggested as a suitable biomarker of environmental stress (Feder & Hofmann, 1999) and a key predictor of the vulnerability of a species to changing conditions. When environmental conditions exceed an organism's ability to adapt physiologically, cellular stress responses such as the production of heat shock proteins decrease

the aggregation of unfolded proteins, assist in protein refolding and maintain the functioning of the cell (Parsell and Lindquist, 1993). Overexpression of one or more Hsps protects cells and tissues against exposures to diverse environmental stressors (Morimoto, 1998) and to oxidative damage at higher temperatures (Gonzalez et al., 2016).

Biomarkers of oxidative stress were observed in *P. stalagmia* in the 1°C treatment as enzymes involved in the oxidative stress response such as glutathione peroxidase and catalase were up-regulated in this treatment. These are however often present in the resting transcriptome of Antarctic species and thought to be a response to life in hyperoxygenated waters and the increased potential for damage from reactive oxygen species in the Southern Ocean (Chen et al., 2008; Clark et al., 2010; 2011). The up-regulation of both heat shock proteins and enzymes involved in oxidative stress indicated a metabolic response at the cellular level to cope with the temperature increase. This response was supported further by the up-regulation of genes involved in ATP synthesis such as ATP synthase and cytochrome genes, possibly to meet the high energy demands involved in the production of Hsps (Somero 2002, Sharma et al., 2010). However, the up-regulation of death associated proteins such as caspase observed in the transcriptome indicated the beginning of apoptosis in these organisms and suggested a lack of capability to deal metabolically with the higher temperature.

The above hypothesis was supported by the results observed in the 2°C treatment: ribosomal genes such as elongation factors and cell cycle genes (mitotic and translation inhibition factors) were up-regulated in the 2°C treatment compared to the control, indicating a substantial requirement for the enhanced generation of proteins, protein turnover and cell renewal in warmer conditions (Appendix 2) in *P. stalagmia*. There was also evidence of the activation of the classical cellular stress response (Parsell and Lindquist, 1993) represented by the up-regulation of genes involved in the thermal stress response such as *hsp70* and *hsp90*. The production of Hsps is energetically costly (Sørensen & Loeschcke, 2007) and generates high cellular demands for energy in terms of ATP production (Somero, 2002, Sharma et al., 2010). As such, these processes generate physiological trade-offs in order to cope with the high energy demands. The trade offs associated with the production of Hsps and environmental stressors have been previously observed in other marine organisms, such as the marine snail *Concholepas concholepas*. Under a reduced nutritional status, the snail showed lower levels of Hsp70 induction upon exposure to stress factors during low tide compared with snails in a good nutritional status (Jeno & Brokordt, 2014). Furthermore, Brokordt et al., (2015) also observed the reduced capacity of mature and spawned *Argopecten*

pupuratus scallops to increase Hsp70 production following an exposure to thermal and hypoxia stressors compared to that of immature individuals. In this case, reproductive investment limited the availability of energy in terms of ATP production for *hsp70* expression in the organisms exposed to environmental stress and increased their vulnerability to environmental stressors in comparison to immature individuals.

Trade offs associated with reproduction might have been observed in *P. stalagmia* over a longer deployment but due to the long generation times of Antarctic marine organisms (Clarke, 1988; Pearse et al., 1991) it was not possible to observe them in this study. However, it is possible that *P. stalagmia* individuals were not able to ingest sufficient food to fuel the increased metabolic demand at the higher temperatures. This is particularly relevant in encrusting filter feeders in Antarctica where food supply is highly seasonal and restricted to the summer months of primary production (Clarke, 1988). Although Ashton et al., (2017) observed the continuous increase in growth rates throughout the Austral summer (December-February) in *P. stalagmia* individuals in the heated panels, the transcriptional profile here indicated that the animals were close to, a tipping point in their ability to survive and unable to fuel their metabolism. The enhanced production of Hsps to cope with the aggregation of unfolded proteins and lack of energy reserves due to the death of phytoplankton over the Antarctic winter to fuel this increased metabolic demand, would eventually lead to oxidative stress and cell death in these organisms.

In some organisms such as the clam *Corbicula fluminea*, there appears to be a trade off between the heat shock response and the oxidative stress response. Both the thermal and oxidative stress responses are activated at intermediate temperatures but at high temperatures, the heat shock response is prioritized over the antioxidant protection, causing oxidative lesions to accumulate in clam tissues (Falfushynska et al., 2016). This was not the case in *P. stalagmia* where both systems are activated in the heated treatments (1°C and 2°C). The up-regulation of translation inhibition factors and actin cytoskeleton transcripts, which are known to be important indicators of cell health and are up-regulated in response to temperature increase (See Tomanek et al., 2011; Fields et al., 2012; Clark et al., 2017) indicated the start of cell death in these organisms.

The induction of antioxidant enzymes is an important line of defence against oxidative stress in biological systems but it can be compromised under temperature stress because of the thermal impairment of protein function (reviewed by Abele and Puntarulo, 2004). Impairment of antioxidants that act against free radicals such as superoxide dismutase (SOD) and glutathione

peroxidase (Halliwell et al., 1985) under thermal stress has been reported for different marine invertebrates (Abele et al., 2001, 2002). This loss of enzymatic antioxidant activity beyond critical temperatures might relate to heat-induced protein denaturation or disturbances of protein synthesis (Pörtner, 2002; Kregel, 2002). The up-regulation of *hsps* such as *hsp90* in the 2°C treatment known to be involved in apoptosis control (Lanneau et al., 2008) and the up-regulation of antioxidant transcripts such as glutathione peroxidase in the 1°C treatment in *P. stalagmia* indicated that the organisms are unable to sustain cellular homeostasis and were likely in a process of extended senescence.

These molecular data supported the UTL trials in Chapter 3 conducted on the congeric species *R. perrieri* were we observed a lack of acclimation in the species and all animals on the warmer panels were in a permanent state of resistance and/or decline. Given the lack of acclimation in these organisms, it was of interest to identify if there had been any post-recruitment selection in relation to temperature. Bayenv2 was chosen as the analysis tool because it can identify associations between allele frequencies and environmental variables while accounting for sampling error in pooled data (Günther & Coop, 2013). Small but significant allele frequency differences were observed in a total of 91 genes (0.14% of the total number of transcripts obtained in this study). However, Blast searching and GO analysis of individual genes produced few annotations. Although individual transcripts had putative functions associated with translation, the cytoskeleton and serine/threonine kinases, which linked directly with the major transcriptome results above, the selection of these genes was weak and it seems that they did not provide the animals with a sufficient physiological buffer in the warmer conditions. Hence, there was little evidence for post-recruitment selection and genetic adaptation within the *P. stalagmia* spirorbid population.

Overall, these molecular and UTL results suggest a lack of physiological and genetic flexibility in the encrusting species to warming. Organisms in the heated treatments had not acclimated to the elevated temperatures and were in fact resisting. This was further supported by the up-regulation of genes involved in thermal stress (*hsps*), respiration (ATP synthase) and oxidative stress (glutathione peroxidase) to cope metabolically with the effect of temperature on metabolism. The up-regulation of apoptotic transcripts such as caspase was an indication that even at 1°C, organisms were starting to experience cellular level problems. These impacts on cellular homeostasis may not be sustainable long-term especially with regard to the ability of these animals to maintain enhanced growth rates and sufficient food stores to ensure longevity. The

deployment of the panels for a longer period would have almost certainly led to the mortality of the organisms. It seems unlikely that these Antarctic benthic marine organisms are therefore, going to be able to cope to with a predicted end of century warming (IPCC, 2014).

4.6 References

Abele, D., Tesch, C., Wencke, P. and Pörtner, H. O. (2001). How oxidative stress parameters relate to thermal tolerance in the Antarctic bivalve *Yoldia eightsi*. *Antarct. Sci.* **13**, 111-118.

Abele, D., Heise, K., Pörtner, H. O. and Puntarulo, S. (2002). Temperature dependence of mitochondrial function and production of reactive oxygen species in the intertidal mud clam *Mya arenaria*. *J. Exp. Biol.* **205**, 1831-1841.

Abele, D. and Puntarulo, S. (2004). Formation of reactive species and induction of antioxidant defence systems in polar temperate marine invertebrates and fish. *Comp. Biochem. Physiol. A. Mol. Integr. Physiol.* **138**, 405-15.

Bateman, A., Coin, L., Durbin, R., Finn, R. D. et al. (2004). The Pfam protein families database. *Nucleic. Acids. Res.* **1**, D138-41.

Brokordt, K., Perez, H., Herrera, C. and Gallardo, A. (2015). Reproduction reduces HSP70 expression capacity in *Argopecten purpuratus* scallops subjected to hypoxia and heat stress. *Aquat. Biol.* **23**, 265-274.

Buckley, B. A. (2007). Comparative environmental genomics in non-model species: heterologous hybridization to DNA-based microarrays. *J. Exp. Biol.* **210**, 1602-6.

Buttergereit, F. and Brand, M. D. (1995). A hierarchy of ATP-consuming processes in mammalian cells. *Biochem. J.* **15**, 163-7.

Camacho, C., Coulouris, G., Avagyan, V., Ma, N., Papadopoulos, J., Bealer, K. and Madden, T. L. (2009). BLAST+: architecture and application. *BMC. Bioinform.* **10**, 421.

Chen, Z., Cheng, C., Zhang, J. et al. (2008). Transcriptomic and genomic evolution under constant cold in Antarctic notothenioid fish. *Proc. Natl. Acad. Sci. USA.* **105**, 12944-12949.

Chown, S. L., Hodgins, K. A., Griffin, P. C., Oakeshott, J. G., Byrne, M. and Hoffman, A. A. (2015). Biological invasions, climate change and genomics. *Evol. Appl***. 8**, 23-46.

Clark, M. S., Thorne, M. A. S., Vieira, F. A., Cardoso, J. C. R., Power, D. M. and Peck, L. S. (2010). Inshights into shell deposition in the Antarctic bivalve *Laternula elliptica*: gene discovery in the marine transcriptome using 454 pyrosequencing. *BMC. Genom*. **11**, 362.

Clark, M. S., Thorne, M. A. S., Toullec, J. Y., Meng, Y., Guan, L. L., Peck, L. S. and Moore, S. (2011). Antarctic krill 454 pyrosequencing reveals chaperone and stress transcriptome. *PLoS One.* **6**, e15919.

Clark, M. S., Ulf, S., Sihra, J., Thorne, M., Morley, S., King, M., Viant, M. and Peck, L. S. (2017). Biodiversity in marine invertebrate responses to acute warming revealed by a comparative multi-omics approach. *Glob. Change. Biol.* **23**, 318-330.

Clarke, A. (1988). Seasonality in the antarctic marine environment. *Comp. Biochem. Physiol. B. Comp. Biochem.* **3***,* 461-473.

Conesa, A., Madrigal, P., Tarazona, S., Gomez-Cabrero, D., Cervera, A., McPherson, A., Szczesniak, M. W., Gaffney, D. J., Elo, L. L., Zhang, Z. and Mortazavi, A. (2016). A survey of best practices for RNA-seq data analysis. *Genome. Biol.* **17**, 181.

De Wit, P. and Palumbi, S. R. (2013). Transcriptome-wide polymorphisms of red abalone (*Haliotis rufescens*) reveal patterns of gene flow and local adaptation. *Mol. Ecol*. **22**, 2884-2897.

DePristo, M. A., Banks, E., Poplin, E. B., Garimella, K. V., Maguire, J., Hartl, C. et al. (2011). A framework for variation discovery and genotyping using next-generation DNA sequencing data. *Nat. Genet.* **43**, 491-498.

Doblin, A., Davis, C. A., Schlesinger, F., Drenkow, J., Zaleski, C., Jha, S., Batut, P., Chaisson, M. and Gingeras, T. R. (2013). STAR: ultrafast universal RNA-seq aligner. *Bioinformatics*. **29**, 15-21.

Eddy, S. R. (2011). Accelerated profile hmm searches. *PLOS. Comput. Biol.* **7**, e1002195.

Edinburgh Genomics, https://genomics.ed.ac.uk/resources/sample-requirement.

Ern, R., Huong, D. T. T., Phuong, N. T., Madsen, P. T., Wang, T. and Barley, M. (2015). Some like it hot: Thermal tolerance and oxygen supply capacity in two eurythermal crustaceans. *Sci. Rep.* **5**, 10743.

Evans, T. G., Pespeni, M. H., Hofmann, G. E., Palumbi, S. R. and Sanford, E. (2017). Transcriptomic responses to seawater acidification among sea urchin populations inhabiting a natural pH mosaic. *Mol. Ecol*. **8**, 2257-2275.

Feder, M. and Hofmann, G. (1999). Heat-shock proteins, molecular chaperones, and the stress response: Evolutionary and Ecological Physiology. *Annu. Rev. Physiol*. **61**, 243–282.

Falfushynska, H. I., Phan, T. and Sokolova, I. M. (2016). Long term acclimation to different thermal regimes affects molecular responses to heat stress in a freshwater clam *Corbicula Fluminea*. *Sci. Rep.* **6**, 39476.

Fields, P. A., Marcus, J. Z. and Tomanek, L. (2012). Proteomic responses of blue mussel (*Mytilus*) congeners to temperature acclimation. *J. Exp. Biol.* **215**, 1106-1116.

Fletcher, D. A. and Mullins, R. D. (2010). Cell mechanics and the cytoskeleton. *Nature.* **436***,* 485-492.

Fu, L., Niu, B., Zhu, Z., Wu., S. and Li, W. (2012). Cd-hit: accelerated for clustering the next-generation sequencing database. *Bioinformatics.* **28**, 3150-3152.

Gao, Q., Liao, M., Wang, Y., Li, B. and Zhang, Z. (2015). Transcriptome analysis and discovery of genes involved in immune pathways from coelomocytes of sea cucumber (*Apostichopus japonicus*) after *Vibrio splendidus* challenge. *Int. J. Mol. Sci*. **16**, 16347-16377.

Gonzalez, K., Gaitan-Espitia, J., Font, A., Cardenas, C. and Gonzalez-Aravena, M. (2016). Expression pattern of heat shock proteins during acute thermal stress in the Antarctic sea urchin, *Sterechinus neumayeri*. *Rev. Chil. Hist. Nat*. **89**.

Grabherr, M. G., Hass, B. J., Yassour, M. et al. (2011). Full-length transcriptome assembly from RNA-Seq data without a reference genome. *Nat. Biotechnol.* **29**, 644-652.

Gross, M. (2004). Emergency services: a bird's eye perspective on the many different functions of stress proteins. *Curr. Protein. Pept. Sci.* **5**, 213-223.

Güther, T and Coop, G. (2013). Robust identificaiton of local adaptation from allele frequencies. *Genetics*. **195**, 205-20.

Haas, B. J., Papanicolaou, A., Yassour, M., Grabherr, M., Blood, P. D., Bowden, J., Couger, M. B. et al. (2013). De novo transcript sequence reconstruction from RNA-seq using the Trinity platform for reference generation and analysis. *Nat. Protoc*. **8**, 1494-512.

Halliwell, B. and Gutteridge, J. M. C. (1985). Free radicals in biology and medicine (2nd ed), Clarendon Press, Oxford, 188-276.

Helberg, M. E. (2009). Gene flow and isolation among populations of marine animals. *Ann. Rev. Ecol. Evo. Syst*. **40**, 291-310.

Hereford, J. (2009). A quantitative survey of local adaptation and fitness trade-offs. *Am. Nat*. **173**, 579-88.

Hilbish, T. J. (1985). Demographic and temporal structure of an allele frequency cline in the mussel *Mytilus edilus. Mar. Biol.* **86**, 163-171.

Hummel, H., Sommer, A., Bogaards, R. H. and Pörtner, H. O. (1997). Variation in genetic trait of the lugworm Arenicola marina: temperature related expression of mitochondrial allozymes? *Mar. Ecol. Prog. Ser*. **159**, 189-195.

Ighodaro, O. M. and Akinloye, O. A. (2017). First line defence antioxidants-superoxide dismutase (SOD), catalase (CAT) and glutathione peroxidase (GPX): Their fundamental role in the entire antioxidant defence grid. *Alexandria. Med. J*. In press.

IPCC (2014) Climate Change 2014 Synthesis Report Summary for Policymakers.

Jeno, K. and Brokordt, K. (2014). Nutritional status affects the capacity of the snail *Concholepas concholepas* to synthesize the Hsp70 when exposed to stressors associated with tidal regimes in the intertidal zone. *Mar. Biol.* **161**, 1039-1049.

Knight-Jones, P. and Walker, A. J. M. (1972). Spirorbidae (Serpulidae: Polychaeta) on limpets from the South Orkney Islands. *BAS. Bulletin.* **31**, 33-40.

Kopfler, R., Orozco-terWengel, P., De Maio, N., Pandey, R. V., Nolte, V., Futschik, A., Kosiol, C. and Schlötterer, C. (2011). PoPoolation: A toolbox for population genetic analysis of next generation sequencing data from pooled individuals. *PLos ONE*. **6**, e15925.

Kopylova, E., Noe, L. and Touzet, H. (2012). SortMeRNA: fast and accurate filtering of ribosomals RNAs in metatranscriptomic data. *Bioinformatics.* **28**, 3211-3217.

Kregel, K. C. (2002). Heat shock proteins: modifying factors in physiological stress responses and acquired thermotolerance. *J. Appl. Physiol.* **95**, 2177-86.

Lanneau, D., Brunet, M., Frisan, E., Solary, E., Fontenay, M. and Garrido, C. (2008). Heat shock proteins: essential proteins for apoptosis regulation. *J. Cell. Mol. Med.* **3**, 743-761.

Lesoway, M. P., Abouheif, E. and Collin, R. (2016). Comparative transcriptomics of alternative developmental phenotypes in a marine gastropod. *J. Exp. Zool.* **32**, 151-167.

Li, B. and Dewey, C. N. (2011). RSEM: accurate transcript quantification from RNA-Seq data with or without a reference genome. *BMC. Bioinform.* **12**, 1471-2105.

Li, H., Handsaker, B., Wysoker, A., Fennell, T., Ruan, J., Homer, N., Marth, G., Abercais, G. and Durbin, R. (2009). The sequence of alignment/map format and SAMtools. *Bioinformatics*. **15**, 2078-9.

Li, H. and Durbin, R. (2010). Fast and accurate long-read alignment with burrows-wheeler transform. *Bioinformatics.* **26**, 589-595.

Li, W. and Godzik, A. (2006). Cd-hit: a fast program for clustering and comparing large sets of protein or nucleotide sequences. *Bioinformatics.* **22**, 1658-1659.

Logan, C. A. and Buckley, B. A. (2015). Transcriptomic responses to environmental temperature in eurythermal and stenothermal fishes. *J. Exp. Biol.* **218**, 1915-1924.

Lv, F., Wang, T., Liu, F., Yu, Y., Qiao, G., Lv, L., Wang, Z. and Qi, Z. (2017). De novo assembly and characterization of transcriptome in somatic muscles of the polychaete *Perinereis aibuhitensis. J. Coast. Res*. **33,** 931-937.

Martin, M. (2011). Cutadapt removes adapter sequences from high-throughput sequencing reads, *EMBnet.journal, 17*. URL http://journal.embnet.org/index.php/embnet-journal/article/view/200.

McCormick, R. F., Truong, S. K. and Mullet, J. E. (2015). RIG: recalibration and interralation of genomic sequence data with the GATK. *G3.* **5**, 655-665.

McKenna, A., Hanna, M., Banks, E., Sivachenko, A., Cibulskis, K. et al. (2010). The genome analysis toolkit: A mapreduce framework for analyzing next-generation DNA sequencing data. *Genome. Res.* **20**, 1297-1303.

Meredith, M. P. and King, J. C. (2005). Rapid climate change in the ocean west of Antarctic Peninsula during the second half of the 20th century. *Geophys. Res. Lett.* **32**, L19604.

Mistry, J., Finn, R. D., Eddy, S. R., Bateman, A. and Punta, M. (2013). Challenges in homology search: Hmmer3 and convergent evolution of coiled-coil regions. *Nucleic. Acids. Res*. **41**, e121-e121.

Morimoto, R. I. (2018). Regulation of the heat shock transcriptional response: cross talk between a family of heat shock factors, molecular chaperones and negative regulators. *Genes. Dev.* **12**, 3788-3796.

Morley, S. A., Lemmon, V., Obermuller, B. E., Spicer, J. I., Clark, M. S. and Peck, L. S. (2011). Duration tenacity: a method for assessing acclimatory capacity of the Antarctic limpet, *Nacella concinna*. *J. Exp. Mar. Biol. Ecol*. **399**, 39-42.

Neave, M. J., Streten-Joyce, C., Nouwens, A. S., Glasby, C. J., McGuiness, K. A., Perry, D. L. and Gibb, K. S. (2012). The transcriptome and proteome are altered in marine polychaetes (Annelida) exposed to elevated metal levels. *J. Proteomics*. **75**, 2721-2735.

Nicholls, R. J. and Cazenave, A. (2010). Sea-level rise and it's impact on coastal zones. *Science*. **238**, 1517-1520.

Nielsen, E. E., Hemmer-Hansen, J., Poulsen, N. A. et al. (2009). Genomic signatures of local directional selection in a high gene flow marine organism; the Atlantic cod (*Gadus morhua*). *BMC. Evol. Biol.* **9**, 276.

Nielsen, H. (2017). Predicting secretory proteins with signalp. *Methods. Mol. Biol.* **1611**, 59-73.

Panova, M. and Johannesson, K. (2004). Microscale variation in Aat (aspartate aminotransferase) is supported by activity differences between upper and lower shore allozymes of *Littorina saxitalis*. *Mar. Biol*. **144**, 1157-1164.

Parsell, D. A. and Lindquist, S. (1993). The function of heat-shock protein in stress tolerance-degradation and reactivation of damaged proteins. *Ann. Rev. Genet.* **27**, 437-496.

Patro, R., Duggal, G., Love, M. I., Irizarry, R. A. and Kingsford, C. (2017). Salmon provides fast and bias-aware quantification of transcript expression. *Nat. Methods.* **14**, 417-419.

Pearse, J. S., Mcclintock, J. B. and Bosch, I. (1991). Reproduction of Antarctic benthic marine invetebrates: tempos, modes and timing. *Integr. Comp. Biol.* **31**, 65-80.

Peck, L. S. (2002). Ecophysiology of Antarctic marine ectotherms: limits to life. *Polar. Biol.* **25**, 31-40.

Peck, L. S. (2018). Antarctic marine biodiversity: adaptations, environments and responses to change. *Oceanogr. Mar. Biol. Annu. Rev.* in press.

Pespeni, M. H. and Palumbi, S. R. (2010). The purple sea urchin genome suggests local adaptation along a latitudinal gradient despite high gene flow. *Integr. Comp. Biol*. **50**, E136.

Pespeni, M. H., Chan, F., Menge, B. A. and Palumbi, S. R. (2013). Signs of adaptation to local pH conditions across an environmental mosaic in the california current ecossytem. *Integr. Comp. Biol*. **53**, 857-870.

Pfaffl, M.W., Horgan, G.W. and Dempfle, L. (2002). Relative expression software tool (REST) for group-wise comparison and statistical analysis of relative expression results in real-time PCR.

Pörtner, H. O. (2002). Climate variations and the physiological basis of temperature dependent biogeography : systemic to molecular hierarchy of thermal tolerance in animals. *Comp. Biochem. Physiol. A. Mol. Integr. Physiol.* **132**, 739–761.

Pörtner, H. O. and Gutt, J. (2016). Impacts of climate variability and change on (marine) animals: physiological underpinning and evolutionary consequences. *Integr. Comp. Biol.* **56**, 31-44.

Reid, P. C., Fisher, A. C., Lewis-Brown, E. et al. (2009). Impacts of the oceans on climate change. *Adv. Mar. Biol*. **56**, 1-150.

Rhee, J. S., Won, E. J., Kim, R. O., Choi, B. S., Choi, I. Y., Park, G. S., Shin, K. H., Lee, Y. M., Lee, J. S. (2011). The polychaete *Perinereis nuntia* ESTs and its use to uncover potential biomarker genes for molecular ecotoxicological studies. *Environ. Res.* **112**, 48-57.

Robinson, M. D., McCarthy, D. J. and Smyth, G. K. (2010). Edger: a bioconductor package for differential expression analysis of digital gene expression data. *Bioinformatics.* **26**, 139-140.

Sanford, E. and Kelly, M. W. (2011). Local adaptation in marine invertebrates. *Annu. Rev. Mar. Sci*. **3**, 509-35.

Schmidt, P. S. and Rand, D. M. (2001). Adaptive maintenance of genetic polymorphism in an intertidal barnacle: habitat- and life- stage specific survivorship of MPI genotypes. *Evolution.* **55**, 1336-1344.

Sharma, S., Singh, R., Kaur, M. and Kaur, G. (2010). Late-onset dietary restriction compensates for age-related increase in oxidative stress and alterations of HSP70 and synapsin1 protein levels in male Wistar rats. *Biogerontology.* **11**, 197-209.

Sharma, P., Jha, A. B., Dubey, R. S. and Pessarakli, M. (2012). Reactive oxygen species, oxidative damage and antioxidative defense mechanism in plants under stressful conditions. *J. Bot.* **217037**, 1-26.

Somero, G. N. (2002). Thermal physiology and vertical zonation of intertidal limits and costs of living. *Integr. Comp. Biol.* **4**, 780-789.

Somero, G. N. (2010). Effects of climate change: how potentials for acclimatization and genetic adaptation will determine 'winners' and 'losers'. *J. Exp. Biol*. **213**, 912-920.

Somero, G. N. (2015). Temporal patterning of thermal acclimation: from behaviour to membrane biophysics. *J. Exp. Biol.* 167-169.

Somero, G. N. and DeVries, A. L. (1967). Temperature tolerance of some Antarctic fishes. *Science*. **156**, 257-8.

Sommer, A., Klein, B. and Pörtner, H. O. (1997). Temperature induced anaerobiosis in two populations of the polychaete worm *Arenicola marina*. *J. Comp. Physiol. B.* **167**, 25-35.

Sonnhammer, E. L., Von Heijne, G., Krogh, A. et al. (1998). A hidden markov model for predicting transmembrane helices in protein sequences. *Proc. Int. Conf. Intell. Syst. Mol. Biol.* **6**, 175-182.

Sørensen, J. G., Nielsen, M. M. and Loeschcke, V. (2007). Gene expression profile analysis of *Drosophila melanogaster* selected for resistance to environmental stressors. *J. Evol. Biol.* **20**, 1624–1636.

Sotka, E. E. and Palumbi, S. R. (2006). The use of genetic clines to estimate dispersal distances of marine larvae. *Ecology*. **87**, 1094-103.

Tomanek, L., Zuzow, M. J., Ivanina, A. V., Beniash, E. and Sokolova, I. M. (2011). Proteomic responses to elevated pCO2 level in eastern oysters, *Crassostrea virginica*: evidence for oxidative stress. *J. Exp. Biol.* **1**, 1816-44.

Turner, J., Lu, H., White, I., King, J. C., Phillips, T., Hosking, J. S. et al., (2016). Absence of 21st century warming on Antarctic Peninsula consistent with natural variability. *Nature*. **535**, 411–415.

Wernberg, T., Thomsen, M. S., Tuya, F. and Kendrick, G. A. (2011). Biogenic habitat structure of seaweeds change along a latitudinal gradient in ocean temperature. *J Exp Mar Biol Ecol*. **400**, 264-271.

Wiberg, R. A., Gaggiotti, O. E., Morrissey, M. B. and Ritchie, M. G. (2017). Identifying consistent allele frequency differences in studies of stratified populations. *Methods. Ecol. Evol*. **8**, 1899-1909.

Zielinski, S. and Pörtner, H. O. (1996). Energy metabolism and ATP free-energy change of the intertidal worm *Sipunculus nudus* below a critical temperature. *J. Comp. Physiol.* **166B**, 492-500.

Chapter 5

Analysis of the biodiversity of biofilm communities from the heated settlement panels

5.1 Abstract

Biofilms are critical components of marine systems that induce settlement and metamorphosis in many marine invertebrates, an essential process critical to establish marine communities. The composition of biofilms and their subsequent biofouling communities is dependent on a range of environmental factors, including temperature. To date, there are few studies looking at the effects of *in situ* oceanic warming on the marine benthic biofilm community. In this study, we analysed the biodiversity of biofilm communities from the Ashton et al., (2017) experiment, after a further period of 9 months *in situ* warming (total exposure of 18 months). Amplicon sequencing of bacterial 16S rRNA was used to evaluate the effects of a +1°C and +2°C temperature increase in the microbial composition of the benthic biofilm. Biofilm community composition was similar in the +1°C and control treatment and different in the +2°C. Analysis of the rare oligotypes removed from the original analysis revealed similar presence and abundance of oligotypes across treatments with the exception of two oligotypes that were more abundant in the +2°C treatments. This initial study only evaluated bacterial species at the DNA level, i.e. presence/absence and in the future it could be more useful to conduct such studies alongside transcriptomic analyses. There were small differences in the biofilm community observed within a panel of the same treatment, which would be expected given the differences in bare space and in benthic assemblages observed in Ashton et al., (2017) study. As with many other marine bacterial studies, the lack of reference genomes made it difficult to assign a taxonomic identity to the species level for many samples. Nevertheless, this is one of the few studies to look at the effects of *in situ* elevated temperature on marine biofilm communities and the first Antarctic study. With the development of heated settlement panels, studies that look at the development of benthic assemblages and biofilm communities will become key in order to understand the effects of predicted end of century oceanic warming.

5.2 Introduction

Settlement and metamorphosis of marine invertebrates have drawn great interest because of their role in establishing benthic marine communities (Fraschetti et al., 2003). Recruitment to optimal habitats is essential for sessile invertebrates, as metamorphosis is often irreversible and successful recruitment is therefore largely linked to post-settlement environmental pressures (Whalan et al., 2014). Early studies of invertebrate reproduction assumed that the massive production of eggs by many marine invertebrates allowed larval settlement to be a random process, i.e. the few larvae fortunate enough to descend to a suitable site at the end of larval life were sufficient to establish and maintain communities. However, by the 1950s the studies of Wilson (1952, 1954 and 1955) revealed that larvae of some polychaetes settle selectively on suitable substrata and avoid unsuitable substrata. Subsequent investigations focused on selective settlement of larvae and it is now well established that larval settlement is far from random and that the larvae of many species settle in response to specific environmental cues: cues induced by adults of the same species, induced by prey and by biofilms (Hadfield and Paul 2001).

Some marine invertebrates settle preferentially on or among individuals of their own species, resulting in gregarious or aggregative settlement. An example of this this is that of oyster larvae responding to waterborne cues from adult oysters (Zimmer-Faust et al., 1994). Further examples can be found in the polychaete literature. Marine polychaete worms of the family Sabellariidae live in tubes of cemented sand grains and often form extensive colonies of these sand tubes by recruiting larvae from the plankton. Evidence that chemical cues in the tube cement triggered larval settlement were first reported by Wilson (1968). Chemicals cues induced by prey organisms induce the metamorphosis in larvae of the coralivorous nudibranch *Phestilla sibogae* (Hadfield et al., 1985). For many species, it is clear that the cues are associated with surface biofilms composed of bacteria, diatoms and other microorganisms. The latter is particularly well documented in the polychaete literature: the serpulid polychaete *Hydroides elegans* will not settle in the absence of a biofilm (Hadfield et al., 1994). Biofilms also effectively induce larval settlement on the congeneric species *Hydroides dianthus* (Toonen & Pawlik, 1994) and on the spirorbid worm *Janua brasiliensis* (Kirchman et al., 1982), where competent larvae typically attach to a surface, secrete a primary tube and commence metamorphosis within 15 minutes of contact with an inductive biofilm (Carpizo-Ituarte and Hadfield, 1998).

As such, biofilms are critical components of biofouling in most marine systems. The generation of biofouling communities is a sequential process starting with the accumulation of adsorbed organics, followed by the settlement and growth of pioneering microorganisms, which secrete a matrix of extrapolymeric substances (EPS) that form a highly complex, dynamic three-dimensional structure. This is then followed by the colonisation of micro- and macrofoulers (Chambers et al. 2006). Bacterial biofilm communities contribute to fundamental microbial processes including the degradation of organic matter and environmental pollutants and are often involved in biological processes such as photosynthesis, nitrogen fixation, sulphate reduction and fermentation (Lock et al., 1984).

The composition of biofilms and their subsequent biofouling communities is dependent on geographical and seasonal variations (Dang & Lovell, 2016). More importantly, biofilm community composition can change when exposed to variable environmental conditions and as such, strongly affect larval settlement and subsequent community development. As temperature impacts the development and composition of biofilms, studies elucidating the influences of temperature on biofilm community composition and development of micro and macrofoulers are particularly relevant given predicted oceanic warming conditions (IPCC, 2014). Increased oceanic warming could influence the production of chemical cues that induce larval settlement and impact the overall community composition. Currently there is very little understanding on how future oceanic warming (IPCC, 2014) will impact benthic biofilm communities and subsequently, the larvae that settle on them (Keough & Raimondi, 1996; Pritivera et al., 2011).

To date there have been several studies manipulating biofilms generated or maintained in aquaria. For example, in a study by Huang et al., (2003) benthic biofilms were shown to influence whether the tube worm*, Hydroides elegans*, attached and metamorphosed from its larval stage to an adult. This is particularly important since the pelagic larval phase of sessile marine invertebrates is critical to species distributions and settlement is often irreversible (Marshall et al., 2010; Whalan & Webster, 2014). Larval settlement of the coral reef sponge *Rhopoloeides odorabile* was induced by biofilms developed at higher temperatures in comparison to those developed at lower ones (Whalan & Webster, 2014), with more larvae settling in the heated treatments. This is also true for other marine species i.e. Lau et al., (2005) reported that larval settlement of the barnacles *Balanus amphitrite* and *B. trigonus* were also induced by biofilms developed at high temperatures (23°C and 30°C) compared to those at lower temperatures. Temperature also alters the proteomic responses of individual organisms within a biofilm community. In a study by Mosier et al., (2014)

elevated temperature repressed carbon fixation proteins from two *Leptospirillum* genotypes whereas carbon fixation proteins were up regulated at higher temperatures by a third member of this genus.

In contrast to terrestrial (Walker et al., 2006) and freshwater (Williamson et al., 2016) ecosystems, there have been very few field based controlled manipulations of temperature in the marine environment. The vast majority of our existing knowledge stems from laboratory-based mesocosm experiments (Neal & Yule, 1994). For example, Jeong et al., (2014) used a microfluidic system where continuous temperature gradients were generated to look at the effects of temperature on biofilm conformation in the lab. Mesocosm experiments are important because they increase experimental tractability, but they typically focus on one or a few target species in isolation and fail to mimic natural biotic and abiotic variation (Wernberg et al., 2012). Furthermore, many of these experiments are short term and thus do not take into account the seasonal and inter annual changes in the effects of marine biofilms (Lidbury et al., 2012; Villanueva et al., 2011). For example, in a short term intertidal study (5 weeks) by Russell et al., (2013) looking at the combined exposure of elevated temperature and carbon dioxide on biofilms and their consumers, the combination of elevated temperature and CO_2 caused a decrease in the amount of primary productivity consumed by grazers while the abundance of biofilms increased. However, when exposed to a much longer period (5 months) the abundance of benthic biofilms decreased due to an increase in the grazing rates of the gastropod species *Littorina littorea* (Russell et al., 2013). Thus emphasising that laboratory experiments may be confounded by the exposure time and the effects of being held in an artificial environment.

In some cases, anthropogenic activities such as the thermal discharges from power plants, give rise to unique opportunities to study temperature changes in the natural environment i.e. an increase in water temperature near a nuclear power plant enhanced the metabolism of bacteria and increased biofilm growth in the experimental area (Rao, 2010). Therefore, given the highly complex interactions between biofilms, larval responses and environmental fluctuations, studying benthic biofilms in the field is an essential step towards gaining a more holistic understanding on how temperature affects recruitment potential and the development of biofouling communities.

The development of heated panels capable of manipulating temperature *in situ* is key in bridging the gap between mesocosm and field experiments to evaluate warming effects on biofilms. A recent study (Smale et al., 2017) used this technology by deploying panels in the marine

environment that heated the water at +3°C and +5°C above ambient temperature, over a total period of 40 days. Increased temperature resulted in significant shifts in community structure across bacteria, protists and metazoans, which supports previous findings on how temperature can alter biofilm community composition (Mosier et al., 2014; Romaní et al., 2014). Other studies (Ashton et al., 2017) have utilised this technology to study the effects of temperature on growth rates and community composition of benthic invertebrates.

The panels in (Ashton et al., 2017) are different to those of Smale et al., (2017): they heat the water at +1°C and +2°C above ambient, thus matching the IPCC's end of century oceanic warming predictions (IPCC, 2014) and were deployed for a longer period, 9 months prior to evaluating the effect on the biodiversity of biofouling organisms. The authors reported the near doubling of growth rates of the bryozoan *Fenestrulina rugula* and a reduction in the overall species diversity and evenness in heated panels due to the spatial dominance of *F. rugula*. As previously mentioned, the interplay between biofilms, larval settlement and environment stressors and the complexity of these makes it hard to dissect the causes and changes observed at the community level in benthic communities. As such, it was unclear whether changes in biofilm diversity due to increased temperature (as observed in Smale et al., 2017) could have contributed to the observed findings in Ashton et al., (2017). In this study, we analysed the biodiversity of biofilm communities from the Ashton et al., (2017) experiment, after a further period of 9 months *in situ* warming. Amplicon sequencing of bacterial 16S rRNA was used to evaluate the effects of a +1°C and +2°C temperature increase in the microbial composition of the benthic biofilm in the heated settlement panels, after an 18 month immersion at Rothera Research Station, Antarctica.

5.3 Methods

Two independent experiments were carried out to investigate the differences in microbial composition in the biofilm formed in heated and non-heated settlement panels. As sample sizes were very small, an initial set of test biofilm samples were collected after a two month immersion (short-term) from heated and non-heated panels deployed on the benthos at 15m to validate laboratory methodologies prior to NGS sequencing. The aim was to identify an appropriate DNA extraction technique and to verify the presence of Antarctic microbial communities using 16S rRNA PCR amplification, with subsequent transformation of amplified products into *Escherichia coli* cells and limited Sanger sequencing. A subsequent set of biofilm samples was taken after 18 month immersion (long-term) and the differences in the microbial composition of the biofilm on the panels at different temperatures (Control, +1 °C, +2 °C) were investigated through 16S rRNA amplicon sequencing.

5.3.1 Test samples: Short-term immersion panels

5.3.1.1 Sample collection

Biofilm samples were obtained after two months immersion from heated and non-heated panels (1 of each +1°C, +2°C and control) deployed in January 2011 at Rothera Research Station, Adelaide Island, Antarctic Peninsula (67° 4' 07" S, 68° 07' 30" W). Two biofilm swabs per treatment (n=2 for each +1 °C, +2 °C and control) were taken by wiping a sterile gauze across the panel and were snap frozen in liquid nitrogen for subsequent analysis.

5.3.1.2 DNA extraction and PCR

For each treatment (n=2 for each +1°C, +2°C and control) one of the biofilm swabs was cut in to three equal pieces to allow for technical replicates. Total genomic DNA was extracted from the biofilm swabs using the PowerBiofilm DNA isolation kit (MO BIO Laboratories, Inc.) following manufacturer's instructions. DNA samples were quantified using Nanodrop (NanoDrop, ND-1000) and electrophoresed on a 1.5 % agarose gel (90 v, 20 min) to check DNA integrity.

The hypervariable V4 region of the 16S rRNA genes were PCR-amplified using the forward primer 16s_515Fw (5' GTGCCAGCMGCCGCGGTAA) and the reverse primer 16S_806Rv (5' GGACTACHVGGGTWTCTAAT). PCR reactions were carried out in a total volume of 25µL containing Q5 Hot Start High Fidelity 2 X Master Mix (BioLabs Inc.), 10µM of each primer, 1µL of Bovine Serum Albumin (BSA) and 1µL of genomic DNA template following manufacturer's instructions. The amplification was carried out in a GS4 thermal cycler (G-Storm) under the following conditions: 98°C for 30s, 25 cycles of 98°C for 10s, 50°C for 30s and 72°C for 30s. A final elongation step at 72°C for 2min was performed. Resulting PCR products were checked for efficient amplification by standard agarose gel (1.5%) electrophoresis (80v, 50min). Primer efficiency was optimised across a temperature gradient and for number of PCR cycles. Each round of PCR reactions included a no template control to check for contamination.

5.3.1.3 Transformation and Sequencing

Amplification products were cloned using the NEB PCR Cloning kit (BioLabs Inc) following manufacturer's instructions. Amplified products were ligated into plasmid vectors (Linearized pMiniT 2.0) and transformed in to *Escherichia coli* competent cells (DH5α) following manufacturer's instructions (Invitrogen). The resultant mixture (containing 950µl of SOC medium and the vector-cell reaction) was plated on to pre-warmed agar plates containing 100µg/ml ampicillin. Clones were left to develop overnight (16h) at 37°C. Plates were inspected for recombinant colonies (white plaques) and colonies containing inserts were handpicked into a 96 well micro-plate (containing TYE media and ampicillin (100ug/ml)) and sent to a commercial sequencing facility, Source Bioscience (Cambridge, UK) for Sanger sequencing. Sequences were obtained in an ABI file format and viewed in Finch TV version 1.4.0 (Geospiza, Inc., Seattle) to check the quality. Processed sequences were compared to those available in GenBank using the BLAST tool in Finch TV to determine the highest sequence similarity match.

5.3.2 Long-term immersion panels

5.3.2.1 Sample collection

Biofilm samples were taken from heated and non-heated panels deployed on the benthos at 15m after 18 months immersion at Rothera Research Station, Adelaide Island, Antarctic Peninsula (67° 4' 07" S, 68° 07' 30" W). Panels were brought up to the surface by SCUBA divers and placed in a 10l tank on the boat with sea water at the same temperature as the ambient sea water (0°C). 4-5

biofilm swabs were taken per panel (n=1 panel for each of +1 °C, +2 °C and control) and stored in 100% ethanol for subsequent analysis.

5.3.2.2 DNA extraction and PCR

Total genomic DNA was extracted from the biofilm swabs using the PowerBiofilm DNA isolation kit (MO BIO Laboratories, Inc.) following manufacturer's instructions. A blank swab was also included and extracted as a non-template control to check for background contaminants (Kim et al., 2017). DNA samples were assessed for concentration and quality using a NanoDrop ND-100 Spectrometer (NanoDrop Technologies) and an Agilent 2200 Tapestation (Agilent Technologies). To enable compatibility with the Illumina 16S Metagenomic Sequencing Protocol, a set of primers different to those in the test samples were used. The hypervariable V4 region of the 16S rRNA genes were PCR-amplified using the 16S Amplicon PCR forward primer (5' TCGTCGGCAGCGTCAGATGTGTATAAGAGACAGCCTACGGGNGGCWGCAG) and the 16S Amplicon reverse PCR primer (5' GTCTCGTGGGCTCGGAGATGTGTATAAGAGACAGGACTACHVGGGTATCTAATCC). PCR reactions were carried out in a total volume of 25µL containing 2X KAPA Hifi HotStart ReadyMix, 1µM of each primer and 2.5µL of DNA sample. Amplifications were carried out in an AlphaCycler (PCRmax) under the following conditions: 95°C for 30s, followed by 25 cycles of 95°C for 30s, 55°C for 30s and 72°C for 30s. A final elongation step at 72°C for 5min was performed. Resulting PCR products were checked by standard agarose gel (1.5%) electrophoresis (80v, 50min). PCR products were purified using the QIAquick PCR Purification kit (Qiagen) following manufacturer's instructions.

5.3.2.3 Sequencing

Library preparation and sequencing was carried out by the Department of Biochemistry at the University of Cambridge. A total of 13 samples including a blank swab were sequenced. For each sample (n=4-5 swabs per panel per treatment: +1 °C, +2 °C and control) DNA was converted in to a sequencing library using the 16S Metagenomic Sequencing Library preparation kit (DNA input 1ug, 8 PCR cycles), and sequenced in triplicate (39 samples total) on an Illumina MiSeq using 300 base paired-end reads, to generate 44-50 million raw reads per pool.

5.3.2.4 Bioinformatics

We used Oligotyping analysis to explain biofilm community composition differences in heated and non-heated settlement panels. Oligotyping entails systematically identifying nucleotide positions that represent information-rich variation among closely related sequences and generating oligotypes. The identification of similarities and differences between DNA sequences requires the comparison of nucleotide residues at positions that share a common evolutionary history. For oligotyping, the artificial insertion or deletion of bases in sequence reads versus naturally occurring length variation requires the use of alignment tools for the insertion of gaps that will dissipate artificial length variations and align sites that share a common evolutionary history. The concatenation of nucleotides from information-rich variable positions in sequencing reads defines an oligotype. Oligotypes converge towards the minimal number of nucleotide positions that will explain the maximum amount of biological diversity. The oligotyping software pipeline utilizes Shannon entropy (Shannon, 1948) as the default method to identify positional variation to facilitate the identification of nucleotide positions of interest.

Adapters were trimmed from the raw reads using Trimalore software (Krueger, 2015). Reads were merged using mothur v.1.35.1 (Kozich et al., 2013, MiSeq SOP site accessed on the 18/08/17). Entropy and oligotyping analyses were conducted according to Eren et al., (2013). Sequences were not aligned to a reference alignment since length read varied due to partially overlapping reads. Hence the *0-pad-with-gaps* script from the Minimum entropy decomposition (MED) pipeline 1.2 (Eren et al., 2015) was run on the reads. All analyses were carried out using default parameters unless otherwise specified. MED analysis was performed using the MED pipeline version 1.2. The minimum substantive abundance criterion (M) was set to 50 to filter noise in the data. After the initial round of oligotyping, high entropy positions were chosen (-C option). To minimise the impact of sequences errors, we required an oligotype to be represented in at least 1000 reads (-M option). Moreoever, rare oligotypes present in less than 5 samples were discarded (-s option). These parameters led to 1,478,129 sequences being left in the database.

5.3.2.5 Statistical analysis

Matrix output files from the oligotype pipeline were exported into R studio (RStudio Team, 2015). Abundance of oligotypes across treatments was compared using multivariate analysis models in the R environment for statistical computing using the *vegan* package. The reference model included an interaction between treatment and oligotype:

>Permanova <- adonis (Data~ Treatment*oligotype, method = “bray”, header = “TRUE”, perm = 999).

5.4 Results

5.4.1 Oligotype analyses

Oligotyping analysis of biofilm composition in panels subjected to different treatments (control, +1°C and +2°C) yielded 16 unique oligotypes across 14 samples from 1,478,129 sequences. The minimum relative abundance threshold removed 350 rare oligotypes. The most abundant oligotypes represented 90% of the reads. Oligotypes that were abundant in at least one sample (>1% relative abundance) were always found across all treatments, meaning abundant oligotypes were ubiquitous across all host-associated treatments. Oligotype richness varied across treatment.

The abundance of each oligotype varied across the treatments although not significantly (PERMANOVA, P = 0.16). The TG oligotype was the most relative abundant overall and it was observed in all of the samples and across all treatments (control, +1°C and +2°C). The relative abundance of the TG oligotype was similar across all samples and treatments, with the highest relative abundance observed in control- swab 4 (19.4%) and in the 2°C- swab5 (19.9%) samples and the lowest relative abundance observed in the 2°C- swab1 (12.8%) sample. The relative abundance of the TG oligotype ranged in the control treatments from 15.5% (in the control- swab3 sample) to 19.8% (in the control- swab4 sample). In the 1°C treatment, the relative abundance of the TG oligotype ranged from 13.9% (in the 1°C- swab1 sample) to 17% (in the 1°C- swab3). In the 2°C treatment, the relative abundance of the TG oligotype ranged from 12.8% (in the 2°C- swab1 sample) to 19.9% (in the 2°C- swab5 sample).

The AG oligotype was the second most relative abundant oligotype in all samples and across all treatments. The highest abundance was observed in the 2°C- swab5 sample (11.5%) and the lowest relative abundance was observed in the control- swab3 sample (5.8%). The AG oligotype was more abundant in the samples in the 2°C and 1°C treatments (ranging from 8-11.5%) than in the samples in the control treatment (ranging from 5-8%). The TA oligotype was more dominant in samples from the control and 1°C treatments (ranging from 7.3% in the 1°C- swab4 sample to 11.3% in the control- swab4 sample) than in samples in the 2°C treatment (ranging from 4.4% in the 2°C- swab2 sample to 7.8% in the 2°C- swab1 sample).

In contrast, the GG oligotype was more relative abundant in 2°C treatments (ranging from 2.1% in the 2°C –swab2 sample to 8.9% in the 2°C- swab3 sample) than in the control and 1°C treatments (ranging from 1.6% in the control- swab3 sample to 2.8% in the 1°C- swab4 sample). The CA

oligotype was more relative abundant in the 2°C treatment (ranging from 4.3% in the 2°C- swab5 sample to 9.6% in the 2°C- swab1 sample) than in the control and 1°C (ranging from 3.6% in the control- swab4 sample to 6.5% in the 1°C- swab4 sample). A complete list of each oligotype and distribution across each sample can be found in Figure 5.1.

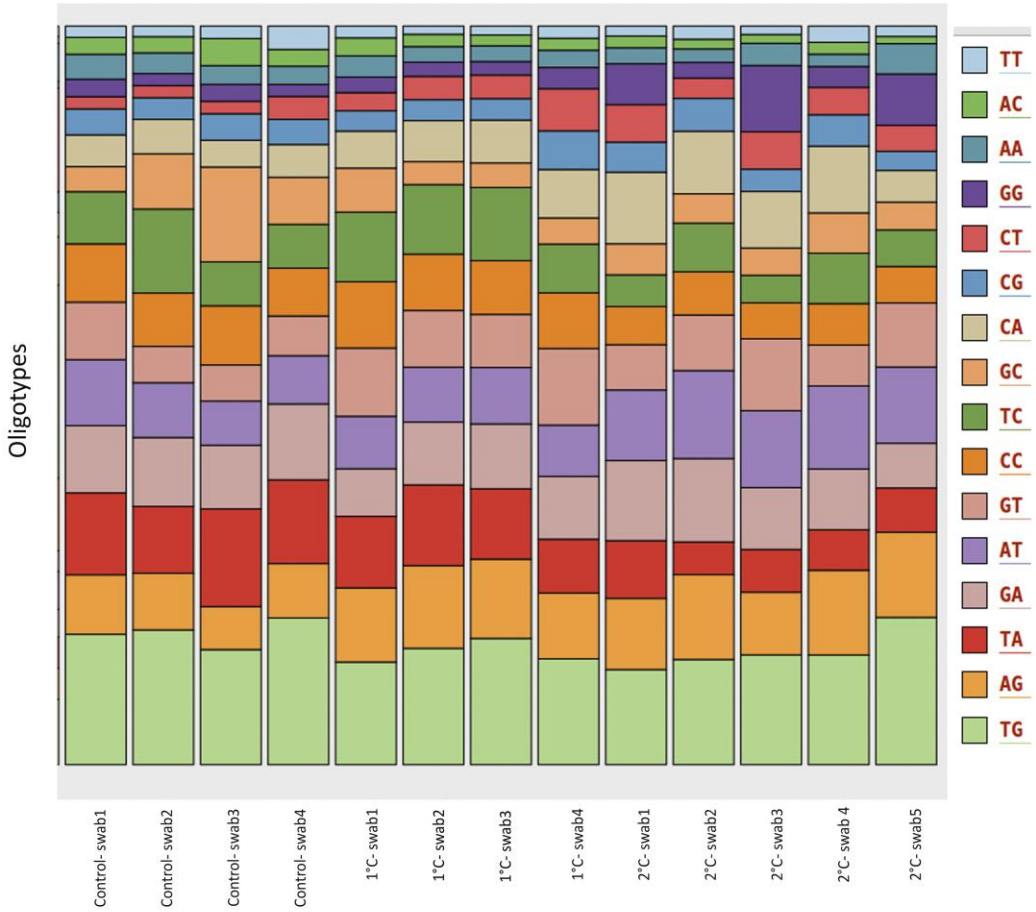

Figure 5.1. Proportions of abundant oligotypes in the biofilm samples for the different treatments (Control, +1°C and +2°C) and swabs

5.4.2 Community and treatment relationships

Cluster analysis using Bray-Curtis similarity ratio obtained from normalised oligotype data revealed no biofilm community differences between the +1°C and control treatment. Samples (represented by swabs) in the control treatment in general clustered together, with swabs 2 and 4 being more similar in composition than swab 3. In the 1°C treatment, swabs 2 and 3 were more similar in composition than swab 1. Swab 4 in this treatment did not cluster with the 1°C swabs, instead it clustered with the 2°C treatment, under the 2°C- swab5 sample (Figure 5.2). The 2°C treatment community composition was different to the 1°C and control treatment, with the exception of the swab 4 from the 1°C treatment as previously stated.

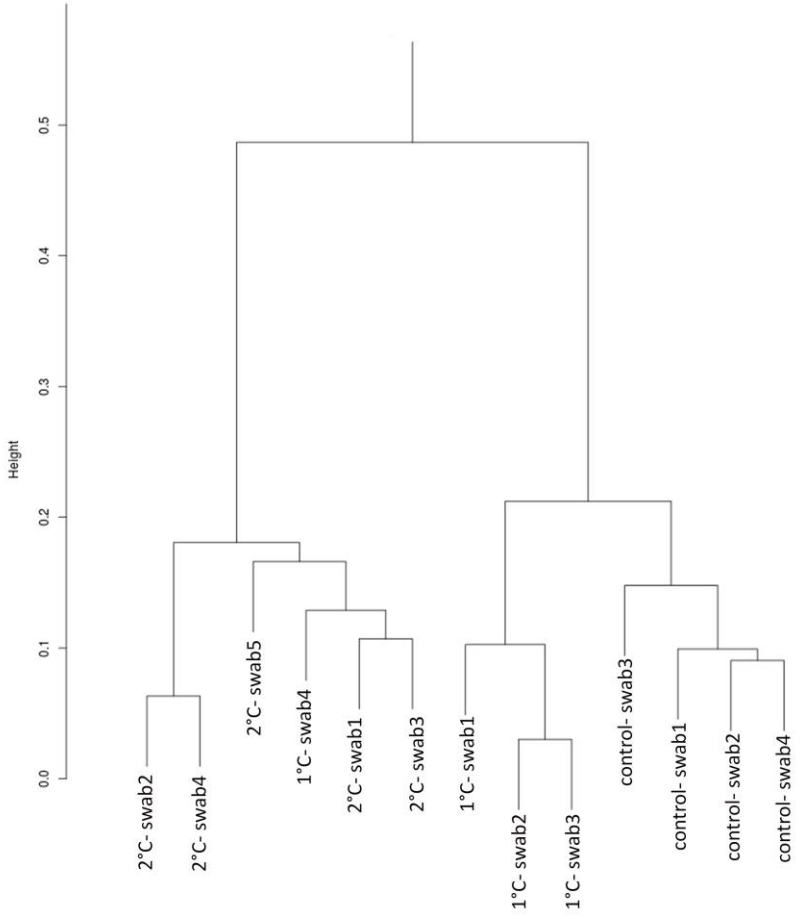

Figure 5.2. Bray-Curtis distances measures for oligotypes from biofilm communities from heated (1°C and 2°C) and non-heated (Control) panels for different samples (Swab1-5)

These cluster-analysis results are also reflected in the NMDS analyses which showed no differences in the biofilm community composition of panels in the control and 1°C treatment but a difference in community composition of panels in +2°C treatment compared to the control and 1°C treatment (Figure 5.3).

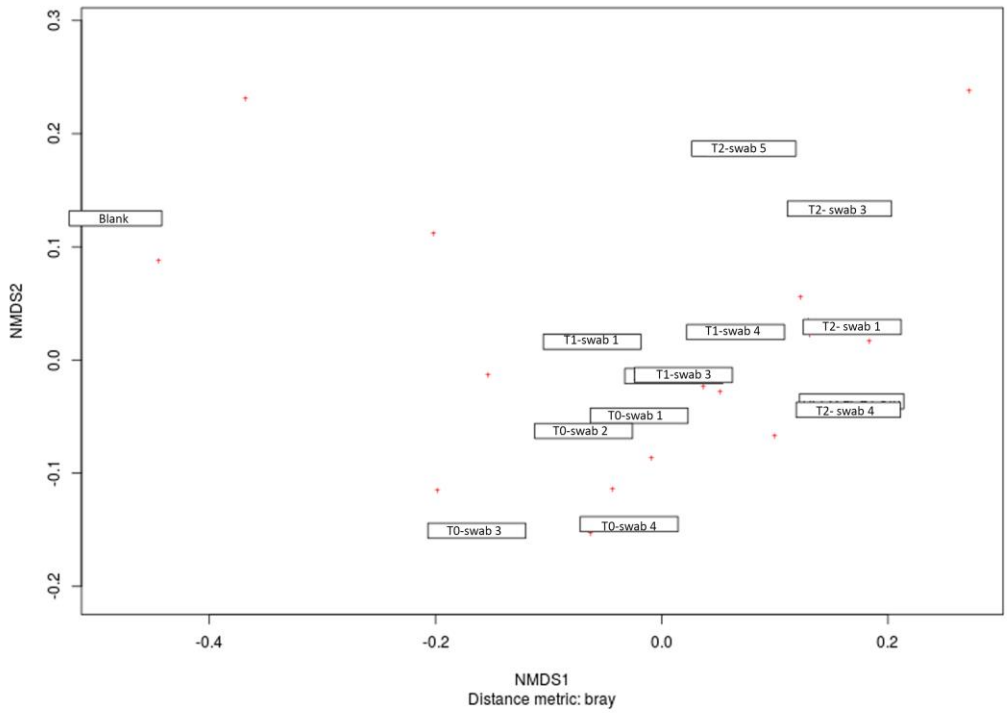

Figure 5.3. Non-metric dimensional scaling (NMDS) ordination for oligotypes of 14 biofilm samples, for 4-5 swabs per treatment: control, +1°C and +2°C. T0 = control, T1 = 1°C and T2 = 2°C.

5.4.3 Blast matches and Taxonomy

Individual oligotype sequences were Blast searched against reference sequences in the NCBI's nr database. Most of the sequence matches of the oligotypes against the database yielded uncultured marine bacterium and uncultured gamma proteobacterium, as is often the case with Antarctic marine bacteria due to poor database coverage and annotation of marine bacterium databases (Countinho et al., 2017). This was true for the oligotypes AC, TT, CT, CC, GT, AT, GA, TG, AA and AG with highest identity score against uncultured marine bacterium or uncultured gamma proteobacterium. A phylogenetic tree was constructed based on maximum likelihood analysis (Figure 5.4). The oligotype TC clustered with the *Shewanella* bacterium spp. This is a species of marine bacteria consisting of gram-negative proteobacteria with a wide distribution, from the deep sea to the shallow Antarctic Ocean (Dikow et al., 2011). The AG oligotype was most closely related to the *Aureispira* and *Saprospira* spp, both also marine bacteria of the *Saprospiraceae* family. Three strains of gliding bacteria belonging to the genus *Saprospira* have been isolated from marine sponges and algae from the southern coastline of Thailand (Hosoya et al., 2006). The genus *Aureispira* contains two species: *Aureispira marina* (Hosoya et al., 2006) and *Aureispira maritima* (Hosoya et al., 2007). Members of the *Saprospiraceae* are generally associated with the degradation of organic material (Cottrell et al., 2000).

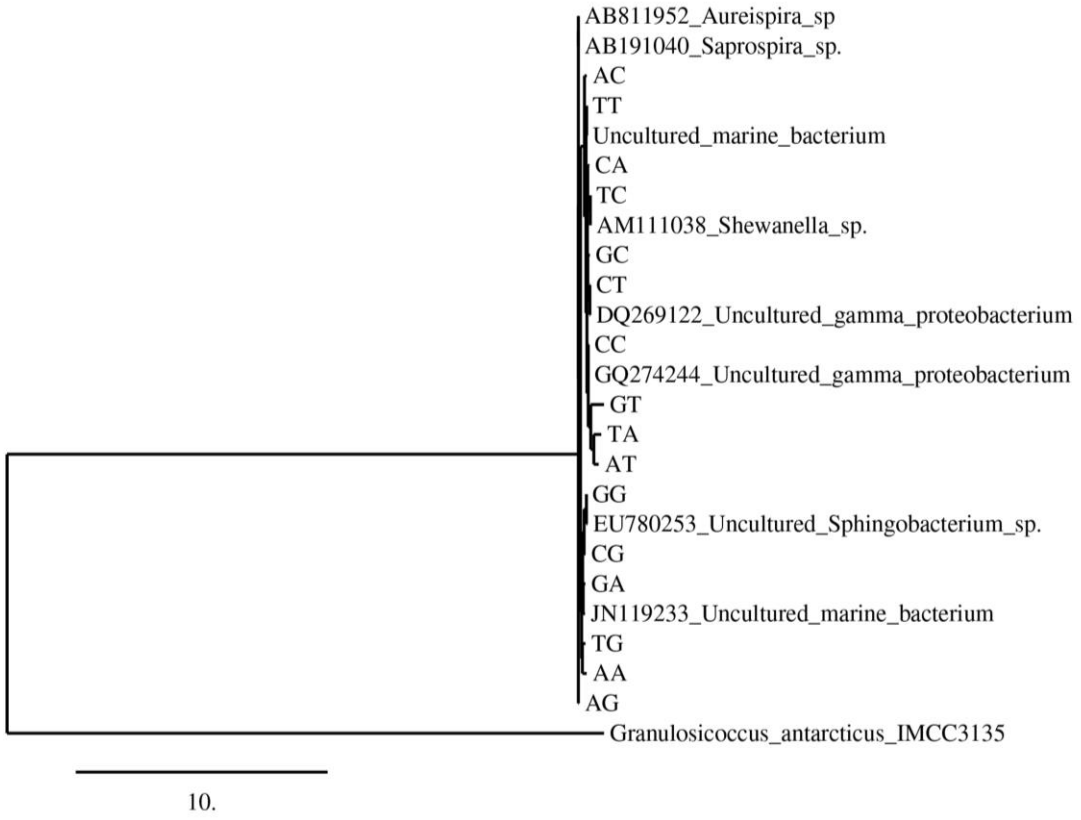

Figure 5.4. Maximum likelihood phylogenetic tree showing the affiliation of oligotypes identified through oligotyping analyses against reference sequences.

5.4.4 Analysis of rare oligotypes

Further oligotyping analysis was performed on the rare oligotypes removed from the original analysis to look at differences in microbial diversity in the rarer species between treatments (Control, +1°C and +2°C). Oligotyping analysis of the rare oligotypes revealed similar presence of oligotypes and similar abundances across treatments. There were two oligotypes however, that were slightly different across treatments. The GAGGTTAGTCTGATCTGGGACCCAACGT oligotype was more relative abundant in the 2°C treatment (ranging from 4.8-25.6%), in particular in the 2°C- swab3 (25.6%) and in the 2°C-swab5 (17.7%) than in the 1°C treatment (5.9-7.7%) and absent in the control treatment. BLAST search against NCBI's nr database revealed closest similarity to *Leucothrix* spp, a *Gammaproteobacteria* associated with epiphytes on marine plants and algae (Brock, 2006). The relative abundance of the AGGTTGTTAACAGCTGAATCAACTG oligotype was similar across treatments except in the 2°C-swab3 (25.6%) and 2°C-swab 5 (17.2%) sample, where it was more abundant than in any of the other samples and treatments (ranging from 0.2% in the Control- swab1 sample to 13.5% in the 2°C- swab1 sample) . BLAST search against NCBI's nr database revealed closest similarity to an uncultured marine bacteria of the *Gammaproteobacteria* Class.

5.5 Discussion

In this study we examined biofilm communities from heated and non-heated settlement panels after 18 months immersion from the Ashton et al., (2017) experiment. Oligotyping analysis revealed 16 unique oligotypes with similar abundance across treatments (Control, +1°C and +2°C) and samples (Figure 5.1.). The community and treatment oligotype Bray-Curtis cluster analysis revealed that the biofilm community was similar between the control and 1°C treatment but different in the 2°C treatment in comparison to the control and 1°C (Figure 5.2.) It is possible that a 1°C increase in temperature might not be enough to drive differences in biofilm composition and community structure in the panels but a 2°C increase could.

Only one other study has looked at the effects of *in situ* elevated temperature on community structure and composition of biofilms (and also metazoans and protists) (Smale et al., 2017). The study reported significant shifts in the community structure of bacteria with greater richness in the communities held at higher treatments as determined by the number of bacterial OTUs. The temperatures employed in the Smale et al., (2017) study however, were much greater: a 3°C and 5°C increase instead of the 1°C and 2°C increase employed in this study. Furthermore, the experiment was performed in a temperate habitat during which maximum temperatures fell below thermal maxima for most taxa, and as such, the taxa were more likely to have responded positively to the higher temperatures. In the Antarctic, there is a lack of knowledge about most bacterial biofilms and their response to environment conditions (Jeong et al., 2014). Of the few studies performed, the results indicate that there are optimal temperature ranges for biofilm development of Antarctic marine bacteria (Jeong et al., 2014) e.g. in a *Pseudoalteromonas* species this range is from -2°C to 10°C. Furthermore, as temperature regulates many environmental genes in microorganisms, higher temperature increases might result in a cell surface change of the extra-polymeric substance production that can subsequently affect the development of microbial biofilms (Nevot et al., 2008). The extent to which this might be the case in Antarctica, is unknown.

The effect of temperature on biofilm development and production of extra-polymeric substances is particularly important in polychaetes as cues released by bacterial biofilms are known to mediate the settlement and metamorphosis of their larvae. For example lectins released by bacterial biofilms in the spirorbid worm *Janua brasiliensis* mediate the settlement and metamorphosis of the polychaete larvae (Kirchman et al., 1982). In some cases, a single bacterium has been shown to strongly influence the settlement of larvae of *Hydroides elegans* in single-species biofilms. Huang et al., (2012) identified that a set of genes is essential to the inductive

capacity of *Pseudoalteromonas luteoviolacea*: *P. luteoviolacea* produce complex arrays of organelles known as bacteriocins that must be present in their entirety for metamorphosis in larval *H. elegans* to occur.

There were small differences observed in the biofilm community within a single panel of the same treatment (Figure 5.2). In the 2°C treatment, swab2 and swab4 were different to swab1 and swab3. Similarly, swab 4 in the 1°C treatment was more similar to the 2°C treatment community, according to the Bray-Curtis cluster analysis. These biofilm community differences within a single panel reflect the importance of considering the micro-scale differences in biofilm community and composition within a small area, which is often overlooked at in such studies. Small biofilm community differences within a panel can be driven by the benthic organisms that have settled next to where the biofilm samples were taken or the availability of free space. For benthic sessile communities, where competition for space can influence Darwinian fitness, availability of free space for recruitment is criticall. Free space results in bare surfaces with associated biofilm communities that can vary according to the age of the biofilm and temperature (Diaz-Villanueva, 2011). For example, the polychaete *Hydroides elegans* in Hawaii preferentially settles on aged biofilms over un-filmed surfaces (Hadfield et al., 1994). When considering Ashton et al., (2017) results, a 1°C increase in temperature produced an increase in the overall percentage cover of the panels whilst coverage in the 2°C panels was highly variable. This availability of free space in the 2°C panels compared to the 1°C, could have influenced the biofilm community composition differences we observed in this study.

Furthermore, the development of the benthic community after 18 months almost certainly influenced the biofilm community over time. In terms of the benthic assemblages established on the panels, the 1°C panels were dominated by the bryozoan *Fenestrulina rugula* whilst the 2°C panels were again highly variable (Ashton et al., 2017). These differences in benthic community structure with a higher dominance of *F. rugula* in the 1°C panels, could also drive some of the differences observed in the biofilm samples between the 1°C and 2°C treatments. The presence of antibacterial compounds has been demonstrated to allow bryozoans to manipulate the microbial film growing on them, which in turn may influence the types of organisms that are able to settle near them or on them. This ability makes the substrate nearby more suitable for the settlement of their own larvae (Schellenberger and Ross, 1998). Scholz et al., (2005) also looked at the relationship between bryozoan spatial variance and biofilms in cool-temperate to subtropical latitudes, revealing that in tropical reefs, the occurrence of bryozoans is mainly linked to the

competitive pressure of microbial mats and not the competitive pressure with macroorganisms. Therefore, whilst biofilms play an important role in initiating settlement of marine invertebrates (Whalan et al., 2014), marine invertebrates also influence the development of microbial mats. Thus, the 18 month biofilms on these plates are a result of these complex interactions.

A major limitation of any study involving a marine biofilms (including the present one) is the lack of reference genomes, even for dominant taxa (Heidelberg et al., 2010). Metagenomic outputs of the most current high-throughput sequencing technologies (such as Illumina) often result in a mixture of multiple genomes most of which do not cover a complete genome of the organisms of interest since the complete reference genomes of known organisms are lacking in the databases (Simon and Daniel, 2011; Teeling and Glöckner, 2012). This is even more predominant in Antarctic marine biofilms that are under-studied (Webster et al., 2006). Therefore, many studies rely on universally occurring DNA sequences, either partial or complete such as 16S rRNA genes. Oligotyping however, enables the detection and classification of distinct subpopulations within a genus or even within a single species as shown for *Gardnerella vaginalis* in humans (Eren et al., 2011). However, due to the absence of genome-specific libraries from Antarctic marine bacteria, it was therefore difficult to assign a taxonomic identity at the species level to many samples.

In our study, many of the oligotypes yielded highest similarity against uncultured marine bacteria (Figure 4.4) of the *Gammaproteobacteria* class. Of the few oligotypes that were more closely identifiable to species level, the AG oligotype was most closely related to the *Aureispira* and *Saprospira* species of the *Saprospiraceae* family and the oligotype TC to the *Shewanella* spp, of the *Gammaproteobacteria* class. These species, in particular *Shewanella*, are known to play an important role in bioremediation and the biogeochemical cycles of elements in freshwater and marine ecosystems (Li et al., 2018). *Saprospiraceae* are also found in bacterial biofilm communities that colonise algal surfaces (Burke et al., 2011) and are considered of interest as they play an active role in controlling algal blooms in oceans (Hau et al., 2007). The *Gammaproteobacteria* and in particular the *Saprospiraceae* are also often found in close proximity to waste water due to their ability to hydrolise and utilise carbon sources (McIlroy et al., 2014).

These results are similar to those of Webster et al., (2006) who observed benthic Antarctic marine biofilms around McMurdo station. In that study, community structure and composition of marine microbial biofilms established on glass surfaces was investigated across three differentially contaminated sites within McMurdo Sound. Each of the sites were dominated by different

bacterial groups: *Alphaproteobacteria*, *Gammaproteobacteria* and cytophaga-flavobacterium-bacteroides (CFB) depending on the level of contamination from the station. The least impacted site contained high *Gammaproteobacteria* whilst *Planctomycetales* dominated the highly impacted site. Whilst, our site in North Cove where the panels were deployed, was in close proximity to Rothera Research Station's waste management facility, the lack of *Planctomycetales* indicates that contamination from the station was minimal. In addition, when Webster et al., (2006) compared the diversity of the biofilms in the least impacted site to that in a previous study (Webster et al., 2004) on a tropical reef and the biofilm diversity was similar to that of a 4-week-old reef. Thus, the presence of *Gammaproteobacteria* and *Saprospiraceae* spp in this study indicates that the biofilms were reflecting the natural microbial community around the station. However, further sites and samples taken at multiple sites further away from the waste management facility would be necessary in order to confirm this, but such studies are constrained by access to power supplies.

In this study, temperature seems to have an effect on the biofilm community in the 2°C panels in comparison to the 1°C and control treatment. There were small differences in biofilm community observed within a panel of the same treatment, which would be expected given the differences in bare space and in benthic assemblages observed in Ashton et al., (2017) study i.e. biofilms next to the bryozoan *F. rugula* might be different in composition to those next to the spirorbid worm *Romanchella perrieri*. These micro-scale differences reflect the importance of considering the diversity of biofilms within a small area and should be taken in to account in future studies. Although biofilm community composition was relatively stable between treatments, those on the +2°C plates are starting to show changes, as is the biodiversity of the biofouling species. This initial study only evaluated bacterial species at the DNA level, i.e. presence/absence and in the future it could be more useful to conduct such studies alongside transcriptomic analyses. The aim would be to determine how temperature affects the functionality of the bacterial community, especially in terms of the nutrients or exudates produced which may be metabolised by the biofoulers, which in turn could affect their resilience or sensitivity.

As with many other marine bacterial studies, the lack of reference genomes makes it difficult to assign a taxonomic identity to the species level for many samples. Nevertheless, this is one of the few studies to look at the effects of *in situ* elevated temperature on marine biofilm communities and the first Antarctic study. With the development of heated settlement panels, studies that look at the development of benthic assemblages and biofilm communities will become key in order to

understand the effects of predicted end of century oceanic warming (IPCC, 2014) on marine communities.

5.6 References

Adams, C. M., Shumway, S. E., Whitlatch, R. B. and Getchis, T. (2011). Biofouling in marine molluscan shellfish aquaculture: a survey assessing the business and economic implications of mitigation. *J. World. Aquac. Soc.* **42**, 242-252.

Ashton, G. V., Morley, S. A., Barnes, D. K. A., Clark, M. S. and Peck, L. S. (2017). Warming by 1°C Drives Species and Assemblage Level Responses in Antarctica's Marine Shallows. *Curr. Biol.* **27***,* 2698–2705.

Brock, T. D. (2006). The Genus Leucothrix. The Prokaryotes, pp3247-3255.

Burke, C., Thomas, T., Lewis, M., Steinberg, P. and Kjelleberg, S. (2011). Composition, uniqueness and variability of the epiphytic bacterial community of the green alga *Ulva australis*. *ISME.* **5**, 590-600.

Carpizo-Ituarte, E. and Hadfield, M. G. (1998). Stimulation of metamorphosis in the polychaete *Hydroides elegans* Haswell (Serpulidae). *Biol. Bull*. **194**, 14-24.

Chambers, L. D., Stokes, K. R., Walsh, F. C. and Wood, R. J. K. (2006). Modern approaches to marine antifouling coatings*. Surf. Coat. Technol.* **201***, 3642-3652.*

Cottrell, M. T. and Kirchman, D. L. (2000). Natural assemblages of marine proteobacteria and members of the Cytophaga-Flavobacter cluster consuming low-and high-molecular-weight dissolved organic matter. *Appl. Environ. Microbiol.* **66**, 1692-1697.

Countinho, F. H., Silveira, C. B., Gregracci, G. B., Thompson, C. C., Edwards, R. A., Brussaard, C. P. D., Dutilh, B. E. and Thompson, F. L. (2017). Marine viruses discovered via metagenomics shed light on viral strategies throughout the oceans. *Nat. Commun.* **8**, 1038.

Crisp, D. J. and Ryland, J. S. (1960). Influence of filming and of surface texture on the settlement of marine organisms. *Nature. 4706*.

Dang, H. and Lovel, l. C. R. (2016). Microbial Surface Colonization and Biofilm Development in Marine Environments. *Microbiol. Mol. Biol. Rev*. **80**, 91–138.

Dikow, R. B. (2011). Genome-level homology and phylogeny of *Shewanella* (Gammaproteobacteria: Iteromonadales: Shewanellaceae). *BMC. Genomics.* **12**, 1471-2164.

Eren, M. A., Zozaya, M., Taylor, C. M., Dowd, S. E., Martin, D. H. and Ferris, M. J. (2011). Exploring the diversity of *Gardnerella vaginalis* in the genitourinary tract microbiota of monogamous couples through subtle nucleotide variation. *PLoS. One.* **6**, e26732.

Fitridge, I., Dempster, T., Guenther, J. and Nys, RDe. (2012). The impact and control of biofouling in marine aquaculture : a review. *Biofouling.* **7***, 649-669.*

Fraschetti, S., Giangrande, A., Terlizzi, A. and Boero, F. (2003). Post-settlement events in benthic community dynamics. *Oceanol. Act*. **25**, 285-295.

Hadfield, M. G., Unabia, C. C., Smith, C. M. and Michael, T. M. (1994). Settlement preferences of the ubiquitous fouler Hydroides elegans. In: Thompson, M. F., Nagabhushanam, R., Sarojini, R., Fingerman, M. (eds). Recent development in biofouling control. Oxford and IBH Pub. Co., New Delhi, pp 65-74.

Hadfield, M. G. and Paul, V. J. (2001). Natural chemical cues for settlement and metamorphosis of marine invertebrate larvae. In: McClintock J. B., Baker, W. (eds). Marine chemical ecology. CRC Press, pp 431-461.

Hau, H. H. and Gralnick, J. A. (2007). Ecology and biotechnology of the genus *Shewanella*. *Annu. Rev. Microbiol.* **61**, 237-258.

Heidelberg, K. B., Gilbert, J. A. and Joint, I. (2010). Marine genomics: at the interface of microbial ecology and biodiscovery. *Microb. Biotechnol.* **3**, 531-543.

Hosoya, S., Arunpairojana, V., Suwannachart, C., Janjana-Opas, A. and Yokota, A. (2007). *Aureispira maritima* sp. nov., isolated from marine barnacle debris. *Int. J. Syst. Evol. Microbiol.* **57**, 1948-51.

Hosoya, S., Arunpairojana, V., Suwannachart, C., Kanjana-Orpas, A. and Yokota, A. (2006). *Aureispira marina* gen. nov., sp. nov, a gliding, arachidonic acid-containing bacterium isolated from the southern coastline of Thailand. *Int. J. Syst. Evol. Microbiol.* **56**, 2931-2935.

Huang, S. and Hadfield, M. G. (2003). Composition and density of bacterial biofilms determine larval settlement of the polychaete *Hydroides elegans*. *Mar. Ecol. Prog. Ser.* **260***,* 161–172.

Huang, Y., Callahan, S. and Hadfield, M. G. (2012). Recruitment in the sea: bacterial genes required for inducing larval settlement in a marine worm. *Sci. Rep*. **2**, 228.

IPCC (2014) Climate Change 2014 Synthesis Report Summary for Policymakers.

Jeong, H. H., Jeong, S. G., Park, A., Jang, S. C., Hong, S. G. and Lee, C. S. (2014). Effect of temperature on biofilm formation by Antarctic marine bacteria in a microfluidic device. *Anal. Biochem.* **446***,* 90–95.

Keough, M. J. and Raimondi, P. T. (1996). Responses of settling invertebrate larvae to bioorganic films : Effects of large-scale variation in films. *J. Exp. Mar. Bio. Ecol.* **207***,* 59-78.

Kirchman, D., Graham, S., Reish, D. and Mitchell, R. (1982). Bacteria induce settlement and metamorphosis of *Janua* (Dexiospira) *brasiliensis* Grube (Polychaeta: Spirorbidae). *J. Exp. Mar. Biol. Ecol.* **56**, 153-163.

Lau, S. C. K., Thiyagarajan, V., Cheung, S. C. K. and Qian, P. (2005). Roles of bacterial community composition in biofilms as a mediator for larval settlement of three marine invertebrates. *Aquat. Microb. Ecol*. **38***,* 41–51.

Lidbury, I., Johnson, V., Hall-spencer, J. M., Munn, C. B. and Cunliffe, M. (2012). Community-level response of coastal microbial biofilms to ocean acidification in a natural carbon dioxide vent ecosystem. *Mar. Pollut. Bull*. **64***,* 1063–1066.

Li, B. B, Cheng, Y. Y., Fan, Y. Y., Liu, D. F., Fang, C. Y., Wu, C., Li, W. W., Yang, Z. C. and Yu, H. Q. (2018). Estimates of abundance and diversity of *Shewanella* genus in natural and engineered aqueous environments with newly designed primers. *Sci. Total. Environ.* **637**, 926-933.

Lock, M. R., Wallace, R. W., Costerton, J. M., Ventullo, R. and Charlton, S. (1984). River Epilithon: Toward a Structural-Functional Model. *Oikos.* **42***,* 10-22.

Marshall, D. J., Monro, K., Bode, M. and Swearer, S. (2010). Phenotype – environment mismatches reduce connectivity in the sea. *Ecol. Lett.* **13***,* 128–140.

Maruzzo, D., Aldred, N., Clare, A. S. and Høeg, J. T. (2012). Metamorphosis in the Cirripede Crustacean *Balanus amphitrite*. *PLoS One.* **7***,* 1–8.

McIlroy, S. J., Albertsen, M., Andresen, E. K., Saunders, A. M., Kritiansen, R., Stokholm-Bjerregaard, M. et al. (2014). "*Candidatus Competibacter*" - lineage genomes retrieved from metagenomes reveal functional metabolic diversity. *ISME.* **8***,* 613-624.

Mittelman, M. W. (1999). Bacterial Biofilms and Biofouling: Translational research in marine biotechnology. O*pportunities for Environmental Applications of Marine Biotechnology: Proceedings of the October 5-6, 1999, Workshop*. Washington, DC: The National Academies Press.

Mosier, A. C., Li, Z., Thomas, B. C., Hettich, R. L., Pan, C. and Banfield, J. F. (2014). Elevated temperature alters proteomic responses of individual organisms within a biofilm community. *ISME.* **9***,* 180–194.

Neal, A. L. and Yule, A. B. (1994).The tenacity of *Elminius modestus* and *Balanus perforatus* cyprids to bacterial films grown under different shear regimes. *J. Mar. Biol. Assoc. U.K.* **74***,* 251–257.

Nevot, M., Deroncele, V., Montes, M. J. and Mercade, E. (2008). Effect of incubation temperature on growth parameters of *Pseudoalteromonas antarctica* NF3 and it's production of extracellular polymeric substances. *J. Appl. Microbiol.* **105**, 255-263.

Pritivera, D., Noli, M., Falugi, C. and Chiantore, M. (2011). Benthic assembalges and temperature effects on *Paracentrotus lividus* and *Arbacia lixula* larvae and settlement. *J. Exp. Mar. Bio. Ecol.* **407**, 6-11.

Rao, T. S. (2010). Comparative effect of temperature on biofilm formation in natural and modified marine environment. *Aquatic. Ecol.* **44***,* 463–478.

Romaní, A. M., Borrego, C. M., Díaz-villanueva, V., Freixa, A., Gich, F. and Ylla, I. (2014). Shifts in microbial community structure and function in light- and dark-grown biofilms driven by warming. *Environ. Microbiol.* **16***,* 2550–2567.

RStudio Team. (2015). RStudio: Integrated Development for R. RStudio, Inc., Boston, MA.

Russell, B. D., Connell, S. D., Findlay, H. S., Tait, K., Widdicombe, S. and Mieszkowska, N. (2013). Ocean acidification and rising temperatures may increase biofilm primary productivity but decrease grazer consumption. *Philos. Trans. R. Soc. Lond. B. Biol. Sci*. **368***,* 20120438.

Schellenberger, J. S. and Ross, J. R. P. (1998). Antibacterial activity of two species of bryozoans from northern Puget Sound. *Northwest. Sci.* **72**, 23-33.

Scholz, J., Kaselowsky, J., Mawatari, F. S., Probert, K. P., Gerdes, G., Kadagies, N. and Hillmer, G. (2005). Bryozoans and microbial communities of cool-temperate to subtropical latitudes - paleoecological implications. *Facies.* **50**, 349-361.

Schultz, M. P. (2007). Effects of coating roughness and biofouling on ship resistance and powering. *Biofouling.* **23***,* 331–341.

Schultz, M. P., Bendick, J. A., Holm, E. R. and Hertel, W. M. (2011). Economic impact of biofouling on a naval ship surface. *Biofouling.* **27**, 87-98.

Schultz, M. P., Walker, J. M., Steppe, C. N. and Flack, K. A. (2015). Impact of diatomaceous biofilms on the frictional drag of fouling-release coatings. *Biofouling.* **31***,* 759–773.

Simon, C. and Daniel, R. (2011). Metagenomic analyses: past and future trends. *Appl. Environ. Microbiol.* **77**, 1153-61.

Smale, D. A., Taylor, J. D., Coombs, S. H., Moore, G. and Cunliffe, M. (2017). Community responses to seawater warming are conserved across diverse biological groupings and taxonomic resolutions. *Proceedings. B.* **284***,*20170534.

Teeling, H. and Glockner, F. O. (2012). Current opportunities and challenges in microbial metagenome analysis--a bioinformatic perspective. *Brief. Bioinform.* **13**, 728-42.

Toonen, R. J. and Pawlik, J. R. (1994). Foundations of gregariousness. *Nature*. **370**, 511-512.

Villanueva, V., Font, J., Schwartz, T. and Romaní, A. (2011). Biofilm formation at warming temperature: Acceleration of microbial colonization and microbial interactive effects. *Biofouling.* **27***,* 59–71.

Walker, M. D., Wahren, C. H., Hollister, R. D., Henry, G. H. R., Ahlquist, L. E., Alatalo, J. M. et al. (2006). Plant community responses to experimental warming across the tundra biome. *PNAS.* **103**, 1324-1346.

Webster, N. S., Smith, L. D., Heyward, A. J., Watts, J. E., Webb, R. I., Blackall, L. L. and Negri, A. P. (2004). Metamorphosis of a scleractinian coral in response to microbial biofilms. *Appl. Environ. Microbiol.* **70**, 1213-21.

Webster, N. S. and Negri, A. P. (2006). Site-specific variation in Antarctic marine biofilms established on artificial surfaces. *Environ. Microbiol.* **8**, 1177-90.

Wernberg, T., Smale, D. A., Tuya, F., Thomsen, M. S., Langlois, T. J., Bettignies, T. De. et al. (2012). An extreme climatic event alters marine ecosystem structure in a global biodiversity hotspot. *Nat. Clim. Change.* **3***,* 78–82.

Whalan, S. and Webster, N. S. (2014). Sponge larval settlement cues : the role of microbial biofilms in a warming ocean. *Sci. Rep.* **4***,* 28–32.

Wilson, D. P. (1952). The influence of the nature of the substratum on the metamorphosis of the larvae of marine animals, especially the larve of *Ophelia bicornis* Savigny. *Ann. Inst. Oceanogr.* **27**, 49-156.

Wilson, D. P. (1954). The attractive factor in the settlement of *Ophelia bicornis* Savigny. *J. Mar. Biol. Assoc. U.K*. **33**, 361-380.

Wilson, D. P. (1955). The role of micro-organisms in the settlement of *Ophelia bicornis* Savigny. J. *Mar. Biol. Assoc. U.K*. **34**, 531-543.

Wilson, D. P. (1968). The settlement behaviour of the larvae of *Sabellaria alveolata*. *J. Mar. Biol. Assoc. U.K.* **48**, 387.

Williamson, T. J., Cross, W. F. and Benstead, J. P. (2016). Warming alters coupled carbon and nutrient cycles in experimental streams. *Glob. Change. Biol.* **22**, 2152–2164.

Chapter 6

Deployment of heated panels in the Menai Strait: applications to a temperate ecosystem and community analysis of a short-term panel deployment

6.1 Abstract

Predicting the impacts of future oceanic warming on marine ecosystems has been traditionally approached via mesocosm installations and via long term correlation studies based on historical datasets. Only recently has the use of *in situ* oceanic warming through field manipulation experiments using heated settlement panels provided an experimental link between observational and laboratory studies. In this study, we employed the Ashton et al., (2017) panel design to evaluate the effects of *in situ* oceanic warming on marine benthic recruitment and community development in a temperate ecosystem, the Menai Strait (UK). Multiple arrays with heated panels (1°C and 2°C above ambient temperature and non-heated) were deployed subtidally in the Menai Strait for a period of 13 months. The effect of temperature on species composition of the assemblage, seasonal effects and on the growth rates of one of the main colonisers, the polychaete *Spirobranchus triqueter* was assessed. Species composition was similar across treatments but varied across seasons. Growth rates of *S. triqueter* increased with temperature in Spring and Autumn and were significantly lower in the 1°C panels in Summer in comparison to the 2°C and control. This difference was thought to be due to differences in availability of free space. Temperature had no effect on the percentage cover and community composition except when comparing the months of June 2015 and June 2016. Further analysis revealed that overall percentage cover was significantly higher in the control and 1°C treatment in June 2016 compared to June 2015. This difference in percentage cover was attributed to differences in sea water temperature across years, with surface sea water temperature being 1.3°C warmer in June 2015 than in June 2016. There is mounting evidence from terrestrial and marine ecosystems to suggest that discrete climate events (e.g. warmer years) interact with chronic stressors such as warming to reach and exceed the ecological tipping point that cause abrupt shifts in populations and communities (Thibault et al., 2008), and this is supported for the marine biofouling community data in this study. This study demonstrated that although in shorter time-scales, heated panel

technology can be successfully applied to biofouling communities in temperate climates, previously thought to be more resilient than polar or tropical assemblages to small changes in temperature.

6.2 Introduction

The marine biome provides >60% of the value of ecosystem services derived from nature (Costanza et al., 1998; de Groot et al., 2012), from global nutrient cycling to human provisioning food-chains, but recent anthropogenic climate change threatens these services. The earth's climate is changing with sea temperatures predicted to increase 1.5-3°C by 2070 (Wernberg et al., 2011). The predicted increase in ocean temperatures is one of the most important impacts of climate change, as temperature influences physiological and ecological processes across biological scales, from genes to ecosystems. The impacts of anthropogenic warming have already been observed in a variety of systems and taxa (Hawkins et al., 2009). For example, relative abundances of higher latitude species have declined and those of lower latitude have increased in temperate latitudes e.g. Southern trochids (*Gibulla umbilicalis*) have increased in abundance and their ranges have extended into northern Scotland, Northern Ireland, North Wales and the eastern English Channel (Mieszkowska et al., 2006). Climate change also impacts the performance of individuals at various stages in their life history cycle, in particular early life history stages since these are often thought more vulnerable to environmental stress than adults (Harley et al., 2006; Clark et al., 2016). The timing of ontogenic transitions may be affected with temporal mis-matches between larval production and food supply. For example increased temperatures have advanced spawning times in the bivalve mollusc *Macoma balthica* causing a slight mis-match between the phytoplankton bloom and the occurrence of early life stages dependent on that food resource (Philippart et al., 2003).

Although the impacts of climate change have been noted in marine systems since the early twentieth century (Harley et al., 2006), there are still many unknowns (Lurgi et al., 2012). Our ability to predict responses to altered climatic patterns relies on an understanding of how warming affects all levels of organisation: from individuals to ecosystems (Peck, 2011). Community level predictions are particularly challenging due to the fact that species' sensitivities to climate change are often determined on a species by species basis in laboratory experiments. Species-specific responses to biotic and abiotic factors vary considerably especially when interacting with other species. For example, abiotic stress may remove the dominant competitors, allowing subordinate species to persist (Poloczanska et al., 2008). Thus, water temperature influenced the strength with which the sea star *Pisaster ochracenus*, a keystone predator, interacted with its principal prey (Sanford, 1999). Exposure to warmer waters increased both *Pisaster's* mid-intertidal abundance and *per capita* consumption rate. Such responses to warming could allow *P.*

ochracenus to progressively eliminate large sections of mussel beds and secondarily displace hundreds of species that inhabit the mussel matrix. Moreover, biological communities are often connected across a range of spatial and temporal scales, which extend beyond the confines of an aquarium in a laboratory (Borthagaray et al., 2009).

To date, predicting the impacts of future oceanic warming on marine ecosystems has been approached in a variety of ways. Mesocosm installations (experimental enclosures usually based in the laboratory, but sometimes field based) are used to improve knowledge of how functional traits can predispose species to range changes under shifting climates and their associated effects on community structure and stability. In a study by McElroy et al., (2015) using laboratory based mesocosms both nutrient enrichment and warming had a strong influence on an assemblage containing *Carcinus maenas* crabs compared to those without crabs. Recent technological and methodological developments in this field include multifactorial mesocosm installations capable of simulating combined climate change scenarios including, for example, alterations in temperature, acidification, nutrient enrichment and sea level rise on marine intertidal communities (Pansch et al., 2016).

Whilst these types of experiments have provided valuable information, due to the confinement and highly controlled nature of the physiochemical and biological environments, they reduce realism and are limited to an artificial habitat (Carpenter et al., 1997). Other approaches to study effects of warming on marine systems are “opportunistic and natural experiments”. These have long been advocated, and predominantly report that community composition changes with warming in the field. In a study by Schiel et al. (2004) a 3.5°C rise in seawater temperature induced by the thermal outfall of a power generating station resulted in significant community wide changes in 150 species of algae and invertebrates over 10 years. The responses of the benthic communities to oceanic warming were strongly coupled to the direct effects of temperature on key taxa. Similarly, an *in situ*, but relatively uncontrolled manipulation was carried out on intertidal communities in the Salish Sea (Kordas et al., 2014). This study placed black and white settlement panels in the intertidal zone. Passive warming meant that the black panels were on average 2.6°C warmer than the white panels, with the former showing a decline in invertebrate assemblages. The authors concluded that a decline in the number of species in invertebrate assemblages was due to the reduced numbers of local thermally-stressed species and the lack of replacement by warm-adapted species (Kordas et al., 2014). This suggested that communities in thermally

stressful habitats respond to warming via the interplay between species-specific thermal responses and secondary adaptive strategies.

Given the advantages of the above studies, assessing the impacts of oceanic warming *in situ* through field manipulation experiments has become an essential step towards understanding how marine benthic communities will respond to change. They can mimic abiotic stress and incorporate a realistic species pool, providing a crucial experimental link between observational and laboratory studies (Kordas et al., 2014). On land, some of the most valuable insights into the resistance of communities to predicted climate change have come from field manipulation experiments (e.g. Grime et al., 2008; Yergeau et al., 2011). However, in the marine environment this knowledge is lacking primarily due to the logistical limitations of manipulating temperature in marine systems in the field (Smale et al., 2011). The recent development of heated settlement panels, capable of recreating ecologically relevant controllable temperatures *in situ*, is a key contributor in addressing this gap in the literature (Smale et al., 2011; Ashton et al., 2017).

Heated settlement panels deployed for 36 days at a Harbour in Australia showed no significant difference between controls and heated treatments, but reported changes were of shifts in community structure of the heated panels, with the bryozoan *Watersipora subtorquata* and spirorbid polychaete worms covering less space on warmed surfaces than controls. This was associated with a greater biomass of a colonial ascidian *Didemnum perlucidum* (Smale et al., 2011). Smale's latest panel design (2017) also reported shifts in community structure in bacteria, protists and metazoans and increases in community abundance of the latter due to warming. More recently and using a different panel design and protocol that matches oceanic warming predictions for the end of the century (IPCC, 2014), Ashton et al., (2017) reported the near doubling of growth rates in the bryozoan *Fenestrulina rugula* and a reduction in the overall community diversity caused by an increase of +1°C at a site in Antarctica. Whilst the Smale et al. (2017) study used heated settlement panels, these panels warmed the surface layer of the water to higher temperatures (3°C and 5°C) than those predicted by the IPCC (IPCC, 2014) for end of century conditions, for a short time-scale of 40 days. The results obtained are thus not representative of future warming predictions for the next 100 years.

In the study reported here, the Ashton et al. (2017) panel design was employed to evaluate the effects of *in situ* oceanic warming on marine benthic recruitment and community development in the field. The panels heated the surfaces and a thin layer of overlying water to 1°C and 2°C above

the ambient temperature, thus reproducing temperatures predicted for oceanic warming for the end of the century (IPCC, 2014) in the natural environment. Multiple arrays with heated panels (1°C and 2°C above ambient temperature and non-heated) were deployed subtidally in the Menai Strait for a period of 12 months. The aims of this study were to evaluate the effect of a 1°C to 2°C increase in water temperature on temperate marine species. In particular to analyse the effect on species composition of the assemblage, identify any seasonal effect and evaluate in more detail the effect of altered temperature on the main coloniser, the worm *Spirobranchus triqueter.*

6.3 Methods

6.3.1 Site description

The Menai Strait is a narrow area of water separating Anglesey Island from North Wales, UK (53.2400° N, 4.0803° W). It is a special area of conservation (SAC) where the diversity of habitats and the strong tides have promoted a high benthic diversity (Young and Kay, 1999). Community composition includes both warm water (Lusitanian) and cold water (boreal) species, as the UK is located on a biogeographic boundary, hence providing a good site to study community interactions (Mieszkowska et al., 2006). The area is typified by muddy sand substrata with some boulders and rocky outcrops, creating islands for settlement and development of hard substratum communities.

The dynamics of the water flow in the strait are dominated by strong tides, causing the water column to remain vertically mixed throughout the year, with little difference between surface and bottom water temperatures (Roberts et al., 2014). Surface sea water temperature in the Menai Strait varies annually in the range of 6.7°C-16.7°C (CEFAS, https://www.cefas.co.uk/cefas-data-hub/wavenet). Temperatures for the duration of the experiment varied from year to year. The Summer of 2015 was on average 1.3°C cooler than the Summer of 2016, with a mean sea surface temperature of 18.65°C as oppose to 19.95°C. The mean sea surface temperature for Autumn was 17.45°C and the mean sea surface temperature for Spring was 15°C (https://www.cefas.co.uk/cefas-data-hub/smartbuoys) (See Figure 6.1).

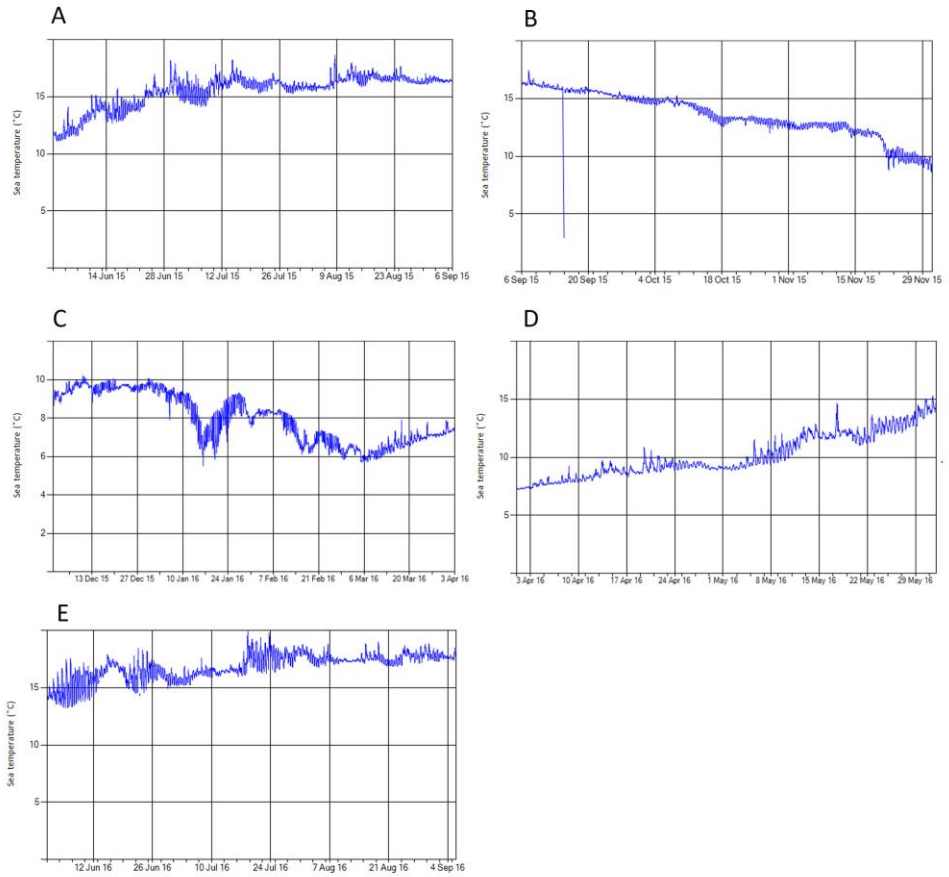

Figure 6.1. Sea water temperature (°C) from CEFAS wave buoy data in the Menai Strait during the experimental deployment. A) Summer 2015, B) Autumn 2015, C) Winter 2015/16 D) Spring 2016 and E) Summer 2016. Mean temperature for the June July period in 2015 was 18.75°C and 19.95°C in 2016.

A total of 12 panels were mounted on to 4 steel frames (3 panels per frame, 4 replicates per treatment) and were deployed in the Menai Stait, Wales, at one site near Ynys Faelog Island in a fan shape design. Panel treatment (control, +1°C, +2°C) was randomly distributed around the frame. Due to the strength of the flow through the Menai Strait and the risk of equipment loss due to the latter, only three panels (one each of 1°C, 2°C and control) were attached at random to each frame. This was to ensure that the loss of any single frame would not negatively impact data collection. The rest of the spaces were left empty. Please refer to Chapter 2 for a more detailed description of the experimental set up.

6.3.2 Data acquisition

6.3.2.1 Monitoring and panel photography

As previously discussed in Chapter 2, the experiment was conducted for 13 months with an overlap of one month in June 2015 and June 2016. Panels were deployed on the 05/06/15 and photographed regularly for the duration of the experiment (see Table 6.1). Separate trials were run in Summer, Autumn, Winter and Spring. Panels that were deployed during the Winter period (December-March) were only photographed at the start and end of the deployment, due to low recruitment and slow growth during the winter months.

Table 6.1. Season and date the panels were deployed, photographed and sampled. The last column is the month the panels were recruited for each season.

Deployment Season/year	Deployment date	Photographed	Retrieved and sampled	Recruitment
Summer 15	05/06/15	15/07/15 06/08/15 02/09/15	02/09/15	June
Autumn 15	10/09/15	26/10/15 24/11/15	24/11/15	September
Winter 15/16	26/11/15	05/04/16	05/04/16	November
Spring 16	07/04/15	05/05/16 03/06/16	03/06/16	April
Summer 16	06/06/16	20/07/16	20/07/16	June

Steel frames (n=4) containing the panels were lifted from the seabed to the side of a boat and brought to the shore near the sampling sites, but held under water at all times. The plastic frame securing the panels to the array was removed and the panels were moved onto an *in situ* tank filled with filtered sea water. Panels were turned over so that the experimental surface was facing up and photographs of the associated fauna were taken. Following image capture of all panels the arrays were reattached to the frame and the frames returned to the relevant site. Throughout the whole process panels were kept underwater at all times. Panels were photographed using a Nikon D7000 with a Nauticam Nikon D7000 Underwater housing and a 60mm macro lens (following the setup in Ashton et al., 2017). The underwater housing was fitted on to a sliding frame that in turn was rested on the panel, thus keeping the camera lens at a constant distance from the panel. The camera was slid across the panel to a series of roughly predetermined positions, and a total of 24 photographs or more (lens focal ratio 1:2) were taken per panel, with a 50% overlap between image. Each photograph captured approximately an area of 3.5-2.5cm of the panel. Photographs

were taken in both RAW and JPEG formats and were subsequently merged in to a single image using Photoshop CS5. Images were cropped to the central 9.8 x 9.8cm heated area of each panel.

6.3.2.2 Sampling

Every 3 months panels were brought back to inland aquaria to the School of Ocean Sciences at Bangor University (Menai Bridge, Anglesey, LL59 5AB) for sampling. This deployment period was determined by the growth rate of colonisers in summer that reached high levels of panel surface coverage in 3 months. Species composition was assessed under low power microscopy (10x). The majority of the panel communities comprised common species such as the barnacle *Balanus crenatus* and the bryozoan *Electra pilosa*. However, species with unconfirmed taxonomic ID's were present. These were sampled and stored in 95% ethanol for subsequent DNA barcoding to confirm the species. Post-sampling, panels were scraped clean and re-deployed. Panels had to be scraped clean and re-deployed every 3 months to prevent organisms growing above the heated layer post this period. Sampling periods were timed to coincide with each season.

6.3.3 Statistical analysis

6.3.3.1 Species ID

Organisms recruited on the panels were identified using Hayward and Ryland (1990). Organisms with unconfirmed taxonomic ID's previously stored in 95% ethanol were barcoded. These unidentified organisms were washed with phosphate-buffered saline (PBS) to remove any excess ethanol that could contaminate the extraction. Total genomic DNA was extracted using the DNeasy Tissue kit (Qiagen) following manufacturer's instructions. DNA samples were quantified using Nanodrop (NanoDrop, ND-1000) and electrophoresed on a 1.5% agarose gel (90v, 20mins) to check DNA integrity. PCR amplifications were performed in 25µL volumes containing final concentrations of 0.5 units of Taq DNA Polymerase (Bioline), 10x buffer (Bioline), 5% bovine serum albumin 10mg/ml (Sigma), 200µM of dNTP mix, 3.5mM of Magnesium chloride, 0.5µM of each 18S rRNA primer (NSF4: CTGGTTGATYCTGCCAGT and NSR581: ATTACCGCGGCTGCTGGC) and 1µL of template DNA. Cycling conditions were at 94°C for 30s followed by 35 cycles of 94°C for 30s, 60°C for 30s (annealing temperature) and 72°C for 1min. This was followed by a 5min extension at 72°C. PCR products were sent to a commercial sequencing facility, Source Bioscience (Cambridge, UK), for product clean-up and Sanger sequencing. Sequences were obtained in an ABI file format and viewed in Finch TV version 1.4.0 (Geospiza, Inc., Seattle) to check the quality. Processed sequences

were compared to those available in GenBank using the BLAST tool in Finch TV to determine the highest sequence similarity match.

6.3.3.2 Growth rate

Spirobranchus triqueter (n=30 per panel) were identified and measured for each sampling period using Fiji (ImageJ). *S. triqueter* is commonly found sublitorally around the British coastline (Hayward and Ryland, 1995) and in very exposed water flow rates such as the Menai Strait (Riley et al., 2005). *S. triqueter* larvae settle all year round (Castric-Frey, 1983) and the species was the main coloniser on the panels across the 13 months of the experiment. As such, *S. triqueter* was chosen to evaluate in more detail the effects of altered temperature on growth rate. The area occupied by each worm was traced and growth rates were calculated on an area basis according to Bowden et al., (2006) using the formula:

$$\mu = \ln(N/N_0) / t$$

Where μ is the growth rate, N is the area at the end of the growth period, N_0 is the area at the start of the growth period and t is the growth period in days. Growth rates were analysed using a general linear model (GLM) in the R environment for statistical computing. Post-hoc Tukey tests were performed using the *agricolae* package.

6.3.3.3 Species richness and diversity

Percentage cover data for sessile taxa at the end of each sampling period were analysed using the colour threshold plugin in Fiji (an image analysis package that is an enhanced version of ImageJ). Presence and percentage cover data for sessile taxa on panels at the end of each sampling period were compared using multivariate analysis models in the R environment for statistical computing using the *vegan* package. The reference model included an interaction term between treatment, month and panel:

>Permanova <- adonis (Data~ Treatment*Frame*Month, method = “bray”, header = “TRUE”, perm = 999).

6.4 Results

The community growth on panels was analysed for the percentage area covered across individual months and seasons (Summer, Autumn and Spring) across panels of different treatments. The community growth on panels was also analysed for species composition and the growth rates of one of the key species, the polychaete worm *Spirobranchus triqueter* was analysed.

6.4.1 Percentage cover

Over the 13 months of the experiment, overall percentage cover on the panels varied considerably between months: from 19% (1℃ treatment) and 37% (control) in the month of June 2015, 11% (2°C treatment) and 77% (control) in August 2015 to 2.9% (2℃ treatment) and 7.75% (control) in March 2016 (Figure 6.2). Percentage cover on panels was not significantly different across treatments (ANOVA, F (2), = 1.43, *P* = 0.3) except in the months of June 2015 and June 2016 (See section 5.3.5 for further analysis).

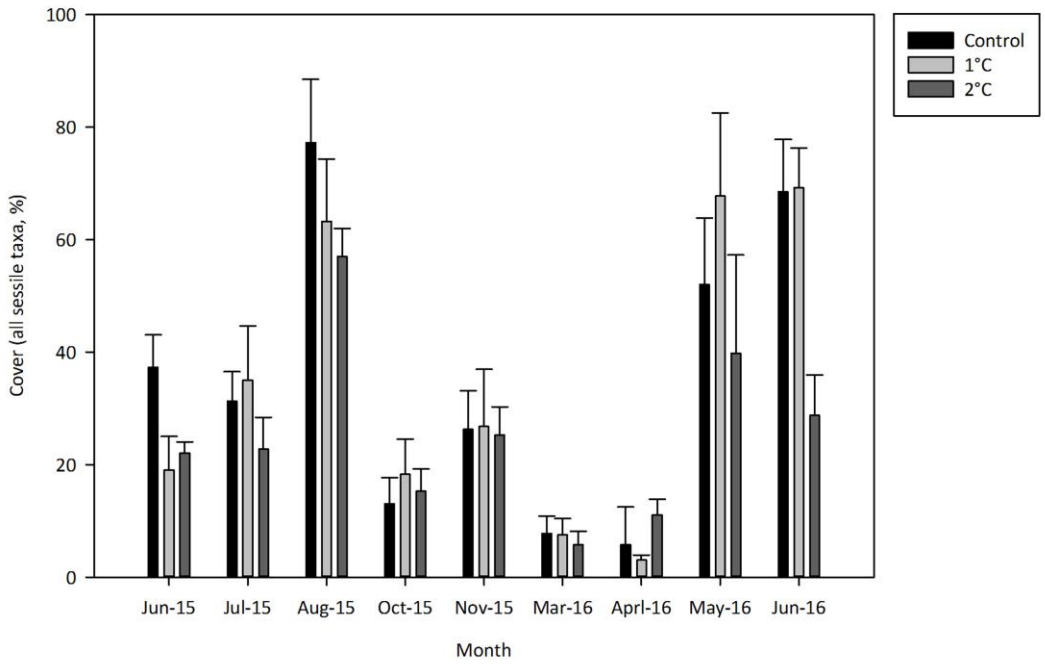

Figure 6.2. Total area colonised by community assemblages from June 2015 up to, and including June 2016 (mean and SE).

An analysis of variance (ANOVA) revealed that coverage of panels was significantly different across seasons (F (2), = 17.32, $P < 0.01$) (Figure 6.3). Post hoc comparisons using the Tukey HSD test indicated that percentage cover in the summer was significantly higher to the coverage in Autumn ($P < 0.05$) but not to the coverage in Spring ($P = 0.1$). The percentage cover in Spring and Autumn were not significantly different from each other ($P = 0.1$).

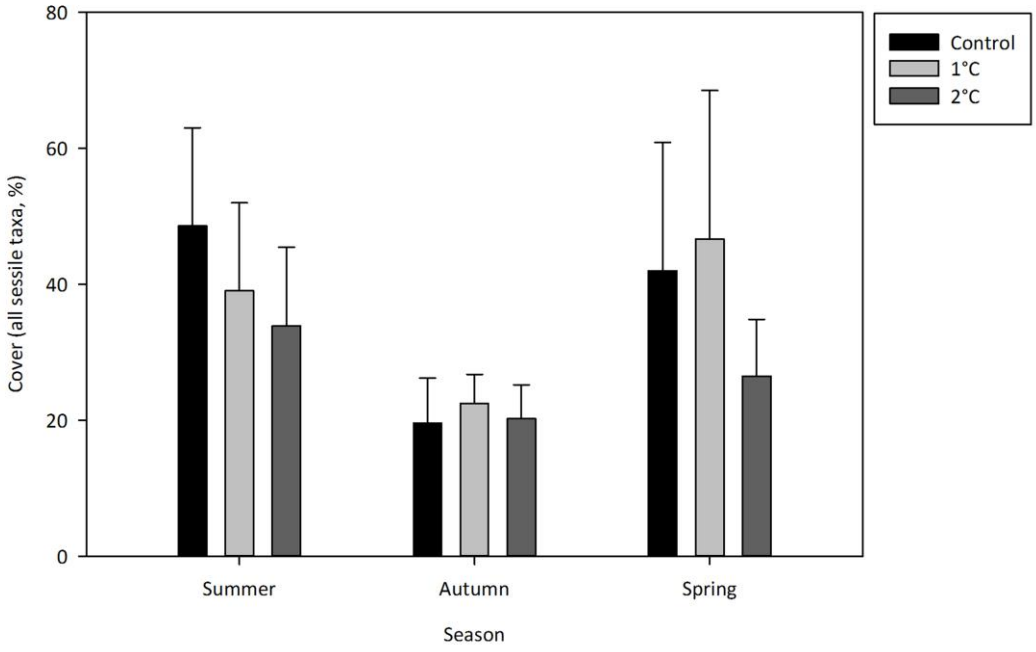

Figure 6.3. Total area colonised by community assemblages per season (Summer, Autumn and Spring) (mean and SE).

6.4.2 Species composition

Across the 13 months, 25 taxa were identified on the panels, with species assemblages dominated by the polychaete *Spirobranchus triqueter* and *Sabellaria alveolata,* the barnacle *Balanus crenatus,* the bryozoan *Electra pilosa,* the hydroid *Plumaria setacea* and the ascidian *Diplosoma listerianum*. All 25 species occurred on all treatments. The ascidian *Ciona intestinalis* occurred in small numbers in the control treatment (0.75%) and in the heated treatments (0.50%) and only in August 2015. Similarly the sponge *Sycon ciliatum* also occurred in small numbers in the control treatment (1.00%) and in the heated treatments (0.25%) and only in August 2015. The presence of

these two species in August 2015 was probably a random occurrence and not of ecological relevance.

Species composition was very similar across treatments but varied across seasons (Figure 6.4.). In the Summer (June, July, August), the ascidian *Diplosoma listerianum* and the polychaetes *Sabellaria alveolata* and *Spirobranchus triqueter* dominated the coverage. Coverage was highest in the control (55%) and lowest in the 1℃ treatment (40%). There was a higher coverage of *S. triqueter* (15.7%) on the control than on 1℃ and 2℃ heated treatments (6.75% and 6.50% respectively), but there was a higher coverage of *D. listerianum* (21.7%) on the 2℃ treatment compared with the control (12%) and 1℃ (13%) panels. An analysis of variance (ANOVA) revealed that overall coverage of the above 6 species was not significantly different across treatments ($F_{(10)} = 0.70$, $P = 0.7$). During Autumn (October and November) overall coverage of the above 6 species was again similar across treatments with 14.5% in the control and slightly lower in the 1℃ treatment (13.5%) (Figure 6.4). *B. crenatus* dominated the assemblage during this season followed by *S. triqueter* and *S. alveolata.* An analysis of variance (ANOVA) revealed that overall coverage of the above 6 species was not significantly different across treatments ($F_{(10)} = 0.84$, $P = 0.5$). The main difference in this assemblage was the absence of the ascidian *D. listerianum* and *P. setacea* in the control treatment, but both were present in the 1℃ and 2℃ treatments with *P. setacea* present in the 2℃ treatment at relatively high levels.

Overall coverage of the 6 species varied in Spring (April-May) between treatments, with the 2℃ treatment having the highest coverage (10.5%) and once again, the lowest coverage being contributed by the 1℃ treatment (2.50%)(Figure 6.4). An analysis of variance (ANOVA) revealed that this difference was significant ($F_{(10)} = 2.20$, $P = 0.03$). *B. crenatus* and *P. setacea* dominated the assemblage during this season, with the highest coverage in the 2℃ treatment contributed by *P. setacea* (6.50%) followed by a similar coverage of *B. crenatus* across all treatments (3.25%). Post hoc comparisons using the Tukey HSD test indicated that the difference in coverage between *B. crenatus* and *P. setacea* was significantly ($P < 0.05$).

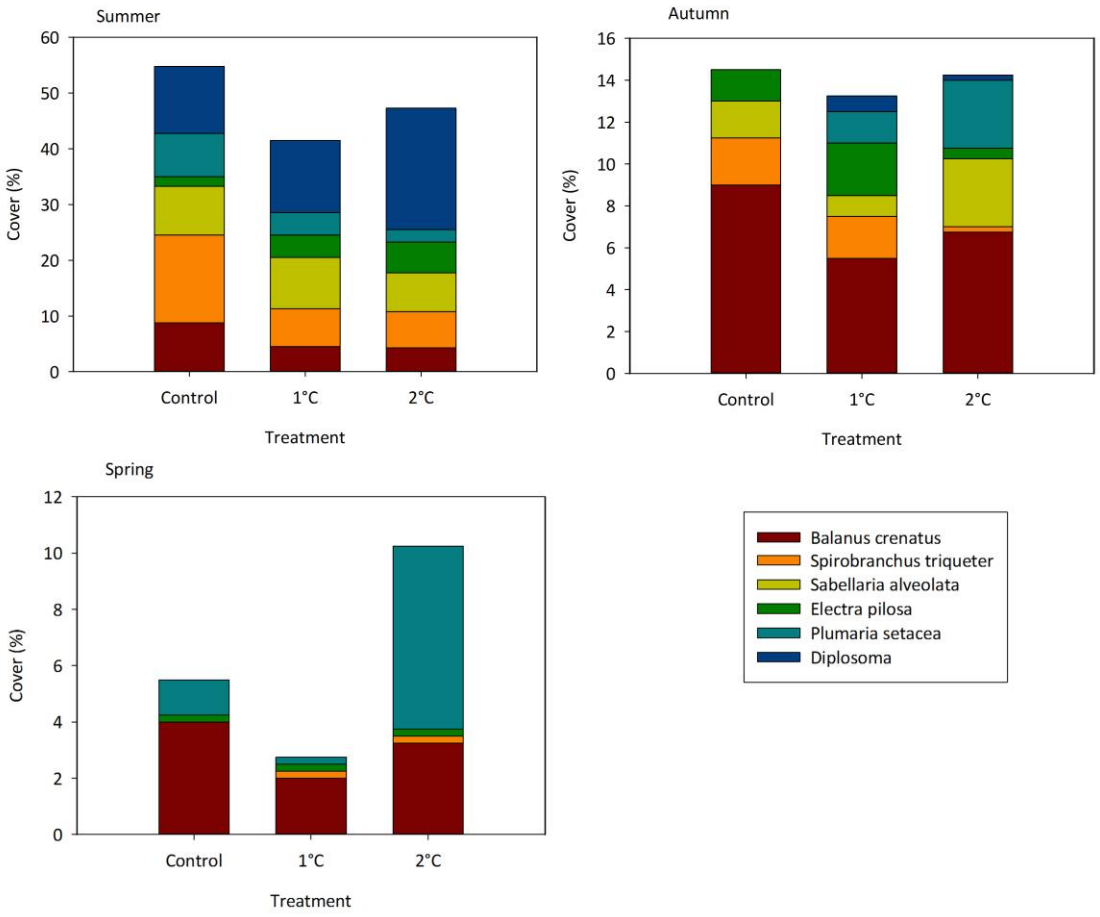

Figure 6.4. Panel composition of the 6 most dominant species colonising panels across seasons (Summer, Autumn, Spring). Winter not shown due to very low colonisation rates and recruitment success

6.4.3 Growth rates

The effect of temperature on the growth rate of one of the main colonisers *Spirobranchus triqueter* was evaluated across seasons. Growth rates of *S. triqueter* were highest in the Summer across all treatments and lowest in Autumn (Figure 6.5). An analysis of variance revealed that in Summer, growth rates across treatments were significantly different from each other (F (2), = 5.59, $P < 0.01$). A post hoc Tukey test revealed that growth rates were significantly different in the 1℃ treatment ($P < 0.01$) but not in the control and 2℃ treatment ($P = 0.7$). An analysis of variance (ANOVA) revealed that in spring, growth rates were significantly different across treatments (F (2), = 3.69, $P < 0.05$). Post hoc comparisons using the Tukey HSD test indicated that the growth rates were significantly different between the 2°C, control and 1℃ treatment ($P < 0.05$) but not between the 1℃ treatment and the control ($P = 0.1$). Despite the trend described above, there were no significant differences in growth rates across treatments in autumn (F (2), = 7.49, $P = 0.2$).

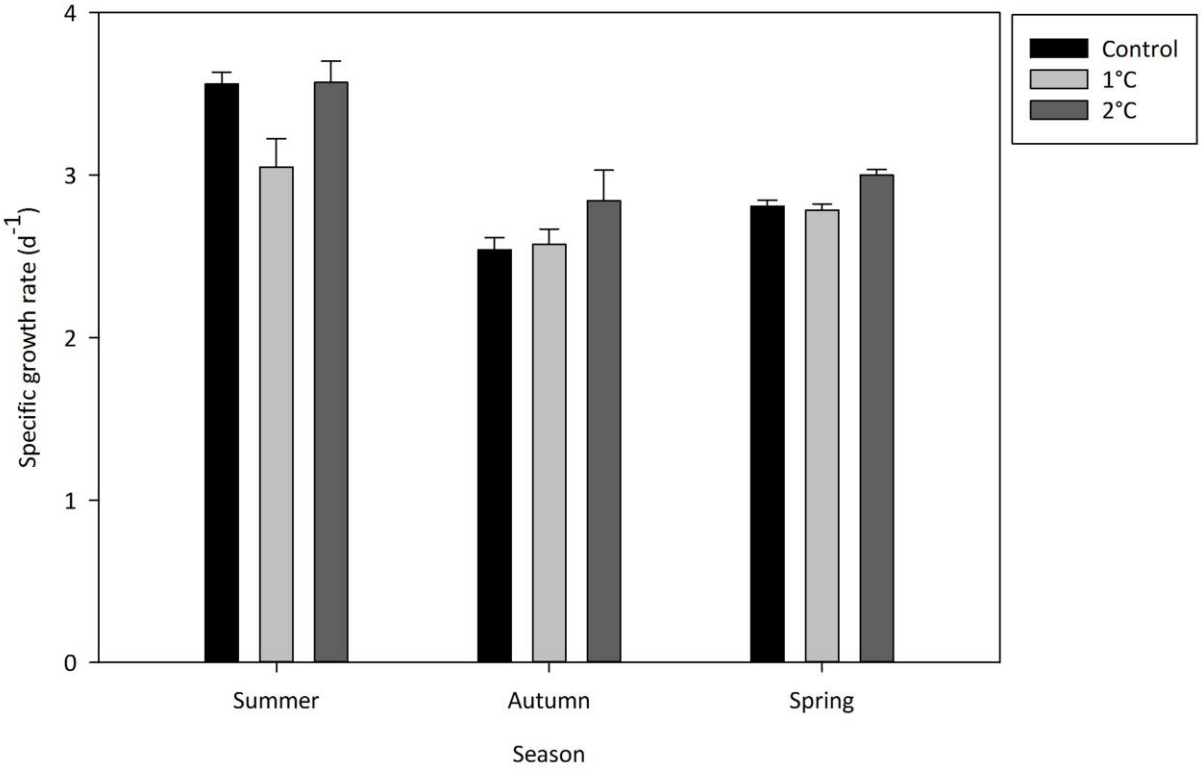

Figure 6.5. Specific growth rates of *Spirobranchus triqueter* (Mean and SE) across different treatments (Control, 1°C and 2°C).

6.4.4 Community analysis

Community assemblages established on heated panels (+1℃ and +2℃) were different to panels in non- heated treatments but not significantly so (PERMANOVA, $P = 0.1$).

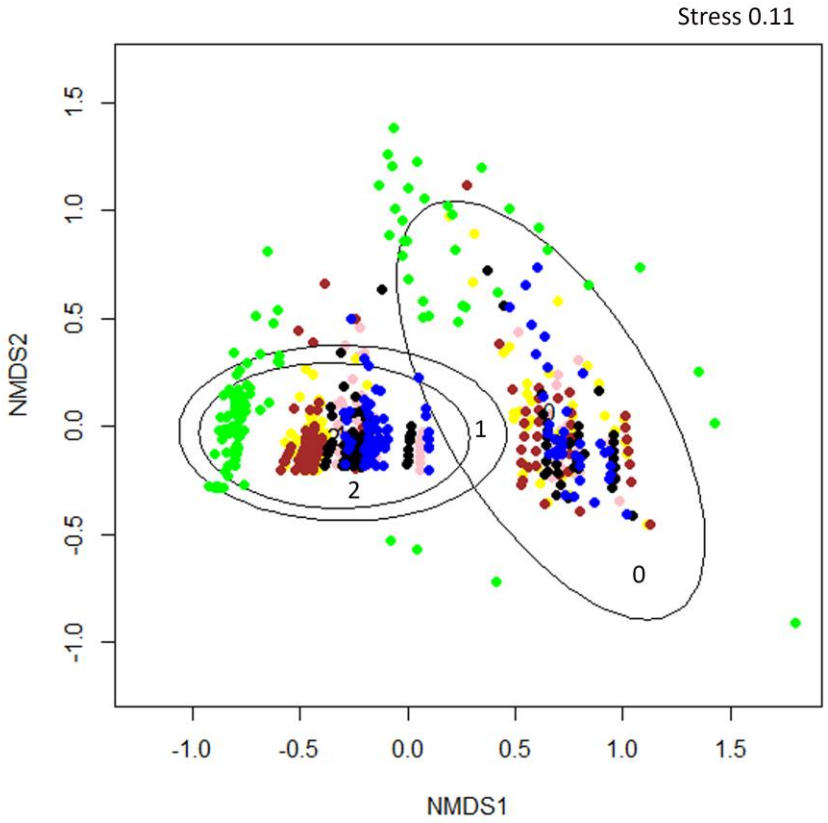

Figure 6.6. Non-metric multidimensional scaling (nMDS) plots illustrating differences in species composition of assemblages recruiting to panels across treatments and all seasons (Summer, Autumn and Spring). 0 = control, 1 = 1°C and 2 = 2°C. Green = *Balanus crenatus*, blue = *Spirobranchus triqueter*, pink = *Sabellaria alveolata*, yellow = *Electra pilosa*, brown = *Diplosoma listeranium* and black = *Plumaria setacea.*

During summer, species composition in the control panels was different from heated panels at the early stages of assemblage development (Stress = 0.11). However, species composition became similar across treatments as the community developed (Figure 6.7). The opposite was true in Autumn, species composition was not different across treatments at the early stages of assemblage development. However, as the community developed, species composition in the control panels was different to that in heated panels (Stress = 0.11). In Spring, species composition was not different across treatments.

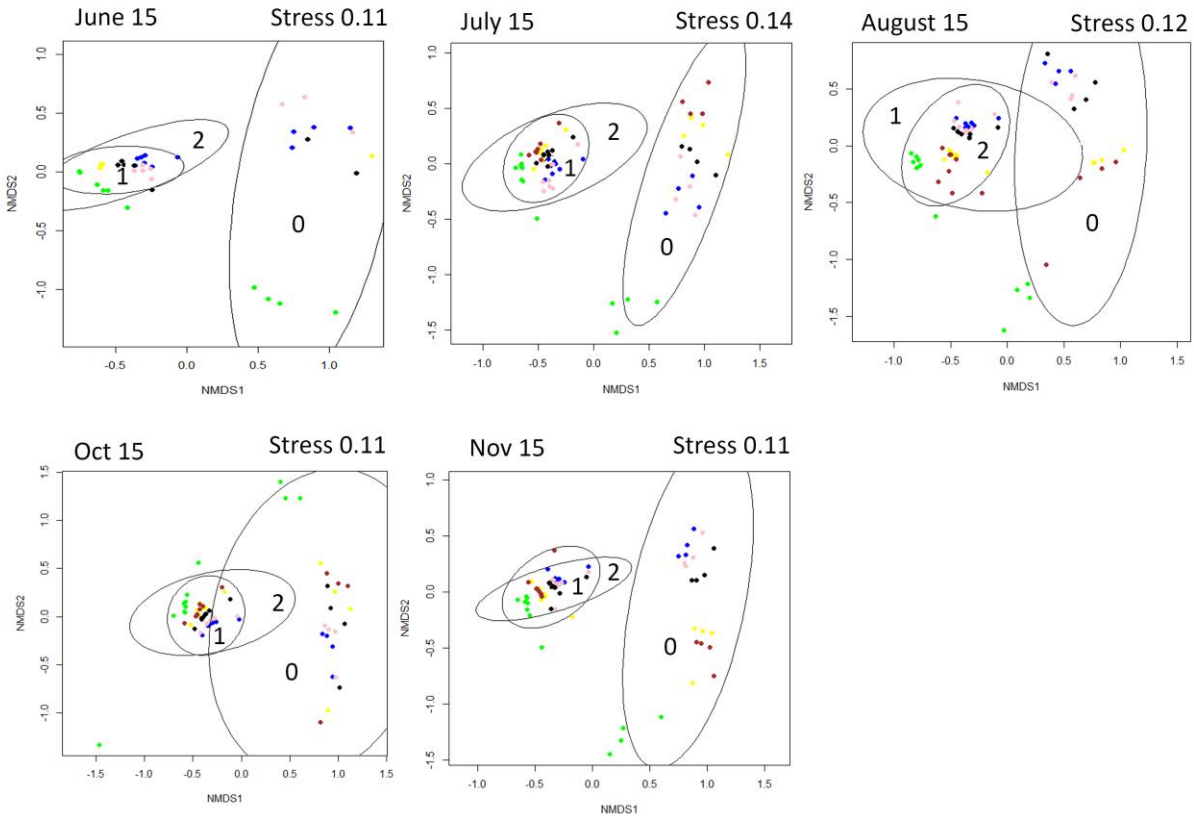

Figure 6.7. Non-metrix multidimensional scaling (nMDS) plots illustrating differences in species composition of assemblages recruiting to panels across treatments, summer and autumn seasons. 0 = control, 1 = 1°C and 2 = 2°C. Green = *Balanus crenatus*, blue = *Spirobranchus triqueter*, pink = *Sabellaria alveolata*, yellow = *Electra pilosa*, brown = *Diplosoma listeranium* and black = *Plumaria setacea*.

6.4.5 Comparing June 2015 and June 2016

In this 13 month experiment, there was a period of one month overlap in sampling. In fact treatment had no effect on the overall percentage cover of the panels (P = 0.10) except in the summer of June 2015 and June 2016 (ANOVA, F (2), = 6.16, P < 0.01)(Figure 6.8). Post hoc comparisons using the Tukey HSD test revealed that in June 2015 the +1℃ and control treatment were significantly different from each other (P < 0.01) but the +1℃ and +2℃ were not (P = 0.99*).* In June 2016, overall percentage cover was significantly lower in the 2℃ treatment in comparison to the 1℃ and control treatment (P < 0.01) but the 1℃ and control treatment were not significantly different from each other (P = 1.00). A Tukey HSD further indicated that percentage cover was significantly higher in the control and 1℃ treatment in June 2016 (P < 0.01) compared to June 2015. Overall percentage cover for the 2℃ treatment was not different in June between years (P = 0.1).

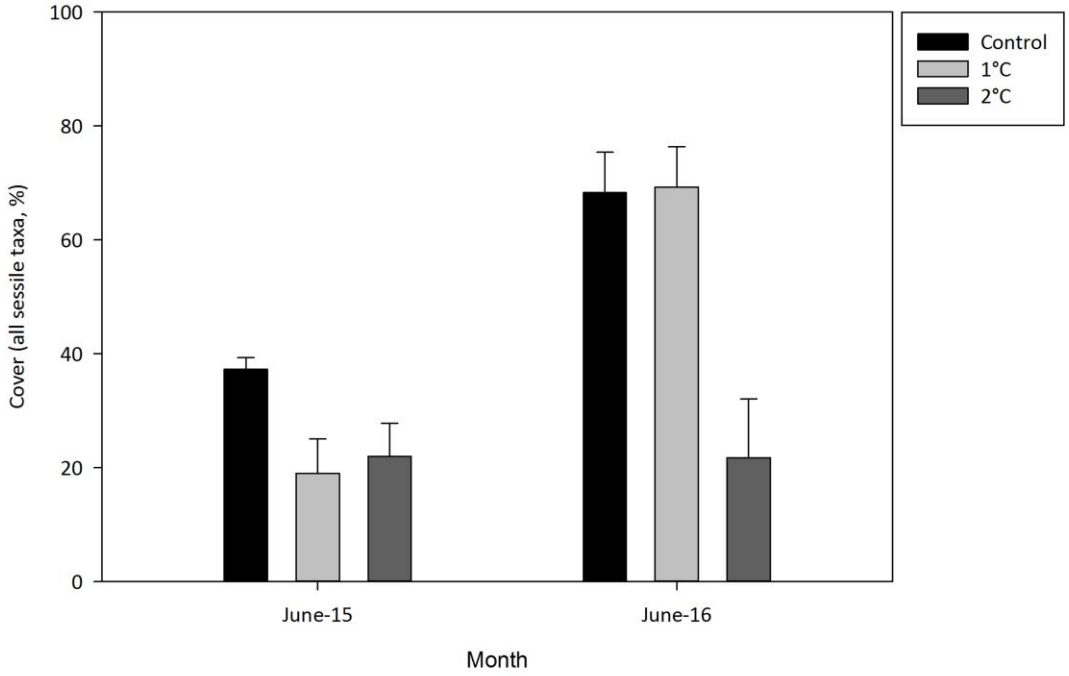

Figure 6.8. Total area colonised by community assemblages per season (Summer, Autumn and Spring) (mean and SE).

In June 2015, assemblages were dominated across treatments by *S. triqueter*, *B. crenatus*, *S. alveolata* and *P. setacea* (Figure 6.9). There was a higher coverage of *S. triqueter* in the control treatment (18.75%) in comparison to the heated 1℃ and 2℃ treatments (6.25% and 6.00%) but this difference was not significant (ANOVA, F (2), = 2.10, *P* = 0.22). In June 2016, assemblage composition was also similar across treatments and dominated by *S. triqueter, B. crenatus and E. pilosa* (Figure 6.9). A notable difference in comparison to June 2015 is the absence of the hydroid *P. setacea* and the polychaete *S. alveolata* and the increased presence of the bryozoan *E. pilosa*. Furthermore, there was a higher coverage of *S. triqueter* in the 1℃ treatment (24.7%) in comparison to that in June 2015 (6.25%), but this difference was not significant (ANOVA, F (2), = 7.41, *P* = 0.05). This could therefore be due to the relative higher overall coverage in the 1°*C* treatment in June 2016. Coverage of *B. crenatus* was higher in the 2°C (15.2%) treatment in June 2016 than in the 2℃ in June 2015 (2.75%) even though the overall coverage was similar across both years (28.7% and 22% respectively). This difference again was not significant (ANOVA, F (2), = 10.9, *P* = 0.08).

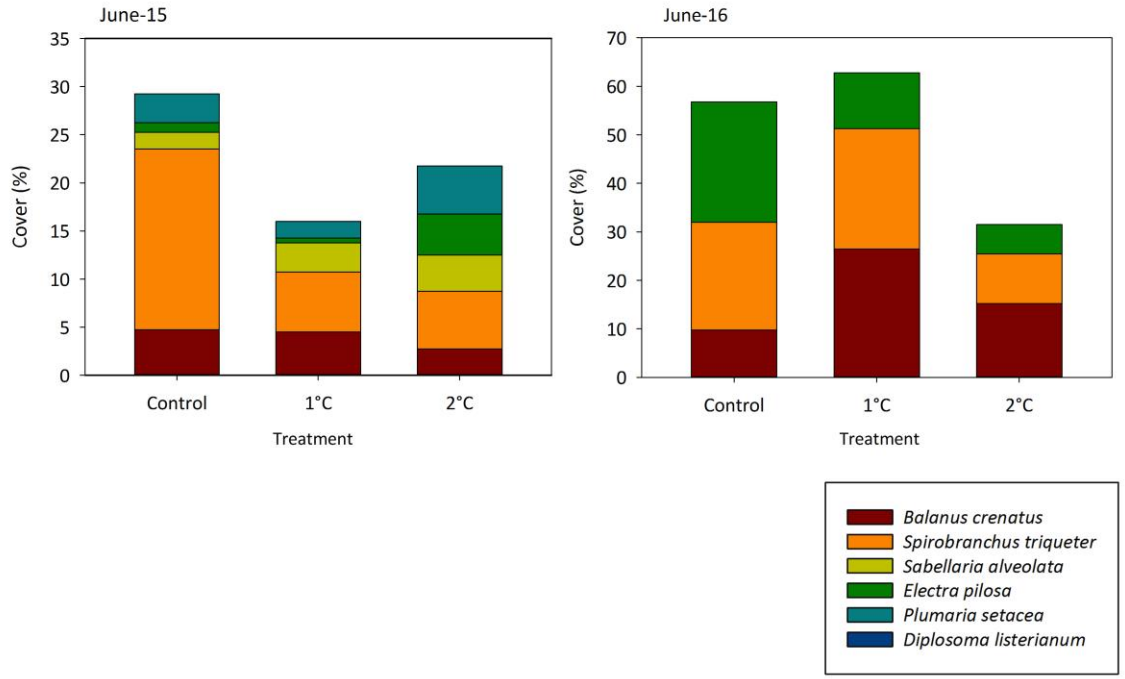

Figure 6.9. Panel composition of the 6 most dominant species colonising panels during June. Left: June 2015: Right: June 2016.

In both June 15 and June 16 species composition in the control panels was different to the composition in heated panels (Stress = 0.11 and 0.10)(Figure 6.10).

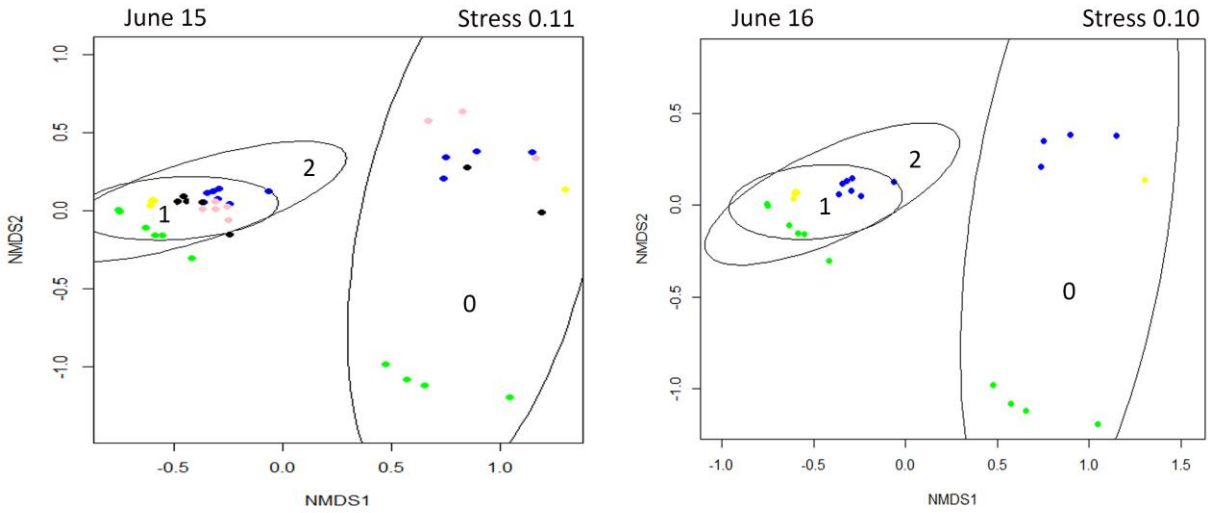

Figure 6.10. Non-metric multidimensional scaling (nMDS) plots illustrating differences in species composition of assemblages recruiting to panels across treatments and summer months. 0 = control, 1 = 1°C and 2 =2°C . Green = *Balanus crenatus*, blue = *Spirobranchus triqueter,* pink = *Sabellaria alveolata*, yellow = *Electra pilosa*, brown = *Diplosoma listeranium* and black = *Plumaria setacea*.

6.5 Discussion

6.5.1 Percentage cover

Temperature is a fundamental determinant of survival and performance for all species. In this study we demonstrated that subtidal biofouling organisms living in temperate climates are vulnerable to predicted oceanic warming (IPCC, 2014) and that the higher temperature scenarios (+2°C) during warmer years may exceed the thermal limit of some of these organisms. Overall percentage cover on the panels was not correlated with experimental temperatures except when comparing the coverage between June 2015 and June 2016. Buoy data of the deployment site provided by CEFAS (https://www.cefas.co.uk/cefas-data-hub/smartbuoys) reported the surface sea water temperature was 1.3°C warmer in June 2015 than in June 2016. This increase in oceanic temperature may have driven the differences in coverage between the two months: panels in the control and +1°C treatment were significantly less covered in June 2015 in comparison to June 2016. We suggest that organisms in the heated treatments were living near to or above their long-term thermal limit in June 2015, particularly in the +2°C treatment as overall coverage was significantly lower when compared to the control treatment over both years in June.

During the warmer year (June 2015), coverage in the +1°C treatment (which was similar to that in the control during 2016, a "normal" year), was low and similar to levels in the +2°C treatment in June 2016, supporting the above hypothesis. There is mounting evidence from terrestrial and marine ecosystems to suggest that discrete climate events (e.g. warmer years) interact with chronic stressors such as warming to reach and exceed the ecological tipping point that cause abrupt shifts in populations and communities (Thibault et al., 2008), and this is supported for the marine biofouling community data in this study. In a study by Smale et al., (2012) demonstrated another example when a marine heat wave eliminated the habitat forming seaweed *Scytothalia dorycarpa* at it's warm distribution limit, causing a reduction in its range of approximately 100km.

In this context, the species in this study have variable thermal tolerances. The polychaetes *Spirobranchus triqueter* and *Sabellaria alveolata* have a wide distribution range occurring as far south as the Mediterranean (Castric-fey, 1983), with *S. alveolata* distribution spreading as far south as Morocco. As such, these species have a high thermal tolerance to long-term slight increases in temperature (Riley et al., 2005). On the other hand, the hydroid *Plumaria setacea*, the bryozoan *Electra pilosa* and the barnacle *Balanus crenatus* are less resistant to warming. In the bryozoan *E. pilosa*, growth rates increase with temperature but zooid size decreases. This

decreases in zooid size is thought to be due to an increase in metabolic costs at higher temperatures (Ryland, 1976). In the Menai strait in particular, studies have reported mean zooid size in *E. pilosa* decreases as temperature increases in summer (Okamura, 1987). *E. pilosa* has a wide distribution in temperate seas both north and south of the British Isles and is tolerant to chronic long-term changes in temperature in British waters. However, acute temperature changes such as those from discrete climate events have been reported to affect growth, feeding and reproduction in the species (Tyler, 2005). The barnacle *Balanus crenatus* has a low thermal tolerance to increases in temperature, often being replaced by the subtropical barnacle *Balanus amphitrite* in higher than average temperatures (Tillin, 2016). The impacts of an increase in oceanic temperature during warmer years on the more thermally tolerant species such as the polychaetes *S. alveolata* and *S. triqueter* are likely to be due to a combination of environmental stress factors such as availability of food and the disturbance and creation of open space due to shifts in community composition as less thermal tolerant species such as the bryozoan *E. pilosa* are replaced by more tolerant species.

Previous studies on the influence of temperature on marine ecosystem have focused primarily on intertidal organisms (Firth et al., 2011) or tropical species (Glynn et al., 2001). This is probably because intertidal organisms are thought to live close to their thermal limit and as such, are less resistant to warming (Helmuth, 2009). Studies of differently thermally adapted congeneric ectotherms have shown that warm adapted species may have a more limited ability to increase heat tolerance. For instance a study of thermal acclimation of temperate and tropical fiddler crabs of the genus *Uca*, found that only temperate zone species exhibited acclimation induced adjustment in their thermal tolerance limits. The tropical species, because of the high microhabitat temperatures routinely experienced, were hypothesized to have upper thermal limits that were as high as could be reached through acclimation, so no further acclimation was possible (Vernberg and Tashian, 1959). In this context, Stillman and Somero (2000) suggest that in the absence of selection for heat tolerance, this ability may be lost or that there may be physiological costs involved in maintaining an elevated upper thermal limit.

Furthermore, organisms living in the intertidal have molecular mechanisms to cope with high temperature changes that those in the subtidal do not. For example, temperate zone subtidal species of the gastropod genus *Tegula* are unable to synthesize Hsp70 proteins at the highest temperatures experienced by their intertidal congeners (Tomanek et al., 2002), whereas their intertidal counterparts can. The synthesis of the Hsp family of proteins is a molecular mechanism

responsible for maintaining the folded state of denatured proteins under environmental stress and increased HAP expression is often used as an environmental biomarker of stress (Clark et al., 2009). Temperate subtidal biofouling organisms are therefore vulnerable to relatively small amounts of future oceanic warming, particularly during warmer years. This is a growing concern since warmer years/extreme events are predicted to increase in frequency and magnitude as a consequence of global warming but their ecological effects on marine ecosystems are still poorly understood (Wernberg, 2012).

6.5.2 Growth rates

Higher growth rates in the +2°C treatment during Spring and Autumn may elucidate observed alterations in seasonality patterns driven by climate change, with Spring temperatures matching those predominantly experienced during "normal" Summers and Summer temperatures exceeding normal averages. These patterns have already been observed in a variety of systems: climate warming is causing spring to start earlier and summer to last longer, shifting the timing of reproduction, larval release and settlement in many species (Philippart et al., 2003) e.g. Southern species of the limpet *Patella depressa* are breeding earlier and for a longer period during the year (Moore et al., 2011). There is a good understanding of the impact of temperature on biochemical processes, but our ability to expand, integrate and apply this knowledge to the organism level is still limited (Clarke, 2003; Pörtner et al., 2007; Ashton et al., 2017), with a few exceptions such as the predicted impact of warming on some host-parasite interactions (Kirk et al., 2018).

In this study we would expect growth rates in the main coloniser *S. triqueter* to increase with temperature, as increased temperature raises metabolic rates (Clarke et al., 2004) and growth rates (Schmidt-Nielsen, 1997; Peck, 2016). This pattern is observed across the seasons in this study: growth rates increase with temperature in Spring and Autumn. However, in the Summer season growth rates were significantly lower in the +1°C treatment in comparison to the control and +2°C treatment. Availability of free space may explain some of the differences observed: panels in the +1°C treatment were less covered than those in the other treatments. Rapid growth rates are reported to be advantageous in benthic biofouling communities where space is limiting (Sutherland et al., 1977; Barnes et al., 2014; Ashton et al., 2017) hence higher growth rates in the control and +2°C might suggest a competitive advantage for new colonisers over those in the +1°C treatment during summer, where space is limited. However, higher growth rates come at an energetic cost due to the trade-offs associated with metabolism at higher temperatures: as

temperature increases, metabolic rates increase, eventually leading to insufficient ATP production and reducing oxygen supply to the tissues (Pörtner, 2001; Pörtner, 2002), and also increasing the formation of reactive oxygen species (ROS) due to heat stress (Heise et al., 2002).

Furthermore, higher metabolic rates increase the requirement for food consumption in order to meet the increased requirements e.g. in a study by Clark et al., (2013) oysters at higher temperatures were unable to consume enough food to fuel their increased metabolic requirements, resulting in reduced shell growth. It is unclear whether the oysters would have been able to sustain these growth rates over a prolonged exposure (e.g. a year) to the experimental temperatures, or whether seasonal food supplies would have had an impact (Peck, 2018). In serpullids, food supply is known have a major influence in growth rates, more than temperature changes. In the polychaete *Hydroides elegans*, low food concentration reduced the survivorship and settlement of newly settled juveniles whilst temperature was not a limiting factor (Qiu et al., 1997). This pattern is also observed across other calcareous species such as the coral *L. pertursa*. Although *L. pertusa* is capable of calcifying under elevated CO2 and temperature, growth rates are more strongly influenced by food availability (Büsher et al., 2017). A 10-fold higher food supply stimulated growth under elevated temperature, which was not observed in the combined elevated temperature and CO2 treatment, indicating that increased food supply does not compensate for adverse effects of temperature. These studies further underly the importance of considering the nutritional status in studies investigating organism responses under environmental changes.

As temperature is known to influence the growth rate of serpulid tubes (Ten Hove, 1979), growth rates of *Spirobranchus triqueter* were measured using tube dimensions as oppose to tissue measurements. Water temperature and salinity influence the biomineralization and the growth of serpulids. Lowenstam & Weiner (1989) showed that the calcite-aragonite ratio changes along the tube of *Hydroides gracilis* (previously known as *Eupomatus gracilis*) with seasonal changes in ambient water temperature, showing a positive correlation between aragonite content and temperature. Both entirely calcitic tubes as well as tubes of mixed mineralogy show an increase in MgCO3 content within the calcite with increasing water temperatures (Bornhold & Milliman, 1973). Further studies investigating effects of temperature on growth rates of serpullids have used tube dimensions as oppose to tissue as a proxy for growth rates (Ni et al., 2018; Li et al., 2016).

6.5.3 Assemblage composition

Despite the differences reported here in percentage cover and growth rate driven by temperature, temperature did not have an effect on the overall community composition on the settlement panels. At the start of each experimental time point, species composition on heated treatments was very different from the control, but as the community developed over time, communities across treatments became more similar. The availability of free space may explain the similar assemblage composition within treatments, as over time panels became more covered and thus species outcompeted each other for space e.g. *Bugula turrita*, a bryozoan that usually settles on rocks along the North American coastlines is overgrown at low densities by *Schizoporella errate*, which has a more rapid growth rate (Michele, 1986). Similar results have been observed among fouling organisms in experimental panels in Tomioka Bay, Japan, with the colonial ascidian *Diplosoma mitsukurii* overgrowing the other species present (Nandakumar et al., 1993). Differences in biofilm composition as a result of environmental temperature changes may also be driving the observed patterns. Studies have shown that changes in temperature drive biofilm differences across species. Larval settlement of the coral reef sponge *Rhopoloeides odorabile* is induced more effectively by biofilms developed at higher temperatures in comparison to those developed at lower ones (Whalan & Webster, 2014). This is also true for other marine species e.g. Lau et al., (2005) reported that larval settlement of the barnacles *Balanus amphitrite* and *B. trigonus* was also induced more by biofilms developed at high temperatures compared to those at lower temperatures.

Community composition in this study, however, was different within panels of the same treatment e.g. panels that were in different frames. These frames were deployed within close proximity of each other but due to the topography of the site (Simpson et al., 2007), there was a large intra-site variability. Panels in frame 4 were closer to the mouth of the strait, potentially experiencing slightly stronger currents than those in frame 1, closer to the sheltered inlet of the bay. Thus panels deployed on frames on either end (the faster flowing region of the strait or the inlet) of the site would have been subjected to somewhat different physical and biological conditions, even though they were at the same deployment site. This highlights the importance of microscale differences within benthic habitats: within a single site, differences in topography or microcurrents can have profound effects on the biofouling communities that settle on panels (Barnes, 2014).

It is interesting to note however that in contrast to other studies (Ashton et al., 2017), community composition here was similar across treatments. The biofouling species observed on the settlement panels in this study have a wide intertidal-subtidal distribution (Mettam, 1994) and some of the main biofoulers (*Spirobranchus triqueter, Sabellaria alveolata* and *Diplosoma listeranium)* have high thermal limits (Somero, 2002) as previously discussed. Hence we would expect species to settle on all panels regardless of treatment. Perhaps differences in community composition driven by temperature would have been observed over a longer deployment (9 months as in Ashton et al., 2017) due to the differences in behavioural and physiological coping strategies and species-specific responses to temperature over time, as observed in other systems (Kordas et al., 2014).

The short-term experimental period of the study although annual, precluded studying long-term growth and assemblage development of individual organisms across time (see Ashton et al., 2017). This was due to the limitations of the technology: the panels warm a 2mm layer of water, making deployments challenging in temperate and tropical environments as organisms here have much faster growth rates. The faster growth rates also result in panels becoming fully covered in shorter periods of time than in Antarctica that then reduces the ability to measure attributes such as growth rates because organisms impinge on each other. Replication of this experiment across multiple years would elucidate environmental variability and organism responses across time, and include factors such as El Niño or NAO (North Atlantic Oscillation) years. Nevertheless, this study demonstrated that although in shorter time-scales, heated panel technology can be successfully applied to biofouling communities in temperate climates, previously thought to be more resilient than polar or tropical assemblages to small changes in temperature.

6.6 References

Ashton, G. V., Morley, S. A., Barnes, D. K. A., Clark, M. S. and Peck, L. S. (2017). Warming by 1°C drives species and assemblage level responses in Antarctica's marine shallows. *Curr. Biol*. **27**, 2698–2705.

Barnes, D. K. A., Fenton, M. and Cordingley, A. (2014). Climate-linked iceberg activity massively reduces spatial competition in Antarctic shallow waters. *Curr. Biol*. **24**, 553–554.

Borthagaray, A. I., Brazeiro, A. and Giménez, L. (2009). Connectivity and patch area in a coastal marine landscape : Disentangling their influence on local species richness and composition. *Austral. Ecol*. **34**, 641–652.

Bowden, D. A., Clarke, A., Peck, L. S. and Barnes, D. A. K. (2006). Antarctic sessile marine benthos: colonisation and growth on artificial substrata over three years. *Mar. Ecol. Prog. Ser.* **316**, 1-16.

Büscher, J. V., Form, A. U. and Riebsell, U. (2017). Interactive effects of ocean acifification and warming on growth, fitness and survival of the col-water coral *Lophelia pertusa* under different food availabilities. *Front. Mar. Sci*. **4**, 101.

Carpenter, S. R. and Pace, M. L. (1997). Dystrophy and eutrophy in lake ecosystems: implications of fluctuating inputs. *Oikos.* **78**, 3-14.

Castric-Frey, A. (1983). Recruitment, growth and longevity of *Pomatoceros triqueter* and *Pomatoceros lamarckii* (Polychaeta, Serpulidae) on experimental panels in the Concarneau area, South Brittany. Ann. Inst. Oceanogr. (Paris). **59**, 69-91.

CEFAS, https://www.cefas.co.uk/cefas-data-hub/wavenet.

Clark, M. S. and Peck, L. S. (2009). Marine Genomics HSP70 heat shock proteins and environmental stress in Antarctic marine organisms : A mini-review. *Mar. Genomics*. **2**, 11–18.

Clark, M. S., Thorne, M. A. S., Amaral, A., Vieiram, F., Bautista, F. M., Reis, J. and Power, D. M. (2013). Identification of molecular and physiological responses to chronic environmental challenge in an invasive species: the Pacific oyster, *Crassostrea gigas*. *Ecol. Evol.* **3**, 3283-3297.

Clark, M. S., Thorne, M. A. S., Burns, G. and Peck, L. S. (2016). Age-related thermal response: the cellular resilience of juveniles. *Cell. Stress. Chaperones*. **21**, 75-85.

Clarke, A. and Fraser, K. P. P. (2004). Why does metabolism scale with temperature? *Funct. Ecol.* **18**, 243-251.

Costanza, R., Groot, R. De., Farber, S., Grasso, M., Hannon, B. and Limburg, K. (1998). The value of ecosystem services: putting the issues in perspective. *Ecol. Econ.* **25**, 67-72.

De Groot R, Brander L, Ploeg SV, Costanza R, Bernard F, Braat, L. et al. (2012). Global estimates of the value of ecosystems and their services in monetary units. *Ecosystem services,* **1**, 50-61.

Firth, L. B., Knights, A. M. and Bell, S. S. (2011). Air temperature and winter mortality: implications for the persistence of the invasive mussel, *Perna viridis* in the intertidal zone of the south-eastern United States. *J. Exp. Mar. Biol. Ecol.* **400**, 250-256.

Glynn, P. W., Mate, J. L., Baker, A. C. and Calderon, M. O. (2001). coral bleaching and mortality in Panama and Ecuador during the 1997-1998 El Niño - Southern Oscillation event: Spatial/temporal patterns and comparisons with the 1982-1983 event*. Bull. Mar. Sci.* **69***, 79-109.*

Grime, J. P., Fridley, J. D., Askew, A. P., Thompson, K., Hodgson, J. G. and Bennett, C. R. (2008). Long-term resistance to simulated climate change in an infertile grassland. *Proc. Natl. Acad. Sci. USA.* **105**, 10028-10032.

Harley, C. D. G., Hughes, A. R., Kristin, M., Miner, B. G., Sorte, C. J. B. and Carol, S. (2006) The impacts of climate change in coastal marine systems. *Ecol. Lett.* **9**, 228–241.

Hawkins, S. J., Sugden, H. E., Mieszkowska, N., Moore, P. J., Poloczanska, E., Leaper, R. et al. (2009). Consequences of climate-driven biodiversity changes for ecosystem functioning of North European rocky shores. *Mar. Ecol. Prog. Ser*. **396**, 245–259.

Hayward, P. J. and Ryland, J. S. (1990). The Marine fauna of the British Isles and North-West Europe. (Clarendon Press).

Hayward, P. J. and Ryland, J. S. (1995). Handbook of the Marine Fauna of North-West Europe. (Oxford Univ. Press).

Heise, K., Puntarulo, S., Pörtner, H. O. and Abele. D. (2003). Production of reactive oxygen species by isolated mitochondria of the Antarctic bivalve *Laternula elliptica* (King and Broderip) under heat stress. *Comp. Biochem. Physiol.* **134C**, 79-90.

Helmuth, B. (2009). From cells to coastlines: how can we use physiology to forecast the impacts of climate change? *J. Exp. Biol.* **212**, 753-760.

IPCC .(2014). Climate Change 2014 Synthesis Report Summary for Policymakers.

Kirk, D., Jones, N., Peacock, S., Phillips, J., Molnár, P. K., Krkošek, M. et al. (2018). Empirical evidence that metabolic theory describes the temperature dependency of within-host parasite dynamics. *PLoS. Biol.* **16**, e2004608.

Kordas, R. and Dudgeon, S. (2014). Intertidal community responses to field-based experimental warming warming. *Oikos.* **124**, 888-898.

Lau, S. C. K., Thiyagarajan, V., Cheung, S. C. K. and Qian, P. Y. (2005). Roles of bacterial community composition in biofilms as a mediator for larval attachment of three marine invertebrates. *Aquat. Microb. Ecol.* **38**, 41-51.

Li, C., Meng, Y., Chong, H., Vera, B. S. C., Yao, H. and Thiyagarajan, V. (2016). Mechanical robustness of the calcareous tubeworm Hydroides elegans: warming mitigates the adverse effects of ocean acidification. *Biofouling*. **32**, 191-204.

Lowenstam ,H. A. and Weiner, S, (1989), On Biomineraliztion. Oxford University Press, Oxford.

Lurgi, M., Lopez, B. C. and Montoya, J. M. (2012). Climate change impacts on body size and food web structure on mountain ecosystems. *Philos. Trans. R. Soc. Lond. B. Biol. Sci*. **367**, 3050–3057.

McElroy, D. J., Gorman, E. J. O. and Schneider, F. D. (2015). Size-balanced community reorganization in response to nutrients and warming. *Glob. Change. Biol.* **21**, 3971–3981.

Mettam, C., Conneely, M. E. and White, S. J. (1994). Benthic macrofauna and sediments in the Severn Estuary. *Biol. J. Linn. Soc.* **51**, 71-81.

Michele, S. (1986). Sessile macrofauna and marine ecosystem. *Ital. J. Zool.* **53**, 329-337.

Mieszkowska, N., Kendall, M. A., Hawkins, S. J., Leaper, R. and Williamson, P. (2006). Changes in the range of some common rocky shore species in Britain – a response to climate change? *Mar. Biodivers*. **555***,* 241–251.

Moore, P. J., Thompson, R. C. and Hawkins, S. J. (2011). Phenological changes in intertidal con-specific gastropods in response to climate warming. *Glob. Change. Biol.* **17**, 709-719.

Nandakumar, K., Tanaka, M. and Kikuchi, T. (1993). Interspecific competition among fouling organisms in Tomioka Bay, Japan. *Mar. Ecol. Prog. Ser.* **94**, 43-50.

Ni, S., Taubner, I., Böhm, F., Winde, V. and Böttcher, M. E. (2018). Effect of temperature rise and ocean acidification on growth of calcifying tubeworm shells (*Spirorbis spirorbis*): an in situ benthocosm approach. *Biogeosciences*. **15**, 1425-1445.

Okamura, B. (1988). The influence of neighbours on the feeding of an epifaunal bryozoan. *J. Exp. Mar. Biol. Ecol*. **120**, 105-123.

Pansch, A., Winde, V., Ragnhild, A. and Asmus, H. (2016). Tidal benthic mesocosms simulating future climate change scenarios in the field of marine ecology. *Limnol. Oceanogr-methods.* **14**, 257-267.

Peck, L. S. (2011). Organisms and responses to environmental change. *Mar. Genomics*. **4**, 237-243.

Peck, L. S., Clark, M. S., Power, D., Reis, J., Batista, F. M. and Harper, E. M. (2015). Acidification effects on biofouling communities: winners and losers. *Glob. Change. Biol.* **21**, 1907-1913.

Peck, L. S. (2018). Antarctic marine biodiversity: adaptations, environments and responses to change. *Oceanogr. Mar. Biol. Annu. Rev. in press.*

Philippart, C. J. M., Aken, H. M., VanBeukema, J. J., Bos, O. G., Cade, G. C. and Dekker, R. (2003). Climate-related changes in recruitment of the bivalve *Macoma balthica*. *Limnol. Oceanogr.* **48**, 2171–2185.

Poloczanska, E. S., Hawkins, S. J., Southward, A. J. and Burrows, M. T. (2008). Modeling the response of populations of competing species to climate change. *Ecology.* **89**, 3138-3149.

Pörtner, H. O. (2001). Climate change and temperature-dependent biogeography: oxygen limitation of thermal tolerance in animals. *Naturwissenschaften.* **88**, 137-146.

Pörtner, H. O. (2002). Climate variations and the physiological basis of temperature dependent biogeography : systemic to molecular hierarchy of thermal tolerance in animals. *Comp. Biochem. Physiol. Part A Mol. Integr. Physiol.* **132**, 739–761.

Pörtner, H. O., Peck, L. S. and Somero, G. (2007). Thermal limits and adaptation in marine Antarctic ectotherms : an integrative view. *Philos. Trans. R. Soc. Lond. B. Biol. Sci.* **362**, 2233–2258.

Qiu, J. W. and Qian, P. Y. (1997). Combined effects of salinity, temperature and food on early development of the polychaete *Hydroides elegans*. *Mar. Ecol. Prog. Ser*. **152**, 79-88.

Riley, K. and Ballerstedt, S. (2005). *Spirobranchus triqueter* A tubeworm. In Tyler-Walters, H. and Hiscock, K. (eds) Marine Life Information Network: Biology and Sensitivity Key Information Reviews, (online). Plymouth: Marine Biological Association of the United Kingdom. (Cited 09-03-2019). Available from: https://www.marlin.ac.uk/species/detail/1794.

Roberts, E. M., Bowers, D. G. and Davies, A. J. (2014). Springs – neaps cycles in daily total seabed light : Daylength-induced changes. *J. Marine. Syst.* **132**, 116–129.

Ryland, J. S. (1976). Physiology and ecology of marine bryozoans. *Adv. Mar. Biol*. **14**, 285-443.

Sanford, E. (1999). Regulation of Keystone Predation by small changes in ocean temperature. *Science.* **283***,* 2095-2097.

Schiel, D. R., Steinbeck, J. R. and Foster, M. S. (2010). Ten years of induced ocean warming causes comprehensive changes in marine benthic communities. *Ecology*. **85**, 1833–1839.

Schmidt-Nielsen, K. (1997). *Animal Physiology: Adaptation and Environment*, 4th edn, Cambridge: Cambridge University Press, 602 pp.

Simpson, J. H., Berx, B., Gascoigne, J. and Saurel, C. (2007). The interaction of tidal advection, difussion and mussel filtration in a tidal channel. *J. Mar. Syst.* **68**, 556-568.

Simpson, T. J. S., Smale, D. A., McDonald, J. I. and Wernberg, T. (2017). Large scale variability in the structure of sessile invertebrate assemblages in artificial habitats reveals the importance of local-scale processes. *J. Exp. Biol. Ecol.* **494**, 10-19.

Smale, D. A., Taylor, J. D., Coombs, S. H., Moore, G. and Cunliffe, M. (2017). Community responses to seawater warming are conserved across diverse biological groupings and taxonomic resolutions. *Proc. R. Soc. Lond. B. Biol. Sci.* **284***,* 20170534.

Smale, D. A. and Wernberg, T. (2012). Ecological observations associated with an anomalous warming event at the Houtman Abrolhos Islands, Western Australia. *Coral. Reefs.* **31**, 441-441.

Smale, D. A., Wernberg, T., Peck, L. S. and Barnes, D. K. A. (2011). Turning on the Heat: Ecological response to simulated warming in the sea. *PLos. One*. **6**, e16050.

Somero, G. N. (2002). Thermal physiology and vertical zonation of intertidal animals: optima, limits and costs of living. *Integr. Comp. Biol.* **42**, 780-789.

Stillman, J. H. and Somero, G. N. (2000). A comparative analysis of the upper thermal tolerance limits of eastern Pacific porcelain crabs, genus Petrolisthes: influences of latitude, vertical zonation, acclimation, and phylogeny. *Physiol. Biochem. Zool.* **73**, 200-8.

Sutherland, J. P. and Karlson, R. H. (1977). Development and stability of the fouling community at Beaufort, North Carolina. *Ecol. Monogr.* **47**, 425-446.

Ten Hove, H. A. (1979). Different causes of mass occurrence in serpulids. In: Biology and systematics of colonial organisms. Academic Press, London, Systematics Association Special Volume, 11, pp. 281-298.

Thibault, K. M. and Brown, J. H. (2008). Impact of an extreme climatic event on community assembly. *Proc. Natl. Acad. Sci. USA.* **105**, 3410-3415.

Tomanek, L. and Helmuth, B. (2002). Physiological ecology of rocky intertidal organisms: a synergy of concepts. *Integr. Comp. Biol.* **42**, 771-775.

Tillin, H. M. (2016). Filamentous red seaweds, sponges and Balanus crenatus on tide-swept variable salinity infralittoral rock. In Tyler-Walters H. and Hiscock K. (eds). Marine Life Information Network: Biology and Sensitivity key information Reviews, (online). Plymouth: Marine Biological Association of the United Kingdom. (Cited 09/03/19). Available from: https://www.marlin.ac.uk/habitat/detail/218.

Tyler-Walters, H. (2005). *Electra pilosa* a sea mat. In Tyler-Walters H. and Hiscock, k. (eds). Marine life information network: Biology and sensitivity key information reviews, (online). Plymouth: Marine Biological association of the United Kingdom. (Cited 09/03/2019). Available from: https://www.marlin.ac.uk/species/detail/1694.

Vernberg, F. J. and Tashian, R. E. (1959). Studies on the physiological variation between tropical and temperate zone fiddler crabs of the genus Uca. II. Thermal limtis. *Ecology.* **40**, 589-593.

Wernberg, T., Thomsen, M. S., Tuya, F. and Kendrick, G. A. (2011). Biogenic habitat structure of seaweeds change along a latitudinal gradient in ocean temperature. *J. Exp. Mar. Biol. Ecol.* **400**, 264–271.

Wernberg, T., Smale, D. A., Tuya, F., Thomsen, M. S., Langlois, T. J., de Bettignies, T. et al. (2012) An extreme climatic event alters marine ecosystem structure in a global biodiversity hotspot. *Nat. Clim. Change*. **3**, 78–82.

Whalan, S. and Webster, N. S. (2014). Sponge larval settlement cues: the role of microbial biofilms in a warming ocean. *Sci. Rep.* **4**, 4072.

Yergeau, E., Bokhorst, S., Kang, S., Zhou, J., Greer, C. W., Aerts, R. and Kowalchuk, G. A. (2011). Shifts in soil microorganisms in response to warming are consistent across a range of Antarctic environments. *ISME.* **6**, 692–702.

Young, A. and Kay, P. (1999). *Marine Wildlife of Atlantic Europe*: Muze Media.

Chapter 7

In this project I used state of the art technologies: heated settlement panels, to evaluate the effects of *in situ* oceanic warming on marine benthic recruitment and community development. The aims of the project were to evaluate whether marine benthic Antarctic organisms will be able to acclimate to end of century oceanic warming predictions (IPCC, 2014) at the molecular level. Upper thermal limit (UTL) and heat shock experiments were carried out on one of the main colonisers, the spirorbid worm *Romanchella perrieri*. Insights into the genes associated with thermal stress were obtained from an analysis of differential gene expression on another main coloniser, the spirorbid worm *Protolaeospira stalagmia*. Differences in the biofilm communities of panels across heated and non-heated treatments provided insights on the effect of heating on the composition of the microbial communities and whether differences in colonisation observed in panels were due to differences in biofilm communities. The heated settlement panels were also deployed in a temperate ecosystem, the Menai Strait (North Wales, UK) to provide insights on the use of this technology in other ecosystems and the effects of 1-2°C warming (predicted end of century oceanic temperatures (IPCC, 2014) on temperate communities.

7.1 Lack of acclimation in Antarctic marine organisms to end of century oceanic warming predictions

R. perrieri spirorbid worms were unable to acclimate to either a 1°C or 2°C temperature increase after 18 months of exposure to the heated treatments: the organisms' upper thermal temperatures declined with an increase in the ambient temperature. These data therefore suggested that *R. perrieri* were resisting in the higher temperatures rather than acclimating to them. As highlighted previously in Chapter 3, the acclimation timings allowed for *R. perrieri* were far beyond those previously identified as necessary in Antarctic marine organisms to acclimate. These findings were further validated by the transcriptomic analysis on the congeneric species *Protolaeospira stalagmia*, which showed the massive up-regulation of the cellular stress response at +2°C. These data suggested that these encrusting organisms will be unable to cope with predicted end of century oceanic warming (IPCC, 2014).

Thus, organisms on the warmer panels were in a permanent state of resistance and/or decline depending on the individual and temperature. The fact that this was still in process after 18 months exposure, much longer than any previously identified time line (Morley et al., 2011) is probably a reflection of the low energy lifestyle of these species and their very slow metabolisms (Peck, 2018). Furthermore, it highlights a critical factor in understanding Antarctic marine responses to climate change: that of extended senescence. These processes can only be evaluated using molecular techniques as this study shows, as persistence with decline in physiological capacity may not be accompanied by outward morphological signs in such long- lived species with calcareous exoskeletons. In the 9 month preliminary ecological study using these heated panels, Ashton et al., (2017) observed accelerated invertebrate growth and colonisation rates for *R. perrieri* on the heated panels in the warmed treatments throughout the summer (the exception being a decline in March), but this situation was clearly not sustainable long-term as the molecular data demonstrates.

Different guilds may respond differently to climate change depending on their feeding mode: whether they are suspension feeders, scavengers etc. In a study by Suckling et al., (2015), the sea urchin *Sterechinus neumayeri* was exposed to the combined stresses of temperature and low pH in laboratory conditions for 17 months to 2°C and showed no significant physiological effects. In contrast to *R. perrieri* and *P. stalagmia*, the sea urchin *S. neumayeri* is a scavenger/detritivore, capable of actively finding food. *R. perrieri* and *P. stalagmia* on the other hand, are suspension feeders and depend on the seasonal algal bloom to feed, making them more susceptible to changes in the primary productivity and the extreme seasonality of the Antarctic marine environment (Barnes and Clarke, 1995). The Ashton et al., (2017) study hinted at a potential problem for sustained growth rates with seasonality effects. *R. perrieri* growth rates accelerated on the warmed treatments throughout the summer with the exception of March, where the decline in growth rates coincided with the end of the algal bloom (and the relevant food source). This highlights the impacts on cellular homeostasis that a 1°C or 2°C temperature increase in the environment of these Antarctic encrusting species can have, especially with regard to the ability of these animals to maintain not only enhanced growth rates, but also sufficient food stores over winter to ensure longevity in the species as highlighted previously.

The effects that predicted oceanic warming (IPCC, 2014) might have on the primary productivity and as a consequence, on the feeding of Antarctic organisms are hard to predict. The Western Antarctic peninsula (WAP) is one of the fastest warming regions on Earth, with a rise in surface

ocean temperature of over 1°C (Meredith and King, 2005). The increase in surface temperature and the inflow of warm, mid-depth Upper circumpolar deep water (UCDW) from the Antarctic circumpolar current (ACC) has resulted in a massive reduction in the number of days of winter sea ice (Ducklow et al., 2013) and the rapid retreat of the majority of glaciers along the peninsula (Cook et al., 2005) with impacts for the ecosystem. Over the past three decades, primary productivity in the WAP has declined as sea ice cover has diminished and wind mixing has increased (Montes-Hugo et al., 2009). Reductions in sea ice have significant effects on filter feeding assemblages through change in the seasonal production of phytoplankton, in terms of the magnitude, timing quality and duration of the plankton bloom (Lohrer et al., 2013). Rapid warming in the WAP has already led to shifts within the size class distribution of phytoplankton, where low winter sea-ice cover leads to low phytoplankton biomass and enhanced proportions of nanophytoplankton (Rozema et al., 2016). These changes can potentially alter the Southern Ocean food web drastically (Atkinson et al., 2004). The impacts described above are not unique to Antarctica, as changes in the primary productivity of the Southern Ocean have pronounced implications on a global level for the marine biosphere, carbon sink and biogeochemistry of Earth (Falkowski et al., 2000). Understanding the impacts of temperature on the cellular homeostasis of Antarctic encrusting species is a key element in a wider understanding of changes in primary productivity and the effects on filter feeders, in order to predict the impacts of end of century oceanic warming (IPCC, 2014) at a global level.

Future work: Given the strong seasonality patterns in Antarctica in light and primary productivity, replication of the upper thermal limit and transcriptome analysis and sampling of the organisms across different time points in the season i.e. the beginning of summer (at the start of the plankton bloom), the end of summer and the end of winter should be explored in future experiments in order to elucidate the extent of the vulnerability of these organisms to thermal stress during the winter period when food is limited. This would also highlight on a global scale, the effects of primary productivity on the thermal stress of Antarctic organisms. In particular, these studies should incorporate more detailed oceanographic data on phytoplankton constitution (species, size and relative proportion in the bloom) linked to the Rothera Time Series (RaTS), which is collected on a year round basis at Rothera Research Station. These data could be provided by either by microscopical observations, chemical analyses and/or molecular analyses of the bloom (Rozema et al., (2016)).

7.2 Little evidence of post-selection recruitment and genetic adaptation in *Protolaeospira stalagmia* with warming

Protolaeospira stalagmia spirorbid worms showed little evidence of post-selection recruitment and genetic adaption, supported by no significant differences when analysing SNPs individually. These results together with the transcriptomic and upper thermal limit (UTL) data in *R. perrieri* discussed previously, suggest a lack of physiological and genetic flexibility in encrusting species to warming. As Somero (2010) argues, acclimation via physiological flexibility is the most important process that dictates the survival or failure of a long-lived species, as given the current rates of change, these species will have very few generations in which they can genetically adapt. Following from this argument, is the fact that the knowledge of the extent of phenotypic plasticity within populations and the capacity of genotypes to produce different phenotypes in response to environmental variation is key, in order to predict biodiversity change in face of end of century predicted oceanic warming (IPCC, 2014). But, in this study, these encrusting worms were unable to acclimate and the population genetic data suggests a lack of genetic flexibility to warming. It therefore seems unlikely that *P. stalagmia* will be able to recruit and survive predicted end of century oceanic warming (IPCC, 2014). The strong frontal systems associated with the Antarctic circumpolar current (ACC) and the fact that Antarctica is a circular continent which is universally cold restrict the migration of Antarctic marine species to more favourable areas. The Southern Ocean is warming, there are no colder refuges for marine species to migrate to in the future.

However, responses of species and ecosystems to climate change are multifactorial and potentially more complex than the analyses presented here. Recent analysis suggests that the atmospheric warming seen along the Peninsula during the second half of the 20th century has ceased (Turner et al., 2016), but, it is still uncertain whether these atmospheric trends are also reflected in the oceanographic data, where sea ice changes and glacier retreat are still occurring (Barnes & Souster, 2011; Cook et al., 2016). Increasing periods of thermal stress will produce directional selection for resistance, particularly in species that live close to their physiological limits. Rapid climate change is likely to produce a range of new selection pressures on populations as several ecological factors may become important that are outside of acclimation and genetic flexibility limits. These include but are not limited to availability of food and space for settlement and colonisation (Barnes & Peck, 2008; Chown & Gaston, 2008). As previously discussed, primary productivity changes in the WAP have already been observed (Schofield et al., 2018) but the impacts of these on encrusting organisms are still uncertain. Coupled with these pressures is the very slow larval development rates and long generation times of Antarctic species (Peck, 2005)

which means that rapid genetic adaptation in these species is also unlikely. So although from the molecular data presented in this thesis, the spirorbids appear unlikely to survive even small increases in warming, the actual responses may well be a result of the complex interactions between the rate of change together with the above mechanisms.

The pressures and mechanisms discussed above can be observed on a global scale, not only in Antarctica. Tropical ectotherms living close to their upper thermal tolerance (Tewksbury et al., 2008), intertidal organisms where post-settlement selection leads to different genotypes becoming established in different physical or biotic conditions (Schmidt and Rand, 2001) are all examples of how species with the adequate genetic variation to generate phenotypes with different thermal tolerances prove to be winners in a warming world. Clearly more data are required in Antarctic species, such as the longer term studies suggested above.

In this study it is important to highlight the constrains of the population genetic analysis: analyses were carried out on pools and not individuals. Since sequencing errors confounded with the alleles present at low frequency in the pools can give rise to false positive variants (Anand et al., 2016), the results in these study were analysed conservatively, in order to reduce the rise of false positives. Future experiments should therefore aim to explore SNP data using individual samples rather than pools. Although using individuals rather than pools was not possible in this study for this particular species and for the sequencing kit used (TruSeq) due to the low amounts of RNA in individual *P. stalagmia* samples, there are other kits available such as the SMARTer kit (Clontech Laboratories) that require very low inputs of RNA (10pg-10ng) that could be explored. Whole genome amplification could also be used for analysing SNPs in the DNA. The limitation of this again is the high amounts of DNA required for the analysis (Dagnall et al., 2018), which is often difficult to obtain in small organisms such as the ones in this study.

7.3 Metazoan and bacterial responses to temperature differ dramatically

Biofilm bacterial communities showed no significant differences in community structure with temperature. This contrasts with the findings observed in the metazoan encrusting species above which had a high thermal sensitivity. Of the few studies performed, results have indicated that there are relatively wider temperature ranges for Antarctic marine bacteria when compared with the invertebrates. For example a *Pseudoalteromonas* species from the South Shetlands demonstrated a temperature range from -2°C to 18°C, whilst a *Cellulophaga* species from the same area survived up to 41°C (Jeong et al., 2014), which underpins the findings of bacterial

flexibility identified here. These findings consolidate the hypothesis of greater resilience and adaptability of prokaryotic communities under future climate change compared with the high thermal sensitivity of the Metazoa.

Prokaryotes have a degree of physiological plasticity that is unparalleled in the eukaryotic world: the unique ability to shift to an entirely different lifestyle within a short time in order to accommodate to the changing environment. A classic example of this *is Rhodobacter sphaeroides*, that grows anaerobically as a phototroph but also grows aerobically as a chemoheterotroph (Roh et al., 2000). Future studies incorporating functional differences across microbial groups and transcriptomic analysis might yield insights in to whether these phenotypic traits are also observed on the microbial biofilm of the heated settlement panels. These studies would determine how temperature affects the functionality of the bacterial community, especially in terms of the nutrients produced that may be metabolised by biofoulers, which in turn could affect their resilience.. Given that the panels were deployed *in situ*, these experiments have an opportunity to forge a new understanding between the physical and chemical features of the environment, the composition of microbial communities and their activities, and allow predictions under predicted oceanic warming scenarios.

The vast majority of studies and ecosystem effects of climate change scenarios (Walther et al., 2002; Parmesan et al., 2003; IPCC, 2014) do not accommodate for the enormous physiological plasticity of prokaryotes. This may necessitate the development of new principles applicable to microbial communities, in order to predict the effects of future oceanic warming on ecosystems, as changes at the microbial community level will impact the settlement and metamorphosis of invertebrate larval. Studies observing the interplay between biofilm communities and the resulting benthic assemblages in the context of climate change are lacking in marine studies. The use of heated settlement panels to address these questions would allow us to gain a clearer picture of the interactions between the biofilm community and the benthic assemblages and discriminate which might play a major role in determining the resulting biofilm community. This is particularly relevant to the findings observed in the heated settlement panels, where small differences in the biofilm communities within a single panel of the same treatment were observed (Refer to Chapter 5 for further detail). Biofilms influence what settles on them/next to them but at the same time marine invertebrates also influence the development of biofilm communities. Future experiments should therefore also consider sampling the biofilm community on at least another two time points: towards the beginning of the study (please refer to Rampadarath et al., (2017) for an example of metagenomics and metatranscriptomics to investigate bacterial diversity during early

stage biofilm formation) and in the middle and comparing it to the benthic community developed next to each sample taken. This would require increasing the number of samples for each time period and panel. This, coupled with ecological studies such as the Ashton et al., (2017) would allow us to gain a clearer picture of the interactions between the biofilm and the benthic assemblages and the subsequent effects of temperature on the ecosystem.

Nevertheless, it seems that groups such as prokaryotes that possess more plasticity will be the winners under future oceanic warming predictions, particularly in comparison to the Antarctic invertebrates in this study, that are highly stenothermal and unable to acclimate to predicted end of century oceanic warming (IPCC, 2014).

7.4 Discrete climate events may drive temperate species above their thermal limits (UK studies)

Temperature had no effects on the percentage cover and community composition in the panels deployed in the Menai Strait except when comparing the months of June 2015 and June 2016. Further analysis revealed that overall percentage cover was significantly higher in the control and 1°C treatment in June 2016 compared to June 2015. Surface water temperature from buoy data of the deployment site reported that the temperature was 1.3°C warmer in June 2015 than in June 2016. Thus during the warmer year (June 2015), coverage in the 1°C treatment was low and similar to levels in the 2°C treatment in June 2016, supporting the above hypothesis. There is mounting evidence from terrestrial and marine ecosystems to suggest that discrete climate events such as warmer years, interact with chronic stressors such as warming to reach and exceed the ecological tipping point that cause abrupt shifts in populations and communities (Thibault et al., 2008), and this is supported for the marine fouling community in this study. This is of particular interest as discrete climate events have occurred more frequently in the last decades and are projected to become more frequent in a warming climate (Hobday et al., 2016).

Discrete and extreme climatic events have been observed in temperate and Antarctic ecosystems. In 2012, an ocean heat wave in the Northwest Atlantic produced sea surface temperatures 1-3°C warmer than the 1982-2011 average. Wernberg et al., (2016) linked regime shifts of Western Australian temperate reef ecosystems to continuing ocean warming and extreme marine heatwaves, which resulted in kelp forests being replaced by communities typical of subtropical waters. In Antarctica, exceptional sea ice conditions occurred in the West Antarctic Peninsula

(WAP) region from September 2001 to February 2002, resulting from a strongly positive atmospheric pressure anomaly in the South Atlantic coupled with strong negative anomalies in the Bellingshausen–Amundsen and southwest Weddell Seas. This led to the atypical persistence of highly compact coastal ice through summer. Ecological effects were both positive and negative, the latter including an impact on the growth rate of larval Antarctic krill (Massom et al., 2006). The Antarctic Peninsula is the region of the continent where there is the strongest influence of El Niño-southern oscillation (Turner, 2004), where extensive summer melt in West Antarctica has been linked to a strong el Niño event (Nicolas et al., 2017). The increase frequency of these events couple with El Niño years, can severely impact ecosystems. For example, an ocean heatwave associated with the 2015-2016 El Niño produced extremely high tropical sea surface temperatures in regions where coral reefs experienced the third mass bleaching event in recorded history (NOAA, 2015).

These discrete climate events are not unique to changes in temperature, they include for example severe storms (Byrnes et al., 2011), extreme wave activity (Smale et al., 20167) and salinity changes (Gillanders et al., 2002). How discrete climate events affect ecosystems depends largely on the magnitude, spatial and temporal extent, as well as the timing of the anomalous climate event (Sippel et al., 2016). But, the limitations with collecting ecological time series of sufficient length and ecological monitoring means that it is harder to predict and understand the processes of ecosystem responses to discrete climate events. This is especially pronounced when considering discrete climate events, which by definition are rare events. New technological advances such as heated settlement panels may allow us to bridge these gaps in knowledge. Heated settlement panels could be incorporated into seasonal deployments over multiple years. These time series would elucidate such events and would also us allow to identify patterns observed across El Niño/La Niña or NAO (North Atlantic Oscillation) years. Further studies should also consider sampling the biofilm community as community responses to discrete climate events will differ between prokaryotes and metazoans as previously discussed. The incorporation of such data would improve our understanding on the effects of discrete climate events one ecosystems across organismal groups and improve predictions on the impacts of climate change on marine ecosystems.

However, heated settlement panels have limitations: the current panels only warm a 2-5mm layer of water above the panel and organisms in temperate ecosystems have fast growth rates, which would result in them rapidly growing to a size beyond the heated area. Future studies that wish to

use this technology must therefore consider its limitations in temperate and tropical ecosystems. Heated settlement panels could be deployed at regular intervals in tropical ecosystems to avoid organisms growing beyond the heated layer Nevertheless, this technology has the potential to improve our understanding of the occurrence of these events, predicted to increase in frequency with climate change and the latter effects on ecosystems across biological groups, timescales and environments.

7.5 Final remarks

At the time of this project completion and to the best of my knowledge, this is the first experiment to provide a long-term assessment of the effects of *in situ* elevated oceanic warming on marine benthic recruitment and community development at the molecular level. Experiments such as this one that incorporate ecological findings (Ashton et al., 2017), evaluate sub lethal stress measured at the molecular level and incorporate biofilm communities could potentially lay the foundation for a new era of predicting how marine communities across different levels of biological organisation respond to future ecosystem change.

As the deployment of the heated settlement panels in the Menai strait showed, this technology can be applied to other ecosystems (with limitations) and not only Antarctica. Future studies should look in to deploying heated settlement panels in other fast warming ecosystems such as the Arctic and tropical ecosystems. Such deployments would help to develop a network of *in situ* experiments across different latitudes and ecosystems therefore providing a global assessment of the effects of end of century predicted oceanic warming (IPCC, 2014) on marine benthic ecosystems. Furthermore, heated settlement panels could be deployed in conjunction with ocean observatories as this would allow us to determine how communities respond to physical and chemical changes in the marine environment.

In broader applications, heated settlement panel studies can be used to answer questions about how changes in temperature can modulate toxicity of chemical contaminants to marine life. Future experiments could measure the concentrations of pollutants (e.g. Zn, Pb, Cd) in benthic species that have settled on the panels across different treatments to answer these questions. Heated settlement panels are of particular interest to the anti-fouling compound industry as they can be used to test anti-fouling agents. The fouling of marine organisms on marine structures has

associated costs of $56 million per year, (Schultz et al., 2015). Testing of new anti-fouling compounds with sensitive biomarkers and that are environmentally friendly on heated settlement panels could help to reduce the above costs.

The deployment of heated settlement panels across other ecosystems and in conjunction with ocean observatories could be a very powerful tool which would allows us to make predictions of the effects of predicted end of century oceanic warming (IPCC, 2014) on marine ecosystems. Heated settlement panels have the potential to revolutionise *in situ* studies.

7.6 References

Anand, S., Mangano, E., Barizzone, N., Bordoni, R., Sorosina, M., Clarelli, F., Corrado, L., Boneschi, F.M., D'Alfonso, S. and DeBellis, G. (2016). Polled samples: guideline for variants' filtering. *Sci. Rep*. **6**, 33735.

Ashton, G. V., Morley, S. A., Barnes, D. K. A., Clark, M. S. and Peck, L. S. (2017). Warming by 1°C Drives Species and Assemblage Level Responses in Antarctica's Marine Shallows. *Curr. Biol.* **27***,* 2698–2705.

Atkinson, A., Pakhomov, E. and Rothery, P. (2004). Long-term decline in krill stock and increase in salps within the Southern ocean. *Nature*. **4**, 100-3.

Barnes, D. K. A. and Clarke, A. (1995). Seasonality of feeding activity in Antarctic suspension feeders*. Polar. Biol*. **15**, 335-340.

Barnes, D. K. A. and Peck, L. S. (2008). Vulnerability of Antarctic shelf biodiversity to predicted regional warming. *Clim. Res.* **37***,* 149–163.

Barnes, D. K. A. and Souster, T. (2011). Reduced survival of Antarctic benthos linked to climate-induced iceberg scouring. *Nat. Clim. Change.* **1**, 365–368.

Byrnes, J., Reed, D. C., Cardinale, B. J., Cavanaugh, K. C., Holbrook, S. J. and Schmitt, R. J. (2011). Climate-driven increases in storm frequency simplify kelp forest food webs. *Glob. Change. Biol.* **17**, 8.

Chown, S. L. and Gaston, K. J. (2008). Macrophysiology for a changing world*. Proc. R. Soc. Lond. B*. **275**, 1469-1478.

Cook, A. J., Fox, A. J., Vaughan , D. G. and Ferrigno, J. G. (2005). A new Antarctic peninsula glacier basin inventory and observed area changes since the 1940s. *Antarct. Sci*. **26**, 614-624.

Cook, A. J., Holland, P. R., Meredith, M. P., Murray, T., Luckman, A. and Vaughan, D. G. (2016). Ocean forcing of glacier retreat in the western Antarctic Peninsula. *Science.* **353**, 283–287.

Dagnall, C. L., Morton, L. M., Hicks, B. D., Shengchao, L, Zhou, W. et al. (2018). Successful use of whole genome amplified DNA from multiple source types for high-density Ilumina SNP microarrays*. BMC. Genomics.* **19**, 182.

Ducklow, H. W., Fraser, W. R., Meredith, M. P., Stammerjohn, S. E., Doney, S. C., Martinson, D. G., Schofield, O. M. et al. (2013). *Oceanography.* **26**, 190-203.

Falkowski, P. (2000). The global carbon cycle: A test of our knowledge of earth as a system. *Sci*. **290**, 291.

Gillanders, B. M. and Kingsford, M. J. (2002). Impact of changes in flow of freshwater on estuarine and open coastal habitats and the associated organisms. *Ocean. Mar. Biol*. **40**, 233-309.

Hobday, A. J., Alexander, L., Perkins-Kirkpatrick, S. E. et al. (2016). A hierarchical approach to defining marine heatwaves. *Prog. Oceanogr*. **141**.

IPCC. (2014). Climate Change 2014 Synthesis Report Summary for Policymakers.

Jeong, H. H., Jeong, S. G., Park, A., Jang, S. C., Hong, S. G. and Lee, C. S. (2014). Effect of temperature on biofilm formation by Antarctic marine bacteria in a microfluidic device. *Anal. Biochem.* **446***,* 90–95.

Lohrer, A. M., Cummings, V .J. and Thrush, S. F. (2013). Altered sea ice thickness and permanence affects benthic ecosystem functioning in coastal Antarctica. *Ecosystems*. **16**, 224-236.

Massom, R. A., Stammerjohn, S. E., Smith, R. C., Pook, M. J., Iannuzzi, R. A., Adams, N., Martinson, D. G., Vernet, M., Fraser, W. R., Quetin, L. B., Ross, R. M., Massom, Y. and Krouse, H. R. (2006). Extreme anomalous atmospheric circulation in the West Antarctic Peninsula region in austral spring and summer 2001/02, and its profound impact on sea ice and biota*. J. Clim*. **19**, 3544-3571.

Meredith, M. P. and King, J. C. (2005). Rapid climate change in the ocean west of Antarctic Peninsula during the second half of the 20th century. *Geophys. Res. Lett.* **32**, L19604.

Montes-Hugo, M., Doney, S. C., Ducklow, H. W., Fraser, W., Martinson, D., Stammerjohn, S. E. and Schofield, O. (2009). Recent changes in phytoplankton communities associated with rapid regional climate change along the western Antarctic peninsula. *Sci*. **323**, 1470.

Morley, S. A., Lemmon, V., Obermüller, B. E., Spicer, J. I., Clark, M. S. and Peck, L. S. (2011). Duration tenacity : A method for assessing acclimatory capacity of the Antarctic limpet , *Nacella concinna*. *J. Exp. Mar. Biol. Ecol.* **399**, 39–42.

Nicolas, J. P., Vogelmann, A. M., Scott, R. C., Wilson, A. B., Cadeddu, M. P. et al. (2017). January 2016 extensive summer melt in West Antarctica favoured by strong El Niño. *Nat. Commun.* **8**, 15799.

NOAA News Release (2015). NOAA Declares Third Ever Global Coral Bleaching Event: Bleaching Intensifies in Hawaii, High Ocean Temperatures Threaten Caribbean Corals. Available online at: http://www.noaanews.noaa.gov/stories2015/100815-noaa-declares-third-ever-global-coral-bleaching-event.html (Accessed Feb 10, 2019)

Parmesa, C. and Yohe, G. (2003). A globally coherent fingerprint of climate change impacts across natural systems*. Nature*. **421**, 37-42.

Peck, L. S. (2005). Prospects for survival in the Southern Ocean : vulnerability of benthic species to temperature change. *Antarc. Sci.* **17**, 497–507.

Peck, L. S. (2018). Antarctic marine biodiversity: adaptations, environments and responses to change. *Oceanogr. Mar. Biol*. **56**, 105-236.

Rampadarath, S., Bandhoa, K., Puchooa, D., Jeewon, R. and Bal, S. (2017). Early bacterial biofilm colonizers in the coastal waters of Mauritius. *Electron. J. Biotechn*. **29**, 13-21.

Roh, J. H. and Kaplan, S. (2000). Genetic and phenotypic analyses of the rdx Locus of Rhodobacter sphaeroides 2.4.1. *J. Bacteriol.* **182**, 3475-3481.

Rozema, P. D., Venebles, H. J., Van de Poll, W. H., Clarke, A., Meredith, M. P. and Buma, A. G. (2016). Interannual variability in phytoplankton biomass and species composition in northern Marguerite Bay (West Antarctic Peninsula) is governed by both winter sea ice cover and summer stratification. *Limnol. Oceanogr*. **62**, 235-252.

Schmidt, P. S. and Rand, D. M. (2001). Adaptive maintenance of genetic polymorphism in an intertidal barnacle: habitat- and life- stage specific survivorship of MPI genotypes. *Evolution.* **55**, 1336-1344.

Schofield, O., Brown, M., Kohut, J., Nardelli, S., Saba, G., Waite, N. and Ducklow, H. (2018). Changes in the upper ocean mixed layer and phytoplankton productivity along the West Antarctic Peninsula. *Philos. Trans. Royal. Soc. A.* **376**, 20170173.

Schultz, M. P., Walker, J. M., Steppe, C. N. and Flack, K. A. (2015). Impact of diatomaceous biofilms on the frictional drag of fouling-release coatings. *Biofouling.* **31***,* 759–773.

Sippel, S., Zscheischler, J. and Reichstein, M. (2016). Ecosystem impacts of climate extremes crucially depend on the timing. *PNAS*. **113**, 5768-5770.

Smale, D. A. and Vance, T. (2016). Climate-driven shifts in species' distribution may exacerbate the impacts of storm disturbances on North-east Atlantic kelp forst. *Mar. Fresh. Res*. **67**, 65-74.

Somero, G. N. (2010). The physiology of climate change : how potentials for acclimatization and genetic adaptation will determine " winners " and " losers ". *J. Exp. Biol.* **213***,* 912–920.

Suckling, C., Clark, M. S., Richard, J., Morley, S. A., Thorne, M. A. S., Harper, E. M. and Peck, L. S. (2015). Adult acclimation to combined temperature and pH stressors significantly enhances reproductive outcomes compared to short-term exposures. *J. Anim. Ecol.* **84**, 773-784.

Tewksbury, J. J., Huey, R. B. and Deutsch, C. A. (2008). Putting the heat on tropical animals. *Sci*. **320**, 1296-1297.

Thibault, K. M. and Brown, J. H. (2008). Impact of an extreme climatic event on community assembly. *Proc. Natl. Acad. Sci. USA.* **105**, 3410-3415.

Turner, J., Lu, H., White, I., King, J. C., Phillips, T., Hosking, J. S. et al. (2016). Absence of 21st century warming on Antarctic Peninsula consistent with natural variability. *Nature*. **535**, 411–415.

Walther, G. R., Post, E., Convey, P., Menzel, A., Parmesan, C., Beebee, T. J. C., Fromentin, J. M., Guldberg, O. H. and Bairlein, F. (2002). *Nature.* **416**, 389-395.

Wernberg, T., Bennett, S., Babcock, R. C. et al. (2016). Climate-driven regime shift of a temperate marine ecosystem. *Sci***. 353**, 169-172.

Appendix 1

The following table details the transcripts described in Chapter 4 for the 1°C vs Control contrast. Transcript ID, logCPM values, Top BlastP hits against the Swissprot non-redundant database and the protein descriptions are detailed.

Transcript ID	logCPM	Top BLASTP hit	Protein description
TRINITY_DN690839_c1_g1_i14	0.592300185	.	30S ribosomal protein S10
TRINITY_DN741870_c1_g1_i8	4.39263094	sp|B0BST1|RL3_ACTPJ	30S ribosomal protein S10
TRINITY_DN620745_c1_g1_i10	-1.869694731	.	30S ribosomal protein S12
TRINITY_DN620745_c1_g1_i5	1.22275326	.	30S ribosomal protein S12
TRINITY_DN743099_c11_g1_i1	4.906009906	sp|A1TYJ2|RS12_MARHV	30S ribosomal protein S12
TRINITY_DN743099_c9_g3_i3	2.581116952	.	30S ribosomal protein S12
TRINITY_DN643507_c0_g1_i10	0.807266875	.	30S ribosomal protein S13
TRINITY_DN643507_c0_g1_i14	2.005006323	.	30S ribosomal protein S13
TRINITY_DN643507_c0_g1_i16	-0.517585733	.	30S ribosomal protein S13
TRINITY_DN732871_c3_g3_i1	1.963499257	sp|B3PK59|RS13_CELJU	30S ribosomal protein S13
TRINITY_DN733966_c2_g1_i1	3.845995818	sp|A1SXW5|RS13_PSYIN	30S ribosomal protein S13
TRINITY_DN660373_c0_g1_i8	4.739619596	.	30S ribosomal protein S21
TRINITY_DN637715_c0_g1_i4	0.66034205	sp|Q21M51|RS3_SACD2	30S ribosomal protein S3
TRINITY_DN686995_c0_g2_i1	4.819830034	sp|Q7VKD7|RS3_HAEDU	30S ribosomal protein S3
TRINITY_DN686995_c0_g2_i4	1.411577515	sp|Q7MPI2|RS3_VIBVY	30S ribosomal protein S3
TRINITY_DN687506_c0_g1_i12	2.313414436	sp|A1TYK3|RS3_MARHV	30S ribosomal protein S3
TRINITY_DN687506_c0_g1_i3	1.66913653	sp|A1TYK3|RS3_MARHV	30S ribosomal protein S3
TRINITY_DN700108_c4_g2_i2	-1.584710403	sp|A1TYK3|RS3_MARHV	30S ribosomal protein S3
TRINITY_DN713937_c6_g2_i1	2.063063786	sp|Q2S929|RS5_HAHCH	30S ribosomal protein S5
TRINITY_DN728669_c1_g1_i8	1.00764433	sp|Q488Z6|RS5_COLP3	30S ribosomal protein S5
TRINITY_DN741750_c0_g1_i3	4.756755132	sp|Q2S929|RS5_HAHCH	30S ribosomal protein S5
TRINITY_DN743030_c21_g1_i1	-1.438087165	sp|A1S233|RL6_SHEAM	30S ribosomal protein S5
TRINITY_DN743030_c21_g1_i9	3.576966774	sp|A1S233|RL6_SHEAM	30S ribosomal protein S5
TRINITY_DN640622_c1_g2_i6	3.938141606	sp|Q489U1|RS6_COLP3	30S ribosomal protein S6
TRINITY_DN640622_c1_g3_i8	0.193374483	.	30S ribosomal protein S6
TRINITY_DN731577_c1_g3_i9	5.146838972	sp|A6GZA2|RS7_FLAPJ	30S ribosomal protein S7
TRINITY_DN1330622_c0_g1_i1	-1.980749994	.	40S ribosomal protein S11
TRINITY_DN591865_c0_g1_i7	-0.712637582	.	40S ribosomal protein S11
TRINITY_DN624139_c0_g1_i4	4.297974338	sp|P62282|RS11_RAT	40S ribosomal protein S11

Transcript ID	logCPM	Top BLASTP hit	Protein description
TRINITY_DN692302_c3_g1_i11	1.883696396	.	40S ribosomal protein S11
TRINITY_DN484098_c0_g1_i1	4.054130089	sp|P62264|RS14_MOUSE	40S ribosomal protein S14-2
TRINITY_DN623080_c0_g3_i8	3.603467565	sp|P31674|RS15_ORYSJ	40S ribosomal protein S15
TRINITY_DN671684_c0_g1_i17	4.434696593	sp|P31674|RS15_ORYSJ	40S ribosomal protein S15
TRINITY_DN581427_c0_g3_i8	4.534635113	.	40S ribosomal protein S16
TRINITY_DN636653_c1_g2_i8	-0.702808864	.	40S ribosomal protein S2
TRINITY_DN575296_c0_g1_i3	4.944951488	sp|P60868|RS20_RAT	40S ribosomal protein S20
TRINITY_DN672411_c0_g1_i15	-0.555259744	.	40S ribosomal protein S20
TRINITY_DN716456_c0_g2_i18	5.443824535	sp|Q8TCT9|HM13_HUMAN	40S ribosomal protein S20
TRINITY_DN569078_c0_g1_i5	3.552532313	.	40S ribosomal protein S27-B
TRINITY_DN636430_c1_g2_i1	5.015158092	sp|Q0Z8U2|RS3_PIG	40S ribosomal protein S3
TRINITY_DN666773_c1_g2_i11	3.067920481	sp|Q1QVF0|RL13_CHRSD	50S ribosomal protein L13
TRINITY_DN729330_c2_g1_i19	2.696756271	.	50S ribosomal protein L13
TRINITY_DN641659_c0_g1_i12	2.659732058	.	50S ribosomal protein L14
TRINITY_DN704830_c1_g1_i7	5.785557234	sp|B3PK48|RL24_CELJU	50S ribosomal protein L14
TRINITY_DN705108_c1_g1_i13	4.440796808	sp|A1T0D1|RL24_PSYIN	50S ribosomal protein L14
TRINITY_DN683829_c2_g1_i4	4.677578147	sp|A1TYL6|RL15_MARHV	50S ribosomal protein L15
TRINITY_DN728669_c0_g2_i1	1.383236656	.	50S ribosomal protein L15
TRINITY_DN630680_c0_g1_i1	1.171264143	.	50S ribosomal protein L18
TRINITY_DN630680_c3_g1_i8	-1.208046481	sp|Q488Z6|RS5_COLP3	50S ribosomal protein L18
TRINITY_DN660430_c0_g1_i5	-0.035059863	sp|Q488Z7|RL18_COLP3	50S ribosomal protein L18
TRINITY_DN660430_c0_g1_i9	-0.456276323	sp|Q488Z7|RL18_COLP3	50S ribosomal protein L18
TRINITY_DN675314_c6_g4_i4	3.194706571	sp|Q488Z8|RL6_COLP3	50S ribosomal protein L18
TRINITY_DN675314_c6_g4_i6	-1.511478291	sp|Q488Z7|RL18_COLP3	50S ribosomal protein L18
TRINITY_DN732354_c4_g1_i10	7.288712563	sp|B5FG09|RL3_VIBFM	50S ribosomal protein L2
TRINITY_DN700108_c4_g1_i1	4.173840002	sp|Q21M52|RL22_SACD2	50S ribosomal protein L22
TRINITY_DN625491_c1_g1_i6	0.578246024	.	50S ribosomal protein L23
TRINITY_DN607836_c0_g1_i2	2.721848123	sp|A1T0E2|RL3_PSYIN	50S ribosomal protein L3
TRINITY_DN607836_c0_g1_i5	0.792570018	sp|A1T0E2|RL3_PSYIN	50S ribosomal protein L3
TRINITY_DN703827_c0_g1_i1	1.021994623	sp|Q487Z3|RL3_COLP3	50S ribosomal protein L3

Transcript ID	logCPM	Top BLASTP hit	Protein description
TRINITY_DN703827_c0_g3_i1	1.827686972	.	50S ribosomal protein L3
TRINITY_DN665811_c3_g2_i4	0.063176182	.	60 kDa chaperonin
TRINITY_DN660785_c0_g1_i3	4.253014001	.	60S ribosomal protein L11
TRINITY_DN660785_c0_g1_i7	6.038065198	sp|P46222|RL11_DROME	60S ribosomal protein L11
TRINITY_DN552729_c0_g1_i3	4.257424298	.	60S ribosomal protein L12-3
TRINITY_DN589707_c0_g1_i4	4.241194964	sp|P41126|RL13_DROME	60S ribosomal protein L13
TRINITY_DN640832_c2_g1_i5	6.009377861	sp|Q3SZ90|RL13A_BOVIN	60S ribosomal protein L13a
TRINITY_DN674483_c0_g2_i28	5.421495137	sp|O46160|RL14_LUMRU	60S ribosomal protein L14
TRINITY_DN582912_c0_g1_i1	5.409801135	sp|Q9SIM4|RL141_ARATH	60S ribosomal protein L14-1
TRINITY_DN623103_c0_g1_i2	3.003409835	sp|P46990|RL17B_YEAST	60S ribosomal protein L17-B
TRINITY_DN610360_c0_g1_i12	3.456947742	sp|Q1HR62|RL18_AEDAE	60S ribosomal protein L18-3
TRINITY_DN610360_c0_g1_i17	5.943883847	sp|Q940B0|RL183_ARATH	60S ribosomal protein L18-3
TRINITY_DN665774_c0_g1_i18	4.645426285	sp|Q9LUQ6|RL192_ARATH	60S ribosomal protein L19
TRINITY_DN634448_c0_g1_i9	4.564585827	sp|P52819|RL22_CAEEL	60S ribosomal protein L22
TRINITY_DN644487_c9_g1_i4	4.905713046	sp|P62752|RL23A_RAT	60S ribosomal protein L23a
TRINITY_DN668513_c0_g1_i2	0.526054096	.	60S ribosomal protein L23a
TRINITY_DN590525_c0_g1_i1	4.300818043	sp|Q9DFQ7|RL24_GILMI	60S ribosomal protein L24
TRINITY_DN615508_c2_g1_i7	5.165252464	sp|P61255|RL26_MOUSE	60S ribosomal protein L26
TRINITY_DN562846_c0_g1_i1	2.978669365	.	60S ribosomal protein L32
TRINITY_DN625406_c1_g1_i4	4.774216098	sp|P62912|RL32_RAT	60S ribosomal protein L32
TRINITY_DN600712_c0_g1_i2	3.614738573	sp|O74904|RL35_SCHPO	60S ribosomal protein L35
TRINITY_DN617372_c11_g1_i1	4.102889524	sp|Q8JHJ1|RL35_DANRE	60S ribosomal protein L35
TRINITY_DN617372_c11_g1_i2	5.275939601	sp|Q8JHJ1|RL35_DANRE	60S ribosomal protein L35
TRINITY_DN650649_c0_g3_i2	6.297476623	sp|O01802|RL7_CAEEL	60S ribosomal protein L7
TRINITY_DN650649_c0_g3_i3	4.380389284	sp|O01802|RL7_CAEEL	60S ribosomal protein L7
TRINITY_DN698425_c0_g1_i11	0.944361941	.	60S ribosomal protein L7
TRINITY_DN720053_c0_g2_i18	5.209286395	sp|P46223|RL7A_DROME	60S ribosomal protein L7a
TRINITY_DN589001_c0_g1_i7	4.6237705	sp|Q6PBF0|RL8_XENTR	60S ribosomal protein L8
TRINITY_DN665671_c0_g5_i1	4.493056728	.	60S ribosomal protein L8
TRINITY_DN619147_c0_g2_i9	3.802203962	sp|O74905|RL9B_SCHPO	60S ribosomal protein L9-A

Transcript ID	logCPM	Top BLASTP hit	Protein description
TRINITY_DN634169_c2_g1_i22	-0.239685066	.	70 kDa neurofilament protein
TRINITY_DN634169_c2_g1_i23	1.687594044	sp|Q01241|NF70_DORPE	70 kDa neurofilament protein
TRINITY_DN701044_c0_g1_i6	1.380071677	.	70 kDa neurofilament protein
TRINITY_DN630968_c7_g1_i1	3.766940749	sp|O65315|ACT_COLSC	Actin
TRINITY_DN630305_c4_g1_i18	5.633119551	sp|Q25381|ACTM_LYTPI	Actin, cytoplasmic
TRINITY_DN665210_c2_g5_i2	5.276044664	sp|Q964E0|ACTC_BIOTE	Actin, cytoplasmic 1
TRINITY_DN655864_c3_g1_i6	4.915465826	sp|Q10DV7|ACT1_ORYSJ	Actin, muscle (Fragment)
TRINITY_DN673811_c4_g1_i10	-0.497423681	.	Actin, muscle (Fragment)
TRINITY_DN670119_c1_g1_i22	7.254563358	sp|Q25472|ACT2_MOLOC	Actin, muscle-type
TRINITY_DN688900_c1_g1_i2	-1.0127122	sp|P17126|ACT_HYDVU	Actin, non-muscle 6.2
TRINITY_DN678180_c0_g1_i1	-0.821168248	.	Adenosine kinase
TRINITY_DN685377_c2_g1_i16	5.409142976	sp|P81178|ALDH2_MESAU	Aldehyde dehydrogenase, mitochondrial
TRINITY_DN685377_c2_g1_i17	4.083263947	sp|P12762|ALDH2_HORSE	Aldehyde dehydrogenase, mitochondrial
TRINITY_DN548448_c0_g1_i3	-0.474007056	.	Alpha-(1,3)-fucosyltransferase FucT
TRINITY_DN604710_c3_g1_i5	2.373225304	.	Alpha-(1,3)-fucosyltransferase FucT
TRINITY_DN679538_c5_g1_i10	2.378884846	.	Alpha-(1,3)-fucosyltransferase FucT
TRINITY_DN679538_c5_g1_i3	2.507946412	.	Alpha-(1,3)-fucosyltransferase FucT
TRINITY_DN679493_c1_g1_i7	2.601479454	.	Alpha-actinin, sarcomeric
TRINITY_DN506236_c0_g1_i1	1.580861314	.	Aspartate--tRNA(Asp/Asn) ligase
TRINITY_DN592423_c1_g3_i1	1.812974943	.	Aspartate--tRNA(Asp/Asn) ligase
TRINITY_DN395055_c0_g1_i1	-1.669180123	.	Aspartate/glutamate leucyltransferase
TRINITY_DN637735_c0_g1_i7	-1.241806681	sp|Q8VV78|ATPG_COLMA	ATP synthase gamma chain
TRINITY_DN680871_c1_g2_i1	4.983212842	sp|Q48AW1|ATPG_COLP3	ATP synthase gamma chain
TRINITY_DN685177_c3_g2_i3	1.999650926	sp|Q2S6P0|ATPG_HAHCH	ATP synthase gamma chain
TRINITY_DN685177_c3_g2_i5	2.184384669	sp|Q2S6P0|ATPG_HAHCH	ATP synthase gamma chain
TRINITY_DN685177_c3_g6_i2	4.24023544	sp|Q9HT19|ATPG_PSEAE	ATP synthase gamma chain
TRINITY_DN696148_c0_g1_i2	-1.663627363	sp|Q9HT19|ATPG_PSEAE	ATP synthase gamma chain
TRINITY_DN644771_c0_g1_i6	3.212565602	sp|Q34946|ATP6_LUMTE	ATP synthase subunit a
TRINITY_DN633709_c2_g1_i3	-0.981687457	.	ATP synthase subunit alpha
TRINITY_DN662019_c0_g2_i4	1.181898052	.	ATP synthase subunit alpha

Transcript ID	logCPM	Top BLASTP hit	Protein description
TRINITY_DN646262_c0_g3_i4	-0.306825467	sp|Q9XXK1|ATPA_CAEEL	ATP synthase subunit alpha, mitochondrial
TRINITY_DN646262_c0_g4_i1	4.989875369	sp|P35381|ATPA_DROME	ATP synthase subunit alpha, mitochondrial
TRINITY_DN633120_c6_g1_i9	3.185926166	sp|Q48AW0|ATPB_COLP3	ATP synthase subunit beta
TRINITY_DN671215_c0_g3_i1	0.205890233	sp|Q48AW0|ATPB_COLP3	ATP synthase subunit beta
TRINITY_DN743011_c5_g1_i4	2.161281713	sp|Q48AW0|ATPB_COLP3	ATP synthase subunit beta
TRINITY_DN712491_c2_g2_i1	1.554037398	.	ATP-dependent DNA helicase Rep
TRINITY_DN694383_c2_g2_i1	0.223799106	.	ATP-dependent RNA helicase CshA
TRINITY_DN713508_c0_g1_i16	-0.193281481	.	ATP-dependent RNA helicase DDX3X
TRINITY_DN658364_c2_g3_i1	2.198863313	.	ATP-dependent zinc metalloprotease FtsH
TRINITY_DN718151_c0_g1_i10	0.583968142	sp|Q9ULI0|ATD2B_HUMAN	ATPase family AAA domain-containing protein 2B
TRINITY_DN486256_c0_g1_i1	-0.373198456	.	Autophagy-related protein 3
TRINITY_DN595096_c0_g1_i7	-0.325901692	.	Casein kinase I isoform alpha
TRINITY_DN735979_c2_g1_i2	0.448143309	.	Caspase-8
TRINITY_DN733641_c4_g2_i10	-0.645278523	sp|Q9PWF7|CATA_RUGRU	Catalase
TRINITY_DN600573_c0_g1_i3	4.409633021	sp|P47204|FTSZ_PSEAE	Cell division protein FtsZ
TRINITY_DN593830_c0_g1_i6	0.84761884	.	Cell surface glycoprotein
TRINITY_DN642788_c1_g1_i5	4.638654789	sp|P54423|WPRA_BACSU	Cell wall-associated protease
TRINITY_DN197095_c0_g1_i1	1.140257068	.	Chaperone protein DnaK
TRINITY_DN636510_c5_g6_i1	0.094180328	.	Chaperone protein DnaK 2
TRINITY_DN726746_c1_g2_i1	2.21619419	.	Chaperone protein DnaK 2
TRINITY_DN624192_c5_g2_i1	-0.036346791	.	Chemotaxis protein CheA
TRINITY_DN711686_c0_g1_i16	-0.486506275	.	Chitin biosynthesis protein CHS5
TRINITY_DN733621_c2_g2_i2	0.710263711	.	Cold shock domain-containing protein E1
TRINITY_DN665006_c0_g1_i10	2.900854089	.	Cold shock-like protein CspLB
TRINITY_DN626033_c1_g1_i5	-0.117813849	.	Cubilin homolog
TRINITY_DN663888_c7_g1_i2	2.488807704	sp|Q9D2R6|COA3_MOUSE	Cytochrome c oxidase assembly factor 3 homolog, mitochondrial
TRINITY_DN730799_c1_g1_i7	5.850165619	.	Cytochrome c oxidase subunit 1
TRINITY_DN736646_c1_g3_i1	11.2561721	sp|B0FWD3|NU5M_AEDAE	Cytochrome c oxidase subunit 1
TRINITY_DN702794_c0_g1_i8	2.157750154	.	Cytochrome c oxidase subunit 3
TRINITY_DN636406_c4_g1_i10	2.491920893	.	Cytochrome c-type biogenesis protein CcmF

Transcript ID	logCPM	Top BLASTP hit	Protein description
TRINITY_DN670278_c1_g1_i1	-0.095472146	.	Cytochrome P450 4F22
TRINITY_DN738152_c1_g2_i5	1.066318535	.	Cytosolic carboxypeptidase 3
TRINITY_DN691974_c0_g1_i12	0.909140966	.	Death-associated inhibitor of apoptosis 2
TRINITY_DN623995_c0_g1_i7	0.305924456	sp|Q91XC8|DAP1_MOUSE	Death-associated protein 1
TRINITY_DN733525_c3_g1_i21	0.879941655	.	Death-associated protein kinase 3
TRINITY_DN726487_c0_g1_i1	0.72677467	sp|Q96LJ7|DHRS1_HUMAN	Dehydrogenase/reductase SDR family member 1
TRINITY_DN704096_c1_g5_i3	4.120779376	sp|A4SSY1|RPOA_AERS4	DNA-directed RNA polymerase subunit alpha
TRINITY_DN733410_c1_g1_i18	3.422301693	sp|P74963|RPOA_SHESP	DNA-directed RNA polymerase subunit alpha
TRINITY_DN733410_c1_g1_i2	-0.490441642	.	DNA-directed RNA polymerase subunit alpha
TRINITY_DN733966_c2_g3_i5	6.531966414	sp|A4VHQ5|RPOA_PSEU5	DNA-directed RNA polymerase subunit alpha
TRINITY_DN743030_c20_g1_i1	4.855285314	sp|A4VHQ5|RPOA_PSEU5	DNA-directed RNA polymerase subunit alpha
TRINITY_DN660661_c3_g1_i6	3.234479072	sp|Q6AZ28|PIAS2_RAT	E3 SUMO-protein ligase PIAS2
TRINITY_DN640388_c1_g1_i12	-0.280533944	.	E3 ubiquitin-protein ligase HUWE1
TRINITY_DN605623_c0_g1_i2	4.16641494	.	E3 ubiquitin-protein ligase RNF115
TRINITY_DN703503_c0_g2_i2	0.920224044	sp|Q56R14|TRI33_XENLA	E3 ubiquitin-protein ligase TRIM33
TRINITY_DN673981_c0_g1_i2	-0.758639915	.	G2/mitotic-specific cyclin-A
TRINITY_DN722341_c0_g1_i15	7.771068823	sp|P04962|CCNA_SPISO	G2/mitotic-specific cyclin-A
TRINITY_DN683109_c0_g1_i12	4.973937212	sp|P24862|CCNB_PATVU	G2/mitotic-specific cyclin-B
TRINITY_DN683109_c0_g1_i7	8.303262631	sp|P13952|CCNB_SPISO	G2/mitotic-specific cyclin-B
TRINITY_DN732010_c2_g1_i13	-0.705124678	.	GDP-fucose transporter 1
TRINITY_DN709858_c0_g2_i8	1.060651772	sp|G9JJU2|GPX_PROCL	Glutathione peroxidase 3
TRINITY_DN712896_c0_g2_i12	0.079192787	sp|Q64625|GPX6_RAT	Glutathione peroxidase 6
TRINITY_DN699337_c2_g1_i22	1.57657271	.	Glutathione S-transferase 2
TRINITY_DN562741_c0_g1_i1	-1.622925467	.	GTP cyclohydrolase 1 type 2 homolog
TRINITY_DN1438285_c0_g1_i1	-1.118940825	.	GTP pyrophosphokinase
TRINITY_DN683958_c0_g1_i14	1.929759452	sp|Q5R8Q7|GTPB1_PONAB	GTP-binding protein 1 (Fragment)
TRINITY_DN714648_c0_g1_i7	4.168575073	.	GTP-binding protein 128up
TRINITY_DN737980_c2_g1_i18	3.631503173	.	GTPase HflX
TRINITY_DN649584_c2_g3_i2	5.307113318	sp|Q4R888|HS71L_MACFA	Heat shock 70 kDa protein 1-like
TRINITY_DN698135_c0_g1_i1	3.478798443	sp|P18694|HSP72_USTMA	Heat shock 70 kDa protein 2

Transcript ID	logCPM	Top BLASTP hit	Protein description
TRINITY_DN698135_c1_g1_i4	6.443944892	sp|Q9U639|HSP7D_MANSE	Heat shock cognate 71 kDa protein
TRINITY_DN683946_c2_g1_i12	-0.316595446	sp|Q90474|H90A1_DANRE	Heat shock cognate protein HSP 90-beta
TRINITY_DN683946_c2_g1_i13	1.234297873	.	Heat shock cognate protein HSP 90-beta
TRINITY_DN683946_c2_g1_i6	-0.657975861	sp|P04810|HSP83_DROSI	Heat shock cognate protein HSP 90-beta
TRINITY_DN683946_c2_g1_i7	-0.358336107	.	Heat shock cognate protein HSP 90-beta
TRINITY_DN683946_c2_g1_i8	-0.414347678	.	Heat shock cognate protein HSP 90-beta
TRINITY_DN622357_c0_g2_i2	5.814799003	.	Heat shock factor-binding protein 1
TRINITY_DN735764_c1_g1_i3	-0.775157612	.	Heat shock factor-binding protein 1
TRINITY_DN670310_c4_g3_i4	4.128540369	sp|Q90474|H90A1_DANRE	Heat shock protein 83
TRINITY_DN670310_c4_g3_i7	6.039377511	sp|Q04619|HS90B_CHICK	Heat shock protein 83
TRINITY_DN712943_c3_g7_i1	2.30466779	sp|P04810|HSP83_DROSI	Heat shock protein 83 (Fragment)
TRINITY_DN665271_c1_g1_i10	7.030077542	sp|P30946|HS90A_RABIT	Heat shock protein HSP 90-alpha
TRINITY_DN679451_c1_g2_i2	4.183492025	sp|P11501|HS90A_CHICK	Heat shock protein HSP 90-alpha A2
TRINITY_DN679451_c1_g2_i3	2.697521119	sp|Q14568|HS902_HUMAN	Heat shock protein HSP 90-alpha A2
TRINITY_DN696147_c0_g1_i25	2.648448879	sp|Q9Z2V6|HDAC5_MOUSE	Histone deacetylase 5
TRINITY_DN709828_c1_g1_i2	1.585581277	sp|Q9UQL6|HDAC5_HUMAN	Histone deacetylase 5
TRINITY_DN689521_c0_g1_i14	0.712145682	.	Histone deacetylase 8
TRINITY_DN736276_c2_g1_i4	2.998435844	.	Inhibitor of nuclear factor kappa-B kinase subunit alpha
TRINITY_DN736276_c2_g1_i7	1.10104554	.	Inhibitor of nuclear factor kappa-B kinase subunit alpha
TRINITY_DN653961_c0_g1_i10	3.663466514	sp|P53352|INCE_CHICK	Inner centromere protein
TRINITY_DN653961_c0_g1_i3	6.193136686	sp|O13024|INCEA_XENLA	Inner centromere protein
TRINITY_DN724757_c2_g1_i11	4.067241239	sp|Q8J0D7|SUB3_ARTOT	Intracellular serine protease
TRINITY_DN724757_c2_g1_i12	0.201334942	sp|P20724|ELYA_BACYA	Intracellular serine protease
TRINITY_DN667029_c1_g1_i2	4.124519016	sp|A7MBP4|IFT46_DANRE	Intraflagellar transport protein 46 homolog
TRINITY_DN648580_c1_g1_i3	-0.782422166	sp|Q62559|IFT52_MOUSE	Intraflagellar transport protein 52 homolog
TRINITY_DN717773_c0_g1_i14	2.334489624	.	Lactoperoxidase
TRINITY_DN655234_c4_g2_i7	1.302374663	.	Malate dehydrogenase
TRINITY_DN660359_c0_g1_i11	3.627426077	sp|P86948|MP_PINMA	Mantle protein
TRINITY_DN659119_c1_g1_i20	7.017726655	sp|A4IIN5|TISD_XENTR	mRNA decay activator protein ZFP36L2
TRINITY_DN561643_c0_g1_i2	2.935732814	.	mRNA turnover protein 4 homolog

Transcript ID	logCPM	Top BLASTP hit	Protein description
TRINITY_DN639794_c6_g1_i2	6.650642403	sp|P07291|MLE_ARGIR	Myosin catalytic light chain LC-1, mantle muscle
TRINITY_DN732689_c3_g3_i12	1.973624836	.	NAD kinase
TRINITY_DN694383_c3_g1_i4	1.583563145	.	NAD(P) transhydrogenase subunit alpha
TRINITY_DN677907_c0_g1_i17	2.349547021	.	NAD(P) transhydrogenase, mitochondrial
TRINITY_DN628034_c0_g1_i5	5.649309131	sp|P51899|NU5M_ANOAR	NADH-ubiquinone oxidoreductase chain 5 (Fragment)
TRINITY_DN678190_c0_g1_i1	3.088286094	sp|P34855|NU5M_APILI	NADH-ubiquinone oxidoreductase chain 5 (Fragment)
TRINITY_DN638337_c0_g2_i1	3.116995938	sp|Q9M612|NACA_PINTA	Nascent polypeptide-associated complex subunit alpha-like protein
TRINITY_DN638337_c0_g2_i2	1.219773656	sp|Q9M612|NACA_PINTA	Nascent polypeptide-associated complex subunit alpha-like protein
TRINITY_DN638337_c0_g2_i4	1.998814907	sp|Q9M612|NACA_PINTA	Nascent polypeptide-associated complex subunit alpha-like protein
TRINITY_DN638337_c0_g2_i5	4.065324233	sp|Q9M612|NACA_PINTA	Nascent polypeptide-associated complex subunit alpha-like protein
TRINITY_DN582034_c0_g1_i1	1.080085776	.	Nitric oxide synthase
TRINITY_DN582034_c0_g2_i2	1.049872192	.	Nitric oxide synthase
TRINITY_DN632297_c8_g2_i12	3.709199939	.	Nitric oxide synthase
TRINITY_DN721595_c3_g3_i1	-0.703601279	.	Nitric oxide synthase
TRINITY_DN737442_c5_g1_i2	4.699238505	sp|Q8XGX8|DCOA_SALTI	Oxaloacetate decarboxylase alpha chain
TRINITY_DN737442_c5_g2_i2	4.507126741	sp|P13187|DCOA_KLEPN	Oxaloacetate decarboxylase alpha chain
TRINITY_DN685351_c6_g4_i1	2.657872466	.	Oxygen sensor protein DosP
TRINITY_DN651587_c1_g1_i24	0.653198341	.	Paramyosin
TRINITY_DN711329_c0_g2_i6	0.099561592	.	Peroxidase-like protein 3 (Fragment)
TRINITY_DN594660_c0_g1_i3	5.120908612	sp|Q8BYM7|RSH4A_MOUSE	Radial spoke head protein 4 homolog A
TRINITY_DN683359_c0_g3_i9	6.743165737	sp|P26043|RADI_MOUSE	Radixin
TRINITY_DN653084_c4_g2_i23	4.880304727	sp|Q14692|BMS1_HUMAN	Ribosome biogenesis protein BMS1 homolog
TRINITY_DN674974_c0_g1_i3	5.326943995	sp|P17160|HPF_AZOVI	Ribosome hibernation promoting factor
TRINITY_DN717961_c0_g1_i16	4.140676806	sp|Q9HV53|RIMP_PSEAE	Ribosome maturation factor RimP
TRINITY_DN694352_c0_g1_i2	0.31223443	.	Ribosome modulation factor 1
TRINITY_DN711983_c2_g1_i1	-0.48422897	.	Ribosome modulation factor 1
TRINITY_DN714154_c1_g1_i1	3.518082634	.	Ribosome modulation factor 1
TRINITY_DN714154_c1_g1_i2	1.033238379	.	Ribosome modulation factor 1
TRINITY_DN616082_c4_g1_i11	3.253906026	.	Ribosome-binding protein 1

Transcript ID	logCPM	Top BLASTP hit	Protein description
TRINITY_DN616082_c4_g1_i18	1.507601928	.	Ribosome-binding protein 1
TRINITY_DN616082_c4_g1_i21	-0.136607667	.	Ribosome-binding protein 1
TRINITY_DN616082_c4_g1_i28	3.329843686	.	Ribosome-binding protein 1
TRINITY_DN616082_c4_g1_i3	0.327798285	.	Ribosome-binding protein 1
TRINITY_DN616082_c4_g1_i33	-0.260654022	.	Ribosome-binding protein 1
TRINITY_DN681589_c1_g1_i3	-0.570235386	.	Ribosome-binding protein 1
TRINITY_DN731384_c2_g3_i5	3.839527995	.	RNA polymerase sigma factor RpoS
TRINITY_DN680632_c7_g1_i12	3.989425689	sp|Q92541|RTF1_HUMAN	RNA polymerase-associated protein RTF1 homolog
TRINITY_DN588292_c0_g1_i1	4.928821822	sp|P13585|AT2A1_CHICK	Sarcoplasmic/endoplasmic reticulum calcium ATPase 1
TRINITY_DN735509_c2_g1_i6	3.81378393	sp|Q9YGL9|AT2A3_CHICK	Sarcoplasmic/endoplasmic reticulum calcium ATPase 3
TRINITY_DN706342_c1_g1_i22	6.630566003	sp|Q6DK72|SUMO3_XENTR	Small ubiquitin-related modifier 3
TRINITY_DN644718_c1_g1_i3	2.329987338	sp|P44917|Y883_HAEIN	Sodium/alanine symporter AgcS
TRINITY_DN646949_c2_g1_i2	0.157479394	.	Sodium/alanine symporter AgcS
TRINITY_DN646949_c2_g1_i5	2.80494079	.	Sodium/alanine symporter AgcS
TRINITY_DN657445_c1_g2_i9	0.929538396	.	Sodium/potassium-transporting ATPase subunit alpha
TRINITY_DN688699_c3_g1_i5	3.129302376	sp|Q6RWA9|AT1A_TAESO	Sodium/potassium-transporting ATPase subunit alpha
TRINITY_DN689530_c1_g2_i3	3.853267481	sp|P13607|ATNA_DROME	Sodium/potassium-transporting ATPase subunit alpha
TRINITY_DN739045_c4_g3_i1	5.111326711	.	Sodium/potassium-transporting ATPase subunit alpha
TRINITY_DN739864_c1_g2_i2	3.192288721	.	Sodium/potassium-transporting ATPase subunit alpha
TRINITY_DN670614_c1_g1_i8	2.573770049	.	Sodium/potassium-transporting ATPase subunit alpha-4
TRINITY_DN443151_c0_g1_i1	0.354055583	.	Sodium/potassium-transporting ATPase subunit beta-2
TRINITY_DN614652_c3_g1_i23	0.233615411	.	Stress protein DDR48
TRINITY_DN700269_c1_g1_i12	0.158979435	sp|P0AGE9|SUCD_ECOLI	Succinate--CoA ligase [ADP-forming] subunit alpha
TRINITY_DN725168_c1_g2_i1	-0.515213436	.	Succinate--CoA ligase [ADP-forming] subunit alpha
TRINITY_DN725168_c1_g3_i10	2.316592074	.	Succinate--CoA ligase [ADP-forming] subunit alpha
TRINITY_DN740812_c7_g1_i2	0.693678717	sp|P0AGE9|SUCD_ECOLI	Succinate--CoA ligase [ADP-forming] subunit alpha
TRINITY_DN680049_c2_g1_i13	-1.381724504	.	Succinate--CoA ligase [ADP-forming] subunit beta
TRINITY_DN678077_c3_g1_i12	2.529579431	.	Succinate--CoA ligase [ADP-forming] subunit beta, mitochondrial
TRINITY_DN722163_c2_g1_i5	0.751627293	.	Sulfide:quinone oxidoreductase, mitochondrial

Transcript ID	logCPM	Top BLASTP hit	Protein description
TRINITY_DN634358_c0_g1_i24	3.425059786	sp|P23346|SODC5_MAIZE	Superoxide dismutase [Cu-Zn] 4A
TRINITY_DN623549_c5_g3_i1	0.345428705	sp|P84612|SODF_PSEHT	Superoxide dismutase [Fe]
TRINITY_DN701406_c1_g1_i5	2.964520859	sp|P84612|SODF_PSEHT	Superoxide dismutase [Fe]
TRINITY_DN669452_c0_g1_i1	1.887965368	.	Superoxide dismutase 1 copper chaperone
TRINITY_DN593821_c0_g1_i6	2.6773045	sp|Q8WZ42|TITIN_HUMAN	Titin
TRINITY_DN625726_c0_g3_i2	0.307194126	sp|Q8WZ42|TITIN_HUMAN	Titin
TRINITY_DN648138_c0_g1_i14	3.968790372	sp|Q9I7U4|TITIN_DROME	Titin
TRINITY_DN669875_c0_g1_i13	0.586207873	.	Titin
TRINITY_DN697990_c0_g1_i10	-0.501591973	.	Titin
TRINITY_DN703542_c0_g2_i3	-0.795098561	.	Titin
TRINITY_DN710102_c1_g2_i3	-0.751462793	sp|Q8WZ42|TITIN_HUMAN	Titin
TRINITY_DN710537_c2_g2_i5	3.524637073	sp|Q8WZ42|TITIN_HUMAN	Titin
TRINITY_DN714007_c0_g2_i1	2.884610817	.	Titin
TRINITY_DN729727_c1_g2_i1	3.608331977	sp|Q8WZ42|TITIN_HUMAN	Titin
TRINITY_DN742395_c8_g1_i3	2.715231225	sp|A2ASS6|TITIN_MOUSE	Titin
TRINITY_DN742658_c6_g3_i8	0.529979296	.	Titin
TRINITY_DN742692_c0_g4_i2	1.40150926	.	Titin
TRINITY_DN742742_c3_g1_i9	-0.398792457	sp|A2ASS6|TITIN_MOUSE	Titin
TRINITY_DN742967_c11_g1_i4	2.128278065	sp|Q8WZ42|TITIN_HUMAN	Titin
TRINITY_DN686207_c0_g1_i16	0.825511458	sp|P48553|TPC10_HUMAN	Trafficking protein particle complex subunit 10
TRINITY_DN686207_c0_g1_i5	0.165174863	.	Trafficking protein particle complex subunit 10
TRINITY_DN606607_c9_g2_i2	4.797720865	.	Transcription elongation factor spt5
TRINITY_DN606607_c9_g2_i4	2.373286346	.	Transcription elongation factor spt5
TRINITY_DN674282_c0_g1_i11	3.214855299	sp|Q5M8V0|BT3L4_XENTR	Transcription factor BTF3 homolog 4
TRINITY_DN709114_c1_g1_i19	2.094859488	.	Transcription factor E3
TRINITY_DN673060_c0_g1_i10	2.384069769	.	Transcription factor IIIB 50 kDa subunit
TRINITY_DN741588_c2_g1_i7	-0.782806187	.	Transcription factor MafB
TRINITY_DN700323_c0_g1_i14	4.247755842	.	Transcription factor MafG
TRINITY_DN700323_c0_g1_i2	3.614079464	.	Transcription factor MafG
TRINITY_DN700323_c0_g1_i5	2.644730545	.	Transcription factor MafG

Transcript ID	logCPM	Top BLASTP hit	Protein description
TRINITY_DN678248_c0_g1_i15	0.032903691	sp|Q62318|TIF1B_MOUSE	Transcription intermediary factor 1-beta
TRINITY_DN729451_c3_g2_i5	0.252035266	sp|Q13263|TIF1B_HUMAN	Transcription intermediary factor 1-beta
TRINITY_DN626964_c1_g1_i18	2.979264644	sp|P0AFF9|NUSA_SHIFL	Transcription termination/antitermination protein NusA
TRINITY_DN606359_c1_g1_i11	3.569783208	sp|P15275|ALGQ_PSEAE	Transcriptional regulatory protein AlgQ
TRINITY_DN681107_c1_g1_i11	2.250922228	.	Transforming growth factor-beta-induced protein ig-h3
TRINITY_DN681107_c1_g1_i9	4.014782221	sp|P73392|Y1735_SYNY3	Transforming growth factor-beta-induced protein ig-h3
TRINITY_DN633741_c5_g1_i8	1.477436061	.	Translation factor GUF1 homolog, mitochondrial
TRINITY_DN730774_c2_g2_i23	0.646255888	sp|A7M9B2|TI214_CUSRE	Translation factor GUF1 homolog, mitochondrial
TRINITY_DN730774_c2_g2_i5	1.405400142	.	Translation factor GUF1 homolog, mitochondrial
TRINITY_DN696839_c1_g1_i3	3.792485441	sp|P33319|IF3_PROHU	Translation initiation factor IF-3
TRINITY_DN721452_c1_g3_i10	0.72156839	.	Translation initiation factor IF-3
TRINITY_DN721452_c1_g3_i4	4.464509939	sp|P52833|SYT_PSESY	Translation initiation factor IF-3
TRINITY_DN728119_c1_g3_i4	4.439911127	.	Translation initiation factor IF-3
TRINITY_DN724618_c1_g1_i3	0.201024372	.	tRNA(Ile)-lysidine synthase
TRINITY_DN701388_c0_g1_i25	7.233723402	sp|Q25145|TPM_HALRU	Tropomyosin
TRINITY_DN736548_c3_g2_i1	2.922167687	sp|P09645|TBA8_CHICK	Tubulin alpha chain (Fragment)
TRINITY_DN667350_c5_g1_i2	2.940049888	sp|P06605|TBA3_DROME	Tubulin alpha-1 chain
TRINITY_DN667350_c5_g1_i8	3.394548956	sp|P06605|TBA3_DROME	Tubulin alpha-1 chain
TRINITY_DN625486_c7_g1_i11	2.931379448	sp|P02552|TBA1_CHICK	Tubulin alpha-1 chain (Fragment)
TRINITY_DN625486_c7_g1_i3	4.934380383	sp|P02553|TBA_LYTPI	Tubulin alpha-1 chain (Fragment)
TRINITY_DN634413_c1_g1_i2	3.190169292	.	Tubulin alpha-3 chain
TRINITY_DN634413_c1_g1_i6	1.44899444	.	Tubulin alpha-3 chain
TRINITY_DN666082_c2_g1_i7	-1.371874543	.	Tubulin alpha-4 chain (Fragment)
TRINITY_DN685102_c8_g1_i7	-0.80000954	.	Tubulin alpha-5 chain
TRINITY_DN685102_c8_g1_i9	2.323419541	sp|P09644|TBA5_CHICK	Tubulin alpha-5 chain
TRINITY_DN615282_c4_g2_i15	-0.115515201	sp|Q9HFQ3|TBB_MELLI	Tubulin beta chain
TRINITY_DN615282_c4_g2_i7	0.587301313	sp|P16040|TBB_BLUGH	Tubulin beta chain
TRINITY_DN635926_c3_g1_i2	2.028827834	sp|Q6P9T8|TBB4B_RAT	Tubulin beta chain
TRINITY_DN649550_c3_g1_i3	1.73766727	sp|P11857|TBB_STYLE	Tubulin beta chain
TRINITY_DN655208_c3_g1_i1	3.650928991	sp|P10876|TBB_TETPY	Tubulin beta chain

Transcript ID	logCPM	Top BLASTP hit	Protein description
TRINITY_DN659443_c5_g3_i1	-1.723173271	sp|Q08115|TBB_EUPOC	Tubulin beta chain
TRINITY_DN688671_c4_g1_i1	-0.820413908	.	Tubulin beta chain
TRINITY_DN636052_c2_g3_i3	2.47169526	sp|Q9ZSW1|TBB1_CYAPA	Tubulin beta-1 chain
TRINITY_DN655525_c3_g1_i3	-0.502271393	.	Tubulin beta-1 chain
TRINITY_DN662369_c6_g3_i5	3.04838514	sp|P11833|TBB_PARLI	Tubulin beta-1 chain (Fragment)
TRINITY_DN662369_c6_g3_i7	4.862990828	sp|P68372|TBB4B_MOUSE	Tubulin beta-1 chain (Fragment)
TRINITY_DN711699_c0_g1_i2	-0.430884893	.	Tubulin polymerization-promoting protein family member 3
TRINITY_DN711699_c0_g1_i32	-0.759290204	.	Tubulin polymerization-promoting protein family member 3
TRINITY_DN656733_c2_g1_i1	0.662622742	.	Ubiquitin
TRINITY_DN729001_c1_g4_i5	1.88674398	.	Ubiquitin carboxyl-terminal hydrolase 2
TRINITY_DN629391_c2_g1_i15	2.130722542	sp|P0C276|RL40_SHEEP	Ubiquitin-60S ribosomal protein L40
TRINITY_DN629391_c2_g1_i34	3.800475635	sp|P0C276|RL40_SHEEP	Ubiquitin-60S ribosomal protein L40
TRINITY_DN725323_c0_g1_i5	1.588424114	.	Ubiquitin-60S ribosomal protein L40
TRINITY_DN693537_c0_g1_i25	4.172916652	sp|Q91VX2|UBAP2_MOUSE	Ubiquitin-associated protein 2-like
TRINITY_DN705216_c0_g1_i4	2.462263971	sp|P35129|UBC2_CAEEL	Ubiquitin-conjugating enzyme E2 2
TRINITY_DN637593_c8_g2_i8	3.866806533	.	Ubiquitin-conjugating enzyme E2 4
TRINITY_DN634946_c0_g2_i11	-0.022478809	.	Ubiquitin-conjugating enzyme E2 L3
TRINITY_DN681212_c3_g1_i14	4.615329377	sp|P25867|UBCD1_DROME	Ubiquitin-conjugating enzyme E2-17 kDa
TRINITY_DN681212_c3_g1_i21	3.887971738	sp|P25867|UBCD1_DROME	Ubiquitin-conjugating enzyme E2-17 kDa
TRINITY_DN610446_c2_g1_i1	-0.187115229	.	Ubiquitin-fold modifier-conjugating enzyme 1
TRINITY_DN648535_c2_g1_i5	4.785163114	sp|A7MAZ3|UBA5_BOVIN	Ubiquitin-like modifier-activating enzyme 5
TRINITY_DN669794_c1_g1_i5	0.224432292	sp|Q28970|MYO7A_PIG	Unconventional myosin-VIIa (Fragment)
TRINITY_DN657838_c7_g1_i1	6.084295575	sp|P74897|YQA3_THEAQ	Universal stress protein in QAH/OAS sulfhydrylase 3'region
TRINITY_DN626272_c0_g1_i6	1.662675488	.	Universal stress protein MJ0531

Appendix 2

The following table details the transcripts described in Chapter 4 for the 2°C vs Control contrast. Transcript ID, logCPM values, Top BlastP hits against the Swissprot non-redundant database and the protein descriptions are detailed.

Transcript ID	logCPM	Top BLASTP hit	Protein description
TRINITY_DN741870_c1_g1_i8	5.083002491	sp|B0BST1|RL3_ACTPJ	30S ribosomal protein S10
TRINITY_DN740667_c7_g2_i20	6.146293501	sp|Q47UW1|RS12_COLP3	30S ribosomal protein S12
TRINITY_DN743099_c11_g1_i1	4.6376066	sp|A1TYJ2|RS12_MARHV	30S ribosomal protein S12
TRINITY_DN733966_c2_g1_i1	4.279085075	sp|A1SXW5|RS13_PSYIN	30S ribosomal protein S13
TRINITY_DN660373_c0_g1_i8	4.786979473	.	30S ribosomal protein S21
TRINITY_DN686995_c0_g2_i1	5.219464061	sp|Q7VKD7|RS3_HAEDU	30S ribosomal protein S3
TRINITY_DN741750_c0_g1_i3	4.905722074	sp|Q2S929|RS5_HAHCH	30S ribosomal protein S5
TRINITY_DN640622_c1_g2_i6	4.063788268	sp|Q489U1|RS6_COLP3	30S ribosomal protein S6
TRINITY_DN731577_c1_g3_i9	5.020394569	sp|A6GZA2|RS7_FLAPJ	30S ribosomal protein S7
TRINITY_DN721471_c0_g3_i1	5.928799272	sp|A1TYL1|RS8_MARHV	30S ribosomal protein S8
TRINITY_DN696900_c1_g3_i23	4.499029583	sp|Q26630|IDLC_STRPU	33 kDa inner dynein arm light chain, axonemal
TRINITY_DN624139_c0_g1_i4	4.306124616	sp|P62282|RS11_RAT	40S ribosomal protein S11
TRINITY_DN484098_c0_g1_i1	3.764234078	sp|P62264|RS14_MOUSE	40S ribosomal protein S14-2
TRINITY_DN623080_c0_g3_i8	4.208194577	sp|P31674|RS15_ORYSJ	40S ribosomal protein S15
TRINITY_DN581427_c0_g3_i8	4.762682364	.	40S ribosomal protein S16
TRINITY_DN691690_c2_g2_i6	4.827907803	sp|P27685|RS2_DICDI	40S ribosomal protein S2-3
TRINITY_DN575296_c0_g1_i3	4.164219716	sp|P60868|RS20_RAT	40S ribosomal protein S20
TRINITY_DN569078_c0_g1_i5	4.007695783	.	40S ribosomal protein S27-B
TRINITY_DN636430_c1_g2_i1	4.636381583	sp|Q0Z8U2|RS3_PIG	40S ribosomal protein S3
TRINITY_DN653619_c0_g2_i1	4.421955079	sp|Q5CP76|RS3A_CRYHO	40S ribosomal protein S3a
TRINITY_DN594323_c0_g1_i6	4.742432833	sp|P49395|RS3A_APLCA	40S ribosomal protein S3a
TRINITY_DN613156_c4_g2_i5	5.009647535	sp|Q9BMX5|RS6_APLCA	40S ribosomal protein S6
TRINITY_DN652927_c0_g1_i2	4.43814278	sp|Q9LXG1|RS91_ARATH	40S ribosomal protein S9-1
TRINITY_DN687300_c1_g2_i18	5.525513524	sp|B1JE13|RL11_PSEPW	50S ribosomal protein L1
TRINITY_DN717018_c0_g1_i6	5.282603639	sp|Q47VT1|RL13_COLP3	50S ribosomal protein L13
TRINITY_DN705108_c1_g1_i13	4.076143087	sp|A1T0D1|RL24_PSYIN	50S ribosomal protein L14
TRINITY_DN704830_c1_g1_i7	6.413268727	sp|B3PK48|RL24_CELJU	50S ribosomal protein L14
TRINITY_DN641659_c0_g1_i12	3.902653966	.	50S ribosomal protein L14
TRINITY_DN683829_c2_g1_i4	5.061287298	sp|A1TYL6|RL15_MARHV	50S ribosomal protein L15
TRINITY_DN675314_c6_g4_i4	3.674424283	sp|Q488Z8|RL6_COLP3	50S ribosomal protein L18

Transcript ID	logCPM	Top BLASTP hit	Protein description
TRINITY_DN732354_c4_g1_i10	7.511397489	sp|B5FG09|RL3_VIBFM	50S ribosomal protein L2
TRINITY_DN700108_c4_g1_i1	4.815391147	sp|Q21M52|RL22_SACD2	50S ribosomal protein L22
TRINITY_DN670567_c0_g1_i3	3.776141789	.	50S ribosomal protein L28
TRINITY_DN722580_c2_g1_i20	4.145522826	.	50S ribosomal protein L35
TRINITY_DN729156_c2_g2_i7	4.104281278	.	50S ribosomal protein L35
TRINITY_DN724184_c1_g1_i12	3.78980257	sp|Q487Z4|RL4_COLP3	50S ribosomal protein L4
TRINITY_DN660412_c4_g3_i1	3.628611659	sp|Q487Z4|RL4_COLP3	50S ribosomal protein L4
TRINITY_DN729973_c2_g1_i4	3.703123666	sp|A6W377|RL6_MARMS	50S ribosomal protein L6
TRINITY_DN729973_c2_g1_i23	5.026041939	sp|A1TYL1|RS8_MARHV	50S ribosomal protein L6
TRINITY_DN737596_c3_g1_i2	6.278768542	sp|B5FBQ0|RL9_VIBFM	50S ribosomal protein L9
TRINITY_DN708086_c1_g1_i4	4.192103114	sp|Q9U3U0|RLA0_CERCA	60S acidic ribosomal protein P0
TRINITY_DN590761_c1_g1_i7	3.799924605	sp|Q9DG68|RLA0_RANSY	60S acidic ribosomal protein P0
TRINITY_DN619035_c0_g1_i6	4.044319593	sp|Q0DKF0|RL102_ORYSJ	60S ribosomal protein L10-2
TRINITY_DN689272_c5_g1_i6	5.014166957	sp|Q9VTP4|R10AB_DROME	60S ribosomal protein L10a-2
TRINITY_DN660785_c0_g1_i3	3.745601429	.	60S ribosomal protein L11
TRINITY_DN660785_c0_g1_i7	5.898926458	sp|P46222|RL11_DROME	60S ribosomal protein L11
TRINITY_DN552729_c0_g1_i3	3.677144	.	60S ribosomal protein L12-3
TRINITY_DN589707_c0_g1_i4	4.697424787	sp|P41126|RL13_DROME	60S ribosomal protein L13
TRINITY_DN640832_c2_g1_i5	5.428604298	sp|Q3SZ90|RL13A_BOVIN	60S ribosomal protein L13a
TRINITY_DN560781_c0_g1_i1	4.219329669	sp|O46160|RL14_LUMRU	60S ribosomal protein L14
TRINITY_DN582912_c0_g1_i1	5.088208121	sp|Q9SIM4|RL141_ARATH	60S ribosomal protein L14-1
TRINITY_DN654624_c0_g1_i2	5.531695985	sp|Q4PM54|RL17_IXOSC	60S ribosomal protein L17
TRINITY_DN623103_c0_g1_i2	3.958510268	sp|P46990|RL17B_YEAST	60S ribosomal protein L17-B
TRINITY_DN610360_c0_g1_i12	4.145110996	sp|Q1HR62|RL18_AEDAE	60S ribosomal protein L18-3
TRINITY_DN610360_c0_g1_i17	6.587935327	sp|Q940B0|RL183_ARATH	60S ribosomal protein L18-3
TRINITY_DN665774_c0_g1_i18	4.828294078	sp|Q9LUQ6|RL192_ARATH	60S ribosomal protein L19
TRINITY_DN586644_c0_g1_i4	4.93303639	sp|P36241|RL19_DROME	60S ribosomal protein L19
TRINITY_DN634448_c0_g1_i9	3.915659041	sp|P52819|RL22_CAEEL	60S ribosomal protein L22
TRINITY_DN644487_c9_g1_i4	5.259868141	sp|P62752|RL23A_RAT	60S ribosomal protein L23a
TRINITY_DN590525_c0_g1_i1	3.963241398	sp|Q9DFQ7|RL24_GILMI	60S ribosomal protein L24

Transcript ID	logCPM	Top BLASTP hit	Protein description
TRINITY_DN615508_c2_g1_i7	4.276693982	sp|P61255|RL26_MOUSE	60S ribosomal protein L26
TRINITY_DN668650_c0_g4_i2	6.131662747	sp|O16797|RL3_DROME	60S ribosomal protein L3
TRINITY_DN625406_c1_g1_i4	4.66128917	sp|P62912|RL32_RAT	60S ribosomal protein L32
TRINITY_DN562846_c0_g1_i1	3.776491429	.	60S ribosomal protein L32
TRINITY_DN617372_c11_g1_i1	4.195230237	sp|Q8JHJ1|RL35_DANRE	60S ribosomal protein L35
TRINITY_DN617372_c11_g1_i2	5.062739481	sp|Q8JHJ1|RL35_DANRE	60S ribosomal protein L35
TRINITY_DN600712_c0_g1_i2	4.19603332	sp|O74904|RL35_SCHPO	60S ribosomal protein L35
TRINITY_DN692261_c0_g2_i3	3.748548689	sp|Q5RAZ9|RL36_PONAB	60S ribosomal protein L36
TRINITY_DN720147_c0_g2_i2	3.685064427	sp|P49165|RL4_URECA	60S ribosomal protein L4-1
TRINITY_DN720147_c0_g2_i21	6.140288093	sp|Q9SF40|RL4A_ARATH	60S ribosomal protein L4-1
TRINITY_DN588402_c0_g1_i2	6.092667411	sp|Q9SF40|RL4A_ARATH	60S ribosomal protein L4-1
TRINITY_DN566229_c0_g1_i8	5.514094826	sp|Q26481|RL5_STYCL	60S ribosomal protein L5
TRINITY_DN650649_c0_g3_i2	6.004659681	sp|O01802|RL7_CAEEL	60S ribosomal protein L7
TRINITY_DN650649_c0_g3_i3	4.189163972	sp|O01802|RL7_CAEEL	60S ribosomal protein L7
TRINITY_DN665439_c0_g2_i4	5.194469072	sp|P0DJ14|RL7A_TETTH	60S ribosomal protein L7a
TRINITY_DN665671_c0_g5_i1	4.569500567	.	60S ribosomal protein L8
TRINITY_DN589001_c0_g1_i7	4.57367103	sp|Q6PBF0|RL8_XENTR	60S ribosomal protein L8
TRINITY_DN619147_c0_g2_i9	3.842956537	sp|O74905|RL9B_SCHPO	60S ribosomal protein L9-A
TRINITY_DN684178_c0_g2_i3	4.344454732	sp|P21184|FLICA_PSEAI	A-type flagellin
TRINITY_DN630968_c7_g1_i1	4.995464039	sp|O65315|ACT_COLSC	Actin
TRINITY_DN630305_c4_g1_i18	5.774203318	sp|Q25381|ACTM_LYTPI	Actin, cytoplasmic
TRINITY_DN665210_c2_g5_i2	4.884899918	sp|Q964E0|ACTC_BIOTE	Actin, cytoplasmic 1
TRINITY_DN655864_c3_g1_i6	5.131969112	sp|Q10DV7|ACT1_ORYSJ	Actin, muscle (Fragment)
TRINITY_DN650797_c0_g1_i2	4.131184494	.	Akirin-2
TRINITY_DN685377_c2_g1_i16	5.66056937	sp|P81178|ALDH2_MESAU	Aldehyde dehydrogenase, mitochondrial
TRINITY_DN685377_c2_g1_i17	4.175154161	sp|P12762|ALDH2_HORSE	Aldehyde dehydrogenase, mitochondrial
TRINITY_DN610772_c0_g1_i5	5.75613198	sp|Q29471|ANX13_CANLF	Annexin A13
TRINITY_DN610772_c0_g1_i6	5.20467751	sp|Q29471|ANX13_CANLF	Annexin A13
TRINITY_DN685177_c3_g6_i2	4.333367593	sp|Q9HT19|ATPG_PSEAE	ATP synthase gamma chain
TRINITY_DN680871_c1_g2_i1	4.233084536	sp|Q48AW1|ATPG_COLP3	ATP synthase gamma chain

Transcript ID	logCPM	Top BLASTP hit	Protein description
TRINITY_DN646262_c0_g4_i1	4.207904816	sp|P35381|ATPA_DROME	ATP synthase subunit alpha, mitochondrial
TRINITY_DN600573_c0_g1_i3	4.408806454	sp|P47204|FTSZ_PSEAE	Cell division protein FtsZ
TRINITY_DN642788_c1_g1_i5	4.749758784	sp|P54423|WPRA_BACSU	Cell wall-associated protease
TRINITY_DN651257_c0_g2_i1	6.456112394	sp|P82600|PERC_AEDAE	Chorion peroxidase
TRINITY_DN651257_c0_g2_i21	5.998217115	sp|Q7QH73|PERC_ANOGA	Chorion peroxidase
TRINITY_DN661463_c0_g1_i1	5.656195557	sp|Q6PDQ2|CHD4_MOUSE	Chromodomain-helicase-DNA-binding protein 4
TRINITY_DN611546_c0_g1_i14	4.343396464	sp|Q8BTU1|CFA20_MOUSE	Cilia- and flagella-associated protein 20
TRINITY_DN687111_c0_g1_i2	5.086124708	sp|Q0V8T9|CTP5A_MOUSE	Coagulation factor V
TRINITY_DN644248_c0_g1_i2	5.781730525	sp|Q9GPH3|ATFC_BOMMO	Cyclic AMP-dependent transcription factor ATF-5
TRINITY_DN719675_c2_g1_i1	3.870931764	.	Cysteine-rich protein 1
TRINITY_DN736646_c1_g3_i1	10.768504	sp|B0FWD3|NU5M_AEDAE	Cytochrome c oxidase subunit 1
TRINITY_DN700100_c2_g2_i5	3.803566277	sp|Q56352|NAPC_PARPN	Cytochrome c-type protein NapC
TRINITY_DN704096_c1_g5_i3	4.880226573	sp|A4SSY1|RPOA_AERS4	DNA-directed RNA polymerase subunit alpha
TRINITY_DN733966_c2_g3_i5	6.900969113	sp|A4VHQ5|RPOA_PSEU5	DNA-directed RNA polymerase subunit alpha
TRINITY_DN743030_c20_g1_i1	5.175824619	sp|A4VHQ5|RPOA_PSEU5	DNA-directed RNA polymerase subunit alpha
TRINITY_DN717049_c1_g1_i2	5.477677529	sp|C3LR59|RL7_VIBCM	DNA-directed RNA polymerase subunit beta
TRINITY_DN660661_c3_g1_i6	5.044227084	sp|Q6AZ28|PIAS2_RAT	E3 SUMO-protein ligase PIAS2
TRINITY_DN605623_c0_g1_i2	3.846597941	.	E3 ubiquitin-protein ligase RNF115
TRINITY_DN668298_c2_g1_i6	6.261916026	sp|Q93RV9|ECTD_STRCO	Ectoine dioxygenase
TRINITY_DN735178_c4_g2_i2	3.872958888	sp|Q9HZP6|ETFB_PSEAE	Electron transfer flavoprotein subunit beta
TRINITY_DN722341_c0_g1_i15	7.962202136	sp|P04962|CCNA_SPISO	G2/mitotic-specific cyclin-A
TRINITY_DN683109_c0_g1_i7	8.522036045	sp|P13952|CCNB_SPISO	G2/mitotic-specific cyclin-B
TRINITY_DN683109_c0_g1_i12	4.962805155	sp|P24862|CCNB_PATVU	G2/mitotic-specific cyclin-B
TRINITY_DN697252_c0_g1_i5	5.198592929	sp|P15104|GLNA_HUMAN	Glutamine synthetase
TRINITY_DN606465_c0_g1_i8	4.644222752	sp|Q39769|G3PC_GINBI	Glyceraldehyde-3-phosphate dehydrogenase
TRINITY_DN667022_c2_g3_i8	6.057473927	sp|O42249|GBLP_ORENI	Guanine nucleotide-binding protein subunit beta-2-like 1
TRINITY_DN649584_c2_g3_i2	4.935893178	sp|Q4R888|HS71L_MACFA	Heat shock 70 kDa protein 1-like
TRINITY_DN698135_c0_g1_i1	4.537977487	sp|P18694|HSP72_USTMA	Heat shock 70 kDa protein 2
TRINITY_DN698135_c1_g1_i4	6.42190609	sp|Q9U639|HSP7D_MANSE	Heat shock cognate 71 kDa protein
TRINITY_DN698135_c1_g1_i16	7.298570954	sp|P63018|HSP7C_RAT	Heat shock cognate 71 kDa protein

Transcript ID	logCPM	Top BLASTP hit	Protein description
TRINITY_DN698135_c1_g1_i17	5.295224053	sp|P16627|HS71L_MOUSE	Heat shock cognate 71 kDa protein
TRINITY_DN698135_c1_g1_i18	7.711566456	sp|P63018|HSP7C_RAT	Heat shock cognate 71 kDa protein
TRINITY_DN622357_c0_g2_i2	5.831116432	.	Heat shock factor-binding protein 1
TRINITY_DN670310_c4_g3_i7	6.23704974	sp|Q04619|HS90B_CHICK	Heat shock protein 83
TRINITY_DN679451_c1_g2_i2	4.542294486	sp|P11501|HS90A_CHICK	Heat shock protein HSP 90-alpha A2
TRINITY_DN724757_c2_g1_i11	4.668067611	sp|Q8J0D7|SUB3_ARTOT	Intracellular serine protease
TRINITY_DN667029_c1_g1_i2	4.435789093	sp|A7MBP4|IFT46_DANRE	Intraflagellar transport protein 46 homolog
TRINITY_DN720406_c2_g1_i17	5.346751414	sp|Q4R6T7|IQUB_MACFA	IQ and ubiquitin-like domain-containing protein
TRINITY_DN731569_c3_g2_i9	4.456124505	sp|P81715|LIE1_STREX	Leupeptin-inactivating enzyme 1
TRINITY_DN724217_c4_g1_i12	5.531534385	sp|Q47VL0|MDH_COLP3	Malate dehydrogenase
TRINITY_DN660359_c0_g1_i11	3.671494563	sp|P86948|MP_PINMA	Mantle protein
TRINITY_DN683432_c0_g1_i24	6.891924376	sp|Q8LTE2|MATA2_BPQBE	Maturation protein A2
TRINITY_DN718642_c2_g1_i14	4.375416446	sp|Q88NI1|MCPU_PSEPK	Methyl-accepting chemotaxis protein McpU
TRINITY_DN637492_c5_g1_i6	4.184864387	.	MORN repeat-containing protein 2
TRINITY_DN659119_c1_g1_i20	7.798777221	sp|A4IIN5|TISD_XENTR	mRNA decay activator protein ZFP36L2
TRINITY_DN639794_c6_g1_i2	5.988246731	sp|P07291|MLE_ARGIR	Myosin catalytic light chain LC-1, mantle muscle
TRINITY_DN632818_c7_g1_i11	4.354328858	sp|Q6DBY2|NAA50_DANRE	N-alpha-acetyltransferase 50
TRINITY_DN736646_c1_g1_i2	7.027718203	.	NADH-ubiquinone oxidoreductase chain 4
TRINITY_DN638337_c0_g2_i1	3.694169856	sp|Q9M612|NACA_PINTA	Nascent polypeptide-associated complex subunit alpha-like protein
TRINITY_DN638337_c0_g2_i5	4.375439311	sp|Q9M612|NACA_PINTA	Nascent polypeptide-associated complex subunit alpha-like protein
TRINITY_DN700903_c0_g1_i4	3.988152779	sp|P20397|NUCL_XENLA	Nucleolin
TRINITY_DN611692_c0_g1_i16	4.511166156	sp|P56597|NDK5_HUMAN	Nucleoside diphosphate kinase homolog 5
TRINITY_DN737442_c5_g1_i2	4.719414385	sp|Q8XGX8|DCOA_SALTI	Oxaloacetate decarboxylase alpha chain
TRINITY_DN696023_c0_g1_i2	5.449702521	sp|Q99541|PLIN2_HUMAN	Perilipin-2
TRINITY_DN635792_c2_g1_i10	6.761372531	sp|Q8VEM8|MPCP_MOUSE	Phosphate carrier protein, mitochondrial
TRINITY_DN710346_c7_g1_i1	7.569011498	sp|Q9EPH8|PABP1_RAT	Polyadenylate-binding protein 1
TRINITY_DN617592_c8_g3_i1	4.035026362	sp|P26599|PTBP1_HUMAN	Polypyrimidine tract-binding protein 1
TRINITY_DN680805_c1_g1_i2	4.668029682	.	Primosomal replication protein N
TRINITY_DN642396_c1_g1_i11	4.12233871	sp|Q9FEF8|MD36B_ARATH	Probable mediator of RNA polymerase II transcription subunit 36b
TRINITY_DN695821_c0_g2_i4	3.591712571	.	Probable nucleoredoxin 1-1

Transcript ID	logCPM	Top BLASTP hit	Protein description
TRINITY_DN632375_c2_g2_i4	5.590553092	sp|Q9DEA3|PCNA_CHICK	Proliferating cell nuclear antigen
TRINITY_DN693554_c0_g1_i1	4.82486413	sp|E9PVX6|KI67_MOUSE	Proliferation marker protein Ki-67
TRINITY_DN676890_c2_g1_i12	5.641757427	sp|E9PVX6|KI67_MOUSE	Proliferation marker protein Ki-67
TRINITY_DN693016_c9_g1_i1	4.774527061	sp|P24495|PSA2_XENLA	Proteasome subunit alpha type-2
TRINITY_DN655982_c0_g1_i6	6.165171411	sp|Q99873|ANM1_HUMAN	Protein arginine N-methyltransferase 1
TRINITY_DN707345_c0_g1_i22	5.550307846	sp|Q6DJL7|BORA_XENLA	Protein aurora borealis
TRINITY_DN601575_c0_g1_i1	6.868150254	sp|P62325|BTG1_MOUSE	Protein BTG1
TRINITY_DN618541_c0_g2_i12	3.980517294	sp|Q9Y7Y3|YGR4_SCHPO	Protein gar2
TRINITY_DN651462_c0_g1_i4	5.636084878	sp|P0CW97|PCR3_ARATH	Protein PLANT CADMIUM RESISTANCE 3
TRINITY_DN732871_c3_g1_i5	5.823485607	sp|Q9HWF5|SECY_PSEAE	Protein translocase subunit SecY
TRINITY_DN561515_c2_g1_i2	4.622828695	sp|Q9HWF5|SECY_PSEAE	Protein translocase subunit SecY
TRINITY_DN740662_c1_g1_i10	4.433330751	sp|E9PVD3|PCD16_MOUSE	Protocadherin-16
TRINITY_DN723628_c0_g1_i11	6.493955757	sp|Q6KEQ9|PC11X_PIG	Protocadherin-7
TRINITY_DN610116_c9_g2_i1	4.394074579	sp|B3A0R0|PPI_LOTGI	Putative peptidyl-prolyl cis-trans isomerase
TRINITY_DN618956_c0_g1_i4	5.420466685	sp|P11415|QOR_CAVPO	Quinone oxidoreductase
TRINITY_DN594660_c0_g1_i3	5.270753788	sp|Q8BYM7|RSH4A_MOUSE	Radial spoke head protein 4 homolog A
TRINITY_DN683359_c0_g3_i9	6.794982322	sp|P26043|RADI_MOUSE	Radixin
TRINITY_DN626763_c6_g1_i6	3.608822806	sp|Q5R8Z8|RAB14_PONAB	Ras-related protein Rab-14
TRINITY_DN722375_c1_g1_i20	4.665691419	sp|O57415|RREB1_CHICK	Ras-responsive element-binding protein 1
TRINITY_DN722375_c1_g1_i21	4.537177828	.	Ras-responsive element-binding protein 1
TRINITY_DN722775_c0_g1_i2	3.655367084	.	RE1-silencing transcription factor
TRINITY_DN721604_c0_g1_i14	4.907604351	.	Ribonuclease H1
TRINITY_DN634041_c4_g5_i9	6.123743532	sp|P07201|RIR2_SPISO	Ribonucleoside-diphosphate reductase small chain
TRINITY_DN653084_c4_g2_i23	4.98428359	sp|Q14692|BMS1_HUMAN	Ribosome biogenesis protein BMS1 homolog
TRINITY_DN674974_c0_g1_i3	5.504905541	sp|P17160|HPF_AZOVI	Ribosome hibernation promoting factor
TRINITY_DN731384_c2_g3_i5	4.011551961	.	RNA polymerase sigma factor RpoS
TRINITY_DN680632_c7_g1_i12	4.255513696	sp|Q92541|RTF1_HUMAN	RNA polymerase-associated protein RTF1 homolog
TRINITY_DN693407_c10_g3_i14	5.249411575	sp|Q02427|RBP1_DROME	RNA-binding protein 1
TRINITY_DN721782_c1_g1_i2	5.290355623	sp|Q5TZA2|CROCC_HUMAN	Rootletin
TRINITY_DN651609_c0_g1_i8	6.196153349	sp|P02637|SCP_MIZYE	Sarcoplasmic calcium-binding protein

Transcript ID	logCPM	Top BLASTP hit	Protein description
TRINITY_DN706342_c1_g1_i22	6.492087362	sp|Q6DK72|SUMO3_XENTR	Small ubiquitin-related modifier 3
TRINITY_DN646949_c2_g1_i5	3.944193443	.	Sodium/alanine symporter AgcS
TRINITY_DN739045_c4_g3_i1	5.112654543	.	Sodium/potassium-transporting ATPase subunit alpha
TRINITY_DN681107_c1_g1_i9	4.388247725	sp|P73392|Y1735_SYNY3	Transforming growth factor-beta-induced protein ig-h3
TRINITY_DN728119_c1_g3_i4	4.779850451	.	Translation initiation factor IF-3
TRINITY_DN721452_c1_g3_i4	4.673577197	sp|P52833|SYT_PSESY	Translation initiation factor IF-3
TRINITY_DN696839_c1_g1_i3	4.605472201	sp|P33319|IF3_PROHU	Translation initiation factor IF-3
TRINITY_DN681207_c6_g2_i1	4.692654043	sp|G3LU44|TCTP_LOXIN	Translationally-controlled tumor protein homolog
TRINITY_DN681207_c6_g2_i9	6.625655614	sp|G3LU44|TCTP_LOXIN	Translationally-controlled tumor protein homolog
TRINITY_DN730781_c2_g1_i8	4.849287315	sp|A4XXT6|RIMM_PSEMY	tRNA (guanine-N(1)-)-methyltransferase
TRINITY_DN614259_c2_g1_i9	5.208364404	sp|Q47WV0|TRMD_COLP3	tRNA (guanine-N(1)-)-methyltransferase
TRINITY_DN659725_c3_g1_i5	3.803262502	sp|Q47WV0|TRMD_COLP3	tRNA (guanine-N(1)-)-methyltransferase
TRINITY_DN701388_c0_g1_i25	7.045919739	sp|Q25145|TPM_HALRU	Tropomyosin
TRINITY_DN677250_c1_g1_i1	5.363832112	sp|P07304|TBA1_STYLE	Tubulin alpha chain
TRINITY_DN677250_c1_g1_i5	5.581540538	sp|Q9ZRJ4|TBA_CHLVU	Tubulin alpha chain
TRINITY_DN677250_c1_g1_i9	6.077612195	sp|P10872|TBA_TETPY	Tubulin alpha chain
TRINITY_DN677250_c1_g1_i10	3.985223176	sp|P07304|TBA1_STYLE	Tubulin alpha chain
TRINITY_DN736548_c3_g2_i1	3.79659294	sp|P09645|TBA8_CHICK	Tubulin alpha chain (Fragment)
TRINITY_DN667350_c5_g1_i2	3.844238822	sp|P06605|TBA3_DROME	Tubulin alpha-1 chain
TRINITY_DN667350_c5_g1_i8	3.911006831	sp|P06605|TBA3_DROME	Tubulin alpha-1 chain
TRINITY_DN625486_c7_g1_i3	4.90892602	sp|P02553|TBA_LYTPI	Tubulin alpha-1 chain (Fragment)
TRINITY_DN634413_c1_g1_i2	3.931943102	.	Tubulin alpha-3 chain
TRINITY_DN654595_c1_g2_i3	3.783506164	.	Tubulin alpha-4 chain (Fragment)
TRINITY_DN726552_c2_g6_i4	4.658822173	sp|P79008|TBB_COPC7	Tubulin beta chain (Fragment)
TRINITY_DN636052_c2_g2_i5	3.728551803	sp|P41386|TBB_HALDI	Tubulin beta chain (Fragment)
TRINITY_DN636052_c2_g3_i3	4.638704247	sp|Q9ZSW1|TBB1_CYAPA	Tubulin beta-1 chain
TRINITY_DN662369_c6_g3_i7	5.019567696	sp|P68372|TBB4B_MOUSE	Tubulin beta-1 chain (Fragment)
TRINITY_DN607555_c2_g1_i1	3.789707046	sp|P46575|RL40_EIMBO	Ubiquitin-60S ribosomal protein L40
TRINITY_DN637593_c8_g2_i8	4.41795764	.	Ubiquitin-conjugating enzyme E2 4
TRINITY_DN681212_c3_g1_i14	4.50405472	sp|P25867|UBCD1_DROME	Ubiquitin-conjugating enzyme E2-17 kDa

Transcript ID	logCPM	Top BLASTP hit	Protein description
TRINITY_DN681212_c3_g1_i21	3.906083114	sp|P25867|UBCD1_DROME	Ubiquitin-conjugating enzyme E2-17 kDa
TRINITY_DN657838_c7_g1_i1	5.005667269	sp|P74897|YQA3_THEAQ	Universal stress protein in QAH/OAS sulfhydrylase 3'region

Appendix 3

The following table summarises the Gene ontoloy and BLAST results for Trinity transcripts associated with Trinity genes with significant SNP results from Chapter 4. Please note each Trinity gene is often represented by several Trinity transcripts. Not all SPROT annotations produced GO annotation. Gene Ontology (GO) terms present molecular function, but if not available biological processes (BP) were annotated.

Mean z-score	FDR	Number of SNPs	Transcript_id	SPROT_TopBLASTX_ID	SPROT_TopBLASTX_Gene	E-Value	gene_ontology_pfam	Gene notes
0.498936538	0	8	TRINITY_DN718458_c5_g4_i1					
0.479467766	0.01	14	TRINITY_DN648545_c0_g2_i1					
0.498937	0.02	7						
0.456255128	0.02	20	TRINITY_DN619912_c4_g2_i6					
0.45242906	0.02	15	TRINITY_DN632889_c2_g1_i16					
0.440471795	0.02	6	TRINITY_DN648447_c1_g1_i1					
0.450740385	0.02	8	TRINITY_DN629739_c11_g3_i2					
0.445473767	0.02	13	TRINITY_DN617264_c4_g1_i5					
0.445773504	0.02	6	TRINITY_DN635787_c6_g1_i2					
0.447133937	0.02	17	TRINITY_DN642498_c3_g5_i3					
0.456446154	0.02	13	TRINITY_DN644365_c4_g5_i1					
0.43596	0.025	17	TRINITY_DN666119_c2_g1_i1					
0.43596	0.025	17	TRINITY_DN666119_c2_g1_i2					
0.43596	0.025	17	TRINITY_DN666119_c2_g1_i3					
0.435082353	0.025	17	TRINITY_DN743030_c21_g1_i11	Q488Z6	RS5_COLP3	1.97E-50		Translation
0.435082353	0.025	17	TRINITY_DN743030_c21_g1_i1	Q488Z6	RS5_COLP3	1.81E-99	GO:0003735: structural constituent ribosome	Translation
0.435082353	0.025	17	TRINITY_DN743030_c21_g1_i9	A1S233	RL6_SHEAM	1.26E-92	GO:0003735: structural constituent ribosome	Translation
0.431108718	0.025714286	10	TRINITY_DN738280_c3_g1_i12					

Mean z-score	FDR	Number of SNPs	Transcript_id	SPROT_TopBLASTX_ID	SPROT_TopBLASTX_Gene	E-Value	gene_ontology_pfam	Gene notes
0.428149451	0.029333333	21	TRINITY_DN637768_c7_g1_i28					
0.424650641	0.03875	8	TRINITY_DN718236_c1_g2_i1	A8WYE4	PAR1_CAEBR	5.21E-30		cell division
0.401947578	0.047058824	27	TRINITY_DN611044_c4_g5_i1					
0.398291795	0.047058824	20	TRINITY_DN698079_c5_g3_i1					
0.388163004	0.047058824	14	TRINITY_DN649896_c4_g1_i5					
0.389021004	0.047058824	107	TRINITY_DN742681_c7_g2_i5	Q487Z8	RL22_COLP3	6.18E-72	GO:0003735: structural constituent ribosome	Translation
0.403066422	0.047058824	42	TRINITY_DN624905_c4_g1_i20					
0.385220513	0.047058824	41	TRINITY_DN741750_c2_g1_i7	Q489A1	RL5_COLP3	4.08E-91	GO:0003735: structural constituent ribosome	Translation
0.385220513	0.047058824	41	TRINITY_DN741750_c2_g1_i12	Q489A1	RL5_COLP3	7.88E-93		Translation
0.385220513	0.047058824	41	TRINITY_DN741750_c2_g1_i15	Q489A1	RL5_COLP3	3.17E-93		Translation
0.38297	0.047059	38	TRINITY_DN707721_c5_g2_i1					
0.38297	0.047059	38	TRINITY_DN707721_c5_g2_i2					
0.381668606	0.047059	18	TRINITY_DN622435_c3_g1_i1					
0.391235294	0.047058824	17	TRINITY_DN677665_c6_g5_i1					
0.399041808	0.047058824	18	TRINITY_DN673029_c7_g1_i8					
0.373471795	0.047058824	11	TRINITY_DN630680_c3_g1_i9	Q488Z7	RL18_COLP3	1.92E-32		Translation
0.373471795	0.047058824	11	TRINITY_DN630680_c3_g1_i8	Q488Z6	RS5_COLP3	2.73E-68	GO:0003723: RNA binding	Translation
0.408940793	0.047058824	11	TRINITY_DN630414_c5_g5_i16					

Mean z-score	FDR	Number of SNPs	Transcript_id	SPROT_TopBLASTX_ID	SPROT_TopBLASTX_Gene	E-Value	gene_ontology_pfam	Gene notes
0.3873480	0.047058		TRINITY_DN742681_c7_g			4.62E-		
77	824	8	1_i4	Q488A0	RL16_COLP3	48		Translation
0.3873036	0.047058		TRINITY_DN505940_c0_g					
25	824	29	1_i1					
0.4067630	0.047058		TRINITY_DN624293_c0_g					
77	824	25	2_i16					
0.4020487	0.047058		TRINITY_DN640287_c2_g					
18	824	20	5_i2					
0.4015355	0.047058		TRINITY_DN679445_c4_g					
19	824	61	1_i11					
0.3760435	0.047058		TRINITY_DN647460_c6_g					
9	824	16	2_i3					
0.3845113	0.047058		TRINITY_DN698009_c4_g					
96	824	18	1_i4					
0.4062982	0.047058		TRINITY_DN672550_c4_g					
91	824	36	3_i15					
0.3887303	0.047058		TRINITY_DN672793_c4_g					
64	824	19	2_i8					
0.3980133	0.047058		TRINITY_DN623316_c5_g					
33	824	5	1_i2					
0.3724863	0.047058		TRINITY_DN670777_c2_g			9.44E-		
04	824	41	1_i5	Q3BAI2	YCX91_PHAAO	06		Uncharacterised
0.3724863	0.047058		TRINITY_DN670777_c2_g					
04	824	41	1_i11					
0.4179111	0.047058		TRINITY_DN635514_c2_g					
11	824	12	2_i8					
0.4062521	0.047058		TRINITY_DN671964_c10_					
03	824	25	g1_i6					
0.4189576	0.047058		TRINITY_DN628092_c0_g					
92	824	28	9_i3					
0.3863678	0.047058		TRINITY_DN657568_c4_g					
81	824	19	2_i2					
0.3755723	0.047058		TRINITY_DN622954_c10_					
65	824	18	g1_i3					
0.3789757								
	0.047058		TRINITY_DN670483_c5_g					
35	824	41	3_i1					

Mean z-score	FDR	Number of SNPs	Transcript_id	SPROT_TopBLASTX_ID	SPROT_TopBLASTX_Gene	E-Value	gene_ontology_pfam	Gene notes
0.3870025	0.047058		TRINITY_DN617520_c5_g					
64	824	30	2_i24					
0.4101355	0.047058		TRINITY_DN640665_c1_g			2.38E-		
31	824	14	2_i4	Q487Z6	RL2_COLP3	64	GO:0003735:RNA binding	Translation
0.3957384	0.047058		TRINITY_DN625486_c7_g			4.41E-		Tubulin,
62	824	12	1_i11	P02552	TBA1_CHICK	133		cytoskeleton
0.3957384	0.047058		TRINITY_DN625486_c7_g			2.02E-		Tubulin,
62	824	12	1_i3	P02552	TBA1_CHICK	117		cytoskeleton
0.3957384	0.047058		TRINITY_DN625486_c7_g			1.06E-		Tubulin,
62	824	12	1_i1	P02552	TBA1_CHICK	143		cytoskeleton
0.4168985	0.047058		TRINITY_DN706515_c1_g			2.17E-		
35	824	14	1_i19	Q05974	RAB1A_LYMST	86		
0.3731142	0.047058		TRINITY_DN729286_c1_g					
45	824	36	6_i1					
0.3923715	0.047058		TRINITY_DN652405_c3_g					
1	824	54	2_i21					
0.4193766	0.047058		TRINITY_DN619578_c3_g					
9	824	22	3_i10					
0.4001879	0.047058		TRINITY_DN602732_c7_g					
34	824	17	1_i2					
0.3925128	0.047058		TRINITY_DN741429_c4_g			3.10E-		
21	824	13	1_i9	Q489T9	RS18_COLP3	38		Translation
0.4102150	0.047058		TRINITY_DN646956_c0_g					
43	824	15	2_i7					
0.4181799	0.047058		TRINITY_DN673722_c3_g					
76	824	21	2_i14					
0.3952850	0.047058		TRINITY_DN619912_c4_g					
57	824	29	6_i2					
0.3880235	0.047058		TRINITY_DN704469_c1_g					
9	824	5	1_i4					
0.3859225	0.047058		TRINITY_DN634403_c6_g					
07	824	18	6_i1					
0.3820510	0.047058		TRINITY_DN712909_c5_g			5.48E-		
92	824	27	1_i12	Q487Z7	RS19_COLP3	33		Translation
0.3820510	0.047058		TRINITY_DN712909_c5_g			3.38E-		
92	824	27	1_i23	Q487Z6	RL2_COLP3	47		Translation

Mean z-score	FDR	Number of SNPs	Transcript_id	SPROT_TopBLASTX_ID	SPROT_TopBLASTX_Gene	E-Value	gene_ontology_pfam	Gene notes
0.3820510	0.047058		TRINITY_DN712909_c5_g			5.47E-	GO:0003735: structural constituent	
92	824	27	1_i1	Q487Z6	RL2_COLP3	121	ribosome	Translation
0.3820510	0.047058		TRINITY_DN712909_c5_g			2.53E-		
92	824	27	1_i2	Q487Z7	RS19_COLP3	27		Translation
0.3820510	0.047058		TRINITY_DN712909_c5_g			9.39E-	GO:0003735: structural constituent	
92	824	27	1_i14	Q487Z6	RL2_COLP3	115	ribosome	Translation
0.3780516	0.047058		TRINITY_DN655853_c2_g					
77	824	13	2_i8					
0.4164532	0.047058		TRINITY_DN617797_c4_g					
05	824	16	3_i2					
0.3812051	0.047058		TRINITY_DN674687_c5_g					
28	824	24	4_i1					
0.4096983	0.047058		TRINITY_DN666119_c0_g					
97	824	16	1_i1					
0.4008378	0.047058		TRINITY_DN668861_c7_g					
21	824	8	3_i1					
0.3996351	0.047058		TRINITY_DN742580_c3_g			2.22E-	GO:0003735: structural constituent	
65	824	7	1_i8	Q47UV5	RL11_COLP3	93	ribosome	Translation
0.3996351	0.047058		TRINITY_DN742580_c3_g			2.22E-	GO:0003735: structural constituent	
65	824	7	1_i11	Q47UV5	RL11_COLP3	98	ribosome	Translation
0.4000235	0.047058		TRINITY_DN700907_c9_g					
9	824	20	1_i3					
0.3901327	0.047058		TRINITY_DN685825_c8_g					
3	824	17	1_i6					
0.3842636	0.047058		TRINITY_DN635911_c5_g					
36	824	22	2_i1					
0.3773483	0.047058		TRINITY_DN609892_c5_g					
68	824	44	4_i5					
0.4009853	0.047058		TRINITY_DN731884_c3_g					
48	824	14	7_i1					
0.4052717	0.047058		TRINITY_DN636702_c5_g					
95	824	7	1_i1					
0.4036970	0.047058		TRINITY_DN638801_c3_g					
94	824	15	1_i32					
0.3764276								
	0.047058		TRINITY_DN454068_c0_g					
92	824	5	1_i1					

Mean z-score	FDR	Number of SNPs	Transcript_id	SPROT_TopBLASTX_ID	SPROT_TopBLASTX_Gene	E-Value	gene_ontology_pfam	Gene notes
0.3887303	0.047058		TRINITY_DN690907_c0_g			1.94E-		
56	824	31	1_i14	Q5QXV7	RS4_IDILO	128	GO:0019843: rRNA binding	Translation
0.3887303	0.047058		TRINITY_DN690907_c0_g			2.83E-	GO:0003735: structural constituent	
56	824	31	1_i28	Q488Z0	RS11_COLP3	54	ribosome	Translation
0.3887303	0.047058		TRINITY_DN690907_c0_g			3.73E-	GO:0003735: structural constituent	
56	824	31	1_i9	Q488Z0	RS11_COLP3	57	ribosome	Translation
0.3887303	0.047058		TRINITY_DN690907_c0_g			1.04E-	GO:0003735: structural constituent	
56	824	31	1_i1	Q488Z0	RS11_COLP3	64	ribosome	Translation
0.4056261	0.047058		TRINITY_DN728669_c1_g			1.70E-	GO:0003735: structural constituent	
54	824	20	1_i8	Q488Z6	RS5_COLP3	66	ribosome	Translation
0.4056261	0.047058		TRINITY_DN728669_c1_g			1.48E-		
54	824	20	1_i7	Q488Z6	RS5_COLP3	66	GO:0003735: RNA binding	Translation
0.3911018	0.047058		TRINITY_DN612873_c0_g			1.35E-	GO:0042254: BP: ribosome	
32	824	7	1_i26	Q47UV7	RL10_COLP3	63	biogenesis	Translation
0.3911018	0.047058		TRINITY_DN612873_c0_g			5.15E-	GO:0042254: BP: ribosome	
32	824	7	1_i9	Q47UV7	RL10_COLP3	75	biogenesis	Translation
0.3714435	0.047058		TRINITY_DN695745_c0_g			6.12E-		Transcription
9	824	12	1_i3	Q9VI93	RN_DROME	35		factor
0.3714435	0.047058		TRINITY_DN695745_c0_g			8.65E-		Transcription
9	824	12	1_i2	Q9VI93	RN_DROME	62		factor
0.3899974	0.047058		TRINITY_DN673071_c1_g			2.77E-	GO:0007017: BP: microtubule-based	
36	824	12	2_i6	Q0P5A2	COQ5_BOVIN	88	process	Transferase
0.3899974	0.047058		TRINITY_DN673071_c1_g			2.66E-		
36	824	12	2_i10	Q0P5A2	COQ5_BOVIN	65		Transferase
0.4142051	0.047058		TRINITY_DN658689_c1_g					
28	824	8	2_i5					
0.4006468	0.047058		TRINITY_DN697899_c0_g			1.03E-		
29	824	38	2_i9	Q6P0B1	CELF2_DANRE	58	GO:0003676: nucleic acid binding	Translation
0.4006468	0.047058		TRINITY_DN697899_c0_g			8.18E-		
29	824	38	2_i4	Q6P0B1	CELF2_DANRE	60	GO:0003676: nucleic acid binding	Translation
0.3798564	0.047058		TRINITY_DN661195_c5_g					
1	824	5	2_i10					
0.3756246	0.047058		TRINITY_DN637856_c1_g					
15	824	20	1_i1					
0.3841976								
33	0.047058 824	13	TRINITY_DN670774_c1_g 1_i20	P83510	TNIK_MOUSE	0	GO:0004672: protein kinase activity	Signalling

Mean z-score	FDR	Number of SNPs	Transcript_id	SPROT_TopBLASTX_ID	SPROT_TopBLASTX_Gene	E-Value	gene_ontology_pfam	Gene notes
0.3841976	0.047058		TRINITY_DN670774_c1_g			9.88E-		
33	824	13	1_i12	P83510	TNIK_MOUSE	43		Signalling
0.3816222	0.047058		TRINITY_DN655853_c2_g					
22	824	15	1_i14					
0.3696444	0.048988		TRINITY_DN712378_c3_g			5.79E-		Actin:
44	764	12	1_i13	Q11212	ACT_SPOLI	62		cytoskeleton
0.3696444	0.048988		TRINITY_DN712378_c3_g			1.54E-		Actin:
44	764	12	1_i11	P10984	ACT2_CAEEL	91		cytoskeleton
0.3696444	0.048988		TRINITY_DN712378_c3_g			8.72E-		Actin:
44	764	12	1_i18	P48465	ACT_CRYNH	22		cytoskeleton
0.3696444	0.048988		TRINITY_DN712378_c3_g			2.27E-		Actin:
44	764	12	1_i16	P53464	ACTM_HELTB	99		cytoskeleton
0.3696444	0.048988		TRINITY_DN712378_c3_g			5.10E-		Actin:
44	764	12	1_i6	Q11212	ACT_SPOLI	67		cytoskeleton
0.3696444	0.048988		TRINITY_DN712378_c3_g			1.01E-		Actin:
44	764	12	1_i22	Q11212	ACT_SPOLI	103		cytoskeleton
0.3696444	0.048988		TRINITY_DN712378_c3_g			3.20E-		Actin:
44	764	12	1_i15	P10984	ACT2_CAEEL	91		cytoskeleton
0.3690195	0.049333		TRINITY_DN697274_c3_g					
27	333	26	2_i6					
0.3691080	0.049333		TRINITY_DN728436_c0_g			2.55E-		
87	333	13	1_i8	Q96MR6	CFA57_HUMAN	39		cilia protein
0.3691080	0.049333		TRINITY_DN728436_c0_g			2.62E-		
87	333	13	1_i6	Q9D180	CFA57_MOUSE	07		cilia protein
0.3691080	0.049333		TRINITY_DN728436_c0_g					
87	333	13	1_i19	Q96MR6	CFA57_HUMAN	0	GO:0005515: protein binding	cilia protein
0.3691080	0.049333		TRINITY_DN728436_c0_g			1.18E-		
87	333	13	1_i3	Q96MR6	CFA57_HUMAN	46		cilia protein